Real-time Receding Horizon Optimisation of Gas Pipeline Networks

Hans Aalto

Dissertation for the degree of Doctor of Science in Technology to be presented with due permission of the Department of Automation and Systems Technology, for public examination and debate in Auditorium AS1 at Helsinki University of Technology (Espoo, Finland) on the 20th of May, 2005, at 12 noon.

Real-time optimisation of gas pipelines in transient conditions is considered to be a challenging problem. Many pipeline systems are, however, only mildly non-linear. It is shown, that even the shutdown event of a compressor station can be described using a linear model. A dynamic, receding horizon optimisation problem is defined, where the free response prediction of the pipeline is obtained from a pipeline simulator and the optimal values of the decision variables are obtained solving a Quadratic Programming (QP)problem set up by using linear models, linearised constraints and quadratic approximations of the cost function, which is the energy consumption of the compressor stations (CSs). The problem is extended with discrete decision variables, the shutdown/start-up commands of CSs. A Mixed Logical Dynamical (MLD) system is defined, but the resulting Mixed Integer QP problem is shown to be very high-dimensional. Instead, a series of QP problems, each containing linear constraints modelling the shut down state of CSs, results in an optimisation problem with considerably smaller dimension.

The receding horizon optimisation is tested in a simulation environment and comparison with data from the Finnish natural gas pipeline shows that 5 to 8 % savings in compressor energy consumption can be achieved using optimisation. A new idea, maximisation of energy consumption, is used to calculate maximal energy savings potential of the pipeline.
A new result is that step response models used in conjunction with MLD systems do not produce the same model change behaviour than state space models.

Preface

The very first thoughts on real-time optimisation of gas pipeline networks came into my mind around the year 1990. Since then some small efforts related to that subject were done by myself and some colleagues of mine.

In year 2001, Professor Aarne Halme, head of the Department of Automation and Systems Technology at Helsinki University of Technology, started to guide me through the process of doctoral research. I want to express my warmest gratitude for his inspiring and encouraging supervision.

I also want to express my gratitude to my boss at Neste Jacobs, Dr. Petri Jokinen for his support over the years and to my colleague, Dr. Leif Hammarström for the time and effort he has spent on commenting my research results and on many interesting discussions. There are many persons at Gasum Oy, to whom I owe a lot, but let me express my warmest thanks especially to Mr. Jarmo Aho and Mr. Jorma Rintamäki for the pipeline system data they supplied me with as well as the many interesting discussions we had.

I am also thankful to Professor Arto Visala at the Automation Technology Laboratory of HUT for his support, which started already in 1998 when he for the first time suggested that I should start to work on my doctoral thesis.

Most of all, Raija-Liisa, Erik and Kaisa: how can I be grateful enough for long periods of time, when you only saw my back when I was sitting by my computer or, when I was physically present , but actually I seemed to look at some object far, far away.

Finally, I want to express my gratitude to the Natural Gas Fund of the Finnish Fund for Technology Advancement (Tekniikan Edistämissäätiö) for their financial support.

Helsinki, Finland, 25.4.2005

Hans Aalto

Table of contents

List of Symbols

A	Cross-sectional area of a pipe
a	Constant parameter in the quadratic approximation of compressor head
A	System matrix of a linear, discrete-time system model; Constraint matrix of a QP problem
$A(q^{-1})$	Matrix polynomial in q^{-1}; auto-regressive part of MIMO ARMA model
$A(q^{-1})$	Scalar valued polynomial in q^{-1}; auto-regressive part of ARMA model
$\mathbf{A_1}, \mathbf{A_2},\ldots$	System matrices of linear, discrete-time system models 1,2,...
$a_1, a_2,\ldots$	Compressor cost parameters
a_e	Constant in the general compressor envelope expression
a_{ij}	Constant in envelope limit number "j" for compressor "i"
a_L	Constant parameter in the linear approximation of compressor head
$\mathbf{A_m}$	Averaging matrix used in the equation constraint
b	Constant parameter in the quadratic approximation of compressor head
B	Input matrix of a linear, discrete-time system model; Constraint matrix of a QP problem
b	Matrix in a quadratic cost function
$\mathbf{B}(q^{-1})$	Matrix polynomial in q^{-1}; input polynomial of MIMO ARMA model
$B(q^{-1})$	Scalar valued polynomial in q^{-1}; input polynomial of ARMA model
$\mathbf{B_1}, \mathbf{B_2},\ldots$	Input matrices of linear, discrete-time system models 1,2,...
$b_1, b_2,\ldots$	Compressor cost parameters
b_e	Constant in the general compressor envelope expression
b_{ij}	Constant in envelope limit number "j" for compressor "i"
b_L	Constant parameter in the linear approximation of compressor head
c	Constant parameter in the quadratic approximation of compressor head
C	Output matrix of a linear, discrete-time system model
$\mathbf{C}(q^{-1})$	Matrix polynomial in q^{-1}; disturbance polynomial of MIMO ARMA model
$C(q^{-1})$	Polynomial in q^{-1}; disturbance polynomial of ARMA model
$\mathbf{C_1}, \mathbf{C_2},\ldots$	Output matrices of linear, discrete-time system models 1,2,...
c_e	Constant in the general compressor envelope expression
c_i	Cost function value at time point "i" in prediction horizon
c_{ij}	Constant in envelope limit number "j" for compressor "i"
c_L	Constant parameter in the linear approximation of compressor head
c_p	Average heat capacity of gas at constant pressure
$C_{s,i}$	Start up cost for compressor station "i"
c_v	Specific heat of gas at constant volume
D	Inside diameter of a pipe
d	Constant parameter in the quadratic approximation of compressor head
d	Vector of measured and possibly predicted disturbances of a system
$\mathbf{D_1}, \mathbf{D_2},\ldots$	Output matrices of a general Mixed Logical Dynamic system; matrices used in the quadratic cost function approximation
$\mathbf{D_F}$	Matrix used in the quadratic cost function approximation
$\mathbf{Du_{i,max}}$	Vector of maximum values for CS "i" discharge pressure increments
$\mathbf{Du_{i,min}}$	Vector of minimum values for CS "i" discharge pressure increments
e	Constant parameter in the quadratic approximation of compressor head; disturbance input to a system
E	Disturbance input matrix of a linear, discrete-time system model

$\mathbf{e}(k)$	Vector of stochastic noise inputs; output of a linear, discrete-time disturbance model
$\mathbf{E_1}, \mathbf{E_2}, \dots$	Disturbance input matrices of linear, discrete-time system models 1,2,…
$\mathbf{\hat{e}}$	Vector of correction values for consumption forecasts; difference between measured and estimated system output
f	Fanning friction factor; constant parameter in the quadratic approximation of compressor head
$\mathbf{F}$	Non-linear state propagation vector function of a discrete-time system model
$\mathbf{f}$	Non-linear, vector-valued input/output model of a system
F	Normalised gas flow (volumetric flow in normal conditions)
$\mathbf{F_1}, \mathbf{F_2}, \dots$	Matrices in the inequality part of a general Mixed Logical Dynamic system
F_j	Gas flow through compressor station "j"
$\mathbf{F_j}$	Vector of predicted gas flows for compressor station "j"
$F_j(q^{-1})$	Scalar valued polynomials in q^{-1} used in prediction model; j=1,2,..,P
$\mathbf{F_j}(q^{-1})$	Polynomials in q^{-1} used in prediction model; j=1,2,..,P
f_q	Function in steady state pipeline segment flow equation
g	Acceleration of gravity
$\mathbf{G}$	Non-linear output vector function of a discrete-time system model
$g_{1,i}$	Minimum speed line for compressor no. "i"
$g_{2,i}$	Choke line for compressor no. "i"
$g_{3,i}$	Surge line for compressor no. "i"
$g_{4,i}$	Maximum speed line for compressor no. "i"
$G_j(q^{-1})$	Scalar valued polynomials in q^{-1} used in prediction model; j=1,2,..,P
$\mathbf{G_j}(q^{-1})$	Matrix polynomials in q^{-1} used in prediction model; j=1,2,..,P
h	Elevation of pipe
H	Head of a compressor, in general
$\mathbf{H}$	Impulse response matrix; Shift matrix of a non-minimal system model used to obtain prediction vector
$\mathbf{h}$	Non-linear constraint vector function
H_a	Adiabatic head of a compressor
$H_j(q^{-1})$	Scalar valued polynomials in q^{-1} used in prediction model; j=1,2,..,P
$\mathbf{I_M}$	Vector of length M filled with ones
$\mathbf{I_p}$	Vector of length "P" filled with ones
$\mathbf{I_u}$	Lower triangular matrix filled with ones
$\mathbf{I_w}$	Matrix with vectors of ones for resolving blocking of compressor station on/off variables (w) with respect to the prediction horizon
J	Cost function over prediction horizon (sum of c_i)
j_b	Number of distinct values over the control horizon in the continuous input variable vector
$\mathbf{J_w}$	Matrix with vectors of ones for resolving blocking of compressor station on/off variables (w) with respect to the control horizon
J_w	Number of time intervals, where the compressor shut down/start up command variables are allowed to change
$\mathbf{K}$	Constant estimator gain matrix
K	Gain of a transfer function
$k_1, k_2, \dots$	Time moments, where the compressor shut down/start up command variables "w" are allowed to change
k_{12}	Constant in the steady state pipeline segment flow equation
k_a	Molar specific heat ratio of gas assuming adiabatic compression (adiabatic exponent)
K_H	Constant in the head expression of a compressor

$\mathbf{K_k}$	Estimator (Kalman filter) gain matrix, recalculated at each moment of time "k"
k_n	Exponent of a polytropic compression process
k_s	Shut down or start up moment of a compressor station in the prediction horizon
$k_s^{'}$	Shut down or start up moment of a compressor station in the prediction horizon
M	Length of control horizon
m	Number of inputs of a system model
$\mathbf{M}$	Vector of maximum values for auxiliary variables
$\mathbf{m}$	Vector of minimum values for auxiliary variables
m(t)	Gas mass content (line pack) of a pipeline segment
M'	A large positive number for constraint relaxation
$\mathbf{M_{NP}}$	Identity matrix with a zero element at row "p" and column "p"
$\mathbf{M_P}$	Zero matrix with an element of value one at row "p" and column "p"
$\mathbf{M_s}$	Shift matrix
$\mathbf{M_{ss}}$	Block diagonal matrix containing shift matrices ($\mathbf{M_s}$)
M_w	Molecular weight of gas
n	Rotational speed of compressor (in Chapter 3); number of outputs in a system; number of model change variables (δ_i) in a Mixed Logical Dynamic system
n_a	Degree of a scalar polynomial $A(q^{-1})$ or matrix polynomial $\mathbf{A}(q^{-1})$
n_b	Degree of a scalar polynomial $B(q^{-1})$ or matrix polynomial $\mathbf{B}(q^{-1})$
N_b	Even blocking parameter for continuous input variable
n_c	Degree of a scalar polynomial $C(q^{-1})$ or matrix polynomial $\mathbf{C}(q^{-1})$
N_C	Number of compressor stations in a pipeline system
N_d	Number of disturbance inputs in a system
N_x	Number of checkpoint pressures in a pipeline system
P	Pressure in general; Length of prediction horizon
$\mathbf{P}(t)$	Vector of measured pipeline pressures at time t
P_d	Discharge (outlet) pressure of a compressor station
$\mathbf{P_{d,i,max}}$	Vector of maximum values for discharge pressure of CS "i"
$\mathbf{P_{d,i,min}}$	Vector of minimum values for discharge pressure of CS "i"
$P_{d,j}$	Discharge pressure of compressor station "j"
$\mathbf{P_{d,j}}$	Predicted discharge pressures for compressor station "j"
P_f	Power consumption of gas turbine drive
P_M	Measured pipeline pressure
P_p	Compressor power consumption
P_s	Suction (inlet) pressure of a compressor
$\mathbf{P_{S,j}}$	Vector of predicted suction pressures for compressor station "j"
$\mathbf{P_{x,i,min}}$	Vector of minimum values for checkpoint pressure "i"
$\mathbf{P_{X,j}}$	Vector of predicted pressures for checkpoint "j"
$\mathbf{\hat{P}}(t)$	Vector of estimated pipeline pressures at time t
q	Mass flow rate of gas (kg/s)
$\mathbf{Q,Q_1,Q_2}$	Matrix in a quadratic cost function
q^{-1}	Backward shift operator
q_{12}	Gas mass flow in a pipeline segment
Q_{i0}	A set of values defining, when model change variable δ_i has a value of one
q_{VOL}	Volumetric flow rate of gas (m3/s) in specified conditions
R	Universal gas constant
r	The length of the state vector of a system model
$\mathbf{S}$	Step response matrix
$\mathbf{S_0}$	Matrix for converting incremental inputs to absolute inputs
$\mathbf{S_{00}}$	Block diagonal matrix containing $\mathbf{S_0}$–matrices
$\mathbf{S_1}$	Step response matrix for input increment values in one time point only

$\mathbf{S^1}$	Step response matrix containing step responses for a primary model
$\mathbf{S^{12}}$	Step response matrix containing mixed dynamics from step response matrices $\mathbf{S^1}$ and $\mathbf{S^2}$
$\mathbf{S^2}$	Step response matrix containing step responses for a secondary model
$\mathbf{S_{ij}}$	Sub-matrix for output "i" and input "j" of a step response matrix $\mathbf{S}$
$\mathbf{S^F}$	Step response matrix for all compressor station gas flow responses
$\mathbf{S^P}$	Step response matrix for all compressor station suction pressure responses
$\mathbf{S_i^{P,R}}$	Step response matrix containing zeroed columns (rest response matrix)
$\mathbf{S^X}$	Step response matrix for all checkpoint pressure responses
T	Temperature of gas
t	Time, continuous or discrete
$\mathbf{T}$	Output matrix of a non-minimal system model
$\mathbf{T_M}$	Matrix of time constants for a model change
T_M	Time constant for model change
T_s	Gas temperature at the compressor suction point
ΔT	Sampling time;Optimisation interval;Control interval
u	Scalar input of a linear, discrete-time system
$\mathbf{u}$	System input vector; Decision variable vector
$\tilde{\mathbf{u}}(k)$	Vector of all system input values over the prediction or control horizon
$\mathbf{\Delta u_j}(k)$	Input variable "j" increments over the whole control horizon
$\mathbf{\Delta \tilde{u}}(k)$	Vector of all system input increment values over the prediction or control horizon
v(k)	Prediction error at time k
v_i	Binary variable for compressor station "i" indicating, when station is started up
$\mathbf{v_i}$	Vector of non-measured disturbances of a system, i=1,..4
$\mathbf{V_j}(q^{-1})$	Polynomials in q^{-1}used in prediction model; j=1,2,..,P
w	Gas velocity; shut down/start up command variable for compressor station
$\mathbf{w}$	Vector of shut down/start up command variables for compressor stations
W_f	Energy consumption of gas turbine drive
W_p	Energy consumption of a compressor
x	Length co-ordinate along a pipeline segment
$\mathbf{x}$	State vector of a discrete-time system
$\mathbf{X}$	State vector of a non-minimal system model; Decision variable vector of a Mixed Integer Quadratic Programming problem
$\hat{\mathbf{x}}(k \mid k-1)$	State estimate vector of a linear, discrete-time system
$\mathbf{y}$	Output vector of a system
y	Scalar output of a linear, discrete-time system
$\hat{\mathbf{Y}}(k)$	Vector of predicted system outputs
$\hat{y}(k+j \mid k)$	Predicted value of system output at time k+j calculated at time k
z	Gas compressibility
$\mathbf{z}$	Auxiliary variable of a Mixed Logical Dynamic system
$\mathbf{Z_0}(k)$	Free response prediction vector containing all system variables
$\mathbf{Z_{0,i}}(k)$	Free response prediction vector for system variable "i" only
$z_{0,i}(k+j)$	Free response prediction value for variable "i" at time point k+j
$\mathbf{z_i}$	Auxiliary variable "i" of a Mixed Logical Dynamic system
z_s	Compressibility at compressor suction conditions
α	Model change coefficient
δ_i	Discrete model change variable in a Mixed Logical Dynamic system

δ	Discrete input variable vector in a general Mixed Logical Dynamic system
Δ	Difference operator, $\Delta = 1 - q^{-1}$
ε	Residual error term in prediction model
γ	Pressure ratio exponent in the head expression for a compressor
η_o	Overall compressor efficiency
η_p	Polytropic compressor efficiency
θ	Angle between a pipeline segment and the horizontal direction (x)
ρ	Gas density

List of Abbreviations

bcm	Billion cubic meters (billion m^3)
CPU	Central Processing Unit (of a computer)
CS	Compressor station
CV	Controlled Variable
DP	Dynamic Programming
EKF	Extended Kalman Filter
GA	Genetic algorithm
GPC	Generalised Predictive Control
LMPC	Linear Multivariable Predictive Control
LNG	Liquefied natural gas
LP	Linear programming
MILP	Mixed integer linear programming
MIMO	Multiple Input, Multiple Output
MINLP	Mixed Integer Non-linear Programming
MIP	Mixed integer programming
MIQP	Mixed Integer Quadratic Programming
MLD	Mixed Logical Dynamical
MPC	Multivariable Predictive Control
MV	Manipulated Variable
PC	Pressure controller or Personal Computer
QP	Quadratic Programming
SA	Simulated Annealing
SCADA	Supervisory control and data acquisition
SISO	Single Input, Single Output
SLP	Sequential linear programming
SQP	Sequential Quadratic Programming

Chapter 1

Introduction

1.1 Motivations and background

Natural gas pipeline networks, or *pipeline systems*, are used to transport gas from sources to consumers over long distances. The consumption of natural gas has grown steadily over the past few decades as it is a clean and easy-to-use fuel in energy production and an important raw material for the chemical industry. Consumption has increased partly because old, existing gas reserves are being exhausted within a foreseeable time frame and partly because new geographical regions (with few or no own reserves) are increasing their usage of natural gas. This increase also implies an increase in the transport of gas.

The pipeline network owners and operators have always been faced with the challenge of obtaining sufficient information to support their operations and it has always been their responsibility to transport the gas in a safe and secure manner, fulfilling what has been agreed with gas consumers directly or with external parties providing gas trading services. In the early days, long-term contracts were used and the pipeline system operation remained quite stationary. Seasonal variations in natural gas consumption could, in many cases, be approximated by constant consumption over months or weeks, yielding approximate numbers still enabling an adequate analysis based on steady-state calculations. Steady-state optimisation was also used (and still is) to calculate optimal settings for operating the compressor stations in the pipeline system. Operating a wide pipeline system with large gas throughput requires a lot of compression and consequently, a large amount of energy, which accounts for a significant portion of operating costs.

Over time, customers became increasingly demanding in that they discovered the benefit of short-term contracts and spot markets. This development was supported by government actions: the authorities in both the US and the European Union passed legislation stipulating a free market in natural gas. The free market allows both owners of gas resources and gas customers to select a pipeline system for today's or tomorrow's gas transport. Also the electricity market has been opened up. Short-term electricity trading has led to the use of high-power natural gas fired gas turbine power plants, which may be switched on or off very quickly without prior notice. Based on these factors, we might conclude that the good old days of almost steady-state operation are gone forever, to be replaced with dynamic and rapidly changing pipeline system operations.

One aspect of the challenge facing pipeline system operators in this new dynamic context is to fully utilise their system transportation capacity today, tomorrow, next month and further into the future. They must try to sell any "holes" in their pipeline systems' utilisation profile to avoid operating under capacity. In the new market context, operators need a *dynamic simulator* of the pipeline system for that purpose. Whereas, in the early days, the pipeline system owner used

steady-state optimisation to calculate optimal compressor station settings, this is now more or less outdated and must be replaced by *dynamic optimisation* tools.

The literature on dynamic simulation, steady-state optimisation and dynamic optimisation (*transient optimisation* is frequently used for the latter term) uses the conservation and energy equations of a pipeline system, which are partial differential equations with respect to time and one space co-ordinate, as a basis. Especially dynamic models become very complex if a large and complex pipeline system is considered. If those models are used within an optimisation algorithm, where optimal profiles (functions of time) of important variables concerning compressor station operations are to be calculated, there is very little possibility for convergence to an optimal solution, not to mention in real time.

Very few authors have considered the practical point of view of an industrial control engineer: look at the pipeline system as any process ("we have done this before"), make the necessary approximations, utilise the special structure of the target system, develop and test the method and finally implement it, although some theoretical considerations suggest that "this will probably not work".

The term "pipeline system" will in this work frequently be used instead of "pipeline network" to underline the fact that a system may contain more components, such as control systems, than a network. Also, the word "system" offers a higher degree of abstraction that some parts of this work may need.

1.2 Outline of the thesis

The thesis describes the development of a simplified real-time, receding horizon optimiser for natural gas pipeline systems. It has been run in a simulation environment test bench using the Finnish natural gas pipeline system as the target system. The method developed is based on using linear system models to calculate the optimal values of the decision variables, while the contribution of past values of decision variables as well as past, present and future values of known and predicted disturbances are obtained using a simulation model of the pipeline system. The decision variables are discharge pressures of the compressor stations and the method was extended to allow discrete decision variables, which are the shutdown/start-up command switches of the compressor stations.

Chapter 2 gives a general description of natural gas pipeline systems and some system components. The Finnish natural gas pipeline system is also described.

Chapter 3 contains a brief description of dynamic as well as steady-state models used for pipelines and compressors. These models, or parts of them, are necessary for the optimisation method developed in later chapters. This chapter also includes the results of searching the available literature on the subject of optimum operation of natural gas pipeline systems. The tradition of operations based on modelling knowledge can be said to have started in 1961. Simplified, ad-hoc, rule-based operations support tools have been used and full-blown expert systems have also been developed. Whereas steady-state optimisation is rather extensively studied in the literature, dynamic optimisation studies are rare. Advanced (model-based) control is reported for a few cases, which are actually not natural gas pipeline systems.

Chapter 4 presents the different pressure and gas flow rate responses when compressor stations are operated under discharge pressure control. In a separate appendix (Appendix A), the simulated step responses in three different operating points of the Finnish natural gas pipeline system are presented. From those responses, linear transfer function models are identified, part of which are presented in Appendix B. A simple formula for the gain of a linear transfer function for a pipeline segment is presented. Data from the Finnish pipeline system is presented together with simulated data in the same conditions showing that the simulator reproduces the actual system very well. The "linearity assumption" of the pipeline system is further strengthened by showing that the shut down transient of a compressor station may be constructed using a linear model.

Chapter 5 starts with a definition of a general, non-linear receding horizon optimisation problem, followed by a short review of the literature on receding horizon optimisation problems and a review of linear optimal predictors. The chapter presents the prediction equation, which consists of two parts. The part independent of optimal decision variables, the free response prediction, is obtained from a simulation cycle of the pipeline system simulator and is of particular interest. The energy consumption of the compressor stations, which is a non-linear expression, is approximated by quadratic functions, which, combined with linear system models and linear constraints, gives a quadratic programming (QP) problem to be solved at each cycle of the optimiser. The accuracy of the quadratic cost function approximations is tested by performing a series of steady-state optimisation runs. Results of several test runs of the receding horizon optimiser in a simulator test bench are presented at the end of the chapter.

Appendix C describes the software programs required to combine the commercial pipeline simulator with the receding horizon optimiser. Appendix D lists the details and parameters of the Finnish natural gas pipeline system needed by the optimiser.

Chapter 6 starts with a derivation of the "equation constraint" required in the optimiser to describe compressor stations in shut down mode. Then, the problem of using only one single free response prediction, disregarding the possibility that compressor station shutdowns or start-ups may occur, is discussed. The receding horizon optimisation problem containing discrete decision variables is formulated as a Mixed Logical Dynamical (MLD) problem, but the final optimiser is presented as a procedure executing a defined series of QP optimisations, instead of one large Mixed Integer Quadratic Programming (MIQP) problem. Step response models are used in the QP-based optimiser, but step response models as a basis for MLD systems are also discussed. Results of several test runs using the simulator test bench are presented.

Chapter 7 contains the conclusions and subjects for further research.

1.3 Contributions of the thesis

The approach taken towards solving the problem of minimising the energy used by the compressor stations of a pipeline system while varying gas consumption acts on the system, is a practical one. The target has been to show that linearity assumptions lead to a simple and comprehensive solution, with good prospects for practical application.

On a case basis, a linearity assumption, or at least a mild non-linearity assumption, regarding natural gas pipeline systems holds, which is shown in Chapter 4. This is true even for the

"drastic" event of shutting down a compressor station from high discharge pressure. The mild non-linearity of the shutdown event has not been presented in the literature.

A very simple gain formula for the pressure of a pipeline segment is derived in Chapter 4.

In this work, the free response prediction necessary in the prediction equation is obtained from a dynamic simulator of the pipeline system. The idea is not new and unique, but large-scale industrial applications like the one presented in this thesis have seemingly not been reported.

The approximate quadratic cost function, linear system models and linearised compressor envelope constraints enable a QP solver to be used within the receding horizon optimiser. The approximate quadratic cost function contains some error, as shown in Chapter 5, but while the optimal solutions are usually heavily constrained, the degree of sub-optimality is not large. When compared with the actual pipeline system operating data, the optimiser results reveal that energy consumption savings of 5 to 8% can be achieved.

In order to further verify the capability of the developed optimiser, an energy maximisation case was also simulated, where the energy consumption was 17.5% greater than in the corresponding minimum energy case. Conclusively, the optimiser is capable of providing solutions over a large part of the solution space.

Mixed Linear Dynamical (MLD) systems are based on discrete-time, linear state-space models. Step response matrix models in model predictive control and optimisation can be expressed through a non-minimal discrete-time, linear state-space model. If this non-minimal state-space model is used as a basis for an MLD system, then model changes implemented in the prediction horizon do not produce results equivalent with MLD systems based on (minimal) state-space models. This result, and the use of step response models with MLD systems have not been reported in the literature. If the mixed dynamics, which the non-minimal state-space model does not provide, is necessary, then this can be approximately implemented with an ad-hoc model change method.

Chapter 2

Natural gas pipeline systems

Pipelines are used to transport fluids in large quantities over long distances. In addition, small-scale local pipelines designed for specific purposes exist, for example dedicated pipelines serving an industrial area. Pipelines are used mainly to transport crude oil and natural gas; however, different oil products are also transported. Gas pipelines are also used for nitrogen, oxygen, pressurised air and gases used by the petrochemical industry such as ethane, propane and others. Multiphase pipelines are used increasingly, where liquid and gas phases co-exist in the same pipeline.

A pipeline system consists of pipelines and other components, such as liquid and gas storages, pump and compressor stations, as well as equipment needed for the operations.

2.1 Natural gas

According to the BP Statistical Review of World Energy (2004), the proved reserves of natural gas world-wide totalled 175.78 trillion cubic metres at the end of 2003. The global reserves-to-production ratio, which is equal to how many years the reserves would cover production, is 67.1 years. Of the proved reserves, 40.8% are located in the Middle East, 35.4% in Europe and Eurasia and 4.2% in North America. The North American reserves-to-production ratio in particular, which stands at 9.5, indicates that imports of natural gas must increase in order not to exhaust own reserves within a short time.

The individual area with the second largest reserves-to-production ratio, 81.2 years is the Russian Federation. Russia supplies 30% of the European total natural gas demand.

On a world-wide and annual basis, consumption of natural gas equals production, while storage facilities play a minor role compared to the volumes discussed.

Global consumption of natural gas grew by 2 % in 2003, which is less than the annual growth experienced in previous years. In the US, which is the largest natural gas market, consumption fell by 5 %, while imports of natural gas to the US increased to 16% of total consumption (Imam et al., 2004).

Total consumption of natural gas world-wide was 2618 billion cubic metres (bcm). Of this amount 454.9 bcm were trade movements over national borders through pipelines and 168.8 bcm were through liquefied natural gas (LNG) transports, usually using dedicated LNG tanker ships.

Natural gas consists mostly of methane (CH_4), which makes it a clean fuel. Table 2.1 gives the composition of some selected natural gases (Finnish Natural Gas Association, 2004).

	Russia, Urengoi	Germany, Goldenstedt	USA, Kansas	The Netherlands, Groningen	Norway, Troll
Methane, CH_4	98 %	88 %	84.1 %	81.3 %	93.2 %
Ethane, C_2H_6	0.8 %	1.0 %	6.7 %	2.8 %	3.7 %
Propane, C_3H_8	0.2 %	0.2 %	0.3 %	0.4 %	0.4 %
Butane, C_4H_{10}	0.02 %	-	-	0.4 %	0.5 %
Nitrogen, N_2	0.9 %	10.0 %	8.4 %	14.3 %	1.6 %
Carbon dioxide, CO_2	0.1 %	0.8 %	0.8 %	0.9 %	0.6 %

Table 2.1 Examples of composition (in mol-%) of some types of natural gas.


2.2 Pipeline system overview

A natural gas pipeline system transports natural gas from sources (or supplies) to users through a system of interconnected pipes or pipeline segments. The distance from a source to a user may be thousands of kilometres. The gas in the pipeline is pressurised in order to maintain a pressure difference necessary for moving the gas. *Compressors* are used to pressurise the gas. These are needed at regular intervals along the pipeline– usually every 50 to 150 kilometres, since the gas pressure decreases rapidly due to frictional losses. The most elementary components of a pipeline system are the pipeline segments and the compressors. In many cases one compressor is not sufficient to increase the pressure in the pipeline. In this case several compressors (or compressor units) are grouped to form compressor stations. Other pipeline system components are valves (discrete or continuously operating) and gas storages. Long-distance transmission pipelines operate under high pressures and gas users at the off-takes use *pressure reduction stations* to adapt the gas pressure to their needs. *Blending stations* are used for mixing gas from different sources having different characteristics. A typical task for a blending station is to regulate the heating value to a desired level. In some cases nitrogen is added at blending stations to dilute the gas (Hoeven and Fournier, 1995).

In many cases, a pipeline system may be very complicated having multiple gas sources and multiple off-takes as well as a complex looped or nested loop structure. An example of a principal diagram of a pipeline system is shown in figure 2.1. Pipeline systems are usually classified as *transmission* systems or *distribution* systems. Transmission systems move gas in large quantities over long distances with few or no major supplies or off-takes between the end points of the pipeline. Often this kind of system is referred to as a *gunbarrel* system. Distribution systems have a large number of off-takes and may be significantly branched. However, many pipeline systems are combinations of transmission and distribution systems. The Finnish gas pipeline system is a typical representative of a combined system.
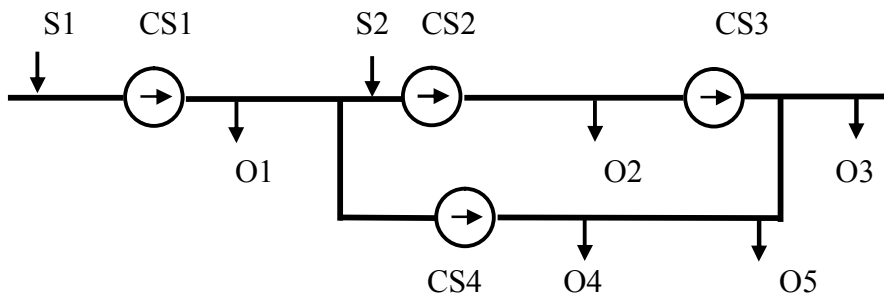
Figure 2.1 Pipeline system with 4 compressor stations (CS1,…,CS4), two gas sources (S1,S2), 5 off-takes (O1,…,O5) and one loop.

Compressor stations with multiple compressors can be arranged in different ways. Figure 2.2 shows alternatives for arranging three units.
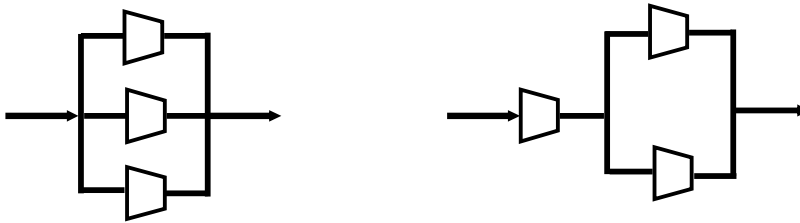
Figure 2.2 Compressor station with 3 parallel units (left) and a series-parallel configuration (right)

Discrete (or "on/off") valves are used to block sections of pipelines and to select paths for the gas to flow through. An example is shown in figure 2.3, where discrete valves (on the left) are used to connect or disconnect pipes belonging to the same parallel pipeline system. The multiple valves at the compressor station to the right are used to select which units are used for the compression and how to distribute the gas between the four outgoing parallel pipes.
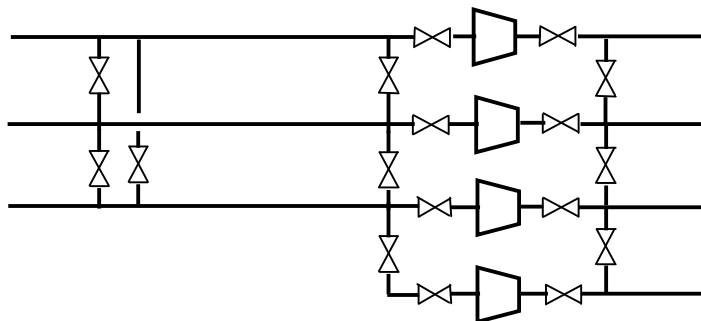
Figure 2.3 An example of a pipeline system with parallel pipes. The number of parallel pipes changes from 3 to 4 at the compressor station.

Two main types of compressor units are *reciprocating* compressors and *centrifugal* compressors, of which the latter is more popular. The compressors are usually driven by gas turbines taking their fuel directly from the pipeline; however, electrical drives are increasingly common. Compressor stations usually have local control systems accepting external *set points* for either discharge pressure, suction pressure or gas throughput flow and *commands* for selecting the running units (start-up and shutdown commands). Such set points and commands may be received from higher-level control or optimisation systems. The local control systems include co-ordinating control of the individual compressor units within the station, such as load balancing and total efficiency maximisation. The local control system also takes care of equipment safety, of which the most important is *surge avoidance*. A compressor surges when the gas flow through it becomes too small. Surge is avoided by circulating gas from the discharge to the suction side by opening a bypass valve in a circulation line. Gas coolers are usually installed downstream each compressor unit, because of gas temperature increase in the compression. The circulation line starts after the gas cooler, otherwise gas circulation would elevate the gas temperature and possibly lead to compressor damage.

Continuously operating control valves may be important components of the pipeline system depending on how the system is operated. A local pressure controller may control either the discharge or the suction pressure. See figure 2.4 for an example of control options.
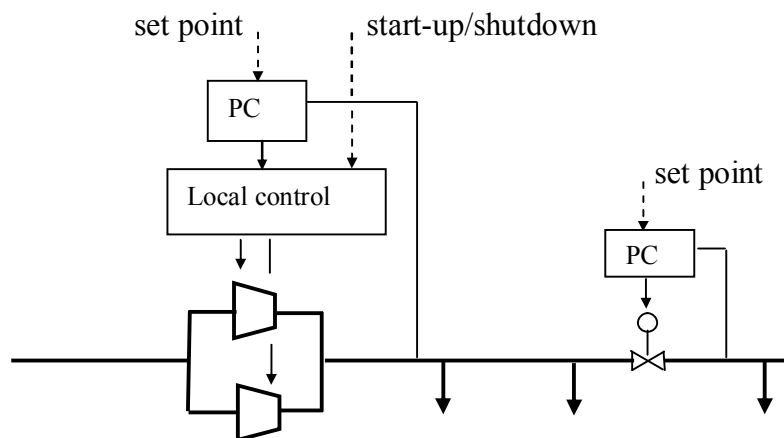
Figure 2.4 Pressure controllers (PC) control the discharge pressure of a compressor station and the discharge pressure of a control valve. Unit selection, or start-up/shut down commands, are received by the local station control system. Dashed arrows indicate external set points and commands.

2.3 Operating a pipeline system: an increasing challenge

From Monitor and Control to Advanced Business Operations

The gas pipeline system is monitored and controlled through a Supervisory Control and Data Acquisition System (SCADA) by human *operators*. If operators are given increased responsibility for managing the gas flow, they can be called *dispatchers* or *gas controllers*. The main part of their job is to keep the pipeline system within physical and contractual limits, in order words, to ensure *feasible operation*, which is not a trivial task. If there is additional time and motivation, they may try to *optimise* the operation of the system in some sense. According

to the literature, minimisation of energy used at the compressor stations is one of the most important optimisation objectives.

Revell and Thorne (1998) describe the liberalisation of the natural gas market in the UK. The owner of the national gas transmission system is obliged to provide third-party access to the system. This means that any natural gas trader may sell gas directly to customers, buying the gas transport service from the system owner, who is responsible for ensuring safe and secure operation of the system, as well as fair and consistent treatment of all system users. Moreover, the system must be balanced so, that the total amount of supplied gas is equal to the total amount of consumed gas over a given time interval, which is usually one day.

Market deregulation in the US has also resulted in an open-access natural gas transportation market allowing customers to choose the lowest cost pipeline services, which in turn forces pipeline owners to reduce their operational costs (Brown and Chui, 1996).

Schoder and Brandt (1999) list new natural gas market requirements such as the increasing number of short-term and spot market deliveries as well as increased trading as motives for improving the tools needed for pipeline system information management. These requirements on a complex pipeline system with a large number of supplies and a number of storage facilities make overall management a challenging task. Communication technology, both data communication within the pipeline owner's organisation as well as data interchange with gas suppliers and customers, is stated to be the most important area to develop and maintain. Once successful communications systems have been implemented, further development of advanced tools like simulation and optimisation can be undertaken.

Flexibility requirements have led to increasingly non-steady-state operation. The newer, high-power gas turbine driven power plants cause large gas consumption variations. The increasing use of electrical drives for compressors connects the natural gas and electrical energy markets. "Park and Ride" services are developed where customers may leave purchased gas un-consumed and consume it later or vice versa. It is not possible to manage such services efficiently without dynamic modelling and simulation tools (Bryant and Varo'n, 2002).

Natural Gas Consumption Forecasts

Reliable and accurate natural gas consumption forecasts for shorter (such as 24 hours) or longer (such as 6 months) periods form the basis for any advance planning or predictive optimal operations. Typically, historical consumption data is used together with other inputs, which are also forecasts: for example, the weather (temperature, rainfall, cloud cover etc.) and the price of energy (natural gas, electricity, coal). Regression, time series or neural network models can be used to process the forecaster inputs to produce the gas consumption forecasts (Piggott, 2003). The various models may also operate on the same input data in parallel and a combined forecast can be formed as a weighted sum of the outputs of the individual models. If there is a danger of too much input data, which may cause over-modelling and consequently performance degradation, genetic algorithms (GA) may be used to create an optimum selection of input data (Piggott et al., 2000). In general, generating good forecasts for natural gas consumption is far from easy, either in the short- or long-term. Most probably, this task will become even more difficult with the global increase in unforeseeable, short-term "spot market" activity in natural gas pipeline systems. It is even more difficult to obtain good forecasts for supply flows and also the achievable off-take flow forecast accuracy falls in the range of 5 to 10% relative error (Shaw et al., 1997).

2.4 The Finnish natural gas pipeline system

The Finnish natural gas pipeline system consists of 1000 km of transmission pipeline and 1440 km of distribution pipelines. There is a single supply point on the border between Russia and Finland. Three compressor stations are installed. The gas entering the Finnish system originates from the largest single natural gas fields in the world, the Urengoi and Jamburg fields in Siberia, 3500 km east of Finland. The gas is very clean, with a methane content of 98% (See table 2.1) and a nitrogen content of only 0.9%. The first 30 km of pipeline became operational in 1974 to service the industry in Eastern Finland. Since then there has been a steady increase in the pipeline system and the number of gas customers. In the period 1974 to end-2003, the total cumulated natural gas consumption stood at 65.1 bcm.

The total number of off-takes in the pipeline system currently stands at 194 while the total number of customers is 35780, including the smallest ones, which are domestic users. The total gas consumption in 2003 was 4.7 bcm.

The distribution of natural gas consumption in Finland for 2003 is shown in table 2.2 (Finnish Natural Gas Association, 2004):

Type of consumption		Share
Heating: residential, commercial greenhouses		1.7 %
District heating		5.7 %
Combined district heat and power		39.5 %
Condensing power		8.8 %
Industrial co-generation		29.0 %
Steam boilers	2.5 %	
Direct processes	10.8 %	
Non-energy use	1.1 %	
Space heating	0.8 %	
Industrial other use	15.2 % →	15.2 %
Natural gas vehicles		0.1 %
Total		100 %

Table 2.2 Natural gas consumption in Finland 2003

The Finnish natural gas pipeline system is supplied by a parallel pipeline (see figure 2.5) at the Finnish – Russian border. From the border, the pipeline continues as a parallel line (700 and 900 mm pipe diameter) for a distance of approximately 100 km. The pipeline system is very branched and it has a "passive" (no compressor stations involved) loop in the northern part in the Tampere area. The system has three compressor stations located at Imatra, Valkeala and Mäntsälä with a total installed compression power of 63 MW and the total number of compressor units is 9. The stations are usually run under discharge pressure control (see figure 2.4). The whole pipeline system, including the compressor stations, is equipped with modern instrumentation and the pipeline data needed for operating and decision making is collected by the SCADA system located in the main control centre in Valkeala.

The pipeline system is owned and operated by Gasum Oy, of which the Finnish state has a 24% share. While the Finnish pipeline system has only one supply point, Finland may derogate from the EU directive concerning open natural gas markets until the Finnish pipeline system is connected to some other EU country's system. However, the Gas Exchange ("Kaasupörssi Oy") providing Internet-based second-hand gas trading services has been in operation since 2001.

Figure 2.5 The Finnish natural gas pipeline transmission system.

Chapter 3

Modelling, control and optimisation of natural gas pipeline systems

3.1 Dynamic and steady-state pipeline models

Non-stationary, isothermal gas flow in a pipeline segment may be modelled by a system of partial differential and algebraic equations as follows (Osiadacz, 1996; Osiadacz and Chaczykowski, 2001):

$$\frac{\partial P}{\partial x} + \frac{2f\rho w^2}{D} + \rho g \sin(\theta) + \frac{\partial(\rho w^2)}{\partial x} + \frac{\partial(\rho w)}{\partial t} = 0 \qquad (3.1)$$

$$\frac{\partial P}{\partial t} + \frac{P}{\rho^2}\frac{\partial(\rho w)}{\partial x} = 0 \qquad (3.2)$$

$$P = \frac{zRT}{M_w}\rho \qquad (3.3)$$

$$z = f_z(P, T) \qquad (3.4)$$

where

x	is the length along the pipeline segment
t	is the time
P	is the pressure
g	is the acceleration of gravity
ρ	is the density of the gas
θ	is the angle between the pipeline segment and the horizontal direction (x)
f	is the Fanning friction factor
D	is the inside diameter of the pipe
A	is the cross-sectional area of the pipe
q	is the mass flow rate
w	is the gas velocity
z	is the gas compressibility
R	is the universal gas constant
T	is the temperature of the gas
M_w	is the molecular weight of the gas
f_z	is the compressibility as a function of pressure and temperature.

The first equation above describes conservation of momentum and the second one is the mass balance equation or continuity equation. The third equation is the state equation for natural gas

and the last one is the expression for gas compressibility, for which a common choice is $z = 1 + k_{z1}P + k_{z2}\dfrac{P}{T}$, where k_{z1} and k_{z2} are constants (Kra'lik et al., 1984 A).

The mass flow rate in the pipe can be calculated from the expression:

$$q = \rho w A \qquad (3.5)$$

Using this expression, the equations can also be written for pressure and mass flow, instead of pressure and density.

For non-isothermal flow in a pipeline segment, the energy equation has to be added to the system of equations. Osiadacz and Chaczykowski (2001) use the following basic form:

$$Q\rho A dx = \frac{\partial}{\partial t}\left[\rho A dx\left(c_v T + \frac{w^2}{2} + gh\right)\right] + \frac{\partial}{\partial x}\left[\rho w A dx\left(c_v T + \frac{P}{\rho} + \frac{w^2}{2} + gh\right)\right] \qquad (3.6)$$

where
Q   is the heat addition to the gas per unit time and per unit mass of gas
c_v is the specific heat of the gas at constant volume
h   is the elevation of the pipe

It is not usually possible to use this basic form as such. A simpler, more practical form of the energy equation is obtained for horizontal pipes (h=0) and neglecting the term $\dfrac{\partial}{\partial x}\left[\left(\rho w A dx\right)\dfrac{w^2}{2}\right]$ from the right hand side of (3.6).

A pipeline system typically contains multiple segments. Each segment requires its own set of equations. A new segment has to be defined each time a compressor station (hereafter abbreviated CS), off-take, junction or branch disturbs the gas flow or when the angle θ, friction factor f or pipe diameter D changes. The value of the friction factor depends on the smoothness of the inside surface of the pipe and on the assumptions on the gas flow conditions (laminar or turbulent), (Schroeder, 2001).

The set of pipeline system equations may be solved numerically for pressure $P(x,t)$ and gas flow $q(x,t)$ given suitable initial and boundary values. Typical boundary values are a given initial pressure profile $P(x, t_0)$ at the initial time $t=t_0$ for all points x of the pipeline system and given mass flows $q(x_i,t)$, where the x_i's are the co-ordinates for supplies and off-takes. From a modelling perspective each CS is a "supply" for the next downstream pipeline segment.

Each pipeline segment has it's own pressure profile $P(x,t)$ and flow profile $q(x,t)$. Segment profiles can be combined to form pipeline system profiles. Figure 3.1 illustrates an example pressure profile for a serial pipeline system with three CSs.

P(x, t₀)
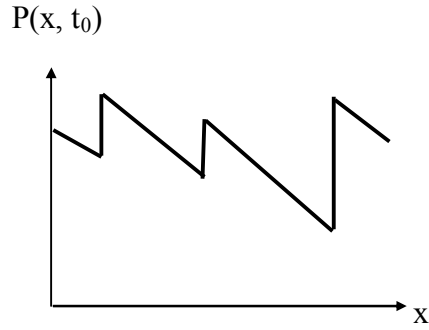
Figure 3.1 Pressure profile for a serial pipeline system with three CSs, which generate positive steps in the profile

The basic dynamic pipeline segment model (3.1 to 3.4) may be adapted for different purposes. The full model presented above is valid for a broad range of gas flow conditions, including high-velocity situations such as pipe rupture. If the gas velocity w can be assumed to be small, then the term $\frac{\partial}{\partial x}(\rho w^2)$ may be neglected. Other simplification possibilities are to assume horizontal pipelines only or to simplify the model down to a diffusion equation model (Osiadacz, 1998) only. It is rather common to assume isothermal conditions, in which case the energy equation (3.6) may be neglected.

In steady state, for a horizontal isothermal pipeline segment with the pressures at the beginning and at the end of the segment, P_1 and P_2 respectively, and gas mass flow q_{12} are related through the equation (Furey, 1993):

$$P_1^2 - P_2^2 = k_{12}z_{12}q_{12}\left|q_{12}\right|^{0.8539} \tag{3.7}$$

where k_{12} is a constant and z_{12} is the average compressibility of the gas in the segment. The exponent 0.8539 can be approximated by the value of 1 (Schroeder, 2001). If the elevation of the pipeline segment is essential, then the following expression yields:

$$P_1^2 - P_2^2 - \frac{k_{12}^{'}g(h_2 - h_1)P_{12}^2}{z_{12}T_{12}} = k_{12}z_{12}q_{12}\left|q_{12}\right|^{0.8539} \tag{3.8}$$

where
$k_{12}^{'}$ is a constant
h_2 is the elevation of the end of the pipeline segment above some basic level
h_1 is the elevation of the beginning of the segment above some basic level
T_{12} is the average gas temperature of the segment

The average pressure P_{12} in the segment is calculated using the expression:

$$P_{12} = \frac{2}{3}\left(P_1 + P_2 - \frac{P_1 P_2}{P_1 + P_2}\right) \tag{3.9}$$

15

In case of non-isothermal steady-state flow, the right hand side of (3.7) or (3.8) is modified so, that k_{12} is actually a function of ambient (or soil) temperature and segment start and end temperatures (Osiadacz and Chaczykowski, 2001).

The properties of natural gas depend on the gas source; consequently, the molecular weight and compressibility of the gas vary with the source. If a pipeline system involves multiple gas sources, mixing rules for molecular weight and compressibility have to be applied, while these influence the flow distribution in the pipeline system. It may also be important to include *property propagation* equations for properties, which do not influence the flow distribution, such as heating value, ownership of gas and gas price. These properties may be calculated by weighted average formulas once the gas flows of the system have been solved (Hoeven and Fournier, 1995; Graham et al., 1996).

The gas content in mass units of a given pipeline segment is defined as the line pack. This is considered to be a very important variable in gas pipeline system operations (Rachford and Carter, 2000; Pietsch et al. 2001; Bryant and Varo'n, 2002, among others). Assuming a constant average temperature, T_{12}, and a constant average compressibility, z_{12}, along the segment, the following general expression for line pack applies when the equation of state (3.3) is applied for each infinitesimal volume element $A dx$ of the segment:

$$m(t) = \frac{M_w}{RT_{12}z_{12}} A \int_{x_1}^{x_2} P(x,t)dx \qquad (3.10)$$

3.2 Compressor models

The active components of a pipeline system are the compressors, which add potential energy to the gas flow by increasing the pressure. The adiabatic head H_a is the energy content increase (kJ/kg) of the gas when it flows through a compressor (Sandler and Luckiewicz, 1987; Coker, 1994):

$$H_a = \frac{z_s RT_s}{\gamma M_w}\left[\left(\frac{P_d}{P_s}\right)^{\gamma} - 1\right] \qquad (3.11)$$

where
P_d is the discharge (outlet) pressure of the compressor
P_s is the suction (inlet) pressure of the compressor
z_s is the compressibility at compressor suction conditions
T_s is the gas temperature at the suction point
γ is defined as:

$$\gamma = \frac{k_a - 1}{k_a} \qquad (3.12)$$

where k_a is the molar specific heat ratio of the gas assuming adiabatic compression. In an adiabatic compression process no heat is transferred into or out from the compressor. Strictly speaking, this assumption does not hold for practical compressors, even though adiabatic compression is assumed in many cases. If polytropic compression is assumed, the expression for polytropic head is the same as (3.11) but with γ defined as:

16

$$\gamma = \frac{k_n - 1}{k_n} \tag{3.13}$$

where k_n is the exponent of the polytropic process having some value between 1 and k_a. Adiabatic and polytropic compression processes are related through the polytropic efficiency η_p:

$$\eta_p = \frac{\dfrac{k_a - 1}{k_a}}{\dfrac{k_n - 1}{k_n}} \tag{3.14}$$

Theoretically, the power needed to pressurise the gas is obtained by multiplying the head by the mass flow of the gas through the compressor. Practical compressors have losses, which are taken into account by dividing the theoretical power by the overall efficiency of the compressor, which is a function of discharge pressure, suction pressure and gas flow, to obtain the power to be supplied by the compressor drive:

$$P_p = \frac{qH_a}{\eta_o(P_d, P_s, q)} \tag{3.15}$$

Despite the rigid thermodynamic basics of the compressor modelling, the fact that practical compressors differ from ideal theoretical compressors and that the commonly used gas turbine drive makes modelling more complicated has led to the use of experimental models in many compressor modelling cases. The rotational speed, n, of the common shaft of the compressor assembly and the gas turbine drive parameterises the model equations for compressor adiabatic head H_a, compressor efficiency η_o, power consumption of the gas turbine P_f and power output of the gas turbine P_p as follows (Kra'lik, 1993):

$$
\begin{aligned}
H_a &= a_1 + a_2 n + a_3 n^2 + \left(a_4 + a_5 n + a_6 n^2\right)q + \left(a_7 + a_8 n + a_9 n^2\right)q^2 \\
\eta_o &= b_1 + b_2 n + b_3 n^2 + \left(b_4 + b_5 n + b_6 n^2\right)q + \left(b_7 + b_8 n + b_9 n^2\right)q^2 \\
P_f &= c_1 + c_2 P_p + c_3 P_p^2 \\
P_p &= d_1 + d_2 n + d_3 n^2 + \left(d_4 + d_5 n + d_6 n^2\right)T_a + \left(d_7 + d_8 n + d_9 n^2\right)T_a^2
\end{aligned}
\tag{3.16}
$$

where T_a is the ambient temperature and $a_1, a_2, ..., a_9$; $b_1, b_2, ..., b_9$; c_1, c_2, c_3 and $d_1, d_2, ..., d_9$ are constants. The power consumption of the gas turbine (third expression of 3.16) can be considered to be linear in many cases ($c_3 = 0$) (Goslinga et al., 1994; Osiadacz, 1998; Rachford and Carter, 2000 among others).

The energy needed over a given time interval $t_0...t_1$ to pressurise the gas is obtained by integrating the gas turbine power over that time interval. Assuming $c_3 = 0$ yields:

$$W_p = \int_{t_0}^{t_1} \frac{1}{\eta_o(P_d(t), P_s(t), q(t))} \frac{q(t)z_s R T_s}{\gamma M_w}\left[\left(\frac{P_d(t)}{P_s(t)}\right)^\gamma - 1\right]dt \tag{3.17}$$

and

$$W_f = c_1(t_1 - t_0) + c_2 W_p \qquad\qquad (3.18)$$

As mentioned earlier, CSs may contain multiple compressors (compressor units). The expressions above are valid for each compressor. The gas flow distribution between parallel compressors or pressures between serial compressors are not arbitrary: they are determined by the fine structure, such as pipe-work properties of the CS or, by how a local control system (Chapter 2, figure 2.4) controls the individual compressors. A complete mathematical model must obviously contain sub-models of the fine structure as well as local control algorithms.

CSs, which are integrated into a pipeline system model, allow one of three variables: gas flow through the station, discharge pressure or suction pressure to be freely selected while the values of the two others are determined by the pipeline system characteristics. Usually the internal dynamics of CSs is neglected as it is much faster than the surrounding pipeline system dynamics.

Centrifugal compressors are constrained to operate within typical "envelopes" (Wu et al., 2000; Osiadacz, 1998; Marque's and Morari, 1988), which are limited by four functions of compressor head and gas flow. The functions are typically non-linear, compressor-specific and must be obtained experimentally. Typically, volume flow in suction conditions is used with the envelopes. An example of a compressor envelope is presented in figure 3.2. The four functions, which apply for each compressor i, i=1,…, N_C, where N_C is the number of CSs in the system, are:

- Minimum speed line $g_{1,i}(H, q_{VOL}) \leq 0$,
- Choke line $g_{2,i}(H, q_{VOL}) \leq 0$,
- Surge line $g_{3,i}(H, q_{VOL}) \leq 0$ and
- Maximum speed line $g_{4,i}(H, q_{VOL}) \leq 0$
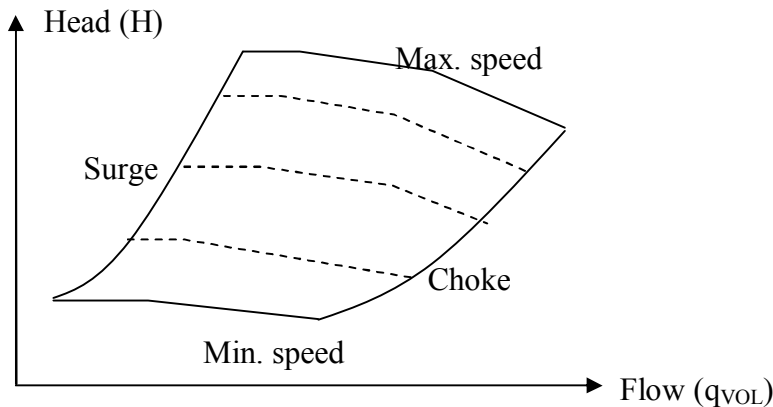
Figure 3.2 A typical compressor envelope

The rotational speed of the compressor shaft parameterises the curves shown in figure 3.2, where constant rotational speed lines are drawn with dashed lines. The working point of a compressor travels around the inside of the envelope without being allowed to violate the envelope limits.

3.3 Improving the performance of natural gas pipeline systems using modelling knowledge

Batey et al. (1961) were one of the first to analyse the dynamics of a gas pipeline system using a partial differential equation model. They obtained an analytical solution to the system of equations in an implicit form. They derived three well-known rules of thumb for minimising energy loss of a pipeline system:
1. Operate the pipeline system at the highest pressure possible
2. Filter the transients as near the load as possible
3. Deliver gas to off-takes at contract pressure and no higher

The rules were further motivated by an elementary analysis of the pipeline:

1. Frictional energy loss in a pipeline segment is proportional to the velocity of the gas, which can be calculated by the expression:

$$w = \frac{q}{k_w D^2 \rho} \qquad (3.19)$$

where k_w is a constant. As the gas density ρ increases, the velocity w decreases and so will the frictional energy loss do. The conclusion is, that gas density is to be maximised (in all pipeline segments, if possible), which is true when the pressure in the segment is as large as possible.

2. A simple calculation shows that the average frictional energy loss with fluctuating gas velocity is greater than with small velocity fluctuations, the conclusion being that the gas velocity (or equivalently, flow) should be as stable as possible. Stable flow cannot be achieved for pipeline segments with off-takes; however, the varying off-take flows of a long-range transmission pipeline system with off-takes only at the other end of the pipeline can be compensated by the CSs near the off-takes, which stabilises the upstream gas flow.

3 . The potential energy of the gas is proportional to the pressure. If the pressure at the off-takes is greater than needed (the minimum delivery pressure is specified by a delivery contract made between the pipeline operator and the customer), then extra potential energy is given to he customer. Avoiding excess pressure saves energy at the CSs, since they do not have to pressurise the gas more than is necessary.

Broadbent and Williams (1990) developed a simplified steady-state optimisation scheme for a pipeline system with two CSs, which essentially builds on steady-state pipe flow (3.7) and adiabatic compressor models (3.11). The optimisation scheme simply calculates a large number of energy consumption values for different combinations of CS discharge pressures and compressor unit selections (two units available per station) and finally lists the 20 most profitable alternatives.

Brown and Chui (1996) discuss a very simple approach to pipeline optimisation for a pipeline system with 5 CSs. The target was to develop a steady-state model "in closed form" without any iterative loops. For each pipeline segment, approximate equations for downstream pressure given the upstream pressure, pipeline flow and temperature were derived based on steady-state simulations and true operational data. The equations are highly accurate despite the fact that the pipeline crosses a mountain-rich area with significant changes in elevation. The optimisation takes place by straightforward search within a large number of feasible operational strategies, the decision variables being CS discharge pressures and compressor unit selections. The strategies with the lowest energy costs are displayed to the operators. Energy savings in excess of US$ 340 000 have been achieved over the first half-year period of use.

Graham et al. (1996) use a dynamic model for a complicated and looped pipeline system, 8000 miles in length and containing 28 CSs. The two main objectives for using the model are state estimation and predictive calculations. The state estimation verifies the correctness of SCADA measurements and calculates values for non-measured process variables. The predictive calculations are performed on an off-line basis, starting from the present state of the pipeline using predicted values of decision variables and off-take flows. The state estimation in particular has proved very beneficial. Instead of investing in expensive flow and pressure metering devices, the calculated values provided by the model can be used.

Shaw et al. (1997) study on-line simulation tools applied to a large pipeline system with more than 9000 miles of pipeline, 74 CSs and a number of gas storages. Pipeline operators cannot apply on-line dynamic simulation as such as everyday working tools, since simulation is very expert intensive. Simulators must be extended with well designed user interfaces for quick and reliable data input, as well as protection against bad data, otherwise they are deemed to be "garbage generators", while small errors in input values may accumulate and lead to disastrous errors in simulation results. Predictive on-line simulation is defined as calculating all relevant pipeline system variables (pressures, flows, temperatures, etc.) from the present moment of time up to a given moment of time in the future, given complete information on present system status and predicted values (forecasts) of off-take and supply flows, as well as decision variables. Decision variable predictions are made based on experience and entered into the simulator by the operators, after which simulation results for up to 5 following days are obtained.

Revell and Thorne (1998) discuss the natural gas transmission system in the UK, which spans a length of 6000 kilometres and contains 21 CSs. On-line simulation is in active and regular use, while steady-state optimisation is used only if constraint conflicts are detected in the on-line simulation runs. The objective of the optimisation is to maximise pressures in the pipeline system.

Wheeler and Whaley (2001) expand the on-line simulation tools of Shaw et al. (1997) to include "Automated Predictive Model Runs". The main objectives of on-line simulation are to decrease compression energy costs, identify unused pipeline system capacity and provide more information to customers. A typical "within day" requirement is set for the operation, this means, that at the end of the day the pipeline system must be restored to a state which enables all operations planned for the next day to be done. Values for the discharge pressures of CSs and compressor unit selections in the predictive simulations are solved using simple rules derived from practical experience, for example: "if all running compressor units at a CS run at more than 90% of maximum power, then start a new compressor unit at this station".

Bryant and Varo'n (2002) use a full dynamic model like Wheeler and Whaley (2001) above for a pipeline system with a total length of 5000 miles and including 22 CSs. The behaviour of the pipeline system is predicted by simulation, given the predicted gas flows at the off-takes. A manual trial-and-error method is used to determine the optimal values for the CS variables and the unit selection. The pipeline operator was able to reduce energy consumption by 12% while increasing the capacity of the pipeline system by 4 %.

3.4 Expert systems

Sandercock (1994) uses an expert system to advise operators of an 800-mile long pipeline system with four CSs on how to operate in order to save energy. This application uses only a knowledge base and an inference engine and does not use dynamic or steady-state pipeline

system models. The content of the knowledge base is built from human experience of operating the pipeline system. Energy savings of 0.5% are reported.

Johnson et al. (2000) apply an expert system together with a dynamic simulator on a pipeline system extending over 15000 miles and including 70 CSs. The expert system performs data validation for the initial and boundary values for the system simulator, which in turn provides simulation results for the expert system for post-processing and preparation of the final operating recommendations. The dynamic simulator was in use long before the expert system, and the routine use of that simulator was seen as a success factor in implementing the integrated solution. The objectives for the combined expert system/dynamic simulator were to reduce energy consumption and to increase gas transportation revenues. Managing line pack was considered important as well. The expert system may operate in an alternative mode making repeated calls to an optimiser which is based on a steady-state model and linear programming (LP). The repeated calls are made to compensate for non-linearities while a linearisation in the current working point is being made at each call.

Uraikul et al. (2000) report a feasibility study on applying an expert system on a pipeline system containing two CSs. The main tasks of the expert system application are to manage line pack, to recommend power input for compressor units and to recommend which units should be running. The expert system uses over 70 rules to conclude whether line pack is high, low or "normal" with respect to the present situation in the pipeline. Conclusions are made based on the same kind of rules used by human operators, i.e. looking at pressure values, rates of changes of pressures and off-take flow values. The predicted line pack behaviour together with pressure and flow conditions in the pipeline generate additional rule-based recommendations on how to run the compressor units.
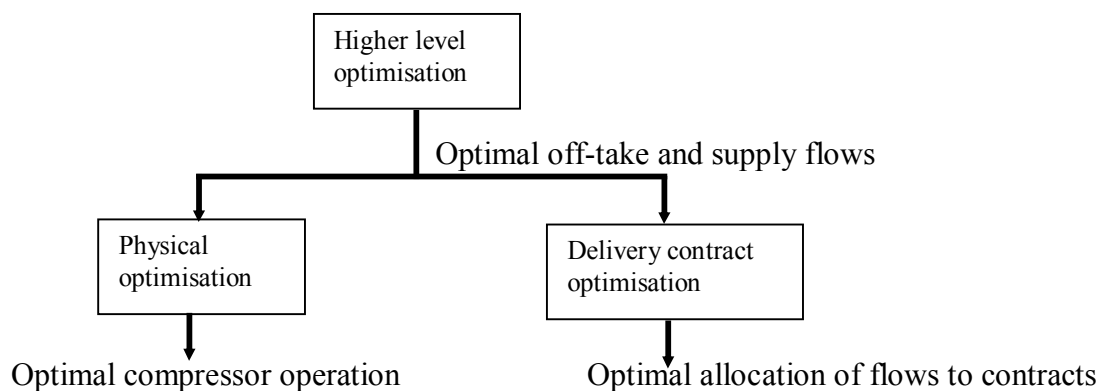
3.5 Steady-state optimisation

Grelli and Gilmour (1986) use a steady-state pipeline system model together with a dynamic programming (DP) algorithm to obtain optimal discharge pressure set points and optimal compressor unit selections for a pipeline system with a length of 719 miles and with 15 CSs. DP is considered to be very well suited to this type of optimisation problem, where compressor unit selections introduce discontinuities in the cost function. Energy saving potential is reported to be 8 to 12%. The steady-state optimisation is manually invoked a few times per day and the optimal discharge pressure and unit selection recommendations are entered manually into the SCADA system. The optimal discharge pressures attain high values at high gas flow rates in the winter, meaning that the results are well in line with the rules of thumb given by Batey et al. (1961). At low gas flow rates in the summertime, optimal discharge pressures are lower.

Luongo et al. (1991) build a hierarchical optimisation method, illustrated in figure 3.3, to perform steady-state optimisation for the physical pipeline system simultaneously with optimising delivery contracts. According to the users' choice, the physical optimisation part can minimise energy, maximise gas throughput or maximise operational profit. At the top of the hierarchy, pipeline system off-take and supply flows are optimised using a dedicated search method. Then, the physical optimisation part at the lower hierarchical level calculates optimal CS pressures (discharge or suction) and compressor unit selections using DP. The delivery contract optimisation, which is based on linear programming (LP), optimally allocates gas flows optimised by the higher level between full delivery contracts and trading contracts. A simple pipeline system optimisation example is demonstrated, but a commercial optimisation

installation is mentioned, expected to deliver energy savings of 19% and an operating profit increase of 15%.

Goslinga et al. (1994) use a repetitive steady-state optimisation method, where non-linear cost function and constraints are linearised in a particular operating point, then an LP-based optimiser provides a feasible and optimal solution for the decision variables. These are then passed to a steady-state pipeline system model, which calculates values for dependent values, after which a linearisation is performed at the new operating point and the LP optimisation is repeated and so on until convergence is obtained. The pipeline system to which the method is applied extends over 12000 miles in length and includes 44 CSs with 102 compressor units as well as 12 control valves. The latter are considered as important elements of the system. It is possible to select energy minimisation, line pack maximisation or throughput maximisation as an objective function for the optimisation.

Optimisation is typically not performed for the whole pipeline system, which is partitioned into smaller sub-systems. Decision variables are discharge or suction pressures of compressor units and pressure ratios of control valves. Compressor unit selection is not a part of the optimisation, but compressor units are shut down during the optimisation cycle in case the heads of the compressor units fall below prescribed minimum limits. Energy savings of up to 18% are reported for a demonstration example of a sub-system containing 17 CSs and 4 control valves.


Figure 3.3 Hierarchical steady-state optimisation of a gas pipeline system

Hoeven and Fournier (1995) discuss steady-state planning problems, where the most important problem to be solved is the feasibility of the solution followed by maximising the pipeline system throughput. The cost function is set up by piecewise linear penalty functions of flow and pressure, where "good" or "preferred" values generate low penalties and non-preferred values generate large ones. An LP problem is set up by linearising a non-linear steady-state model of the pipeline system. The solution of the LP (locally optimal flows and pressures) is sent to the non-linear model, which calculates a new set of variable values to be used iteratively at a new linearisation.

Sekirnjak (1996) describes the development of steady-state optimisation methods applied on the Austrian natural gas pipeline system over many years. The main objective of optimisation is to minimise energy consumption. The steady-state optimisation method of choice is a Sequential Linear Programming (SLP) method. At a given initial solution, linearised expressions for cost function, pipeline pressures and compressor envelopes are obtained, after which an LP is solved.

The optimal solution, such as optimal CS discharge pressures, is supplied to a rigorous steady-state simulator. A new linearisation of the output of the simulator is performed, then a new LP run is performed and so on, until there is a sufficiently small difference between the LP solution and the simulator output (see figure 3.4). The LP can be extended with a mixed integer programming (MIP) part for discrete decision variables like compressor unit selections and pipeline route selections. The linearisation errors of the cost function and compressor envelopes are observed to be very small, which makes convergence of the method easier. Filtering, i.e. weighting of the linearised result with the linearised result from the previous cycle is used to avoid the typical oscillations of LP-based methods.
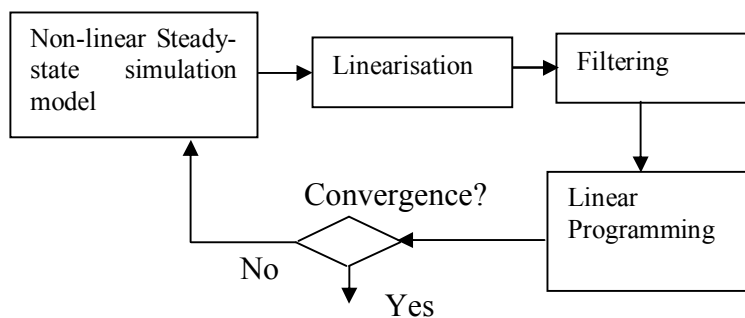
Figure 3.4 A schematic diagram of the iterative SLP method (this figure is adapted from figure 5 in Sekirnjak (1996))

Carter (1996) concentrates on steady-state optimisation inside CSs only. CS energy consumption is minimised by optimising the gas flow distribution through compressor units and by optimally selecting the running units within the station. Four alternative optimisation methods are tested: Mixed Integer Linear Programming (MILP), Mixed Integer Quadratic Programming (MIQP), a heuristic method, where the running unit selection is made by forcing running units to approach their maximum capacity (approximately equal to maximum efficiency) and Mixed Integer Non-linear Programming (MINLP). MINLP and the heuristic method yield better performance than MILP and MIQP because the latter use linear and quadratic approximations of the compressor models.

Carter (1998) discusses DP as a steady-state optimisation tool. From a historical perspective, DP has been successfully applied to gunbarrel pipeline systems, but for branched and/or looped systems, classical DP suffers from long computation times. Therefore, alternative DP formulations, such as different hierarchical approaches, have been developed. The objective of the optimisation has usually been the energy consumption of the compressors in the pipeline system, but alternative objective functions are needed as pipeline systems operations become more complicated. DP- and Genetic Algorithm- (GA) based optimisation are tested on a looped and branched pipeline system with 66 CSs. DP found an optimal solution providing energy consumption savings of 38% relative to the system's known operating strategy. GA required several months to fine tune the different internal parameters of the algorithm, yet it was capable of providing only 28% energy consumption savings.

Wright et al. (1998) extend the analysis performed by Carter (1996) on CS optimisation. GA and Simulated Annealing (SA) are discussed as possibly replacing MINLP. Both GA and SA solve the continuous (selecting the gas flows through compressor units) and combinatorial (selecting

running units) optimisation problems within the same algorithm, whereas MINLP uses a separate algorithm, usually a branch-and-bound method to solve the combinatorial problem. This two-algorithm property of MINLP is seen as a drawback. After a comparison of GA and SA, the SA is selected as the method of choice for large CS optimisation problems as its statistical properties are more attractive. Moreover, SA provides a guaranteed global optimal solution, if the "cooling rate" of the SA algorithm is slow enough. A large number of optimisation cases were run on a test pipeline system with 10 CSs, each containing 25 compressor units. SA was capable of solving all those cases with small variations in the solution times, while MINLP exceeded the defined maximal solution time in almost half of the cases. Also, the solution time variations of MINLP were much larger than for SA.

Ostromuhov (1998) uses a commercial steady-state modelling and optimisation application to demonstrate a test example of a looped pipeline system with 14 CSs and one gas storage. The application, which is based on MINLP with an improved branch-and-bound algorithm providing better local optimum avoidance and lower risk for excessively long solution times, can be used for optimal investment planning, such as optimal pipeline routing and location of equipment, supplies and off-takes as well as optimisation of the pipe diameters. Operational optimisation includes maximising pipeline throughput, minimising energy and maximising profit. The optimisation application provides optimal values for compressor unit selections and pressure settings (discharge to suction pressure ratio, discharge pressure or suction pressure, according to the user's choice). For the test example, energy savings of 11.2% were obtained.

Poe et al. (1999) use a detailed steady-state pipeline system and CS model as the basis for steady-state optimisation of a 250-mile long pipeline system with six CSs. The steady-state optimisation algorithm calculates optimal compressor unit selections and discharge pressure values for the CSs, which, however, are run under suction pressure control. A multivariable predictive control algorithm (MPC, see figure 3.5) is used to convert discharge pressure values to suction pressure values. The cost function options are: energy consumption, pipeline throughput or operating margin. Optimisation is activated manually, typically a few times per day, and the optimal discharge pressure set points are also entered manually into the MPC. The MPC adapts to changing gas demand as well as to CS start-ups and shutdowns, which are done manually by the operators. At decreasing gas flow, up to 10% energy savings are reported. Average or long-term savings are not reported.
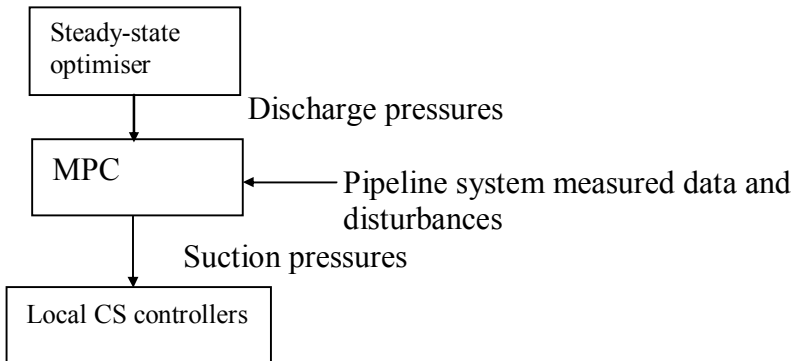

Figure 3.5 An MPC is used to convert optimised discharge pressure values to suction pressure values.

Wu et al. (2000) calculate lower bounds for the cost function values for complex steady-state CS optimisation problems by relaxing the compressor envelope constraints to become convex and partially linear. They also derive linear underestimators for the compressor cost functions. A demonstration example of a complex, looped pipeline system is given, where the steady-state solution was not found at all, but the lower bound was easily obtained. The inability of steady-state optimisers to find an optimal or feasible solution due to problem complexity and non-convexity is seen as the main motivation for developing the lower bound calculation scheme. The authors also report only very modest success to date in dynamic (or "transient") optimisation of gas pipeline systems.

3.6 Advanced process control approaches

Smeulers et al. (1999) discuss MPC of CSs using a simulated case of two parallel compressor units. The pipeline is replaced by a gas header with one or several output flows. Both units have their own throttle valves in the suction line and a bypass valve. A station bypass valve is situated in a line with a cooler from the header to the suction side of the compressors. For each compressor unit, manipulated variables (MV) of the MPC are: the throttle valve position, the bypass valve position and the power input to the compressor. An additional common MV for the whole station is the station bypass valve position (see figure 3.6).
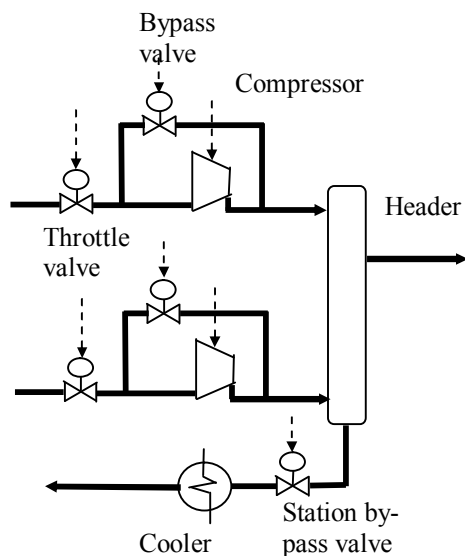
Figure 3.6 CS with two parallel compressor units. Dashed arrows are used to show the manipulated variables of the MPC

The control objectives are to: avoid surge conditions, avoid exceeding the maximum temperature at the compressor discharge sides, keep header pressure within minimum and maximum limits, keep header pressure close to a set point value (optional) and finally, minimise energy consumption of the compressor units.

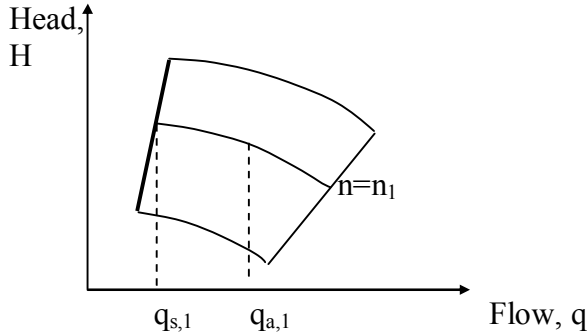The controlled variables (CV) are derived as follows:
For surge avoidance, the distance to the surge line for each unit i=1,2 is defined as (see figure 3.7):

$$DS_i = \frac{q_{a,i}(n_i)}{q_{s,i}(n_i)} \qquad (3.20)$$

where

$q_{a,i}(n_i)$ is the actual mass flow through unit i at rotational speed n_i

$q_{s,i}(n_i)$ is the mass flow at surge line through unit i at rotational speed n_i

Figure 3.7 Calculation of the distance to the surge line, DS_1, for unit 1

If $DS_1 - DS_2$ is a CV with a set point value of zero, then the MPC strives to keep the compressor units at equal distances from the respective surge lines.

The deviation from the minimum required power for the whole station is defined as the ratio between actual power and minimum power:

$$DP = \frac{E_1 + E_2}{q_{tot} c_p T_s \left[\left(\frac{P_d}{P_s} \right)^{\gamma 0} - 1 \right]} \qquad (3.21)$$

where

E_i is the actual power consumption of compressor unit i

q_{tot} is the total mass flow through the station

c_p is the average heat capacity of the gas at constant pressure

T_s is the temperature of the gas at the station suction point

P_d is the header pressure

P_s is the station suction pressure

γ_0 $= \dfrac{k_a - 1}{k_a \eta_m}$ where k_a is the adiabatic exponent and η_m is the ideal (or maximum) efficiency

of the compressor.

When the quantity DP is used as a CV with a set point value of 1, the controller minimises the power consumption of the CS.

A Kalman filter is used to update the internal state of the controller using measured process values. The internal linear model of the MPC is updated at each control cycle by linearising the non-linear compressor unit models. The MPC is capable of avoiding surge and minimising power consumption in various simulated situations and it is also shown to be robust against model mismatch errors.

Zhu et al. (2001) study an oxygen pipeline network, 50 miles in length and with 15 customers (off-takes), supplied by 5 cryogenic process plants. Contractual limits are applied on pressures at given points in the pipeline.

Instead of a partial differential equation model for calculating pressure distributions P(x,t), they use a first-principles model for the pressures at given nodes of the pipeline network assuming constant gas temperature and using molar mass balances and the Virial equation of state. This results in a system of ordinary differential equations for the pressures P_i at the 30 nodes of the pipeline:

$$\frac{dP_i}{dt} = \rho_{sc} \frac{(RT + B_i P_i)^2}{V_i RT} \left[\sum_j k_p \sqrt{P_i^2 - P_j^2} + \sum_k q_{VOL,i,k} \right] \qquad (3.22)$$

where
ρ_{sc} is the molar density of the gas in normal conditions
B_i is the second Virial coefficient at node i, i=1,…,30
V_i is the volume of node i
P_j is the pressure of node j adjacent to node i
k_p is a constant, while gas compressibility is assumed to be independent of pressure
$q_{VOL,i,k}$ are the volumetric flow rates of gas to and from the node i

For Linear Model Predictive Control (LMPC) design, the model is further simplified by combining nodes to produce a final model with 10 nodes. The simplified model is shown to provide responses very close to the original 30-node model. The simplified model is linearised for the LMPC design.

The LMPC has 6 MVs: the gas production rate (flow) of 5 cryogenic plants and the pressure set point of a control valve, which separates the pipeline into high-pressure and low-pressure sections. The LMPC is required to control the pressures at 3 selected nodes to given set points and to keep pressures of the 7 remaining nodes between prescribed minimum and maximum limits. All off-take flows are treated as measurable disturbances. Model states are updated from the measurements using a dead-beat estimator. Since 5 of the 6 MVs are gas flows, the pressure responses are integrating, i.e. unstable in a strict sense. This calls for the LMPC design with an infinite control horizon formulation by Muske and Rawlings (1993).

The final LMPC obtained has a quadratic programming (QP) problem formulation from which the optimal MV values are solved at each control interval. Since some CVs are subject to hard constraints (the pressure limits), a relaxation technique is applied to avoid unfeasible QP solutions. In simulation studies, the LMPC is shown to provide fast and accurate control of the pipeline pressures, even in the case of modelling errors. The authors emphasise, that advanced control is currently not practised in gas pipeline systems and that the literature on control and optimisation is sparse.

3.7 Dynamic optimisation

Marque's and Morari (1988) present a moving (receding) horizon optimisation method as follows where the optimisation spans the prediction horizon from the present moment of time t_0 to a moment of time t_1 in the future. The steps of the basic form of the method are:

1. Obtain measured values such as pressures and flows from the pipeline system
2. Obtain updated consumption forecasts for all off-take flows for the time t_0 to t_1
3. Perform a state estimation step, which corrects the values of the system state variables based on measured values. The state estimator is augmented with expressions for correcting the consumption forecasts based on the difference between measured ($\mathbf{P}(t)$) and estimated ($\hat{\mathbf{P}}(t)$) pressure values near the respective off-takes:

$$\hat{\mathbf{e}}(t+1) = \hat{\mathbf{e}}(t) + \mathbf{K}(\mathbf{P}(t) - \hat{\mathbf{P}}(t)) \qquad (3.23)$$

where $\mathbf{K}$ is a gain matrix

            $\hat{\mathbf{e}}$ is a vector of correction values for the consumption forecasts

4. Enter an optimisation loop, where the value of the cost function to be minimised, the constraints and other system variables are calculated using a rigorous dynamic pipeline model. The optimisation calculates optimal discharge pressure profile values $\mathbf{u}(t_0)$, $\mathbf{u}(t_0+\Delta T),\dots\mathbf{u}(t_1-\Delta T)$ for the CSs from time t_0 to t_1.
5. Implement the first optimal profile values $\mathbf{u}(t_0)$ and wait ΔT time units
6. Define $t_0 = t_0 + \Delta T$ and $t_1 = t_1 + \Delta T$ and go to step 1

Step 6 defines the receding horizon concept, in which the procedure is forced to start all over again and to leave optimal discharge pressure values $\mathbf{u}(t_0+\Delta T)$, $\mathbf{u}(t_0+2\Delta T),\dots$ unused at the next cycle.

The optimisation is based on successive quadratic programming (SQP). Gradient values of the cost function are calculated numerically within the optimisation loop. One optimisation cycle typically needs a large number of cost function and constraint evaluations, which sets hard requirements on the computational speed of solving the dynamic model equations. The cost function is the energy consumption of the CSs, see expression (3.18). The compressor unit envelope constraints are approximated with straight lines as illustrated in figure 3.8. Note, that the vertical axis is the discharge to suction pressure ratio and not the compression head value.

The optimisation is built up of two hierarchical layers. The upper layer performs optimisation once a day (control step ΔT=24 h). The lower layer performs optimisation several times per day for the discharge pressures of only those CSs with off-takes downstream. The other CSs use the discharge pressures provided by the upper optimisation layer.
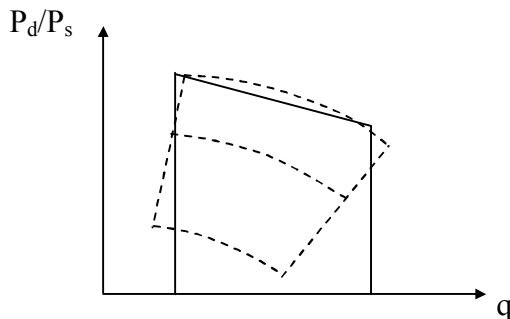
Figure 3.8 Simplified compressor envelope (solid lines) and original envelope (dashed lines)

In order to reduce computational load, the lower level optimisation uses *uneven blocking*, i.e. the control sequence is $\mathbf{u}(t_0)$, $\mathbf{u}(t_0+\Delta T_1)$, $\mathbf{u}(t_0+\Delta T_2)$, $\mathbf{u}(t_0+\Delta T_3)$,… instead of $\mathbf{u}(t_0)$,$\mathbf{u}(t_0+\Delta T)$, $\mathbf{u}(t_0+2\Delta T)$, $\mathbf{u}(t_0+3\Delta T)$,…, each $\Delta T_i > \Delta T$ (see section 5.10).

The optimisation method includes feedback, since measured values from the pipeline system enter the optimisation through the estimator (3.23). The feedback compensates for erroneous consumption forecasts, because simulated case examples on pipeline systems with 2, 3 and 7 CSs show that the optimisation method gives energy savings of 20% even in cases of 10% consumption forecast error.

The length of the prediction horizon is dependent on the size of the pipeline system and should be chosen carefully (see Chapter 5, section 5.10). Values between 6 and 24 hours are considered in the simulation examples presented.

Furey (1993) developed an algorithm for *dynamic optimal control* of complex gas networks. The algorithm calculates optimal compressor MV profiles over a fixed, given time horizon into the future. The cost function is the energy consumption of the compressors plus a terminal cost, which prevents the algorithm from making decisions that are not favourable for the future beyond the time horizon. The compressor envelope constraints are not used as such; they are replaced by minimum and maximum constant limits on suction pressure, discharge pressure and gas flow. A locally linearised, discrete time model is used as the pipeline system model. A two-level algorithm for optimisation is used: at the upper level, a sequential augmented Lagrangian method is used to satisfy the inequality constraints. At the lower level, an SQP problem, with only equality and simple bound constraints, is solved. The algorithm is demonstrated using a large network containing 32 compressor units in 20 CSs using an optimisation horizon of 8 hours. The CPU time required to reach a solution is 1839 seconds. The energy savings potential is not reported.

Vostry et al. (1994) developed a method for *transient optimisation*. The optimisation method finds optimal CS control profiles, which may be discharge pressure, suction pressure, gas flow or discharge to suction pressure ratio. The cost function used is energy consumption augmented with quadratic penalty functions for the pressure limits used in the pipeline system. A method of feasible directions is used as the optimisation algorithm. The dynamic pipeline system model embedded in the optimisation algorithm is a linearised discrete time state equation. A few demonstration examples are presented, where transient optimisation over 3 days is performed for simple pipeline systems with varying off-take and supply flows. The energy savings potential is not reported.

The approach presented by Osiadacz (1998) has much in common with the one in Furey (1993) the main difference being that Osiadacz uses *spatial decomposition* of the gas pipeline system. The interconnections of subsystems to each other are described as pressure and flow constraints (pressure or flow out from a subsystem must be equal to pressure or flow into a neighbouring subsystem), which are represented by multipliers in the cost function of the overall optimisation problem. The higher level of this goal co-ordination problem takes care of fulfilling the interconnecting constraints at the solution. At a local level, subsystems are optimised over a fixed-time horizon using gradient-based minimisation of an augmented Lagrangian function, where inequality constraints are treated as penalties in the cost function. Compressor envelope constraints are replaced by simple pressure and pressure ratio constraints. The cost function is the energy consumption of the CSs. Simulation tests reveal that the method needs a large computational capacity and parallel computation is recommended especially when solving

larger pipeline system optimisation problems. The achievable energy saving potential is not reported.

The objectives for an optimisation method presented by Rachford and Carter (2000) are to minimise energy, to find unused capacity and to assess spot market capability on a short-term basis. Additional objectives are:

- The pipeline system must always be left in a predefined final state at the end of the optimisation horizon, which is expressed as target profiles for some important pipeline pressures $P_i(x,t_1)$, at the final time t_1 of the optimisation horizon.
- Line pack must be managed effectively, meaning that target or minimum/maximum line pack values for sections of the pipeline system must be defined and followed
- Gas inventory depletion must be avoided in all circumstances. Inventory depletion occurs if the potential energy of the gas in the pipeline is allowed to decrease near the end of the horizon, which certainly saves energy in the interval $t_0\dots t_1$ but is an inferior policy for future times beyond t_1.

The optimisation method is based on a rigorous isothermal dynamic simulation model and a full nonlinear optimisation algorithm for finding optimal CS discharge pressure profiles over the optimisation horizon. The constraints of the optimisation problem are CS maximum discharge pressure, minimum suction pressure and maximum CS power, instead of the usual compressor envelopes. The predefined final state at time t_1 is obtained by separate steady-state optimisation. The typical value of the optimisation horizon is 8 hours, which is divided into 15-minute control intervals during which the discharge pressures are constant.

Optimisation with simulated cases show energy savings of up to 17% compared to a "manual" operating strategy, which is over-pessimistic as it assumes that human operators apply large, energy-consuming changes to the CS discharge pressures. Shortening the optimisation horizon to 6 hours is possible, i.e. the final state can be reached in that time without constraint violations, but substantial energy savings cannot be obtained. If the length of the optimisation horizon is increased to 24 hours, the optimisation method can optimally allocate extra spot gas deliveries of given quantities and still reach the final state without violating constraints.

Kelling et al. (2000) develop a method of *transient optimisation* based on, that once a steady-state optimisation method is successfully implemented for a given case, then the extension to a transient optimiser is straightforward under the assumption that the pipeline system considered does not deviate too much from steady-state. The most important objectives of optimisation are energy consumption, maximal gas flow and maximal profit. They use a "large space and time element" approach to approximate the partial differential equations of the pipeline system. Only one pressure value P_{12} is calculated for a pipeline segment between two nodes (such as CSs) using the average pressure expression (3.9). Using an additional assumption -that the system is only mildly non-linear- they apply the SLP method presented by Sekirnjak (1996), where the steady-state model is replaced by the simplified dynamic model. The optimisation is performed for a time period (horizon) of 24 hours with given initial and final pipeline system states. A simulated case example on a looped pipeline system with 8 CSs shows that the assumption on mild non-linearity holds. Benefit estimates, such as energy saving potential, are not reported. The method is expandable with an MIP part for discrete decision variables. Initial experiments indicate, that LP/MIP is a very attractive and robust optimisation method; however, a large number of discrete decision variables rapidly increases the computation time to non-tolerable values.

Pietsch et al. (2001) apply the optimisation method developed by Rachford and Carter (2000) on a pipeline system with two CSs in a simulation test bench. The objectives for optimisation are the same, but expanded with the ability to manage *curtailment* and other abnormal operating conditions.

An optimal initial state, which is defined as a pressure profile given the supply and off-take flows, is calculated by a steady-state optimiser. The optimisation method assumes that the pipeline system is in this initial state each day at midnight and that, whatever happens, the final state of the pipeline system 24 hours later must be the same as the initial state. The optimisation solves optimal discharge pressure profiles over the 24-hour optimisation horizon. The isothermal, rigorous dynamic pipeline system model includes the typical, non-linear compressor envelope constraints. A number of optimisation cases are simulated, where the pipeline system dynamics is taken advantage of in a way not possible with steady-state optimisation. The optimisation method is capable of allocating sudden, short-term spot deliveries to any customer and vice versa, and of optimising situations where planned deliveries and spot deliveries are allocated, but limitations on gas supplies apply. Finally, optimisation of curtailment is also tested, where an unplanned gas supply limitation is compensated for by decreasing some selected off-take flows. For example, figure 3.9 shows a supply limitation for 5 hours, which is compensated by curtailment starting after the supply has returned to normal.

The results are not very encouraging from the point of view of energy minimisation, since no energy savings of practical value were achieved. However, in all optimisation cases studied, the optimiser was capable of avoiding constraint violations while the pipeline system reached the required final state.
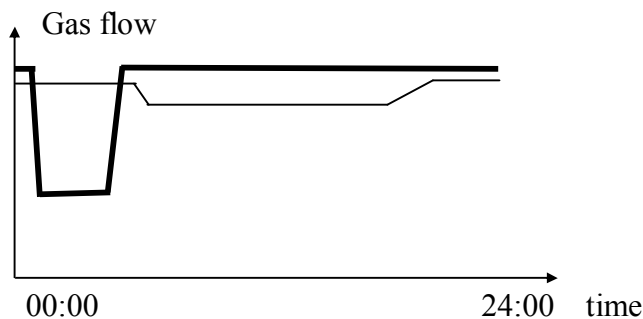
Figure 3.9 Example of curtailment: temporary loss of inlet supply (bold line) is compensated by decreasing off-take flow (thin line) at the other end of the pipeline

3.8 Summary and discussion

Support tools for natural gas pipeline operators not using rigorous optimisation methods are reported. Some of these are built on expert systems, which produce only modest benefits, if *only* heuristic rule bases are used. Expert systems with integrated steady-state or dynamic simulators seem to produce better results. Dynamic simulators must be protected against bad input data, otherwise they may behave as "garbage generators".

Many publishers refer to the pioneer work on efficient pipeline operations performed by Batey et al. (1961) and the majority of these agree with their three rules of thumb. Revell and Thorne (1998) use maximisation of pressures in the pipeline as an explicit optimisation target.

Both steady-state and dynamic optimisation are seen as demanding; the more complex the network, the more difficult is the optimisation problem to solve. The main issue is non-convexity of the problem in general. Faced with solving for optimal compressor unit selections or other discrete optimal decisions, the task of the optimiser is even more challenging. Simplifications are frequently used: compressor envelopes are approximated by linear expressions and sequential linear approximations and/or SLP optimisation have been used. One important conclusion is that both steady-state and dynamic behaviour of a pipeline system is only mildly non-linear.

Some authors touch on a broader issue than just the development of a good optimiser, namely the task of building a whole *optimisation system* including user interfaces, data storage, consumption forecast systems, input data conditioning and so on. This task should be executed in successive steps rather than as one big effort. For example, Johnson et al. (2000) observed that the routine use of a dynamic pipeline simulator before introducing an expert system was a key success factor.

Almost all rigorous optimisation schemes were tested in a simulation environment or test bench only. Poe et al. (1999) report that the steady-state optimisation with MPC was installed in an actual environment, for which the benefits (10% energy savings at *decreasing gas throughputs*) were obtained. Many authors did not clearly express the intention of the developed optimisers, but some optimisers seem to be applicable at least as off-line decision support tools.

State estimation of a pipeline system is essential if optimisation results with relevance are to be obtained. Very little has been published on this subject, but authors do emphasise its importance. The state estimation challenge is often tackled by carefully tuning the pipeline system model to fit the true, measured pipeline data rather than designing optimal estimators.

There has been very little publication activity in the area of real-time optimisation of natural gas pipeline systems. Remarkably, perhaps the most serious contribution to the subject is provided by Marque's and Morari (1988). Transient optimisers for optimally moving the pipeline system from an initial state to a final one, have been developed. Some details of these methods can be questioned. Rachford and Carter (2000) and Pietsch et al. (2001) define a prescribed final state (pressure profile) of the pipeline system *and* constraints on line pack. These requirements are redundant, since pressure profile and line pack are related to each other through (3.10). The use of a final pressure profile obtained by steady-state optimisation may also be questioned, while placing artificial limits between optimisation periods (days) could, intuitively, be replaced by a *receding horizon* optimisation strategy, where the next period's consumption forecasts will influence the optimal solutions in a natural way as the receding horizon slides over the period limit.

The authors referenced in section 3.7 have used prediction horizons from 6 to 24 hours, the latter being popular when commercial aspects are considered. Rachford and Carter (2000) use the prediction horizon as a tuning parameter, which should be chosen carefully; however, it remains unclear how the user should select correct values from case to case. Real-time, repetitive operation and state estimation was thoroughly discussed only by Marque's and Morari (1988). Optimisation including discrete decision variables (compressor unit selections) was, in turn, discussed only by Kelling et al. (2000).

Chapter 4

Dynamics of Natural Gas Pipeline Systems

4.1 Introduction

In this chapter, the dynamics of natural gas pipeline systems will be studied from the point of view of applicability of linear control and real time optimisation methods.

In the sequel, the compressor station (CS) *discharge pressures* are defined as control variables, or manipulated variables, or decision variables of some higher-level control and real-time optimisation algorithms (see Chapter 2, figure 2.4). From a modelling perspective, the discharge pressures are the inputs of the dynamic models needed by those algorithms.

The controlled variables (CVs) or variables needed to calculate cost function values within the control and optimisation algorithms are selected from among the set of pressure and gas flow variables in the pipeline system. These are the outputs of the dynamic models mentioned above. A control task can be either to keep CVs as close as possible to given target values ("control-to-target") or to keep controlled variables above or below given limits. A typical and important control task is to keep pressures along pipeline segments above physical and contractual minimum limits.

A large number of disturbance variables acts on the natural gas pipeline system. Every single gas off-take is a disturbance, since variations in off-take flow will change the pressure at the off-take and the pressure change propagates throughout the pipeline system. Off-take flow rates are usually measured, which gives an opportunity to utilise the information in control and optimisation algorithms. Control valves and block valves along the pipeline system represent disturbance variables as well, but mostly, the valve positions are measured. In this work it will be assumed that off-take flows do not depend on pressures in the pipeline, a realistic assumption, while in real pipeline systems gas consumers control their gas flow rates with their own control valves.

Figure 4.1 schematically illustrates the Finnish natural gas pipeline system. The CS discharge pressure set points are named u1, u2 and u3, respectively. The three particularly interesting pressure "check points" are named Px1, Px2 and Px3 in figure 4.1. The pipeline system consists of three main segments. Important pipeline distances are shown in the figure.

The supply pressure and gas flow rate at the border are measured, the latter with very good accuracy because this is the basis for commercial transactions.

For obvious reasons, only one CV in the control-to-target case may be defined for any pipeline segment between two running CSs, since pressure or flow values in one such segment are related to each other in steady state. However, several pressure and flow variables may be defined for limit-keeping control in one segment, provided, that contradictory limit values are not applied.
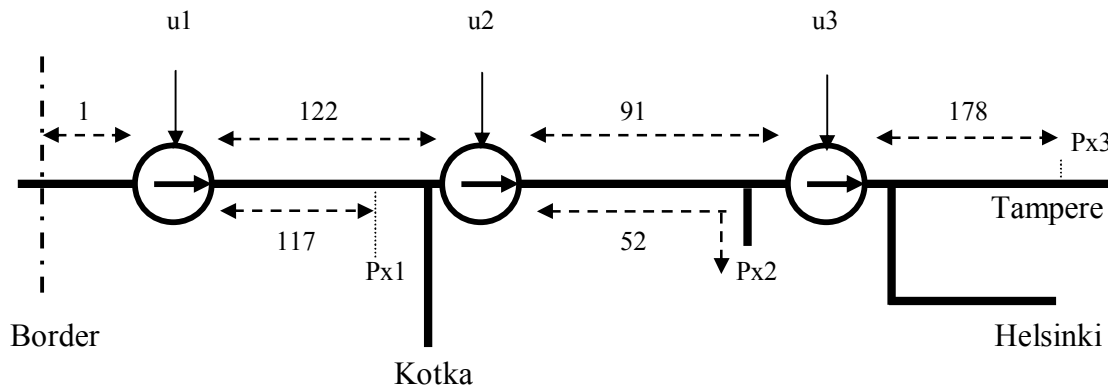
Figure 4.1 The Finnish natural gas pipeline system. Distances are in kilometres.

In discharge pressure control mode, step-wise changes of CS discharge pressure are frequently needed. These steps will generate quite large changes in the gas throughput flow within physical CS equipment limits (see for example figure A.3 in Appendix A).

The physical units used are for pressure bar (absolute pressure) and for flow Nm^3/h (volume flow in normal conditions, 1 atm (1.01325 bar) absolute pressure and 0 °C temperature). In compressor-related analysis, volume flow, m^3/s, in compressor suction conditions is usually used.

4.2 Pipeline system dynamics

In order to investigate the dynamic behaviour of the Finnish natural gas pipeline system, a series of step response tests were executed using a dynamic simulation model. The model is built on the "Simone" pipeline system simulator (Jeni´cek et al., 1991; Kra'lik et al., 1984B). For the control response, steps of 1 bar in the discharge pressures were made and for the disturbance response, steps of 10 000 Nm^3/h in the flow rate of gas off-takes were made. All step tests were executed with the pipeline initially at steady state in three operating points: high, medium and low gas throughput. The operating point data are presented in tables A.1 to A.3 in Appendix A. With respect to CS status, we distinguish between three different cases: all three stations running, CS2 shut down and CS3 shut down. Step responses are presented graphically in Appendix A.

In "Simone", the suction pressure of CS1 is kept at a constant value of 40 bar by an artificial pressure controller, because there is insufficient information on the Russian side of the pipeline system to predict important variables such as CS1 suction pressure.

Eventually, it may be necessary to operate CSs outside their envelopes. This can be achieved in "Simone" by switching off envelope handling (see Appendix C). For example, to switch off a CS at operating point no. 1, where the total gas flow through the pipeline system is high, is not possible (feasible) with the envelopes being active. However, the main interest at this point is to investigate pipeline dynamics without carrying concerns over envelope violations.

4.2.1 Control response

With *control response* we mean the responses of pressure and flow variables to changes in discharge pressures of CSs. The following observations may be made based on data presented in Appendix A:

In a CS's discharge pressure, a step change:
- Generates a pulse in that station's gas flow rate. The dynamics of CS local control systems together with the pipeline characteristics downstream the station determine the shape of the flow pulse.
- Generates a fast change in the station's suction pressure with approximately the same magnitude as the discharge pressure change but with opposite sign, and with time, the suction pressure will return to it's original value.
- Initiates a transient in any pressure value in the pipeline segment downstream the CS. The larger the distance from the CS, the slower the response. Having reached a new steady state, the value of the downstream pressure has experienced a larger change than the change in the station's discharge pressure, provided all gas flows into and out of the pipeline segment are controlled and constant. Using process control terminology, the steady-state gain is larger than one.
- Does not generate any responses on pressure and flow variables downstream the next downstream CS (for example, CS2 discharge pressure has no influence on Px3 when CS3 is in operation). In other words, running CSs "isolate" pipeline segments in the downstream direction.
- Generates a pressure change with a slow return to original value in all pressure variables upstream the CS. The pressure change is slower the larger the distance is from the CS in the upstream direction. The isolating effect is not experienced in the upstream direction.
- Generates a flow pulse in all upstream CSs so that the pulse is "smoothing out" and decreasing in amplitude in proportion to the distance from the CS.

The step response graphs in Appendix A illustrate that at larger gas throughput, the pressure changes downstream are larger and the responses are slower.

If a CS is shut down, then the dynamics becomes considerably slower and steady-state gains increase. Logically, shutting down a CS is equivalent to merging its upstream and downstream pipeline segments into one long segment. Specifically, when making, again, a step change in the discharge pressure of a CS, who's next downstream or upstream station is shut down:
- The gas flow rate pulse looks very much the same as with the downstream station running (compare Appendix A, figures A.6 b with A.25 b for CS2 flow rate when CS3 is shut down and figures A.9 c with A.17 c for CS3 flow rate when CS2 is shut down).
- The recovery of suction pressure is slower (compare figures A.4 b with A.23 b for CS2 suction pressure when CS3 is shut down). In addition, when an upstream station is shut down, the change in the suction pressure is larger (compare figures A.7 c with A.15 c for CS3 suction pressure when CS2 is shut down)

- The CS shut down does not isolate any more. Pressure and flow transients will proceed through the bypass pipe of the station. For example, CS3 suction pressure has a response to CS1 discharge pressure when CS2 is shut down (figure A.12 c) and Px3 pressure has response to CS2 when CS3 is shut down (figure A.24 c).

As can be seen in Appendix A, different gas throughput flow levels (operating points no. 1, 2 and 3) have some influence on gas pipeline system dynamics and shutting down CSs have a considerable influence on the dynamics. Adjusting the CSs to operate on different discharge pressure levels has very little influence on the dynamics (see Appendix A, figures A.28 to A.31).

An observation for later use is that the gas flow has the fastest dynamics of all variables considered and that the dynamics is not very dependent on the operating point, the CS status or the discharge pressure levels.

Note1: The isolation property of a CS does not hold if there is a tendency to violate compressor envelope limits. For example, if a compressor's maximum speed line is threatened, the local control system will override the discharge pressure set point by decreasing its value. The reason for this threat may be that the discharge pressure of the next upstream CS has decreased, leading to decreased suction pressure at the station in question and, in turn, to increased adiabatic head. The overall effect here will be the propagation of the decreased discharge pressure at the upstream CS through this station and the downstream pipeline segment.

Note 2: As the pressure and flow responses in the downstream direction from a CS's discharge pressure is limited (isolated) to the next downstream segment only, it is a good system property from the point of view of control design. The designer does not have to worry about what happens downstream the next CS. Also as upstream responses are temporary by nature – a process variable returning to it's original value is often said to have a "zero gain" response – this would suggest that pipeline system variables should not be controlled by downstream CSs. The control structure is "diagonal", if zero gain responses are not taken into account at all and "triangular" with the zero gain responses in place.

Good control system design practice suggests adjusting the control (sampling) interval to match the dynamics of the target system. In Appendix A, we may see very slow dynamics, which would suggest a larger control interval, but also very fast phenomena, which then would require a small control interval. Let us take a 10-minute control interval as a fair compromise at this point. Throughout this work, we will use a constant 10-minute control and real-time optimisation interval.

4.2.2 Disturbance response

To analyse disturbance response, we selected an off-take near checkpoint no. 3 because of its significance: checkpoint no. 3 is used as one of the critical pressure limits in the pipeline operations. Moreover, moderate changes in gas flow at this point give large local pressure swings, since it is situated far from CS3 (178 km) at the other end of a long pipeline with a gradually decreasing diameter.

A positive step change of 10 000 Nm^3/h at checkpoint no. 3:
- Generates a fast initial pressure decrease in Px3 followed by a slower decrease down to the new steady-state value (Appendix A, Figure A.11 c). The large initial decrease is due to the

fact that the flow change is high compared to the capability of the "narrow pipe" to deliver gas. In the slower part of the response, the actual dynamic characteristics of the whole pipeline segment are seen.

- Generates only a small pressure decrease upstream CS3, because pressure decrease along the pipeline is caused by increased gas flow, but the pipeline diameter and the capacity is larger in the upstream parts of the system.

4.3 Comparing simulator and true pipeline system dynamics

The operations department of Gasum Oy, responsible for operating the Finnish natural gas pipeline system, has for many years successfully used the "Simone" dynamic simulator. Continuous development and model updating has been required in order to keep the simulator up to date.

Operative data from the Finnish pipeline system was collected over the period 1.3. to 31.3.2003. Hourly average values for all off-take flows and 30 pipeline pressures, including CS discharge and suction pressures, were collected. The measured values of each CS's natural gas consumption were also collected. Measured values of CS throughput flow rate were available, but they were not collected, since they are considered inaccurate by the operating personnel.

All test and comparison runs using "Simone" were performed using a sampling time interval of 10 minutes. All collected data was re-sampled from a 60-minute to a 10-minute interval; in addition for discharge pressures, filtering was used to smooth out sharp changes from one hourly value to another.

The re-sampled off-take flows were inserted into Simone's boundary condition file. The CS discharge pressure values were applied to "Simone" through the run command file (see Appendix C for details). A simulation run over the time period 1.3.2003 to 31.3.2003 was performed using true off-take flow rates and station discharge pressures. The simulated pipeline pressures are compared to the true operating data values. In the graphs below, the true suction and checkpoint pressures are not smoothed after re-sampling.

The simulation is based on assumed isothermal conditions throughout the pipeline system. A constant gas temperature of 5°C is assumed.

The first comparison run between "Simone" and the true pipeline uses the values obtained for the period 1.3.2003 00:00 to 4.3.2003 24:00. Throughout this period, all three CSs were in operation, although a very short shutdown attempt of CS2 is observed near time 300 (Figure 4.3). Station discharge pressures are operated at rather high values.

Pipeline pressure (suction and checkpoint pressures) variations stay within 6 bar during the period. Px3 shows the largest variations, since this point is situated at the other end of a long, decreasing-diameter pipeline segment. Operators are obliged to keep this pressure above 29 bar, in which they have succeeded quite well.

A systematic difference, usually less than 1 bar, may be seen between simulated and true values. However, dynamic changes are very well reproduced by "Simone".

In figure 4.7, the simulated gas throughput flows of the CSs are shown. The figure gives an idea of typical gas flow variations in the pipeline system. The figure also shows, that the majority of gas is consumed downstream CS3.
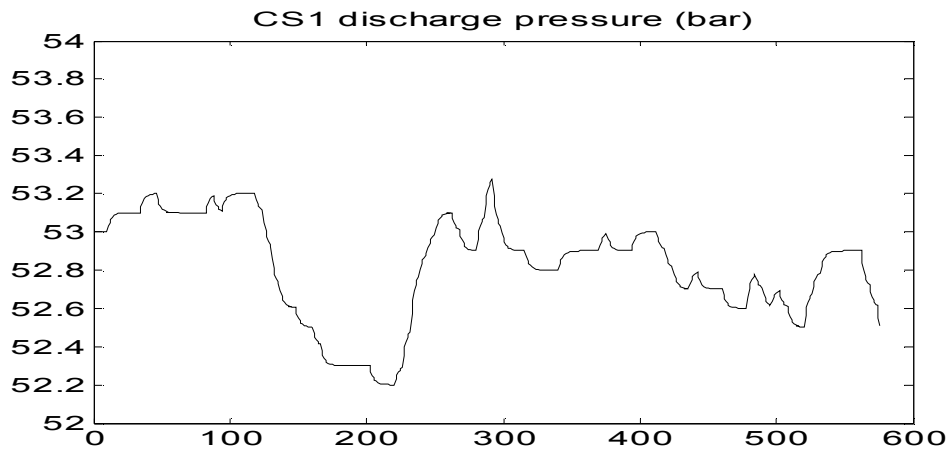

Figure 4.2 CS1 discharge pressure (bar) from operating data, re-sampled and filtered as a function of 10-minute time intervals from 1.3.2003 00:00 to 4.3.2003 24:00.
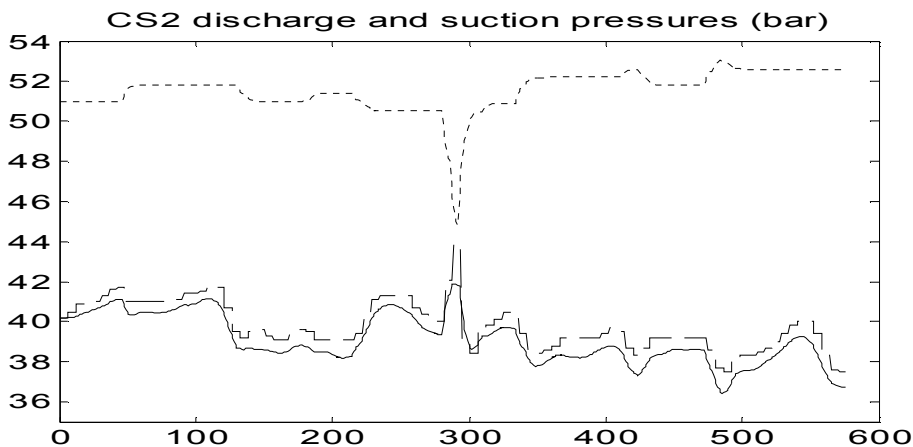

Figure 4.3 CS2 discharge pressure (dotted line), measured suction pressure (dashed line) and simulated suction pressure (solid line) 1.3.2003 00:00 to 4.3.2003 24:00.
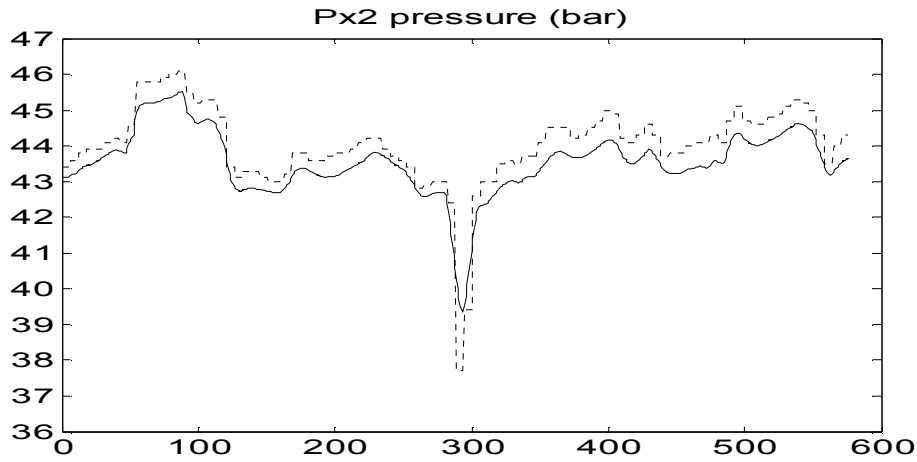
Figure 4.4 Checkpoint Px2 measured pressure (dotted line), and simulated (solid line) 1.3.2003 00:00 to 4.3.2003 24:00.
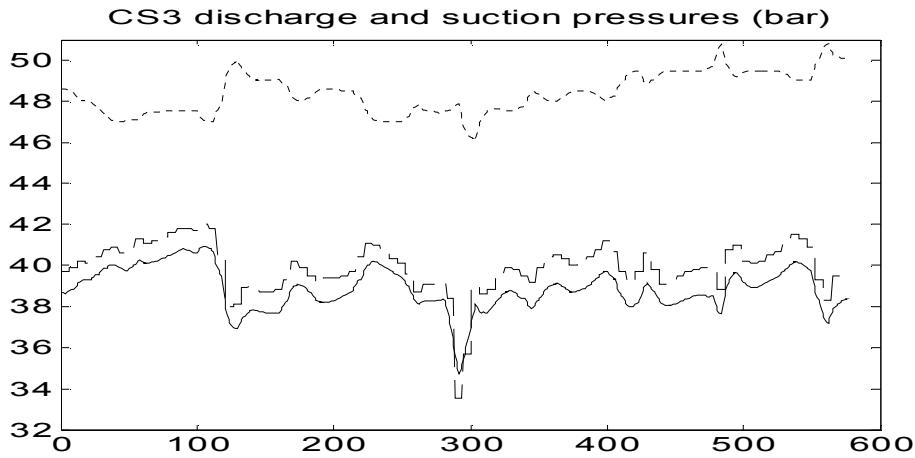
Figure 4.5 CS3 discharge pressure (dotted line), measured suction pressure (dashed line) and simulated suction pressure (solid line) 1.3.2003 00:00 to 4.3.2003 24:00.
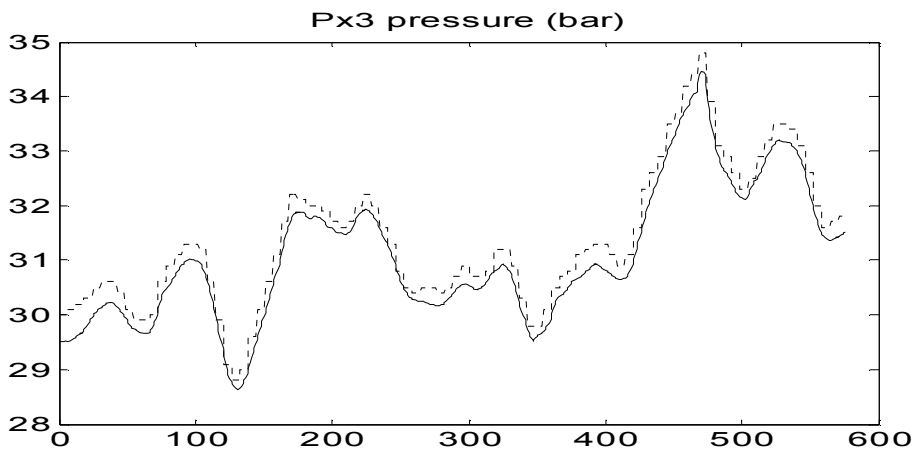
Figure 4.6 Checkpoint Px3 measured pressure (dotted line), and simulated (solid line) 1.3.2003 00:00 to 4.3.2003 24:00. Pressure minimum limit 29 bar not severely violated, except for a temporary violation at time 130.
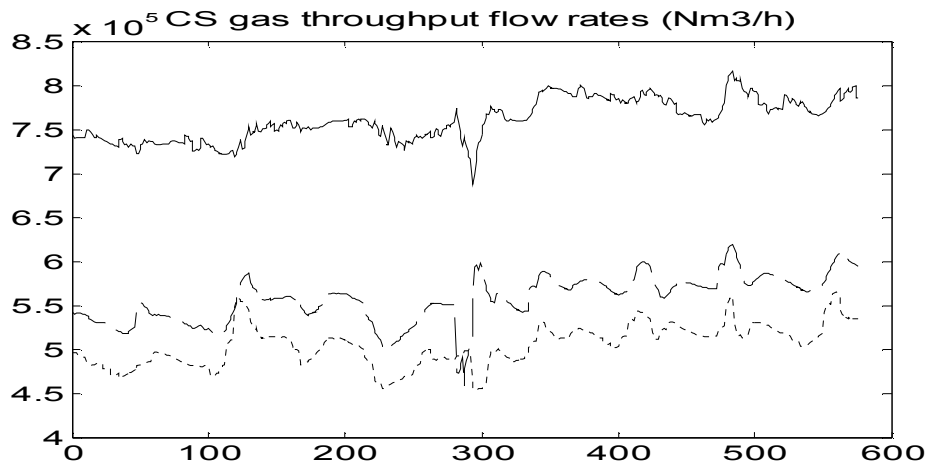
Figure 4.7 Simulated CS gas throughput flows in Nm^3/h 1.3.2003 00:00 to 4.3.2003 24:00. Solid line = CS1, dashed line = CS2 and dotted line = CS3.

Figure 4.8 illustrates a shutdown event of CS2 at time point 200. The time axes of the graphs are 7.3.2003 00:00 to 12.3.2003 15:00 in 10-minute intervals. The re-sampled and filtered CS2 discharge pressure is displayed together with the simulated CS2 discharge pressure. There is a small difference between true and simulated CS2 discharge pressure over the period CS2 is shut down, because when "Simone" receives a CS shutdown command, it starts to internally calculate the discharge pressure instead of receiving set point values. The calculated values are not exactly the same as the values in the operating data.
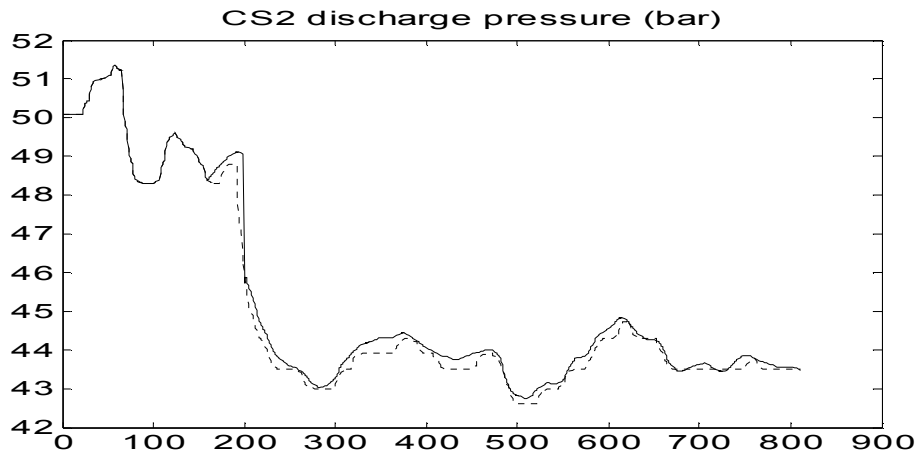
Figure 4.8 CS2 discharge pressure from operating data (dashed line) and simulated discharge pressure (solid line) as functions of 10-minute time intervals from 7.3.2003 00:00 to 12.3.2003 15:00.

40
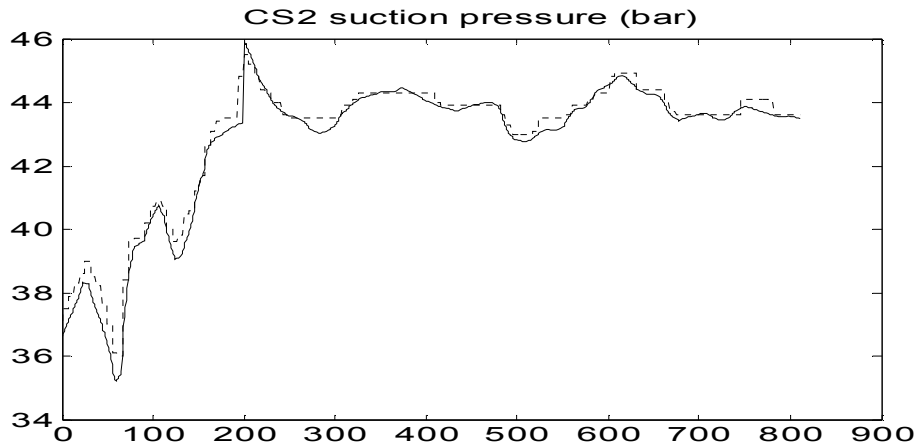
Figure 4.9 CS2 suction pressure from operating data (dashed line) and simulated (solid line) from 7.3.2003 00:00 to 12.3.2003 15:00.
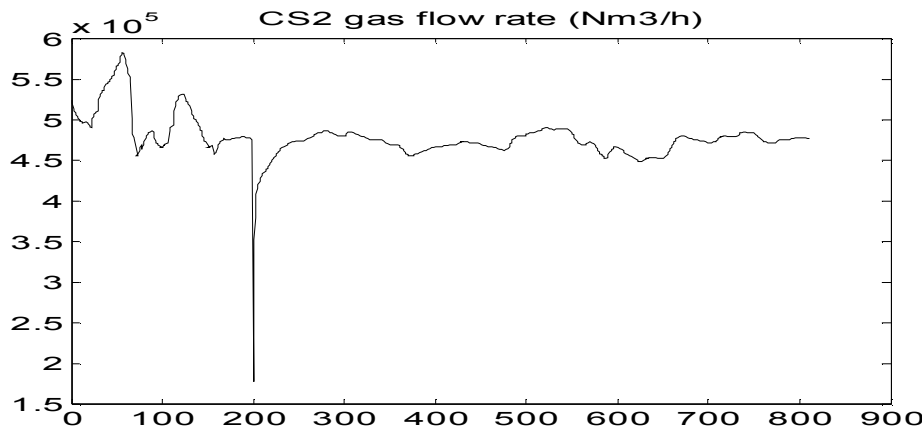
Figure 4.10 Simulated CS2 gas throughput flow, Nm^3/h from 7.3.2003 00:00 to 12.3.2003 15:00. Shutting down CS2 generates a large negative change for a short time period.
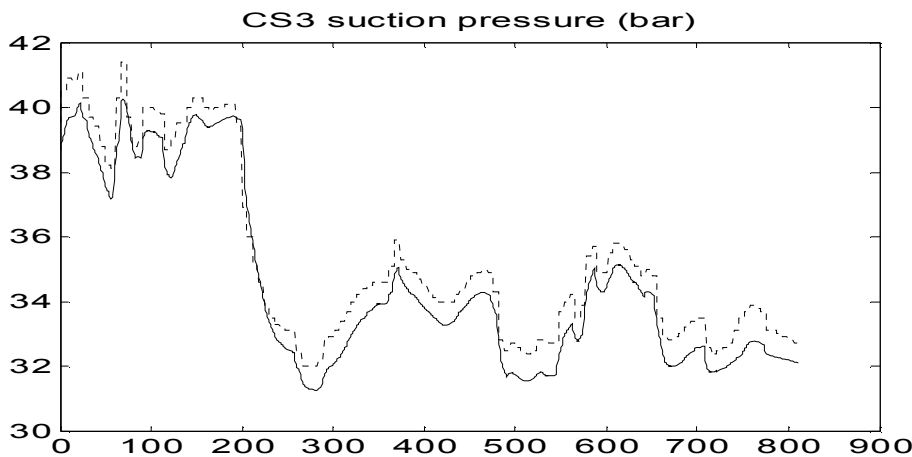
Figure 4.11 CS3 suction pressure from operating data (dashed line) and simulated (solid line) from 7.3.2003 00:00 to 12.3.2003 15:00. Pressure decreases by approximately 9 bar after time 200 due to the shutdown of CS2.

41

4.4 Linear dynamics of natural gas pipeline systems

4.4.1 Linear transfer function models

In the following, we shall identify linear dynamic models for the pressure and flow variables of the Finnish pipeline system *from simulated data* encouraged by the observation that "Simone" offers good correspondence with the true system.

We will limit the study to control response only, as linear disturbance models are not needed in the receding-horizon optimiser development described below. We obtain responses by applying one or a few discharge pressure steps to "Simone" for one CS at a time. Simulated responses are free from noise, unless non-linearity is seen as one variant of noise. Thus, rigorous identification experiment design may be omitted and just a low number of steps is used.

An experimental identification procedure will be used, where the user manually enters continuous transfer function parameters into a simple identification tool. The transfer function takes the general form:

$$G(s) = \frac{K(T_{n1}s + 1)(T_{n2}s + 1)...(T_{nM}s + 1).}{(T_{d1}s + 1)(T_{d2}s + 1)\cdots(T_{dN}s + 1).} \qquad (4.1)$$

where:
  K is the gain
  $T_{n1}, T_{n2}, \ldots$ are real-valued numerator time constants
  $T_{d1}, T_{d2}, \ldots$ are real-valued denominator time constants

The tool converts the continuous transfer function into a discrete one using a selected discretisation interval (10 minutes in this case) and calculates the response using the same input signal (discharge pressure) as "Simone". The output from "Simone" and the output from the identification tool are graphed together and the user may repeatedly adjust the transfer function parameters until the graphs show a satisfactory coincidence. The sum of squared differences of the "Simone" output and the linear model output is also displayed. See figure 4.12 for an illustration.

Discharge pressure step tests for all three CSs were performed in order to identify the transfer functions for CS1, CS2 and CS3 suction pressures, Px1, Px2 and Px3 checkpoint pressures and CS1,CS2 and CS3 gas flows for three operating points (see Appendix A) and three running status alternatives of the CSs. Discharge pressure steps of maximum 1 bar were used.

Discharge pressure step changes are applied to the pipeline system in steady state.

Appendix B shows selected transfer functions together with comparison graphs.

It is fairly easy to obtain linear models offering a good fit, especially for downstream pressure variables. Upstream pressures and flows, which all have a "zero gain" response property, are more challenging, even if the general transfer function structure (4.1) is broken down into a more intuitive form.
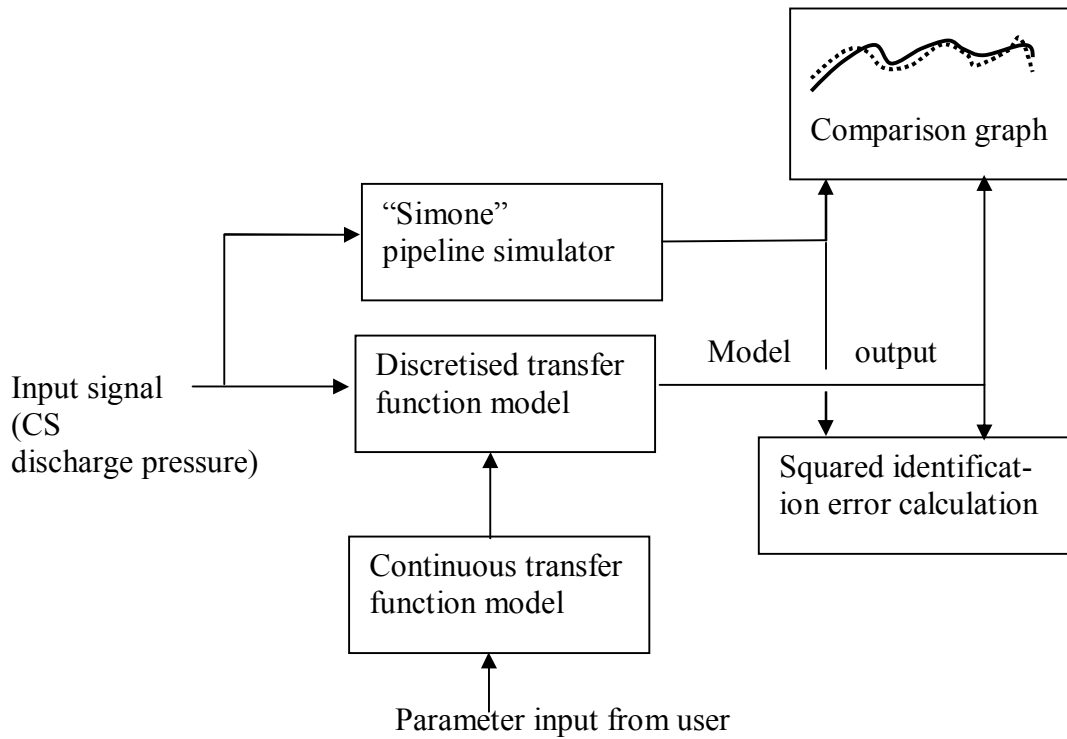
Figure 4.12 An experimental identification procedure

For upstream pressures (for upstream flows, -1 and +1 change places):

$$G(s) = K \left[\frac{-1}{T_1 s + 1} + \frac{1}{(T_2 s + 1)(T_3 s + 1)} \right] \qquad (4.2)$$

Here T_1, which is much smaller than T_2 and T_3, represents the fast decreasing pressure (or fast increasing flow) characteristics for a positive discharge pressure change and T_2 and T_3 the slow recovering response. The delay-free structure means that the gain K influences the linear model response in a non-intuitive way. Standard identification methods would most probably encounter the usual difficulty with identifying numerator dynamics, which is relevant in zero gain transfer functions.

The data in Appendix A reveals that pipeline system dynamics changes with changing operating point and with changing CS status. Using "Simone", a set of models valid for different *operating regimes* (Murray-Smith and Johansen, 1997) of the pipeline system has been obtained. One question may be asked: is it possible to calculate the values of linear model parameters from pipeline system geometry and/or measured data?

4.4.2 A simple gain formula

Let us look at a pipeline segment with the starting point at a CS's outlet and the end point anywhere downstream the station. The end point does not need to be at an off-take. The pipeline segment may have many off-takes. Let us further assume that all gas flows into and out from the pipeline segment are flow controlled, which means that no inflow or outflow of gas is directly

dependent on the pressure in the segment. Let us also assume a steady-state condition, where all inflows, outflows and pressures are constant. Then, the steady-state flow and pressure equation (see chapter 3, expression 3.7) between the pressures at the starting point of the segment, P_1, the end point, P_2, and the gas flow through the segment q_{12}, holds:

$$P_1^{\,2} - P_2^{\,2} = f_q(q_{12}) \tag{4.3}$$

where f_q is a function, which is approximately independent of the pipeline segment pressures.

The steady-state gain between a system input and a system output may be calculated as the derivative of the output with respect to the input at a given steady-state operating point. Solving P_2 from (4.3) yields $P_2 = \sqrt{P_1^{\,2} - f_q(q_{12})}$ and taking the derivative:

$$\frac{dP_2}{dP_1} = \frac{P_1}{\sqrt{P_1^{\,2} - f_q(q_{12})}} = \frac{P_1}{P_2} \tag{4.4}$$

This value for the gain of the transfer function from P_1 to P_2 can be used when the pipeline segment operates not too far away from steady state.

P_1 must be greater than P_2 for gas to flow down the segment. This means, that the gain for any pipeline segment must be greater than 1.

Expression (4.4) applies also to pipeline segments with branches and changing pipe diameter. If new sub-segments with own functions f_{q1}, f_{q2}, ..., f_{qN} and own gas flows are defined, we obtain:

$$P_1^{\,2} - P_{x1}^{\,2} = f_{q1}(q_{x1})$$

$$P_{x1}^{\,2} - P_{x2}^{\,2} = f_{q2}(q_{x2})$$

$$\dots$$

$$P_{xN-1}^{\,2} - P_2^{\,2} = f_{qN}(q_{xN})$$

Adding these N equations eliminates all intermediate pressures P_{xk}, k=1,...,N-1, leaving:

$$P_1^{\,2} - P_2^{\,2} = \sum_{k=1}^{N} f_{qk}(q_{xk}) \tag{4.5}$$

enabling (4.4) to be applied, since the right hand side of (4.5) is still dependent on steady-state gas flows only.

4.4.3 Time constant formulas

For the time constants of the linear continuous-time transfer function models, it is not easy to find simple calculation rules. (Kra'lik et. al., 1984, A) divided a pipeline segment into elements (see figure 4.13), for which linear transfer functions for pressure and mass flow deviations in the element apply:

$$F_{12}(s) = \frac{K_1}{T_1 s + 1}$$

$$F_{21}(s) = \frac{1}{T_1 s + 1}$$

$$F_{11}(s) = \frac{T_2 s}{T_1 s + 1} \qquad (4.6)$$

$$F_{22}(s) = \frac{K_2 (T_3 s + 1)}{T_1 s + 1}$$

The transfer function parameters K_1, K_2, T_1, T_2 and T_3 depend on the geometry of the pipe element, friction and average gas speed. No rules on how to select the length of the element for the model to be accurate, were given, but in their examples, they used element lengths of 10 kilometres. For three or more pipe elements in series, analytical overall pipeline segment transfer function calculation becomes tedious.
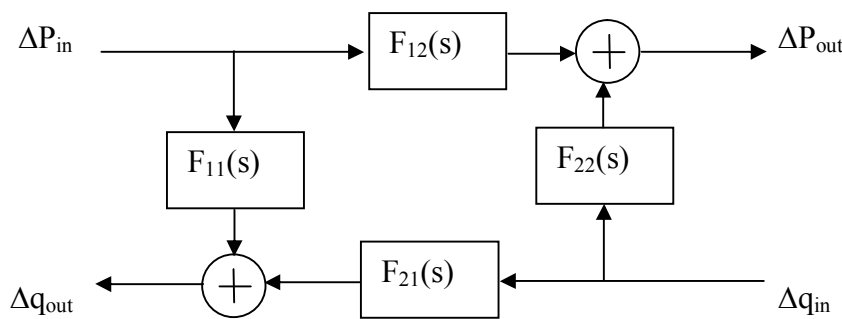
Figure 4.13 Linear transfer function model for small pressure deviations ΔP and gas mass flow deviations Δq for a pipe element.

While time constant formulas seem to be difficult to find, we may think of minimising the number of transfer functions necessary for a particular control or optimisation application. Zero gain responses are not the best ones to use in control and optimisation, since no sustaining (steady-state) change is achieved. Would it be possible to leave aside a part of the zero gain models? In a natural gas pipeline system, the CS envelopes impose constraints on the control/optimisation problem. Even small or short lasting responses must be accounted for when handling constraints. For example, a positive change is made in CS2 discharge pressure (see figure 4.1), which generates a positive gas flow pulse through CS2 and a smoothed positive flow pulse through the upstream CS1. If the latter operates near the maximum speed limit or choke line, the local control system in CS1 adjusts its discharge pressure downward (constrained by the maximum speed limit) or upward (constrained by the choke line) to make a positive flow change possible (see figure 4.14). Consequently, zero gain pressure and flow responses cannot be left out of the problem directly.
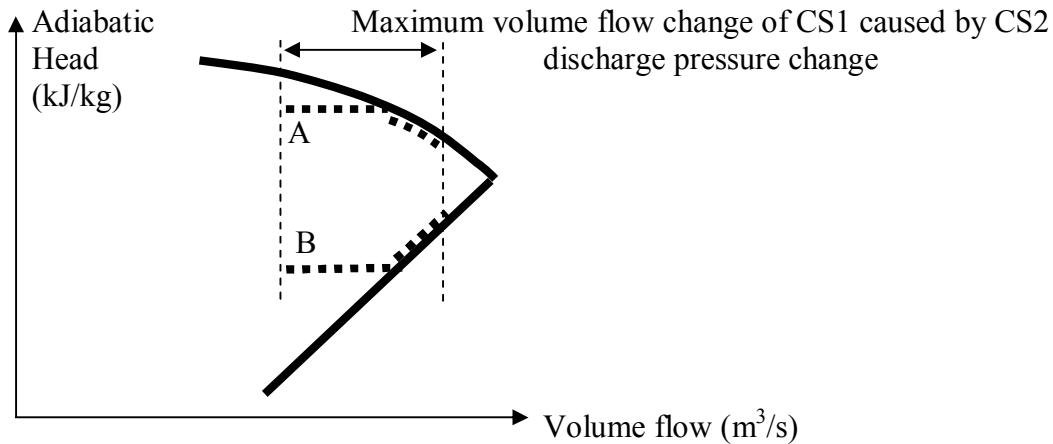
Figure 4.14 CS1 flow response in the envelope co-ordinate system after a CS2 discharge pressure change. "A" and "B" are alternative operating points of CS1 prior to the CS2 discharge pressure change. In both cases, the increase in volume flow is constrained by the envelope limits.

4.5 Discrete events in natural gas pipeline systems

Discrete events are, among others, opening/closing a block valve, starting/stopping a compressor unit in a CS and starting up/shutting down a whole CS.

Let us assume that the block valve "V" in figure 4.15 has only two distinct positions: fully open or fully closed. Opening or closing the block valve initiates a transient in the pipeline system, which depends on the gas flow through the valve at the time of closing or the pressure difference over the valve at opening. Pipeline operators should minimise the transient by trying to minimise the gas flow or pressure difference prior to opening or closing.
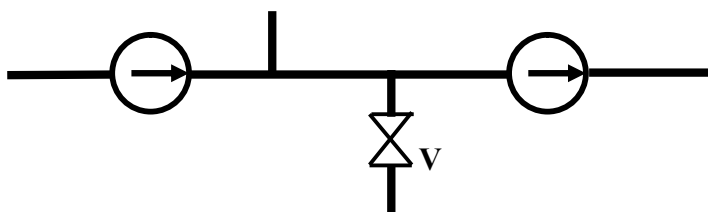
Figure 4.15 A block valve "V" in a pipeline system.

Let us assume a CS with three parallel compressor units running. The envelopes of the individual units may be drawn in the volume flow – adiabatic head co-ordinate system as usual, but the volume flow now means the total flow through the station. The envelopes are partially overlapping in figure 4.16, this means that at an increase in gas flow, a new unit is started before the envelope limits (maximum speed or choke line) are reached by an already running unit. Suppose that the compressor unit with the rightmost envelope is shut down when operating at point "A". The remaining two units cannot maintain the volume flow of gas and the operating point is immediately shifted to the choke line of the middlemost unit although in practice, the

local station control system will ensure optimum distribution of the load between the remaining units. The net effect is a fast gas flow decrease and consequently the pressures in the pipeline downstream the CS start to decrease.

Another case for this CS would be a start up of a third unit, although there is no need for that. The consequence would be that gas flow through the station is forced by unit envelope surge or minimum speed lines to increase rapidly, which in turn increases pressures downstream the station and decreases pressures upstream.
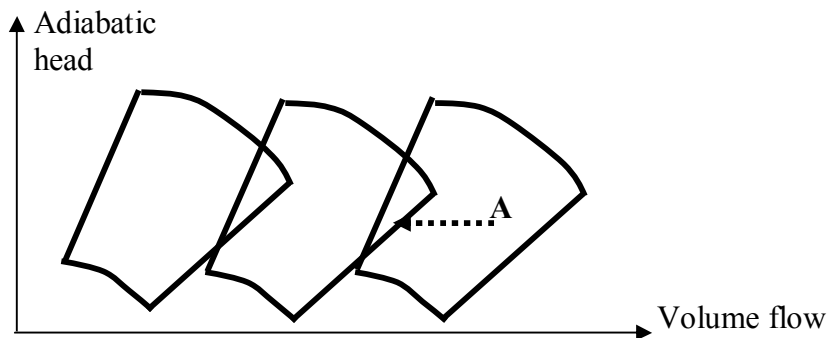
Figure 4.16 Compressor unit envelopes of three units in parallel. Original operating point is "A" with three units running.

Fast changes of gas flow through a CS are part of the everyday life when they are operated in discharge pressure mode. Consequently, the events to start or stop a unit described above are not very challenging to deal with in terms of pipeline dynamics and control.

If we consider a CS with three compressor units in series, the unit envelopes in 4.16 would be stacked on top of each other in the adiabatic head direction. In an analogy with the case above, if a unit is shut down, the discharge pressure of the CS decreases quickly constrained by the envelopes of the remaining two units. The station's gas flow will experience the typical pulse response. If a unit is started prematurely, then the discharge pressure is forced to increase and a positive gas flow pulse is seen. In this case, we have a little more challenging transients to deal with than in the previous case, especially if the discharge pressure is forced to make large changes.

It may be worth pointing out that starting and stopping units as described in the above cases would be more or less mistakes. In most cases, smooth operations should be possible.

As a next case we will consider starting up and shutting down a whole CS, no matter how many units are running (or how many units will be started) or how the units are configured within the station. Schematically, a CS may be presented as surrounded by valves as in figure 4.17 a. Prior to shutting down, the bypass valve ("BP"), which is a control valve, is opened gradually and the discharge pressure is decreased. Typically, shutting down is considered at low gas flow rates, so the opening of the bypass valve circulates more gas through the station and the operating point may move from "A" to "B" in the envelope diagram in figure 4.17.b, where the head and consequently discharge to suction pressure ratio is at a minimum. Shutting down the station at

this point (turn the CS machinery off, close valves "V1" and "V2" and set "BP" fully open) minimises the dynamic transient caused by shutdown.
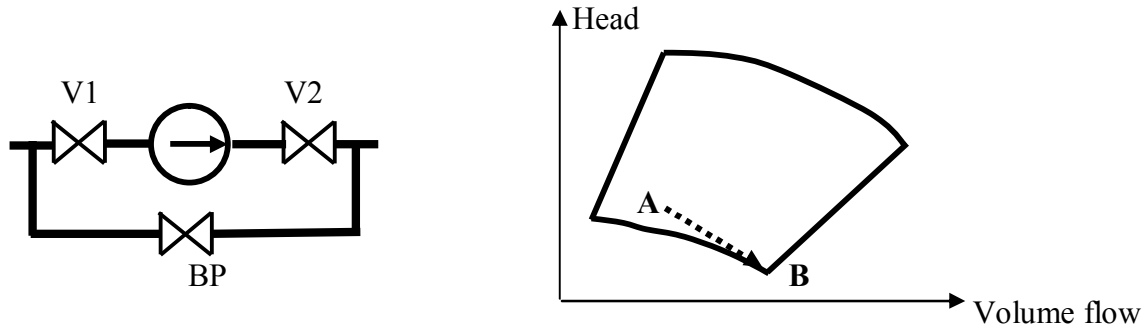
Figure 4.17 a) (left) Schematic CS with valves and **b)** (right) operating point movement in the CS envelope using the bypass valve. Note: the envelope is for one running unit in the station. Multiple running units must be presented as multiple (partially overlapping) envelopes together.

As may be seen from figure 4.17 b), the adiabatic head is not zero at point "B". The discharge to suction pressure ratio at this point may be solved from the equation:

$$\frac{z_s R T_s}{\gamma M_w}\left[\left(\frac{P_d}{P_s}\right)^{\gamma} - 1\right] = H_1\left(q_{VOL}\right) \qquad (4.7)$$

(see equation 3.11, Chapter 3), where $H_1(q_{VOL})$ is the minimum speed line expressed as head as a function of volume flow q_{VOL}. Typically, a pressure ratio greater than one remains at the point where the CS is going to be shut down. This minimum pressure ratio is compressor specific. For example, if the minimum pressure ratio is 1.1, then a suction pressure of 40 bar determines the minimum discharge pressure as 44 bar. Shutting down at this pressure ratio generates a transient in the pipeline system.The reverse operation of starting up a CS is carried out by starting the compressor unit(s) with the bypass valve open. The target is to start at the minimum pressure ratio point "B" in figure 4.17 b, but, similar to shutting down, a transient (or "jump") when moving to point "B" is generated.

In this study, we will not discuss the dynamic events inside CSs related to starting up or shutting down separately. Typically, these dynamic phenomena are very fast and are assumed to fit within the 10-minute control interval. Botros et al. (1996) discuss CS dynamics: for example, the time to achieve the maximum speed from a minimum speed situation is generally less than 3 minutes.

4.6 Constructing the shutdown transient using a linear model

Encouraged by the fact that it is possible to build realistic dynamic simulation models and that the natural gas pipeline system is not severely non-linear, we will construct the shutdown transient of a CS using linear models.

We will limit the discussion to "fast" shutdown events, where the decrease of the discharge pressure and movement to a favourable operating point within the envelope (see figure 4.17), as

well as the final shutdown all take place within the 10-minute basic sampling interval used in this study.

We may write a simple linear, discrete time state-space model for the CS suction pressure as the model output (y) and the discharge pressure as the input (u). The model matrices $\mathbf{A}$, $\mathbf{B}$ and $\mathbf{C}$ can be calculated from the discretised transfer function:

$$\mathbf{x}(k+1) = \mathbf{A}\mathbf{x}(k) + \mathbf{B}u(k),$$
$$y(k) = \mathbf{C}\mathbf{x}(k)$$

(4.8)

Let us assume that the system is in a steady state before the discrete time k=0 and that the CS is running, so that u(k) > y(k) when k<0. If, at k=0, the CS shuts down, the discharge pressure set point u(0),u(1),… cannot be freely determined by operators (or a controller or optimiser), as it must equal the suction pressure. From (4.8), we obtain an expression for y(k), k>0:

$$y(k) = \mathbf{C}\mathbf{A}^k\mathbf{x}(0) + \sum_{i=0}^{k-1}\mathbf{C}\mathbf{A}^{k-1-i}\mathbf{B}u(i)$$

(4.9)

Equating discharge and suction pressures, y(k)=u(k-1) yields a recursive formula, or alternatively, a linear system of equations for computing u(0),u(1),u(2),… If a linear, discrete-time model exists, with model matrices $\mathbf{A_2}$, $\mathbf{B_2}$, $\mathbf{C_2}$ and state vector $\mathbf{x_2}$ for another pipeline variable y_2, which depends on the discharge pressure of the CS shutting down, we may substitute the computed sequence u(0),u(1),u(2),…. into the expression:

$$y_2(k) = \mathbf{C_2}\mathbf{A_2}^k\mathbf{x_2}(0) + \sum_{i=0}^{k-1}\mathbf{C_2}\mathbf{A_2}^{k-1-i}\mathbf{B_2}u(i)$$

(4.10)

The calculation of the shutdown transient is discussed in more detail in Chapter 6.

Next, we will use "Simone" to demonstrate how the shutdown transient construction procedure works.

Figure 4.18 shows the simulated discharge pressure (dashed line) and suction pressure (solid line) when CS2 in the Finnish gas pipeline is shutting down in a steady-state situation. The discharge pressure is 51 bar and the suction pressure about 40 bar prior to shut down, which is a quite large pressure ratio, chosen on purpose in order to demonstrate a large transient. Immediately after shutdown, the suction pressure *exceeds* the discharge pressure for a short time period. There is no physical reason for this; obviously "Simone" does have some difficulties with accurately simulating this type of event.
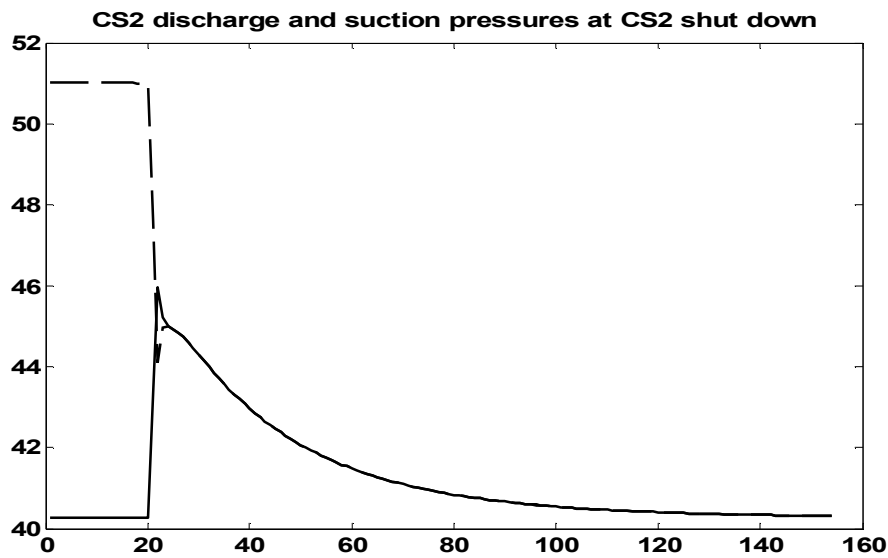
Figure 4.18 Responses to CS2 shut down at time point 20. Time axis in 10-minute intervals.

Figure 4.19 shows the CS2 suction pressure calculated by "Simone" (solid line) from figure 4.18 and the suction pressure constructed with a linear model (dashed line) as explained above.
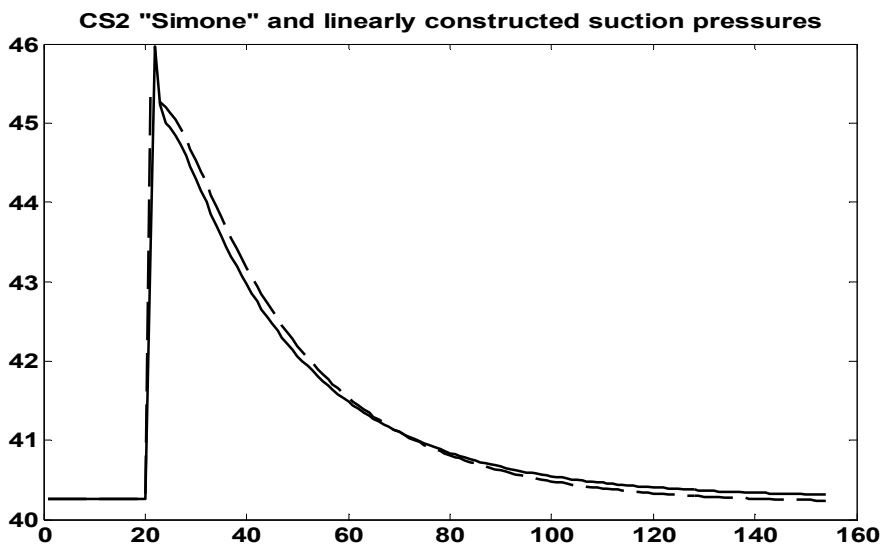

Figure 4.19 Comparison between the CS2 suction pressure from "Simone" and a linear model.

Figure 4.20 shows the suction pressure response of the downstream CS3 to the CS2 shutdown event, calculated using the discharge pressure sequence obtained from the linear model as the input to the discrete, linear model for CS3 suction pressure (compare (4.10)). At the end of the period, a difference of 2 bar can be observed. The reason is that the non-linearity of the pipeline becomes visible when a pressure change of this order occurs. The suction pressure of CS3 decreases as much as 15 bar. The steady-state value of CS2 discharge pressure is 51 bar and

50

CS3 suction pressure is 38.5 bar before shutdown, suggesting a linear model for CS3 suction pressure to have a gain of 51/38.5 = 1.325. After the shutdown, corresponding steady-state values are 40 and 24 bar, respectively, which yields a gain of 1.667.
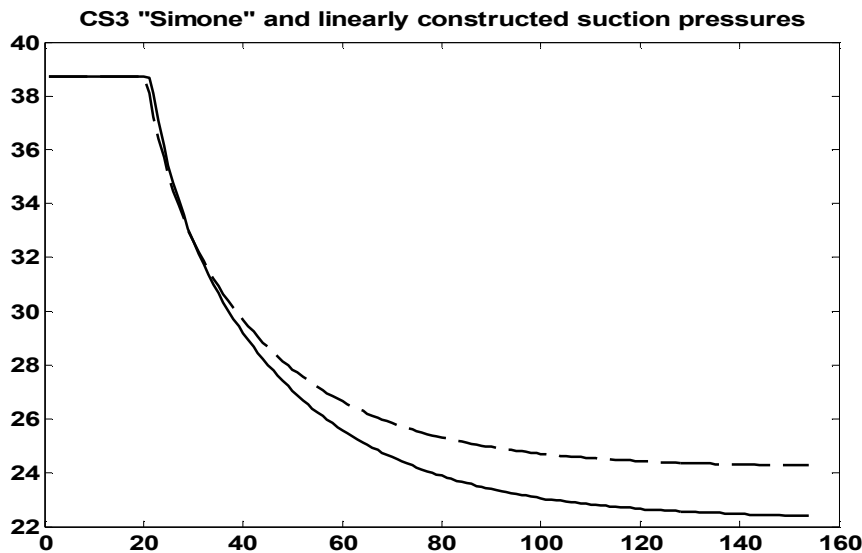
Figure 4.20 CS3 suction pressure when CS2 is shut down. Solid line = "Simone", dashed line = linear model.

The CS2 shutdown was simulated with the CSs in "free mode", which means that the CS envelopes are disabled. The simulation starts at the steady-state conditions of operating point no. 1 (see Table A.1, Appendix A), where the discharge pressure of CS3 is 48.6 bar. Inserting this and the new value 22.5 bar (almost a steady-state value, see table A.2, Appendix A) into the adiabatic head expression gives 101.6 kJ/kg; however the maximum adiabatic head on the maximum speed limit of CS3 configured into "Simone" yields 57.7 kJ/kg. In other words, the CS3 envelope would be violated. Decreasing the CS3 discharge pressure from 48.6 to 36.2 bar yields an adiabatic head of 57.7 kJ/kg, the Px3 pressure will decrease far below the minimum limit of 29 bar, which means that it is *not feasible* to shut down CS2 when the pipeline system is in operating point no. 1.

4.7 Comments and discussion

As can be seen in Appendix A, the dynamics of the pipeline changes when the gas consumption changes and when CSs are shut down and started up. For a moderate number of CSs in a pipeline system, it is not too difficult to identify linear models for different combinations of CSs running and shut down. The simple formula (4.4) is available for a pipeline segment gain, which, in an "adaptive control" setting can be applied by using measured long-term average values for P_1 and P_2.

A simulator may be used to evaluate the pipeline system time constants. As was shown in section 4.3, "Simone" models the Finnish pipeline system with a good level of accuracy. With a reliable simulator, a bank of models for different off-take flow scenarios can be built up. The

logic is simple: if the simulator matches reality and if the linear models match the simulator, then the linear models match the reality. This logic is not foolproof and must be used with care and judgement.

Kra'lik et.al. (1984, B) present a universal dynamic simulation model for pipelines based on linearised transfer function models for pipeline elements as shown in section 4.4.3. This universal model is the basis for "Simone" and matches the dynamics of real pipelines very well.

The temporary "spikes" in the simulated discharge and suction pressures of a CS shutting down from relatively high pressure (see figure 4.18) are probably due to some internal numerical difficulties within the "Simone" differential equation solver. Unfortunately, the version of "Simone" used in this study does not offer any means to adjust integration parameters, such as tolerances and stepping characteristics.

Chapter 5

Real-time receding horizon optimisation

In this chapter, we start with presenting a general, non-linear receding horizon optimisation and control problem. The development of receding horizon, predictive control in the 1970's was initiated by linear methods, since control problems based on linear models are so much easier to solve than non-linear problems. A number of authors have used mixed linear and non-linear approaches.

5.1 Optimisation and control

A discrete-time receding horizon real-time optimisation problem can be defined as finding an optimal sequence of inputs $\mathbf{u}(k)$, $\mathbf{u}(k+1)$,…,$\mathbf{u}(k+M-1)$ at the discrete moment of time "k" based on historical values of measured system outputs $\mathbf{y}(-\infty)$,…,$\mathbf{y}(k-1)$, $\mathbf{y}(k)$ and inputs $\mathbf{u}(-\infty)$, …, $\mathbf{u}(k-2)$, $\mathbf{u}(k-1)$ as well as predicted values of the system output $\hat{\mathbf{y}}(k+1)$, $\hat{\mathbf{y}}(k+2)$, …$\hat{\mathbf{y}}(k+P)$ over the *prediction horizon* P. The optimal inputs are obtained by solving the optimisation problem:

$$\underset{\mathbf{u}(k),\mathbf{u}(k+1),...,\mathbf{u}(k+M-1)}{\text{Min}} \quad J(k) = \sum_{i=1}^{P} c_i [\hat{\mathbf{y}}(k+i)), \mathbf{u}(k+i-1)] \qquad (5.1)$$

where c_i is a suitable cost function. The optimisation problem is subject to the constraints:

$$\mathbf{x}(k+1) = \mathbf{F}(\mathbf{x}(k), \mathbf{u}(k), \mathbf{d}(k), \mathbf{v}_1(k)) + \mathbf{v}_2(k) \qquad (5.2)$$

$$\mathbf{y}(k) = \mathbf{G}(\mathbf{x}(k), \mathbf{v}_3(k)) + \mathbf{v}_4(k) \qquad (5.3)$$

$$\mathbf{h}(\mathbf{x}(k), \mathbf{y}(k), \mathbf{u}(k)) \leq 0 \qquad (5.4)$$

$$\mathbf{u}(k+M+i) = \mathbf{u}(k+M-1), i = 0, 1, ..., P-M-1 \qquad (5.5)$$

where the dimensions of the vectors $\mathbf{u}$, $\mathbf{y}$ and $\mathbf{x}$ are, respectively, m, n and r. $\mathbf{d}(k)$ is a known disturbance acting on the system (at least up to and including time "k", but possibly also over the whole prediction horizon). $\mathbf{v}_1(k)$ to $\mathbf{v}_4(k)$ are unknown disturbances, all of which do not need to be present in the problem. The non-linear discrete-time system model (5.2) and (5.3) is usually not as such available, rather it must be seen as a "short hand notation" for integrating a system of non-linear, continuous time differential equations over the sampling interval ΔT. (5.4) is a set of non-linear inequality constraints for the optimisation problem and (5.5) sets input signals beyond the *control horizon* M, M<P, equal. For a non-linear receding horizon model predictive control (MPC) problem, we define

$$c_i = (\mathbf{y}_i^R - \hat{\mathbf{y}}(k+i))^T \mathbf{W}_i^y (\mathbf{y}_i^R - \hat{\mathbf{y}}(k+i)) +$$
$$(\mathbf{u}_i^R - \mathbf{u}(k+i-1))^T \mathbf{W}_i^u (\mathbf{u}_i^R - \mathbf{u}(k+i-1)) + \qquad (5.6)$$
$$(\mathbf{u}(k+i-1) - \mathbf{u}(k+i-2))^T \mathbf{R}_i (\mathbf{u}(k+i-1) - \mathbf{u}(k+i-2))$$

where $\mathbf{y}_i^R$ are reference value (set point) n-vectors for the outputs, $\mathbf{u}_i^R$ are reference (or target) value m-vectors for the inputs and $\mathbf{W}_i^y, \mathbf{W}_i^u$ and $\mathbf{R}_i$ are, respectively, nxn, mxm and mxm weighting matrices for the control error, input target deviation and control move penalty. If the system model (5.2) and (5.3) as well as the inequality constraints (5.4) are linear, then we have the linear model predictive control (LMPC) problem.

The term "receding horizon" is used, because after solving the optimisation or control problem, $\mathbf{u}(k)$ is implemented and the rest of the optimal input sequence is deleted, while, at the next control interval "k+1" the whole procedure is repeated. In order to achieve closed loop optimisation or control, the measured system output must be accounted for through some estimation mechanism at each sample time "k".

Generally, it is very demanding to solve the general, non-linear MPC problem. Therefore, non-linear systems are frequently approximated by linear ones, so that LMPC can be applied instead. There are different options within LMPC for obtaining optimal output predictions $\hat{\mathbf{y}}(k+1), \ \hat{\mathbf{y}}(k+2), \ ...\hat{\mathbf{y}}(k+P)$, as will be seen below.

There is a vast amount published on the subject of MPC (Morari and Lee, 1999). LMPC is more popular in industrial applications, because of its longer history and proven performance capability. Non-linear MPC is developing and is to some extent applied in industry, but there are still some challenges to be solved. Discrete (or integer) decision variables introduced as a part of the MPC problem will further extend industrial applicability. In recent years, receding horizon optimisation, where a cost function describing the economic performance of the target system is used, has been the subject of research.

One of the early publications on receding horizon optimisation is Marque's and Morari (1988) discussed in Chapter 3.

Abou-Jeyab et al. (2001) combine LMPC of a distillation column with the economic objective to maximise the column's reflux flow rate. The control error objective function is linear and the problem is solved by Linear Programming (LP). The objective function is augmented by subtracting the reflux flow times a weighting factor from the original control error. The reflux flow rate is itself a manipulated variable, i.e. it is a component of the control variable vector $\mathbf{u}$.

Ferrari-Trecate et al. (2002) use MPC to minimise the impact of lifetime changes of power plant components on a plant's asset value. A dynamical lifetime model is derived, including discrete variables (plant component status: "running", "starting up" or "shutting down"), which introduces discrete decision variables into the optimisation problem. Since the dynamic models and cost functions are linear, Linear Mixed Integer Programming (LPMIP) is used. The accuracy of linearised plant and cost models may be increased at will by using piecewise affine model sets, from among which individual models are selected during the optimisation by dedicated discrete decision variables.

Perea-Lo´pez et al. (2003) and Seferlis and Giannelos (2003) use MPC for optimisation of supply chains. The supply chain is a network of raw material suppliers, manufacturers of goods,

warehouses, distribution centres, retailers and end consumers. The flow of goods and information in the supply chain is modelled. Dynamics are introduced by the storage facilities at warehouses, distribution centres and retailers. Transportation delay is also present. The objective is to maximise profit of the complete chain using commands on how much to produce and transport in each part of the network. The problem contains discrete decision variables, but otherwise models are linear whereby it can be solved as an LPMIP problem.

Bemporad and Morari (1999) present an example of MPC of a gas supply system, which actually is a *hybrid system*. Hybrid systems are linear dynamic systems containing both continuous and discrete input, state and output variables. Intensive research has been conducted on this subject during the past few years. A conventional, quadratic control error criterion is used as the cost function of the optimal control problem, to which a linear "non-profit" function is added, which is the difference between the maximum achievable profit and the predicted profit of the supply system.

Gallestey et al. (2003) present a two-level optimisation scheme for the scheduling of industrial processes using MPC and hybrid systems. At the higher level, a general, non-linear cost function, defined as the operating costs of the process subtracted by the revenues, is minimised by finding optimal command sequences of the decision variables, which are given as reference values to be followed by the lower level optimiser, which minimises a quadratic error function like (5.6) above. The optimisation scheme allows a non-linear cost function at the higher level and non-linear process models, but the example presented consists of a combined cycle power plant described by linear models and a linear higher-level cost function.

The receding horizon optimisation or control problem can be illustrated as in Figure 5.1. The past input and output values before the present time "k" are used to calculate the predicted outputs for time steps k+i, i=1,2,...,P in the future under the assumption, that there is no change in future input values from the latest implemented input value $\mathbf{u}$(k-1). This is often referred to as the "free response". The final output response is a combination of the free response and the response to optimal future input variables $\mathbf{u}$(k), $\mathbf{u}$(k+1),..., $\mathbf{u}$(k+M-1) to be determined by the optimiser or controller at time "k". If the system model (5.2) and (5.3) is linear, then the combination is a simple addition, otherwise not.
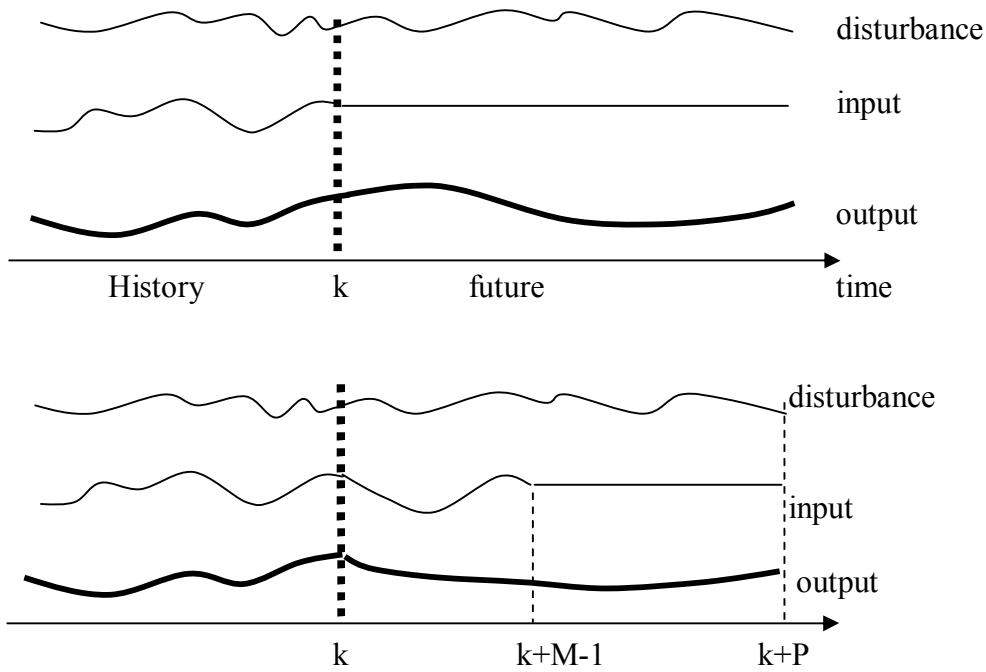
Figure 5.1 The two steps involved with receding horizon optimisation and control. Upper figure: determine free output response assuming no change in input and assumed or known disturbance behaviour. Lower figure: determine future inputs so, that a desired predicted output behaviour is obtained.

The literature dealing with MPC thoroughly discusses unknown and measured disturbances (see (5.2) and (5.3)) and their impact on the system to be controlled or optimised. However, known and predicted disturbances $\mathbf{d}(k+1)$, $\mathbf{d}(k+2),\ldots$, $\mathbf{d}(k+P)$ are rarely dealt with. In this work, both unknown and predicted disturbances are present, the latter being the gas consumption forecasts over the prediction horizon at each off-take. It is fairly straightforward to implement predicted disturbances into MPC or receding horizon optimisation, while, algorithm-wise, they constitute a known feed-forward path.

5.2 Linear optimal predictors

The optimal, stochastic minimum variance predictor (Åström, 1970) was originally derived for a single-input single-output (SISO) system and for one step ahead only (one specific moment of time in then future). De Keyser and van Cauwenberghe (1981) extended the one-step prediction to multi-step self-adaptive prediction for the SISO system:

$$A(q^{-1})y(k)=B(q^{-1})u(k)+C(q^{-1})e(k) \qquad (5.7)$$

where A, B and C are, respectively, n_a-, n_b- and n_c-degree polynomials in the shift operator q^{-1}, $q^{-1}y(k)=y(k-1)$. The prediction error in the future, $P\geq j>0$, is:

$$v(k+j)=y(k+j)-\hat{y}(k+j|k) \qquad (5.8)$$

The optimal prediction problem is defined as finding a value of $\hat{y}(k+j|k)$ to minimise the variance of v(k+j). In the sequel, writing $\hat{y}(k+j|k)$ for the predicted output emphasises, that it is calculated at discrete time "k". The parameters, i.e. coefficients of the polynomials H_j, F_j and G_j of the following j=1,2,...,P prediction models are estimated from process data:

$$v(k)=H_j(q^{-1})v(k-j)+F_j(q^{-1})\hat{y}(k|k-j)+G_j(q^{-1})u(k)+\varepsilon(k) \qquad (5.9)$$

where $\varepsilon(k)$ is a residual error term. The predictions are then calculated from (note, that f_{j0}=-1 in all $F_j(q^{-1}) = f_{j0}+f_{j1}q^{-1}+f_{j2}q^{-2}+...$):

$$\hat{y}(k+j|k)=(1+F_j(q^{-1}))\hat{y}(k+j|k)+G_j(q^{-1})u(k+j)+H_j(q^{-1})v(k) \qquad (5.10)$$

For the first predictor, j=1, the following holds, if the parameter estimates converge: $F_1(q^{-1})$=-$A(q^{-1})$, $G_1(q^{-1})$=$B(q^{-1})$, $qH_1(q^{-1})$=$F_1(q^{-1})$-f_{10}.

If the system model (5.7) is known, no parameter estimation is needed, but the coefficients of the polynomials in (5.10) must be calculated from a set of Diophantine equations.

Separate prediction models for $\hat{y}(k+j|k)$,j=1,2,...,P together with parameter estimation when the system model is unknown requires a large computational capacity when P is large. It can be shown that only the prediction models for $\hat{y}(k+1|k), \hat{y}(k+2|k),..., \hat{y}(k+n_a|k)$ are needed and the remaining P-n_a predictions can be calculated by propagating the original system model (5.7). De Keyser et al. (1988) further simplify the issue by using a predictor only for $\hat{y}(k+1|k)$ and propagating the system model for the remaining 2,…,P predictions.

Clarke et al. (1987 A) introduced Generalised Predictive Control (GPC) for SISO systems based on linear optimal stochastic prediction. Kinnaert (1989) extended GPC for MIMO systems described by the system model:

$$A(q^{-1})\Delta y(k)=B(q^{-1})\Delta u(k)+C(q^{-1})e(k) \qquad (5.11)$$

where **A**, **B** and **C** are matrix polynomials in the shift operator q^{-1}:

$$A(q^{-1}) = I+A_1q^{-1} + A_2q^{-2} +...A_{na}q^{-na}$$
$$B(q^{-1}) = B_1q^{-1} + B_2q^{-2} +...B_{nb}q^{-nb} \qquad (5.12)$$
$$C(q^{-1}) = I+C_1q^{-1} + C_2q^{-2} +...C_{nc}q^{-nc}$$

and the operator Δ is defined as $\Delta =1 - q^{-1}$, for example, $\Delta u(k)$=$u(k)$-$u(k-1)$. A_i and C_i are n x n matrices and B_i are n x m matrices. **I** is an n x n identity matrix. $e(k)$ is a white noise disturbance vector. In the sequel, q^{-1} is left out from the matrix polynomials.

The j-step ahead predictor for (5.11) is:

$$\hat{\mathbf{y}}(k+j|k)=\mathbf{G_j}\mathbf{y}(k)+\mathbf{F_j}\mathbf{B}\Delta\mathbf{u}(k+j)+\mathbf{V_j}\mathbf{e}(k) \ , \ j=1,...,P \qquad (5.13)$$

where $\mathbf{y}(k)$ is the vector of measured outputs and the matrix polynomials $\mathbf{G_j}$ and $\mathbf{F_j}$, where $\mathbf{F_j}$ is of degree j-1, are solved from Diophantine equations:

$$\mathbf{I} = \mathbf{F_j}\mathbf{A}\Delta + q^{-j}\mathbf{G_j} \tag{5.14}$$

and $\mathbf{V_j}$ consists of the last n_c-j+1 terms of $q^j\mathbf{F_j}\mathbf{C}$. Recursion formulas using initial values $\mathbf{F_1} = \mathbf{I}$ and $\mathbf{G_1} = q[\mathbf{I} - \mathbf{A}\Delta]$ for computing $\mathbf{F_j}$ and $\mathbf{G_j}$ can be derived.

Henttonen (1996) uses no linear optimal predictor at all in his simplified version of GPC for MIMO systems, because all predicted output values $\hat{\mathbf{y}}(k+1|k), \hat{\mathbf{y}}(k+2|k),...,\hat{\mathbf{y}}(k+P|k),$ are obtained by propagating the system model equation (5.11).

5.3 Linear state-space model-based predictors

In LMPC, the predicted system output $\widehat{\mathbf{Y}}(k)$ is written as a sum of the predicted free response at moment "k", $\widehat{\mathbf{Y}}(k-1)$ and the contribution of the future inputs using either a step response matrix $\mathbf{S}$ or an impulse response matrix $\mathbf{H}$:

$$\widehat{\mathbf{Y}}(k) = \mathbf{S}\Delta\tilde{\mathbf{u}}(k) + \widehat{\mathbf{Y}}(k-1) \tag{5.15}$$

$$\widehat{\mathbf{Y}}(k) = \mathbf{H}\tilde{\mathbf{u}}(k) + \widehat{\mathbf{Y}}(k-1) \tag{5.16}$$

where:

$\widehat{\mathbf{Y}}(k) = [\hat{y}_1(k+1|k)\ \hat{y}_1(k+2|k)...\hat{y}_1(k+P|k)\ |\ \hat{y}_2(k+1|k)\ \hat{y}_2(k+2|k)...\hat{y}_2(k+P|k)\ |...$

$\qquad \hat{y}_n(k+1|k)\ \hat{y}_n(k+2|k)...\hat{y}_n(k+P|k)\ ]^T$

$\Delta\tilde{\mathbf{u}}(k) \triangleq [\Delta u_1(k)\ \Delta u_1(k+1)\cdots\Delta u_1(k+M-1)\ |\Delta u_2(k)\ \cdots\Delta u_2(k+M-1)\ |\cdots$

$\qquad \Delta u_m(k)\cdots\Delta u_m(k+M-1)\ ]^T$

$\tilde{\mathbf{u}}(k) \triangleq [u_1(k)\ u_1(k+1)\cdots u_1(k+M-1)\ |u_2(k)\ \cdots u_2(k+M-1)\cdots\ |u_m(k)\cdots u_m(k+M-1)\ ]^T$

The prediction expressions (5.15) and (5.16) can be derived based on quite simple intuitive arguments (Cutler and Ramaker, 1980; Martin, 1981).

The nP x mM system step response matrix $\mathbf{S}$ has the structure:

$$\mathbf{S} = \begin{pmatrix} \mathbf{S_{11}} & \cdots & \mathbf{S_{1m}} \\ \vdots & \ddots & \vdots \\ \mathbf{S_{n1}} & \cdots & \mathbf{S_{nm}} \end{pmatrix} \tag{5.17}$$

where each P x M matrix $\mathbf{S_{ij}}$ contains the step response coefficients for input u_j to output y_i :

$$\mathbf{S}_{ij} = \begin{pmatrix} s_{ij}(1) & 0 & 0 & 0 & 0 \\ s_{ij}(2) & s_{ij}(1) & 0 & 0 & 0 \\ s_{ij}(3) & s_{ij}(2) & s_{ij}(1) & 0 & 0 \\ \vdots & & & \vdots & \vdots \\ \vdots & & \cdots & s_{ij}(1) & 0 \\ & & & s_{ij}(2) & s_{ij}(1) \\ & & & \vdots & \vdots \\ s_{ij}(P) & s_{ij}(P-1) & s_{ij}(P-2) & s_{ij}(P-M+2) & s_{ij}(P-M+1) \end{pmatrix} \qquad (5.18)$$

The free response prediction $\hat{\mathbf{Y}}(k-1)$ must, at moment "k", be updated with the latest measured system output values. A non-minimal state-space model can be used as a basis for the estimator design required (Li et al., 1989), among others:

$$\mathbf{X}(k) = \mathbf{M}_{ss}\mathbf{X}(k-1) + \mathbf{S}_{1}\Delta\mathbf{u}(k-1) \qquad (5.19)$$

where

$$\mathbf{X}(k) = [\hat{y}_1(k|k\text{-}1)\ \hat{y}_1(k+1|k\text{-}1)...\hat{y}_1(k+P|k\text{-}1)\ |\ \hat{y}_2(k|k\text{-}1)...\hat{y}_2(k+P|k\text{-}1)\ |...$$
$$\hat{y}_n(k|k\text{-}1)...\hat{y}_n(k+P|k\text{-}1)\ ]^T$$

$$\mathbf{X}(k-1) = [\hat{y}_1(k-1|k\text{-}2)\ \hat{y}_1(k|k\text{-}2)...\hat{y}_1(k+P-1|k\text{-}2)\ |\ \hat{y}_2(k-1|k\text{-}2)...\hat{y}_2(k+P-1|k\text{-}2)\ |...$$
$$\hat{y}_n(k-1|k\text{-}2)...\hat{y}_n(k+P-1|k\text{-}2)\ ]^T$$

The length of the state vector $\mathbf{X}$ is n x (P+1) to include, for each output, the current output value at time "k" and P predicted values.

$\mathbf{M}_{ss}$ is a block diagonal matrix with n shift matrices $\mathbf{M}_s$, diag($\mathbf{M}_s$, $\mathbf{M}_s$,. .., $\mathbf{M}_s$), each of dimension (P+1) x (P+1):

$$\mathbf{M}_s = \begin{pmatrix} 0 & 1 & 0 & \cdots & 0 & 0 \\ 0 & 0 & 1 & \cdots & 0 & 0 \\ \vdots & \vdots & \vdots & \ddots & \vdots & \vdots \\ 0 & 0 & \cdots & 0 & 0 & 1 \\ 0 & 0 & \cdots & 0 & 0 & 1 \end{pmatrix} \qquad (5.20)$$

$\mathbf{S}_1$ is a n(P+1) x m dimensional matrix used to account for the last implemented incremental input and is obtained by expanding the step response matrix $\mathbf{S}$ by one sample interval to a n(P+1) x mM matrix and then, in each sub-matrix $\mathbf{S}_{ij}$, delete all columns except the left-most ones:

$$\mathbf{S_1} = \begin{pmatrix} \begin{array}{c} s_{11}(1) \\ \vdots \\ s_{11}(P+1) \end{array} & \begin{array}{c} s_{12}(1) \\ \vdots \\ s_{12}(P+1) \end{array} & \cdots & \begin{array}{c} s_{1m}(1) \\ \vdots \\ s_{1m}(P+1) \end{array} \\ \begin{array}{c} s_{21}(1) \\ \vdots \\ s_{21}(P+1) \end{array} & \begin{array}{c} s_{22}(1) \\ \vdots \\ s_{22}(P+1) \end{array} & & \begin{array}{c} s_{2m}(1) \\ \vdots \\ s_{2m}(P+1) \end{array} \\ & \vdots & & \\ \begin{array}{c} s_{n1}(1) \\ \vdots \\ s_{n1}(P+1) \end{array} & \begin{array}{c} s_{n2}(1) \\ \vdots \\ s_{n2}(P+1) \end{array} & & \begin{array}{c} s_{nm}(1) \\ \vdots \\ s_{nm}(P+1) \end{array} \end{pmatrix} \tag{5.21}$$

A final state update model for the free response prediction is obtained by using a Kalman filter:

$$\overline{\mathbf{X}}(k) = \mathbf{M_{ss}}\mathbf{X}(k-1) + \mathbf{S_1}\mathbf{\Delta u}(k-1)$$
$$\mathbf{X}(k) = \overline{\mathbf{X}}(k) + \mathbf{K}(\mathbf{y_M}(k) - \mathbf{T}\overline{\mathbf{X}}(k)) \tag{5.22}$$
$$\widehat{\mathbf{Y}}(k-1) = \mathbf{H}\mathbf{X}(k)$$

where $\mathbf{K}$ is a n(P+1) x n dimensional Kalman filter gain matrix. $\mathbf{T}$ is an n x n(P+1) "output" matrix used to pick the predicted output values corresponding to the measured values $\mathbf{y_M}(k)$: for i=1,2,…,n, T_{ij}=1 if j=i(P+1)-P, otherwise T_{ij}=0. $\mathbf{H}$ is an nP x n(P+1) shift matrix modified from $\mathbf{M_{ss}}$ so, that the last row of each $\mathbf{M_s}$ is left away.

The predictor based on the non-minimal state-space model does not perform well, when system outputs have integrating characteristics (Lee et al., 1994). Adding one extra state per output to account for the residual dynamics past P and extra states for an improved disturbance model improves LMPC performance.

Lundström et al. (1995) showed how slow system responses, which are stable but do not reach steady state within P, can severely degrade the performance of MPC. They also showed that the state-space interpretation of Lee et al. (1994) for integrating responses works well in cases with slow responses.

The prediction equations may also be derived based on a (minimal) linear, discrete time state-space representation of the system (Ricker, 1990), with a known and predicted disturbance $\mathbf{d}(k)$ acting on the system:

$$\mathbf{x}(k+1) = \mathbf{Ax}(k) + \mathbf{Bu}(k) + \mathbf{Ed}(k)$$
$$\mathbf{y}(k) = \mathbf{Cx}(k) \tag{5.23}$$

The predicted and corrected (with measured outputs) state estimates are:

$$\overline{\mathbf{x}}(k|k-1) = \mathbf{A}\widehat{\mathbf{x}}(k-1|k-2) + \mathbf{Bu}(k-1) + \mathbf{Ed}(k-1)$$
$$\widehat{\mathbf{x}}(k|k-1) = \overline{\mathbf{x}}(k|k-1) + \mathbf{K}\left(\mathbf{y_M}(k) - \mathbf{C}\overline{\mathbf{x}}(k|k-1)\right) \tag{5.24}$$

and the prediction equation becomes:

$$\hat{\mathbf{Y}}(k) = \mathbf{H} \begin{pmatrix} \mathbf{u}(k) \\ \mathbf{u}(k+1) \\ \vdots \\ \mathbf{u}(k+P-1) \end{pmatrix} + \begin{pmatrix} \mathbf{CA} \\ \mathbf{CA}^2 \\ \vdots \\ \mathbf{CA}^P \end{pmatrix} \hat{\mathbf{x}}(k|k-1) + \begin{pmatrix} \mathbf{CE} & 0 & \cdots & 0 & 0 \\ \mathbf{CAE} & \mathbf{CE} & \cdots & 0 & 0 \\ \mathbf{CA}^2\mathbf{E} & \mathbf{CAE} & \cdots & \vdots & \vdots \\ \vdots & \vdots & \ddots & \vdots & \vdots \\ \mathbf{CA}^{P\text{-}1}\mathbf{E} & \mathbf{CA}^{P\text{-}2}\mathbf{E} & \cdots & \mathbf{CAE} & \mathbf{CE} \end{pmatrix} \begin{pmatrix} \mathbf{d}(k) \\ \mathbf{d}(k+1) \\ \vdots \\ \mathbf{d}(k+P-1) \end{pmatrix} + \ldots$$

$$+ \begin{pmatrix} \mathbf{CK} \\ \mathbf{CAK}+\mathbf{CK} \\ \vdots \\ \mathbf{CA}^{P-1}\mathbf{K}+\ldots+\mathbf{CAK}+\mathbf{CK} \end{pmatrix} (\mathbf{y}_\mathbf{M}(k) - \mathbf{C}\bar{\mathbf{x}}(k|k-1))$$

$$(5.25)$$

where $\mathbf{H}$ is the nP x mP impulse response matrix:

$$\mathbf{H} = \begin{pmatrix} \mathbf{CB} & 0 & 0 & \cdots & 0 & 0 \\ \mathbf{CAB} & \mathbf{CB} & 0 & \cdots & 0 & 0 \\ \mathbf{CA}^2\mathbf{B} & \mathbf{CAB} & \mathbf{CB} & \cdots & \vdots & \vdots \\ \vdots & \vdots & \vdots & \ddots & \vdots & \vdots \\ \mathbf{CA}^{P\text{-}1}\mathbf{B} & \mathbf{CA}^{P\text{-}2}\mathbf{B} & \mathbf{CA}^{P\text{-}3}\mathbf{B} & \cdots & \mathbf{CAB} & \mathbf{CB} \end{pmatrix} \qquad (5.26)$$

The output prediction vector is now organised in a different way as
$$\hat{\mathbf{Y}}(k) = [\hat{y}_1(k+1|k)\, \hat{y}_2(k+1|k)...\hat{y}_n(k+1|k) \;|\; \hat{y}_1(k+2|k)\, \hat{y}_2(k+2|k)...\hat{y}_n(k+2|k) \;|...$$
$$... \; \hat{y}_1(k+P|k)\, \hat{y}_2(k+P|k)...\hat{y}_n(k+P|k)]^\mathrm{T}$$

5.4 Non-linear and linearised predictors

For non-linear systems, the state estimators and predictors are, by nature, non-linear. Because very computation-intensive algorithms result, different simplifications have been proposed. For the state estimation at moment "k", Gattu and Zafiriou (1992) use a Kalman filter, whose gain matrix $\mathbf{K}_\mathbf{k}$ is calculated at each moment based on the linearised system state equation in $\hat{\mathbf{x}}(k|k\text{-}1), \mathbf{u}(k\text{-}1)$. $\hat{\mathbf{e}}(k)$ is the difference between measured and model output, which is assumed to be constant over the whole prediction horizon, while no information regarding the future evolution of that difference is available:

$$\hat{\mathbf{e}}(k) = \mathbf{y}_\mathbf{M}(k) - \mathbf{G}(\hat{\mathbf{x}}(k|k-1)) \qquad (5.27)$$

where $\hat{\mathbf{x}}(k|k-1)$ is the current state estimate. The prediction equations for i=1,2,…,P are now:

$$\hat{\mathbf{x}}(k+i|k-1) = \mathbf{F}(\hat{\mathbf{x}}(k+i-1|k-1), \mathbf{u}(k+i-1), \mathbf{d}(k+i-1)) + \mathbf{K}_\mathbf{k}\hat{\mathbf{e}}(k)$$
$$\hat{\mathbf{y}}(k+i|k) = \mathbf{G}(\hat{\mathbf{x}}(k+i|k-1)) + \hat{\mathbf{e}}(k) \qquad (5.28)$$

To avoid a non-linear optimisation problem for calculating the optimal input sequence $\mathbf{u}(k)$, $\mathbf{u}(k+1),\ldots,$ $\mathbf{u}(k+P-1)$, they choose to set $\mathbf{u}(k+i-1)=\mathbf{u}(k-1)$ in (5.28) which is equivalent to, that the output predictions $\hat{\mathbf{y}}(k+i|k)$ constitute the free response of the system. They assume, that the response to future inputs $\mathbf{u}(k)$, $\mathbf{u}(k+1),\ldots,$ $\mathbf{u}(k+P-1)$ is approximately linear and use the linearised system model to obtain an impulse response matrix. The final result is a prediction equation like (5.16).

Lee and Ricker (1994) improved the disturbance model of Gattu and Zafiriou (1992) to allow the method to be applied with unstable systems and to avoid the high risk of obtaining erroneous state estimates. Inadequate state estimation may be disastrous from an overall performance point of view, since the linearisation performed at each sample interval may fail. The non-linear difference equation model (5.2) and (5.3) is augmented with a linear disturbance model:

$$\mathbf{x}_v(k+1) = \mathbf{A}_v \mathbf{x}_v(k) + \mathbf{B}_v \mathbf{v}(k)$$
$$\hat{\mathbf{e}}(k) = \mathbf{C}_v \mathbf{x}_v(k)$$

(5.29)

The state of the augmented system, $\left[\hat{\mathbf{x}}(k)^T \quad \hat{\mathbf{x}}_v(k)^T \right]^T$ is estimated at each control interval using an extended Kalman filter (EKF). Without showing the detailed equations, the main difference compared to the free response prediction in Gattu and Zafiriou (1992) is that all the output error $\hat{\mathbf{e}}(k+i-1)$, i=1,2,...,P is not constant over the prediction horizon and consequently, each predicted state and output value at all points in the prediction horizon is updated in a distinct way.

Gattu and Zafiriou (1995) further extend the disturbance models in order to obtain good state estimates for step-like disturbances at the system input or output. They also discussed the use of input/output models, such as neural networks, as the non-linear system model:

$$\mathbf{y}(k) = \mathbf{f}(\mathbf{y}(k-1), \mathbf{y}(k-2),..., \mathbf{y}(k-n_y), \mathbf{u}(k-1), \mathbf{u}(k-2),..., \mathbf{u}(k-n_u)) \quad (5.30)$$

where $\mathbf{f}$ is a vector-valued function with dimension n. This is linearised in order to obtain the model with constant matrices $\mathbf{A_1}$, $\mathbf{A_2}$,… $\mathbf{B_1}$, $\mathbf{B_2}$…:

$$[\mathbf{I}+\mathbf{A}_1 q^{-1} + \mathbf{A}_2 q^{-2} +...\mathbf{A}_{ny} q^{-ny}]\mathbf{y}(k)=[\mathbf{B}_1 q^{-1} + \mathbf{B}_2 q^{-2} +...\mathbf{B}_{nu} q^{-nu}]\mathbf{u}(k) \quad (5.31)$$

This input-output model is used instead of a state-space model.

5.5 Selecting the type of predictor and value of the prediction horizon

Early predictor development was based on systems with low complexity, SISO systems initially, and only one future system output value was predicted (Åström, 1970). P in this case was set to T_d+1, where T_d is the discrete dead time of the system, to ensure good closed loop control. Later it became evident that for long-range prediction with large P, several values in the future had to be predicted (de Keyser, et al., 1988). The optimal predictors derived originally for small P and few predicted values became too computation intensive, which suggested different types of

approximations, as was shown in section 5.2. GPC was criticized as not being very suitable for industrial-scale MIMO systems with constraints on the system variables (Morari and Lee, 1999).

The predictor equations obtained by direct application of linear step or impulse response models are simple to understand and do not require much computational load, even if adequate disturbance models and state estimation schemes are applied. Hence, this class of predictors is well suited for large P. As a matter of fact, a large P is a default for these methods, because for good LMPC performance, P should be selected in most cases so that the system responses almost reach steady state within P (Cutler and Ramaker, 1980).

The linear state-space model (5.19) is truly non-minimal, especially for a long prediction horizon P, the number of states being n(P+1). The state-space model (5.23) has a much lower number of states but it increases for higher order dynamics, especially if the system has long dead times. The non-minimal state-space model is most of all needed for an adequate estimator synthesis, but in the early days it was necessary to replace floating-point operations with simple shift operations in order to decrease computer load.

LMPC applications based on a minimal state-space model or input-output polynomial models (5.11) are usually implemented with a smaller value for P. De Keyser and Cauwenberghe (1981), Clarke et al. (1987 B), Ricker (1990) and Gattu and Zafiriou (1992) all use a value of P in the range 5 to 10 sample intervals. If the predictor is used for operator guidance in addition to closed loop control, a very large P may be necessary (De Keyser and Cauwenberghe, 1981).

It is open for discussion, whether linear optimal predictors are better than simplified or approximate predictors. A linear optimal predictor, however optimal it may be, is in industrial applications always based on a linear model, which in any case is only an approximation of the true system.

Whatever predictor mechanism is used for (L)MPC, the final goal is a predictor equation (5.15) or (5.16) in all cases, where the contribution of future inputs is approximated by a linear model.

5.6 Free response predictions using simulators

One variant of input/output model is a commercial, dynamic process simulator. Henson (1998) mentions that use of commercial simulators within MPC schemes has not been reported. Most often, the model equations (or values of the state variables) are not available to the MPC designer or user in an appropriate way. Gattu and Zafiriou (1995) address the input/output model, but their approach seems still to require too much information if a simulator is considered for providing predicted free responses.

The simulator may be seen as solving the system equations (5.2) and (5.3) and can be used for calculating the free response prediction $\hat{Y}(k-1)$. As has been seen in section 5.4, there may be a need to adjust the value of each state and output value at each time point in the prediction horizon. Simulators may or may not provide options to adjust states and outputs, but do they satisfy all possible needs of MPC or optimisation? For example, how do we design the Kalman filter and determine the value of the gain matrix $\mathbf{K_k}$? We will leave this issue outside the scope of this discussion.

The case we are studying more closely, namely the Finnish natural gas pipeline system, has been successfully modelled using the "Simone" simulator, as has been demonstrated in Chapter 4. "Simone" provides an option for so-called state reconstruction, which is "suboptimal" to more rigorous state estimation approaches (Jeni´cek et al. 1991). The gas flow through a pipeline element, which has a gas supply or a gas off-take and a pressure measurement, may be adjusted as follows:

$$\Delta F(k) = k_F \left(P(k) - P_M(k) \right) \tag{5.32}$$

where $\Delta F(k)$ is the adjusted gas flow, which is added to the supply or off-take flow forecast, k_F is a tuning coefficient, $P(k)$ is the pressure of the pipeline element calculated by "Simone" and $P_M(k)$ is the measured pressure. This simple ad-hoc approach is the same as the one used by Marque's and Morari (1988). The maximum number of k_f –parameters is equal to the number of measured pressures in the pipeline system. Although the method is intuitive, it can be difficult to tune the parameter values, because no systematic procedure like the calculation of a Kalman filter gain matrix seems to be available. Also, one might ask, whether the states of the simulator model can be adequately adjusted using this "local way" fixed to supplies and off-takes only. On the other hand, a simple state estimation scheme may be enough, since the better the system model, the smaller the need for state estimation (the smaller the values of the elements of the estimator gain matrix, $\mathbf{K}$). For a perfect model, no state estimation is needed.

The prediction equation to be used for the receding horizon real-time optimisation of natural gas pipeline systems is formed as follows:

At sample interval "k":
For the past input $\mathbf{u}(k-1)$ and known values of present and future disturbances (off-take flow forecasts) $\mathbf{d}(k)$, $\mathbf{d}(k+1)$,..., $\mathbf{d}(k+P-1)$, let the dynamic pipeline system simulator "Simone" calculate the free response prediction vector $\widehat{\mathbf{Y}}(k-1)$ for all variables involved, i.e. suction and check point pressures and CS gas flows. Using the linear models from Chapter 4, define a step response matrix $\mathbf{S}$, which has the general structure of (5.17). The final predicted system output vector $\widehat{\mathbf{Y}}(k)$ is calculated using (5.15), but in the sequel, we will call the free response prediction vector $\mathbf{Z}_0(k)$, $\mathbf{Z}_0(k) \triangleq \widehat{\mathbf{Y}}(k-1)$, which is organised as follows and has a length of $P(2N_c+N_x)$:

$$\mathbf{Z_0}(k) = [\mathbf{Z_{0,1}}(k)^T...\mathbf{Z_{0,Nc}}(k)^T \mathbf{Z_{0,Nc+1}}(k)^T...\mathbf{Z_{0,2Nc}}(k)^T \mathbf{Z_{0,2Nc+1}}(k)^T...\mathbf{Z_{0,2Nc+Nx}}(k)^T]^T \tag{5.33}$$

where N_c is the number of CSs,
N_x is the number of checkpoint pressures
$\mathbf{Z_{0,i}}(k) \triangleq [z_{0,i}(k+1)\, z_{0,i}(k+2)\, ...\, z_{0,i}(k+P)]^T$ are variable specific free response prediction vectors, each of length P: i=1,2,…, N_c are the CS suction pressures, i= N_c+1, N_c+2,…, $2N_c$ are the station gas throughput flows and i= $2N_c$+1, $2N_c$+2,…, $2N_c$ + N_x are the checkpoint pressures.

The final predictions corresponding to (5.15) of individual variables for j=1,2,…, N_c (j=1,2,..., N_x for $\mathbf{P_{xj}}$) are:

$$\mathbf{P_{S,j}}(k) = [\mathbf{S}_{j1}^P \, \mathbf{S}_{j2}^P \, ... \, \mathbf{S}_{jNc}^P] \, \Delta \tilde{\mathbf{u}}(k) + \mathbf{Z_{0,j}}(k)$$

$$\mathbf{F_j}(k) = [\mathbf{S}_{j1}^F \, \mathbf{S}_{j2}^F \, ... \, \mathbf{S}_{jNc}^F] \, \Delta \tilde{\mathbf{u}}(k) + \mathbf{Z_{0,Nc+j}}(k) \qquad (5.34)$$

$$\mathbf{P_{X,j}}(k) = [\mathbf{S}_{j1}^X \, \mathbf{S}_{j2}^X \, ... \, \mathbf{S}_{jNc}^X] \, \Delta \tilde{\mathbf{u}}(k) + \mathbf{Z_{0,2Nc+j}}(k)$$

where $\mathbf{F_j}$ are the throughput flow rate prediction P-vectors for CS "j",

$$\mathbf{F_j}(k) = [F_j(k+1) \, F_j(k+2) \, ... \, F_j(k+P)]^T$$

$\mathbf{P_{sj}}$ are the suction pressure prediction P-vectors for CS "j",

$$\mathbf{P_{s,j}}(k) = [P_{S,j}(k+1) \, P_{S,j}(k+2) \, ... \, P_{S,j}(k+P)]^T$$

$\mathbf{P_{Xj}}$ are the checkpoint pressure prediction P-vectors, and

$\mathbf{S}_{ij}^P$ and $\mathbf{S}_{ij}^F$ are P times M matrices of type (5.18) with step responses for i=1,..., N_c, j=1,.., N_c.

$\mathbf{S}_{ij}^X$ are P times M matrices of type (5.18) with step responses for i=1,..., N_x, j=1,.., N_c

The matrices $\mathbf{S}^F, \mathbf{S}^P$ and $\mathbf{S}^X$ are structured like (5.17) and are the step response matrices of the natural gas pipeline system under consideration.

5.7 A quadratic cost function

As the non-linear cost function of the real-time optimisation problem at hand we will choose the energy consumption of the CSs over the prediction horizon P:

$$J = \sum_{i=1}^{P} \left(\sum_{j=1}^{Nc} a_j F_j(k+i) \left(\left(\frac{P_{d,j}(k+i)}{P_{s,j}(k+i)} \right)^{\gamma} - 1 \right) + b_j \right) \qquad (5.35)$$

where $P_{d,j} \triangleq u_j$ is the discharge pressure of CS j. The values for the parameters a_j and b_j are obtained as described in Appendix D.

In terms of the incremental input vector for CS j, we may write:

$$\mathbf{P_{d,j}} = \left[P_{d,j}(k+1),...,P_{d,j}(k+P) \right]^T = \mathbf{S_0} \Delta \mathbf{u_j}(k) + \mathbf{I_P} u_j(k-1) \qquad (5.36)$$

where $\mathbf{S_0}$ is a P x M matrix with the upper M x M part being a lower triangular matrix filled with ones and the lower (P-M) x M part is filled with ones:

$$\mathbf{S_0} = \begin{pmatrix} 1 & 0 & 0 & \cdots & 0 \\ 1 & 1 & 0 & \cdots & 0 \\ 1 & 1 & 1 & \cdots & 0 \\ \vdots & \vdots & \vdots & \cdots & 0 \\ 1 & 1 & 1 & \cdots & 1 \\ & & \cdots & & \\ 1 & 1 & 1 & \cdots & 1 \end{pmatrix} \qquad (5.37)$$

since, by definition of input increment, $u(k+i) = \sum_{j=0}^{i} \Delta u(k+j) + u(k-1)$.

$\mathbf{I}_p$ is a vector of length P filled with ones: $\mathbf{I}_p = [1 \ 1 \ 1 \ ... \ 1]^T$. $\Delta\mathbf{u}_j(k)$ is defined as: $\Delta\mathbf{u}_j(k) \triangleq [\Delta u_j(k) \ \Delta u_j(k+1) \ ... \ \Delta u_j(k+M-1) \ ]^T$.

We shall use the following two alternatives for arriving at a quadratic approximation $J \simeq \frac{1}{2}\Delta\tilde{\mathbf{u}}^T\mathbf{Q}\Delta\tilde{\mathbf{u}} + \mathbf{b}^T\Delta\tilde{\mathbf{u}}$ of the cost function (5.35):

1. The CS head expression $K_H\left(\left(\frac{P_d}{P_s}\right)^\gamma - 1\right)$ is approximated by a quadratic polynomial in P_d and P_s and F is assumed to be independent of discharge pressures $P_d(k+i)$ over the prediction horizon

2. The head expression is approximated by a linear expression in P_d and P_s and F depends linearly on the discharge pressures over the prediction horizon.

In Chapter 4 and Appendices A and B we saw that CS gas flow rates do indeed respond to the discharge pressures, but for a short time compared to pressure variables. In other words, after a (step-wise) change in a CS's discharge pressure, the gas flow rate of that station and the upstream CSs rapidly return to their original values. This observation motivates the independence of gas flow on discharge pressure in the prediction horizon.

As Goslinga et al. (1994) point out, an assumption of independent flow through the CSs in a looped network (see Chapter 3, Figure 1) is not valid as the optimiser will loose the opportunity to redistribute the gas flow between parallel flow paths. Thus alternative 2 *must* be used with looped networks, whereas either alternative 1 or alternative 2 could be selected for gunbarrel systems.

For the quadratic cost function, alternative 1, we have:

$$\left(\left(\frac{P_d}{P_s}\right)^\gamma - 1\right) \approx aP_d{}^2 + bP_s{}^2 + cP_dP_s + dP_d + eP_s + f \qquad (5.38)$$

As the throughput flows are independent of $\Delta\tilde{\mathbf{u}}(k)$, we will, however, use the newest information on gas flows available in the free response prediction vector $\mathbf{Z}_0(k)$ to update the matrix $\mathbf{D}_F$:

$$\mathbf{Q} = 2(a\mathbf{S}_{00}^T\mathbf{D}_F\mathbf{S}_{00} + b(\mathbf{S}^P)^T\mathbf{D}_F\mathbf{S}^P + c\mathbf{S}_{00}^T\mathbf{D}_F\mathbf{S}^P) \qquad (5.39)$$

and

$$\mathbf{b} = \begin{pmatrix} 2a\mathbf{I}_p u_1(k-1) + c\mathbf{Z}_{0,1}(k) + d\mathbf{I}_p \\ 2a\mathbf{I}_p u_2(k-1) + c\mathbf{Z}_{0,2}(k) + d\mathbf{I}_p \\ ... \\ 2a\mathbf{I}_p u_{Nc}(k-1) + c\mathbf{Z}_{0,Nc}(k) + d\mathbf{I}_p \end{pmatrix}^T \mathbf{D}_F\mathbf{S}_{00} + \begin{pmatrix} 2b\mathbf{Z}_{0,1}(k) + c\mathbf{I}_p u_1(k-1) + e\mathbf{I}_p \\ 2b\mathbf{Z}_{0,2}(k) + c\mathbf{I}_p u_2(k-1) + e\mathbf{I}_p \\ ... \\ 2b\mathbf{Z}_{0,Nc}(k) + c\mathbf{I}_p u_{Nc}(k-1) + e\mathbf{I}_p \end{pmatrix}^T \mathbf{D}_F\mathbf{S}^P \quad (5.40)$$

where $\mathbf{D_F} = \mathrm{diag}(a_1 \mathbf{Z_{0,Nc+1}(k)} \quad a_2 \mathbf{Z_{0,Nc+2}}(k) \cdots a_{Nc} \mathbf{Z_{0,2Nc}}(k))$ and $\mathbf{S_{00}}$ is a PN_c x MN_c-matrix with $N_c \mathbf{S_0}$-matrices on the main diagonal:

$$\mathbf{S_{00}} = \begin{pmatrix} \mathbf{S_0} & & & \mathbf{0} \\ & \mathbf{S_0} & & \\ & & \ddots & \\ \mathbf{0} & & & \mathbf{S_0} \end{pmatrix} \tag{5.41}$$

For the quadratic cost function, alternative 2, we use the first terms of a Taylor series expansion for a function of two variables:

$$f(x,y) \approx f(x_0, y_0) + \left.\frac{\partial f(x,y)}{\partial x}\right|_0 \Delta x + \left.\frac{\partial f(x,y)}{\partial y}\right|_0 \Delta y \tag{5.42}$$

or:

$$\left(\left(\frac{P_d}{P_s}\right)^\gamma - 1\right) \approx a_L \Delta P_d + b_L \Delta P_s + c_L \tag{5.43}$$

where ΔP_d and ΔP_s are small deviations from the nominal values P_{d0} and P_{s0} for the discharge and suction pressures, respectively, and:

$$a_L = \frac{\gamma}{P_{s0}}\left(\frac{P_{d0}}{P_{s0}}\right)^{\gamma-1} \quad , \quad b_L = -\frac{\gamma P_{d0}}{P_{s0}^2}\left(\frac{P_{d0}}{P_{s0}}\right)^{\gamma-1} \quad , \quad c_L = \left(\frac{P_{d0}}{P_{s0}}\right)^\gamma - 1 \tag{5.44}$$

The linear approximation is illustrated in figure 5.2.
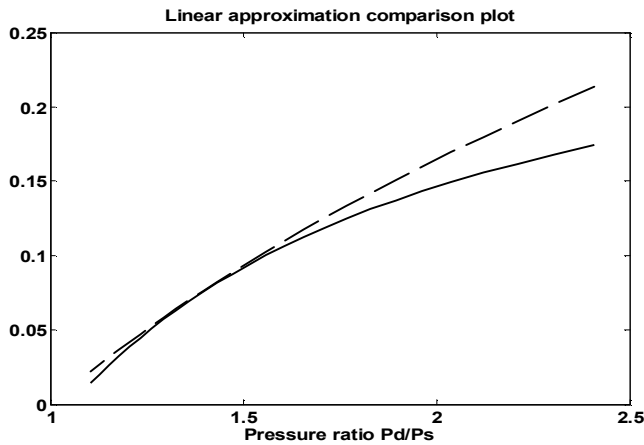
Figure 5.2 The expression $\left(\frac{P_d}{P_s}\right)^{0.22} - 1$ (solid line) and its linear approximation (dashed line). Note, that both are drawn as a function of pressure ratio, which makes also the linear approximation curved. $P_{d0} = 48.5$ bar and $P_{s0} = 33.3$ bar.

The matrices of the QP-problem are as follows, remembering that in this case, we use the linear Δu-dependent expression (see (5.34)) of the CS gas throughput flows instead of Δu-independent flows:

$$\mathbf{Q} = \left(\mathbf{S^F}\right)^T \mathbf{D_1} \mathbf{S_{00}} + \left(\mathbf{S^F}\right)^T \mathbf{D_2} \mathbf{S^P} \tag{5.45}$$

where $\mathbf{D_1}$ and $\mathbf{D_2}$ are diagonal matrices:

$$\mathbf{D_1} = \text{diag}[a_1 a_L \mathbf{I}_p^T \; a_2 a_L \mathbf{I}_p^T \cdots a_{Nc} a_L \mathbf{I}_p^T] \tag{5.46}$$

$$\mathbf{D_2} = \text{diag}[a_1 b_L \mathbf{I}_p^T \; a_2 b_L \mathbf{I}_p^T \cdots a_{Nc} b_L \mathbf{I}_p^T] \tag{5.47}$$

and

$$\begin{aligned}
\mathbf{b} = &\left[a_1(a_L \mathbf{I}_p u_1(k-1) + b_L \mathbf{Z_{0,1}}(k) + c_L \mathbf{I}_P)^T \cdots \right. \\
&\left. a_{Nc}(a_L \mathbf{I}_p u_{Nc}(k-1) + b_L \mathbf{Z_{0,Nc}}(k) + c_L \mathbf{I}_P)^T\right] \mathbf{S^F} + \\
&\left[a_1 a_L \mathbf{Z_{0,Nc+1}}(k)^T \cdots a_{Nc} a_L \mathbf{Z_{0,2Nc}}(k)^T\right] \mathbf{S_{00}} + \\
&\left[a_1 b_L \mathbf{Z_{0,Nc+1}}(k)^T \cdots a_{Nc} b_L \mathbf{Z_{0,2Nc}}(k)^T\right] \mathbf{S^P}
\end{aligned} \tag{5.48}$$

5.8 Linear constraints

The non-linear compressor constraints (compressor envelopes) will be approximated by linear constraints as follows (for details on the Finnish natural gas pipeline system, see Appendix D).

The compressor envelope in the Head – Volumetric flow rate co-ordinate system consists of four inequalities with respect to head (H) and flow (q_{VOL}) of the type $g(H,q_{VOL}) \leq 0$, which may be linearised as $a_e H + b_e q_{VOL} + c_e \leq 0$. Volumetric flow rate in compressor suction conditions q_{VOL}, (m^3/s) and normalised flow F, (Nm^3/h), are related as $F = 3600 P_s q_{VOL}$ where P_s is the suction pressure of the compressor. The approximation $\left(\dfrac{P_d}{P_s}\right)^{\gamma} - 1 \approx c\dfrac{P_d}{P_s} - d$ in the expression for head is used, because it eliminates P_s from the denominator in the expression for q_{vol}. The linear approximation for the CS envelopes becomes:

$$a_e \frac{z_s R T_s}{\gamma M_w} c P_d + (c_e - a_e \frac{z_s R T_s}{\gamma M_w} d) P_s + \frac{b_e}{3600} F \leq 0 \tag{5.49}$$

The general linear envelope constraint expressions for individual CSs are written:

$$a_{ij} P_{d,i} + b_{ij} P_{s,i} + c_{ij} F_i \leq 0 \tag{5.50}$$

where $i=1,2,..,N_c$ and $j=1,..,4$

While the optimiser must apply the CS constraints over the whole prediction horizon in a component-wise fashion, the following vector inequalities can be written:

$$a_{ij}(\mathbf{S_0}\Delta\mathbf{u}_i(k) + \mathbf{I_p}u_i(k-1)) + b_{ij}(\mathbf{S}_i^{\mathbf{P}}\Delta\tilde{\mathbf{u}}(k) + \mathbf{Z}_{0,i}(k)) + c_{ij}(\mathbf{S}_i^{\mathbf{F}}\Delta\tilde{\mathbf{u}}(k) + \mathbf{Z}_{0,Nc+i}(k)) \leq 0 \qquad (5.51)$$

The total number of scalar inequalities is $4\,N_c\,P$.

For each pressure check point i=1,2,…,N_x in the system, linear inequalities apply:

$$\mathbf{S}_i^{\mathbf{X}}\Delta\tilde{\mathbf{u}}(k) + \mathbf{Z}_{0,2Nc+i}(k) \geq \mathbf{P}_{x,i,min} \qquad (5.52)$$

For the discharge pressure, maximum and minimum limits over the prediction horizon may be set by the inequalities:

$$\mathbf{I_u}\Delta\mathbf{u}_i(k) + \mathbf{I_M}u_i(k-1) \leq \mathbf{P}_{d,i,max}$$
$$\mathbf{I_u}\Delta\mathbf{u}_i(k) + \mathbf{I_M}u_i(k-1) \geq \mathbf{P}_{d,i,min} \qquad (5.53)$$

i=1,2,…,N_c where $\mathbf{I_M}$ is a vector with ones of length M and $\mathbf{I_u}$ is an M x M lower triangular matrix filled with ones (the upper M x M part of $\mathbf{S_0}$), see equation (5.37).

Bounds on the decision variables yield $\Delta\mathbf{u}_i(k) \leq \mathbf{Du}_{i,max}$ and $\Delta\mathbf{u}_i(k) \geq \mathbf{Du}_{i,min}$.

5.9 Steady-state optimisation

In this section we will define a steady-state optimisation problem in which we will use three alternative cost functions: the original and the two quadratic approximations.

The steady state optimisation problem, using the original cost function, is:

$$\underset{Pd1,Pd2,Pd3}{\text{Min.}} \; a_1 F_1\left[\left(\frac{P_{d1}}{P_{s1}}\right)^{\gamma} - 1\right] + b_1 + a_2 F_2\left[\left(\frac{P_{d2}}{P_{s2}}\right)^{\gamma} - 1\right] + b_2 + a_3 F_3\left[\left(\frac{P_{d3}}{P_{s3}}\right)^{\gamma} - 1\right] + b_3 \qquad (5.54)$$

under the following equality constraints, which are the steady-state pressure-flow relationships of the pipeline segments involved, assuming isothermal conditions and that gas flows F_i are independent of pressures (see equation 3.7, Chapter 3):

$$P_{d1}^2 - P_{s2}^2 = k_1 F_1^{1.8539} + k_2 F_2^{1.8539}$$
$$P_{d2}^2 - P_{s3}^2 = k_3 F_2^{1.8539} + k_4 F_3^{1.8539} \qquad (5.55)$$
$$P_{d3}^2 - P_{x3}^2 = k_5 F_3^{1.8539} + k_6 (F_3 - F_0)^{1.8539}$$

and the following inequality constraints:

$$P_{di} \leq 53 \;, i = 1...3$$
$$P_{x3} \geq 29 \qquad (5.56)$$
$$g_{ij}(P_{di}, P_{si}, F_i) \leq 0 \;, i = 1...3, j = 1..4$$

where (see also figure 5.3):

a_1, b_1, a_2, b_2 , a_3, and b_3 are CS cost parameters defined in Appendix D, F_1, F_2 and F_3 are gas flow rates through the CSs (Nm³/h), P_{d1}, P_{d2} and P_{d3} are the discharge pressures of the CSs (bar) and the decision variables of the optimisation problem, P_{s1}, P_{s2} and P_{s3} are the suction pressures of the CSs (bar) and P_{x3} is the pressure at check point no. 3 (bar). The functions g_{ij} are the four envelope curves for CS "i" expressed as *quadratic* functions (see Appendix D).
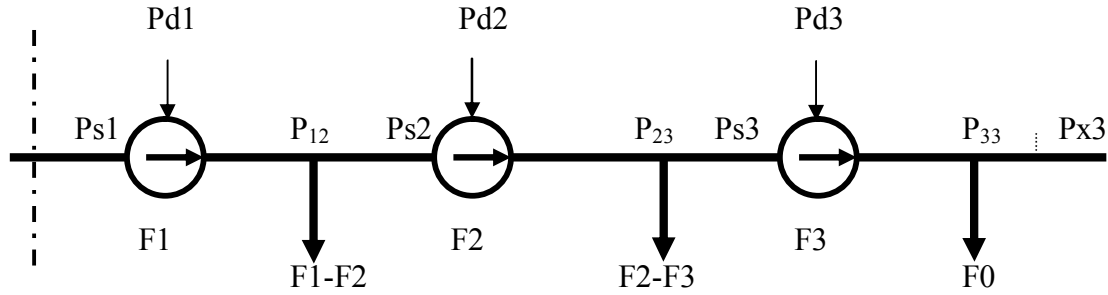
Figure 5.3 The gas pipeline system used for the steady-state optimisation problem. Compare with figure 4.1 in Chapter 4.

The constants k_1 to k_6 are obtained by assuming, that all off-take flows can be lumped into one fictive point somewhere in each segment, where the pressure is the average value of the pressures at the segment ends, i.e. $P_{12} = (P_{d1} + P_{s2})/2$, $P_{23} = (P_{d2} + P_{s3})/2$, $P_{33} = (P_{d3} + P_{x3})/2$. At operating point no. 1 (Appendix A), where the pressures and flows F1, F2 and F3 are given, we have, for example, for the first segment two equations $P_{d1}^2 - P_{12}^2 = k_1 F_1^{1.8539}$, and $P_{12}^2 - P_{s2}^2 = k_2 F_2^{1.8539}$ which added together give the first of the three equations (5.55). F_0 is a constant flow 250000 Nm³/h. The values of the constants k_1 to k_6 as calculated from the pressure and flow data for operating point no. 1 are, respectively: $0.0793 \cdot 10^{-7}$, $0.1224 \cdot 10^{-7}$, $0.1301 \cdot 10^{-7}$, $0.1370 \cdot 10^{-7}$, $0.2223 \cdot 10^{-7}$ and $0.6434 \cdot 10^{-7}$.

The lumping of the off-takes in each segment means, that we are not using an exact model of the Finnish natural gas pipeline system. The essential thing in this study is to compare the quadratic cost functions with the original one. This task is not very much dependent on which kind of *pressure loss formulas* we use for the segments or what is the error introduced by the assumptions and simplifications used.

According to the operating personnel of the Finnish natural gas pipeline system, the operating ranges for the compressor stations CS1, CS2 and CS3 in 2003 were, respectively: $3.0 \ldots 8.9 \cdot 10^5$, $2.5 \ldots 6.2 \cdot 10^5$ and $2.5 \ldots 5.5 \cdot 10^5$ Nm³/h . This broad range of gas flows is caused by gas consumption variations at the off-takes. The given flow ranges are used to create a table of flow rate triplets (F1,F2,F3) for the CSs using even flow rate steps of 59000, 53000 and 50000 Nm³/h, respectively, giving 616 triplet values. When triplets containing values F1<F2 or F2<F3 are deleted, because such flow conditions are not possible (no gas supplies in the three segments involved), this decreases to 256. The flow rate triplets are graphically depicted in figure 5.4.

For each flow rate triplet, the steady-state optimisation problem (5.54 … 56) is solved using the Optimisation Toolbox "fmincon" function (Matlab Optimisation Toolbox User's Guide, 2000).

The optimal discharge pressures using the original cost function for the flow rate values in figure 5.4 are graphed in figure 5.5 a, b and c.
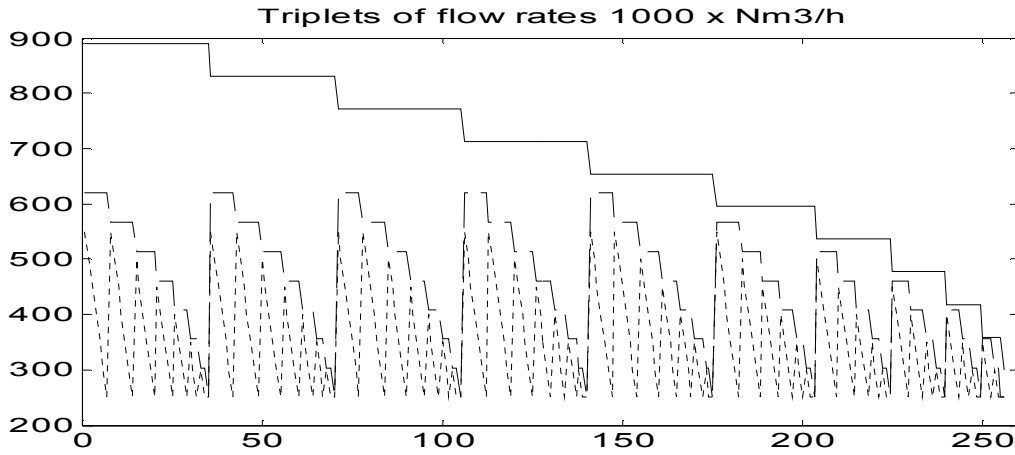
Figure 5.4 The values of the 256 flow rate triplets in Nm^3/h of CSs used for steady- state optimisation. The horizontal axis is the index in the table of the flow rate triplets.
Solid line: F1; dashed line: F2; dotted (short dashed) line: F3.
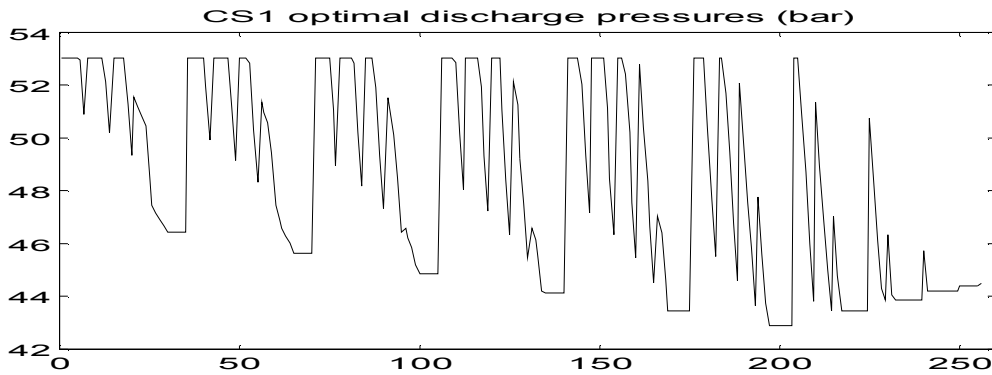
Figure 5.5 a) Optimal CS1 discharge pressures (bar) as function of the flow rate triple index when the original cost function is used.
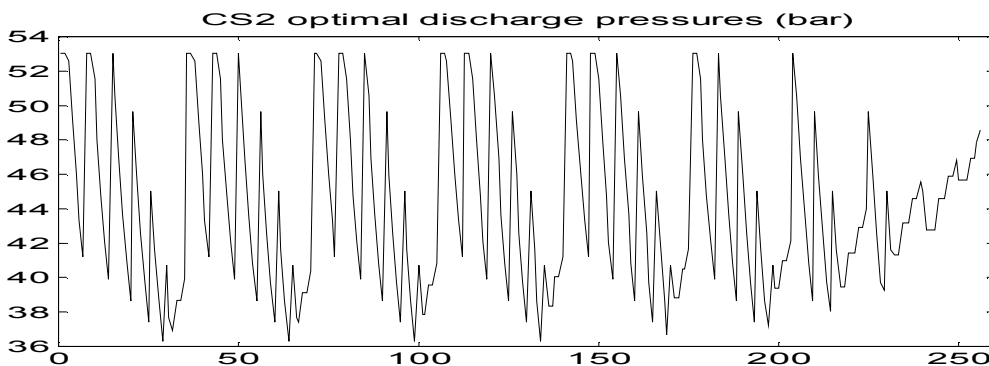
Figure 5.5 b) Optimal CS2 discharge pressures (bar) as function of the flow rate triple index when the original cost function is used.
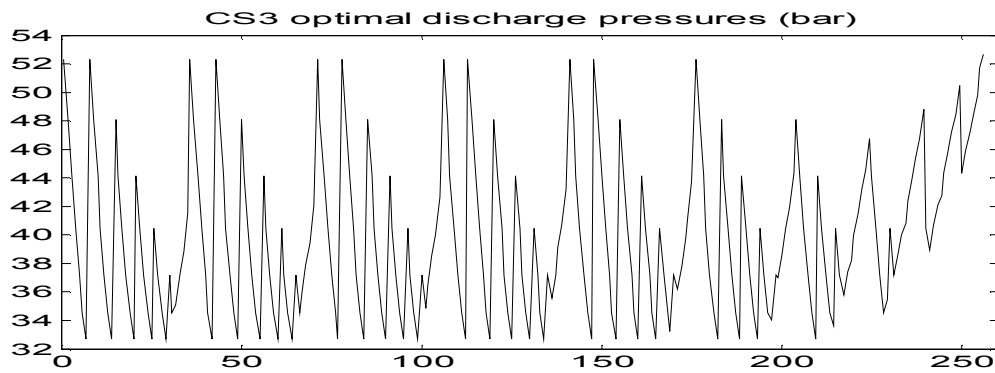
Figure 5.5 c) Optimal CS3 discharge pressures (bar) as function of the flow rate triple index when the original cost function is used.

Next, we will solve the optimisation problem (5.54…56) but with the cost function in (5.54) replaced by the quadratic cost function approximation no.1 (5.38) with the parameter values presented in Appendix D. As expected, some differences are seen in the 256 solutions compared to those obtained using the original cost function, see figure 5.6 below. The maximum difference for CS1 discharge pressure is 1.9 bar and for CS2 discharge pressure 0.1 bar. For CS3 discharge pressure, there is no difference.
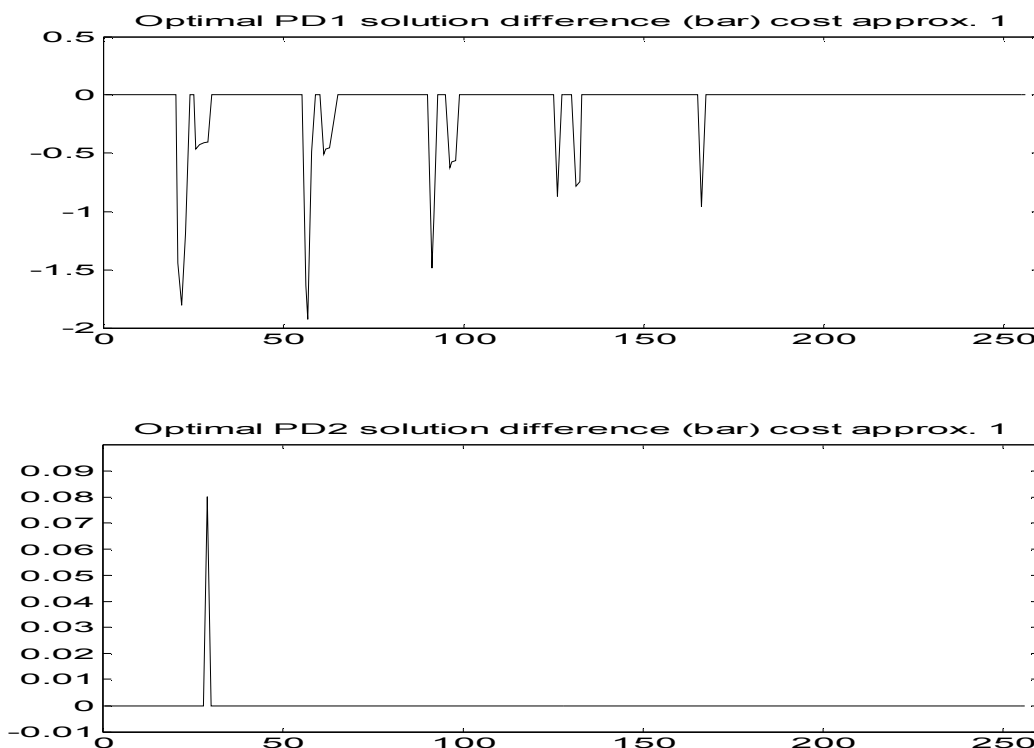
Figure 5.6 a) (Top) Optimal CS1 discharge pressure with original cost function minus optimal CS1 discharge pressure with approximation no.1 b) (Bottom) same for CS2

Next, cost function approximation no. 2 with linear pressure and linear flow is used in (5.54). Figure 5.7 shows that, in this case, the maximum difference for CS1 discharge pressure is 5.9 bar, for CS2 discharge pressure 5.9 bar and for CS3 discharge pressure 9.3 bar.

The steady-state optimisation problem is heavily constrained in the sense that the optimal solution for every flow rate triplet (F1, F2, F3) must satisfy four CS envelope constraints, the minimum Px3 limit as well as minimum and maximum limits of the discharge pressures, all of which adds up to 19 constraints. In this case, the optimal solution is always constrained by one (mostly two) to three constraints from among the 19 possible ones. In figure 5.8 the number of active constraints in each of the 256 optimal solutions is shown using the three cost function variants as discussed. There is one key observation: the differences in the optimal discharge pressures occur when the number of active constraints is less than three. This is not surprising, as three active constraints mean, that the optimum point is completely determined by the constraints and less than three active constraints means, that the shape of the cost function influences the solution. Additionally, we may observe that the discharge pressure differences occur when there is a large off-take in the first two segments (F1-F2 and/or F2-F3 are large).
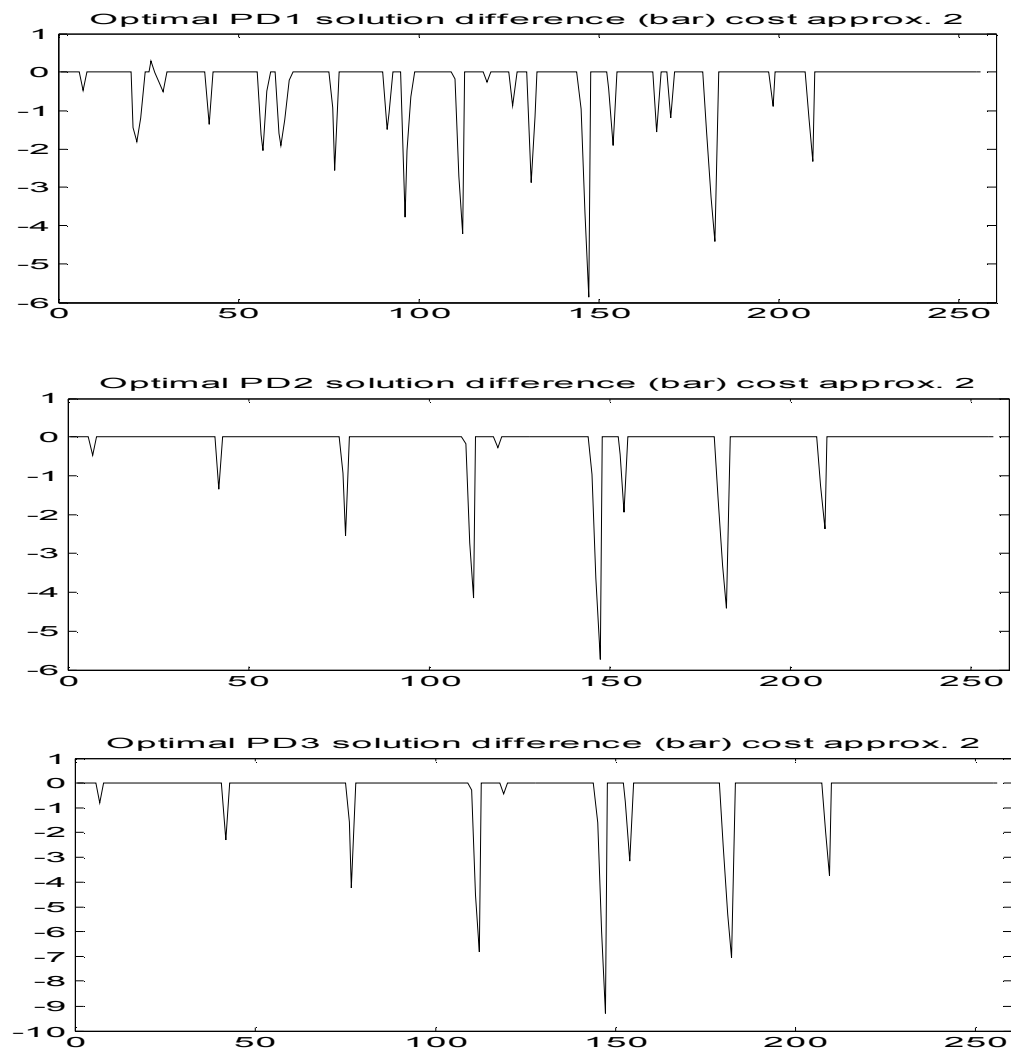
Figure 5.7 a) (Top) Optimal CS1 discharge pressure with original cost function minus optimal CS1 discharge pressure with approximation no.2 **b)** (Middle) same for CS2 **c)** (Bottom) same for CS3.
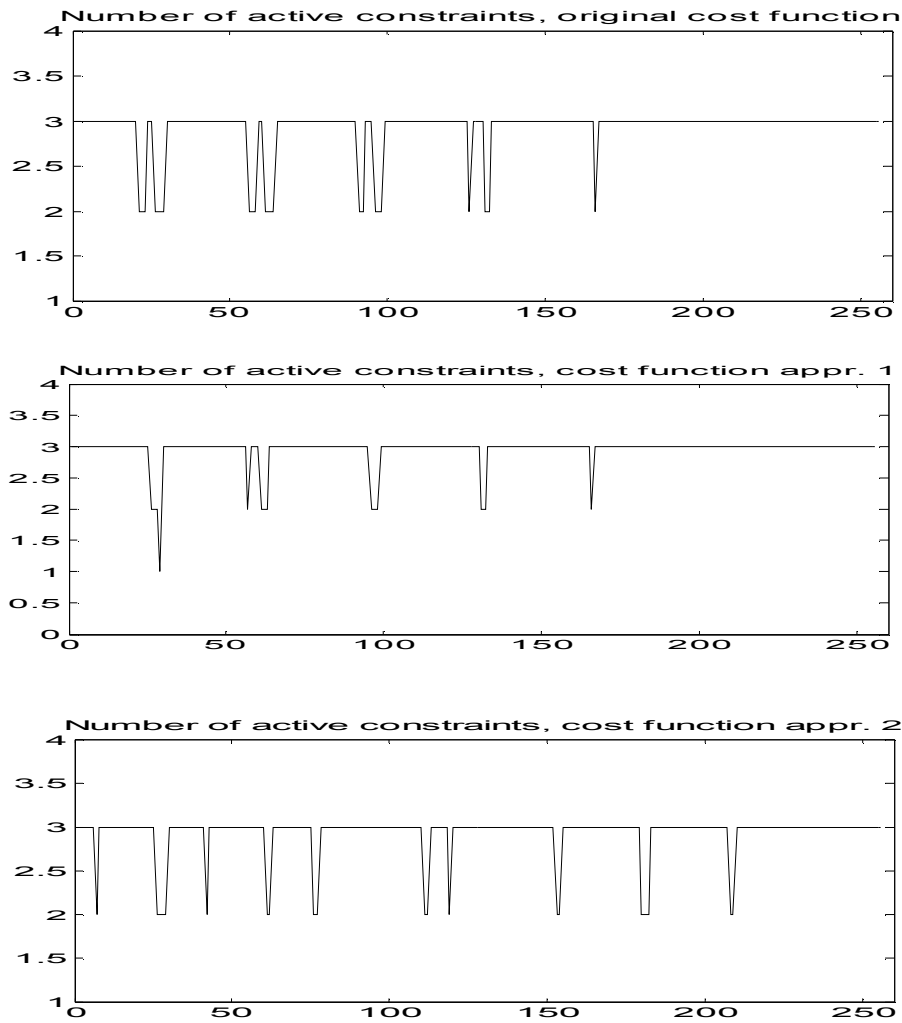
Figure 5.8 a) Number of active constraints as a function of flow rate triplet index, original cost function, **b)** (Middle) same for cost function approximation no.1 and **c)** (Bottom) same for cost function approximation no.2
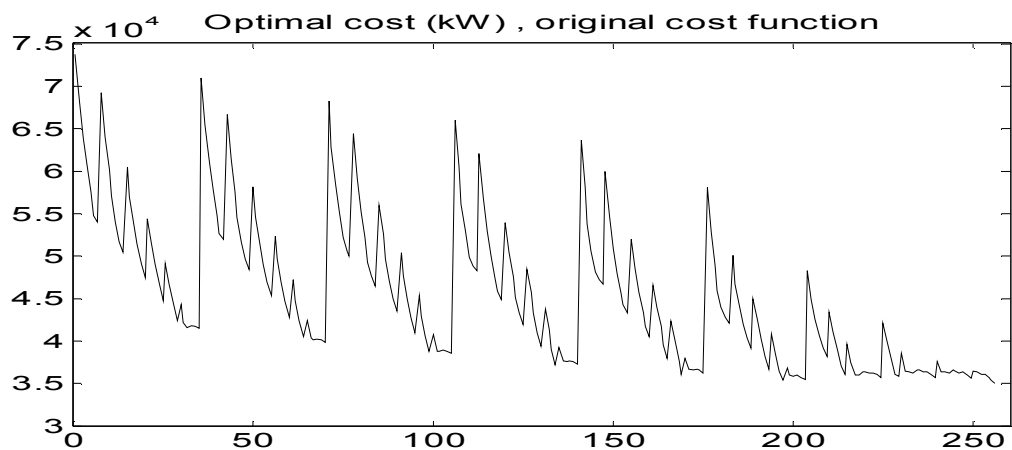
Figure 5.9 Optimal cost function values in kW using original cost function.

74
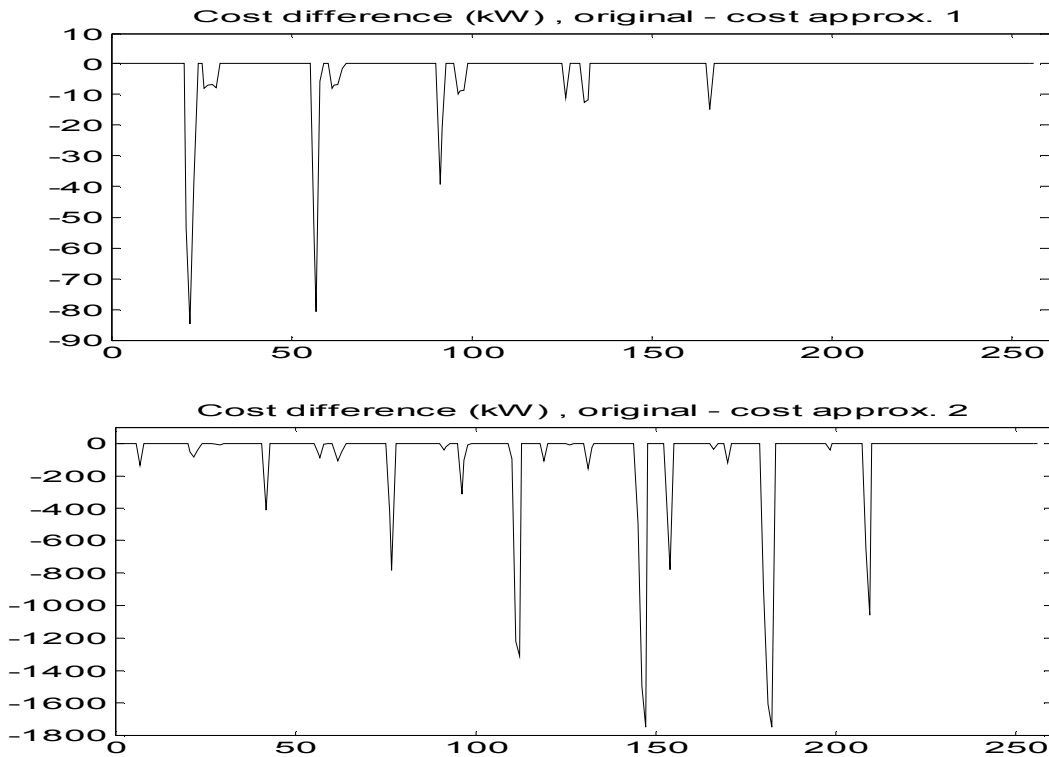
Figure 5.10 a) (Top) Difference in cost function values: original minus approximation no. 1 (kW) **b)** (Bottom) Difference in cost function values: original minus approximation no. 2 (kW).

Figure 5.9 shows the optimal cost values when solving the 256 steady-state optimisation problems using the original cost function. The values fall in the range 35000 to 75000 kW. The cost difference in figure 5.10 a) is calculated as the original cost in figure 5.9 minus the original cost as a function of the optimal discharge pressures (and suction pressures), obtained using cost function approximation no. 1 and the same for cost function approximation no. 2 in figure 5.10 b). The error in cost is maximum 85 kW (0.18 %) for approximation no.1 and maximum 1750 kW (3.85 %) for approximation no. 2. These results reveal that the cost function is flat near the solutions considered, giving such low cost function differences for maximum discharge pressure differences of 1.9 and 9.3 bar, respectively.

If additional limitations on the flow rate triplets (F1,F2,F3) are imposed as follows: F1-F2 < 200000 Nm^3/h and F2-F3 < 200000 Nm^3/h, we obtain 90 flow rate triplets instead of 256. Steady-state optimisation in this case gives equal optimal discharge pressures for all three cost functions and in all cases the number of active constraints is equal to 3 i.e. the optimal solutions are heavily constrained which means that the shape of the cost function and the approximation error play a smaller role. Obviously, when a gunbarrel pipeline system approaches a pure transmission system, the optimal steady-state solutions become more actively constrained, and the approximate cost functions do not disturb the solutions.

A final exercise will be to investigate the steady-state optimisation potential of the pipeline system at operating point no. 1 (Appendix A, Table A.1). The optimal solution to optimisation problem (5.54…56) yields optimal discharge pressures of 53, 53 and 48.61 bar for CS1, CS2 and CS3, respectively. The optimal cost is 58920 kW and Pd1 maximum limit, Pd2 maximum limit and Px3 minimum limit constraints are active. Changing the sign of the cost function

(5.54) yields a *maximisation* problem, for which the optimal discharge pressures are 44.73, 49.67 and 53 bar for CS1, CS2 and CS3, respectively. The optimal cost is 69 394 kW and the CS1 choke limit, CS3 maximum speed limit and Pd3 maximum limit constraints are active. The relative difference of the cost function values is 15.1% and represents the maximum steady-state optimisation potential, i.e. the difference between the most inferior operation strategy and the best one.

5.10 Implementation issues

Blocking of the input variable

Before implementing and using the receding horizon optimisation method described so far, some practical and theoretical issues must be addressed. First, the length of the input vector, which is $N_c M$, may have to be further decreased in order to reduce computational load, especially if large pipeline systems with large N_c are considered. In MPC applications, input variable blocking is sometimes used (Ricker, 1985). Select an integer parameter N_b for *even blocking* and define, for a general case:

$$\Delta u(k+1) = \Delta u(k+2) = ...\Delta u(k+N_b - 1) = 0,$$
$$\Delta u(k+N_b + 1) = \Delta u(k+N_b + 2) = ...\Delta u(k+2N_b - 1) = 0$$
$$...$$
$$\Delta u(k+(j_b - 2)N_b + 1) = \Delta u(k+(j_b - 2)N_b + 2) = ...\Delta u(k+M-2) = 0$$

(5.57)

which reduces the length of the input variable vector to j_b, $j_b < M$ so that $(j_b - 1)N_b = M-1$: $\mathbf{\Delta u} = [\Delta u(k)\ \Delta u(k+N_b)\ \Delta u(k+2N_b)...\Delta u(k+M-1)]^T$. See figure 5.11 for an illustration. Uneven blocking means that we use different blocking interval lengths which gives:

$$\mathbf{\Delta u} = [\Delta u(k)\ \Delta u(k+N_{b1})\ \Delta u(k+N_{b1}+N_{b2})...\Delta u(k+M-1)]^T \text{ and } \sum_{i=1}^{jb-1} N_{bi} = M-1$$
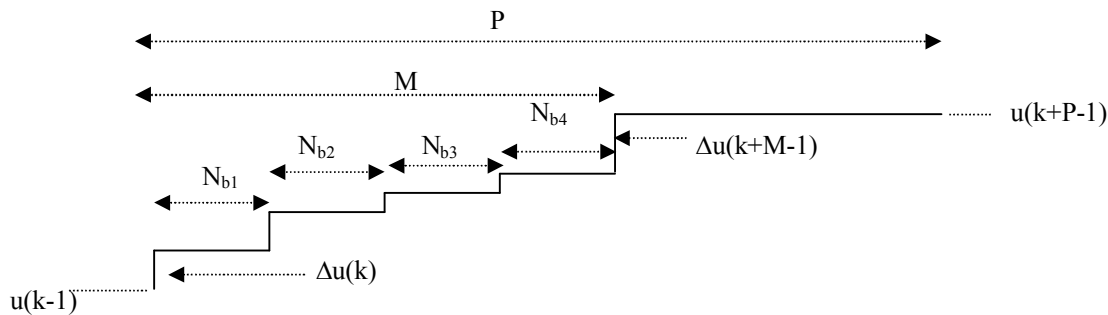
Figure 5.11 Example of even blocking of an input variable. $N_{b1}=N_{b2}=N_{b3}=N_{b4} = N_b$, $4N_b = M-1$, $j_b =5$.

The modification of step response matrices from (5.18) is straightforward, and in general, a modified step response matrix from input j to output i is:

$$\mathbf{S}_{ij} = \begin{pmatrix} s_{ij}(1) & 0 & 0 & 0 \\ \vdots & \vdots & \vdots & \vdots \\ s_{ij}(N_b+1) & s_{ij}(1) & 0 & 0 \\ \vdots & \vdots & \vdots & \vdots \\ s_{ij}(2N_b+1) & s_{ij}(N_b+1) & s_{ij}(1) & \cdots \\ \vdots & \vdots & \vdots & \\ & & & s_{ij}(1) \\ & & & \vdots \\ s_{ij}(P) & s_{ij}(P-N_b) & s_{ij}(P-2N_b) & s_{ij}(P-(j_b-1)N_b) \end{pmatrix} \qquad (5.58)$$

All step response matrices of the natural gas pipeline system, $\mathbf{S^P}, \mathbf{S^F}, \mathbf{S^X}$ and $\mathbf{S_{00}}$, have to be modified in the same way.

The blocking parameter N_b is considered to be one of the MPC tuning parameters as are the prediction horizon P and the number of input steps j_b.

Numerical considerations

QP solvers assume a positive semi-definite and symmetric $\mathbf{Q}$-matrix in the cost function $J(x) = \dfrac{1}{2}\mathbf{x}^T\mathbf{Q}\mathbf{x} + \mathbf{b}^T\mathbf{x}$. In LMPC, these properties are guaranteed, because of the definition of the problem, but in the case at hand (see (5.39) and (5.45)) there is no guarantee; however, it is possible to use symmetrisation where $\mathbf{Q}$ is replaced by $\dfrac{1}{2}\left(\mathbf{Q}+\mathbf{Q}^T\right)$.

Let us substitute the numerical values known for the Finnish natural gas pipeline system from Appendices B and D and calculate $\mathbf{Q_1}$ using (5.39) and $\mathbf{Q_2}$ using (5.45). For pressures and flows we will use constant values over the whole prediction horizon using the steady-state values at operating point no.1 (see Appendix A, table A.1). In table 5.1 below, the minimum and maximum eigenvalues for matrices $\mathbf{Q_1}$ and $\mathbf{Q_2}$ are shown for selected values of j_b, N_b and P. The eigenvalues are calculated using the "eig"-function of Matlab. As can be seen, none of the selected parameter sets produce a positive semi-definite $\mathbf{Q_1}$, while $\mathbf{Q_2}$ is positive semi-definite except for small values of N_b. The latter is an interesting observation because according to the literature, small values of N_b should be used to avoid control performance degradation.

$\mathbf{Q_1}$ and $\mathbf{Q_2}$ are not positive semi-definite and consequently non-convexity, which may cause the solution to converge to a local optimum, and numerical problems may occur with a regular QP solver. The Matlab Optimisation Toolbox "fmincon" function is used on recommendation (Matlab Optimisation Toolbox User's Guide, 2000), instead of the standard "quadprog" QP solver, since it is a general-purpose solver, which can cope with non-convex QP problems but it is still not a global solver.

The first approximation, with quadratic head approximation and decision variable independent gas flow assumption is a better approximation for gunbarrel pipeline systems than the second one, with linear head and gas flow. An interesting question arises: is it better to choose the second approximation, because it produces a convex optimisation problem with the correct choice of tuning parameter values even though it is known to be less accurate?

j_b	N_b	M	P	$\lambda(Q_1)$ min.	$\lambda(Q_1)$ max.	$\lambda(Q_2)$ min	$\lambda(Q_2)$ max
8	4	29	100	-5213	15598	165.2	12003
16	4	61	100	-8954	23411	163.1	19039
22	4	85	136	-16766	42857	149.5	23962
10	4	37	64	-3721	9859	164.15	13237
7	16	97	100	-2838	7090	247.7	6220
4	25	76	100	-1944	4943	354.7	4268
49	2	97	100	-20046	49635	-5.93	45104
97	1	97	100	-39699	98300	-86.75	89720
50	1	50	100	-29791	81692	66.11	64852

Table 5.1 Minimum and maximum eigenvalues of Q_1 and Q_2 for selected parameters.

The matrices R_i are used as tuning parameters in MPC, see (5.6), to damp aggressive inputs and shift the eigenvalues of the Q- matrix of the QP problem in the positive direction. It is easy to see, that eigenvalue correction for Q_1 would require large (diagonal) elements in R_i, which would over-damp and thus disturb the optimal solution. For Q_2, the eigenvalues are only slightly negative (see table 5.1) which enables eigenvalue correction without too much over-damping. For damping, a constant matrix over the prediction horizon, $R_i = R$, is sufficient.

A scope limitation

As mentioned in Chapter 4, the suction pressure of CS1 is set to a constant value of 40 bar because there is not enough information for "Simone" to produce adequate predictions. The information required would be the discharge pressure (or gas flow) of the next upstream CS on the Russian side of the border and gas consumption forecasts for all or at least the major gas off-takes in the pipeline segment upstream CS1, all these off-takes being on the Russian side as well. From an overall perspective, this is somewhat harmful, since CS1 is the station with the largest throughput and the largest energy consumption. Of course, optimal discharge pressure can and will be calculated for CS1, but some special events, for example a disturbance in the pipeline system causing a decrease of CS1 suction pressure, may hinder it from running a typical high discharge pressure strategy.

The length of the prediction horizon

In MPC, the length of the prediction horizon (P) is determined based on stability and control performance criteria (see section 5.5). The (usually linear) disturbance models used to estimate disturbance behaviour over the prediction horizon do not dictate particularly small or large P. The situation is different when there is predicted disturbance information available, i.e. the off-take flow forecasts in our case: There is unique information available over P, something real and physical is predicted to be happening in the future. In order not to overlook significant predicted off-take flow changes, it would be advisable to choose a large enough P. Ratchford and Carter (2000), amongst others, chose a value for P of 24 hours, based on more or less operational and commercial arguments. Marque's and Morari (1988) suggested an empirical formula, $P \geq 2N_S$ hours, where N_S is the number of major pipeline segments. In one of the examples they discussed, they used P=13 hours for a gunbarrel pipeline system with $N_S = 4$ and N_C (number of

CSs) =3. The formula is based on the need to balance the behaviour of the optimiser: a small P leads to minimising the energy content of the system at the end of the horizon, while for larger P the optimiser puts more weight on minimising energy consumption due to frictional losses.

In the simulation studies below in section 5.11 and further on in Chapter 6, we will use P=100 (16 hours 40 minutes, as ΔT=10 minutes) as the basic length of the horizon. P=64 (10 hours 40 minutes) is also used for comparison. P=136 (22 hours 40 minutes) is the largest possible with the version of "Simone" used in the studies.

In-feasibility protection

In-feasibility problems may occur in cases where hard constraints are applied on system output variables. In the case at hand, for example the Px3 checkpoint pressure, it is quite possible that either its current simulated value or a few values in the beginning of the prediction horizon could drop below the minimum limit, without the optimiser being capable of avoiding the situation because of the slow response from CS3 discharge pressure to Px3. To avoid the whole problem being flagged as in-feasible, a constraint relaxation technique resembling the one used by Muske and Rawlings (1993) is implemented: if the current Px3 value or a predicted Px3 value is less than the minimum limit, re-shape the minimum to "follow" the temporary in-feasibility, as shown in figure 5.12.
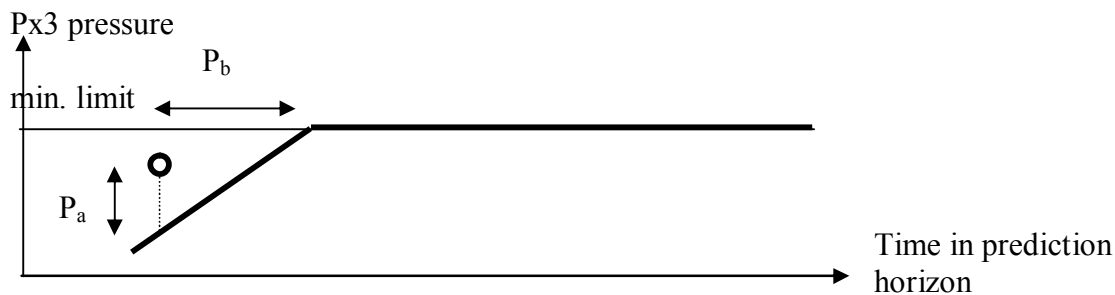
Figure 5.12 Original, constant minimum limit for Px3 (thin line) and re-shaped minimum limit (bold line). "**o**" is the locally infeasible value of Px3 (or the minimum of several values). P_a and P_b are tuning parameters.

5.11 Simulation results

This section presents the receding horizon optimisation results. The receding horizon optimisation is built using Matlab 6.5 scripts which call the non-linear optimisation problem solver "fmincon" of the Matlab Optimisation toolbox. Appendix C explains the details of the simulation test bench used. The objectives of the real-time optimisation are to minimise energy consumption of CS1, CS2 and CS3 as well as to obey the Px3 minimum limit and all CS envelope constraints.

No state estimation or state reconstruction schemes are used. In other words, the pressure and flow "measurements" and predictions provided by "Simone" are assumed to be perfect.

All CSs are running in all simulation runs in this section, although the operators shut down CS2, as is seen in the true operational data. The intention is to test the optimiser with all CSs running,

because the problem becomes more challenging due to more active constraints after the first week of March 2003. The energy consumption of the various simulation runs are compared, however, comparisons with operational data are only made for the first days of March 2003. Actually, shutting down CS2 saves energy and it is not correct to compare optimiser and operational results if the optimiser is not allowed to shut down CSs.

Throughout all the test runs in this study, in both Chapter 5 and Chapter 6, the following limits are used for the CS discharge pressures. Maximum (minimum) change applies to all CS discharge pressure increments along the control horizon M.

	Maximum (bar)	Minimum (bar)	Maximum change (bar)	Minimum change (bar)
CS1	53.3	35	5	-5
CS2	53	35	5	-10
CS3	53	35	5	-10

CS2 and CS3 apply quite large minimum changes, while their discharge pressure changes may be quite large when CSs shut down.

5.11.1 Cost function approximation no.1

In the first two cases the first variant of the cost function approximation (5.38) with quadratic head is used. The simulation time period is 1.3.2003 00:00 to 9.3.2003 24:00, or 1296 10-minute control intervals.

Case1

The values of the tuning parameters are: j_b=8, N_b=4 and P=100. No input variable damping is used, i.e. **R**=0. The results are presented in figures 5.13 to 5.16 below.
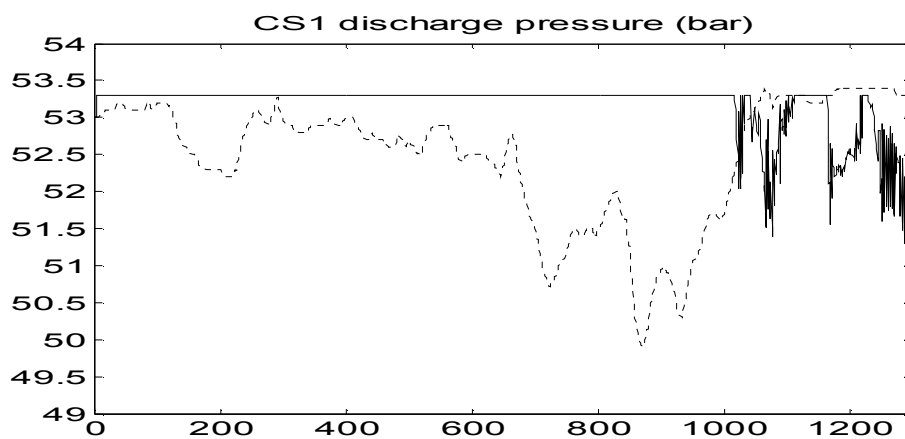
Figure 5.13 CS1 discharge pressure from 1.3.2003 00:00 to 9.3.2003 24:00. The solid line represents the result of the optimiser; the dashed line is as operated.
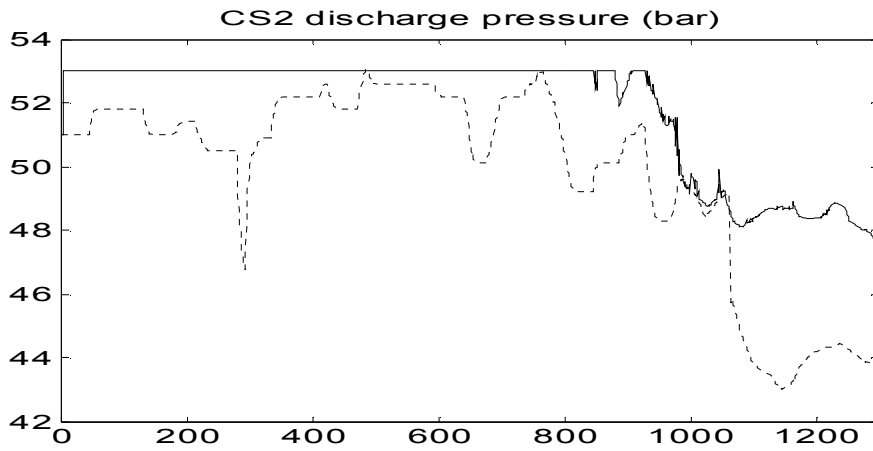
Figure 5.14 CS2 discharge pressure from 1.3.2003 00:00 to 9.3.2003 24:00. The solid line represents the result of the optimiser; the dashed line is as operated.
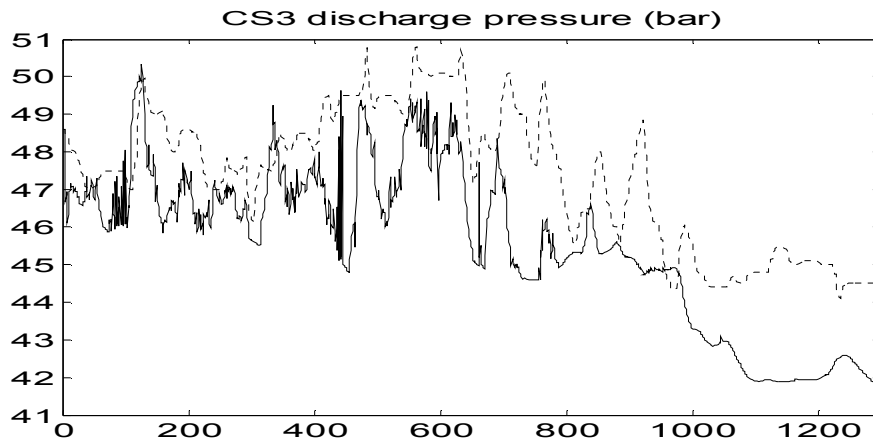
Figure 5.15 CS3 discharge pressure from 1.3.2003 00:00 to 9.3.2003 24:00. The solid line represents the result of the optimiser; the dashed line is as operated.
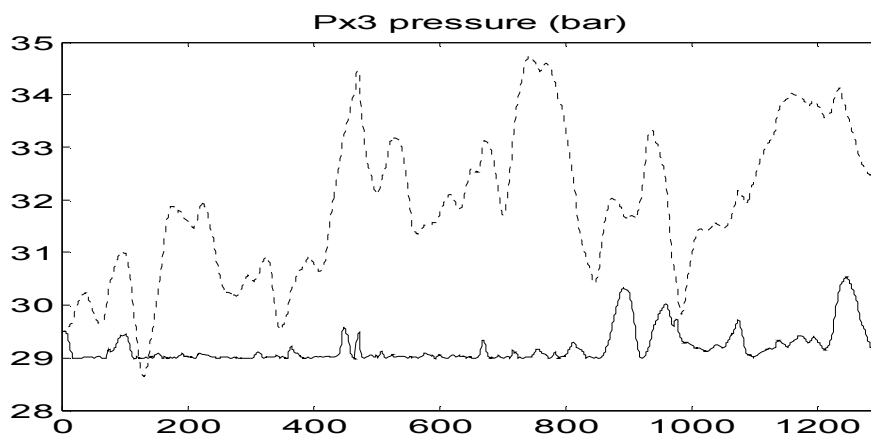
Figure 5.16 Px3 checkpoint pressure from 1.3.2003 00:00 to 9.3.2003 24:00. The solid line represents the result of the optimiser; the dashed line is as operated.

CS1 and CS2 discharge pressures are at their maximum limits over a large portion of the time period. CS1 discharge pressure experiences some ringing behaviour at the end of the period, and ringing is also seen in CS3 discharge pressure.

As a whole, the optimiser seems to be able to run the pipeline system quite optimally, while CS1 and CS2 discharge pressure are high and CS3 discharge pressure is low (lower than the operators have kept it). The Px3 checkpoint pressure is kept very close to the minimum limit 29 bar by the optimiser.

Case 2

The MPC literature frequently claims that the control horizon M should be as large as possible to ensure good control performance. In the second optimisation test run we will repeat the previous case, but with j_b=16, i.e. M=61. The other parameter values are the same as above. The results are presented in figures 5.17 to 5.19 below. CS1 discharge pressure is very close to case 1 and not displayed at all. The other pressure values are displayed together with the corresponding values from case 1.
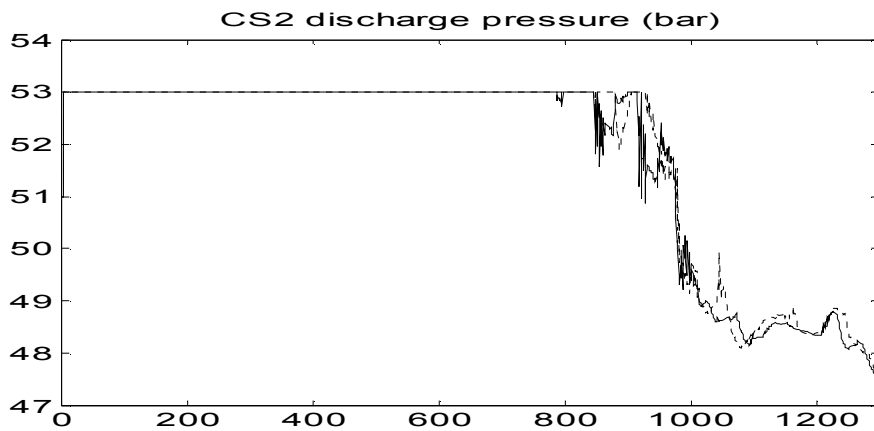
Figure 5.17 CS2 discharge pressure from 1.3.2003 00:00 to 9.3.2003 24:00. The solid line represents the result of the optimiser with j_b=16; the dashed line is from case 1 with j_b=8.
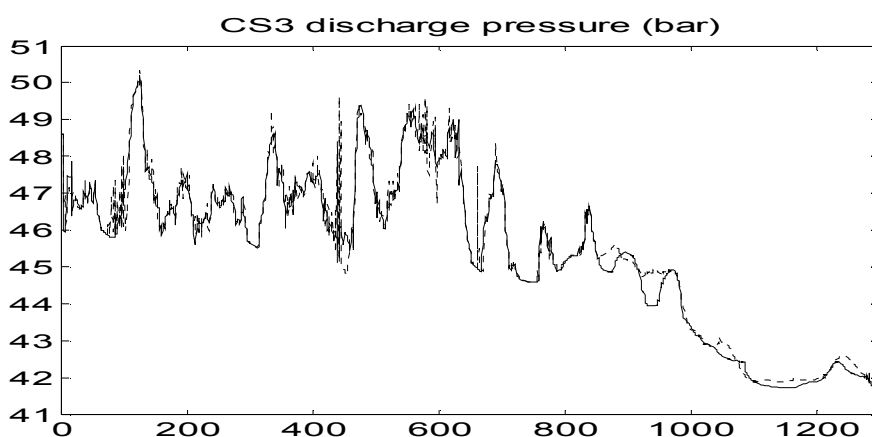
Figure 5.18 CS3 discharge pressure from 1.3.2003 00:00 to 9.3.2003 24:00. Solid line: j_b=16, dashed line: case1, j_b=8.
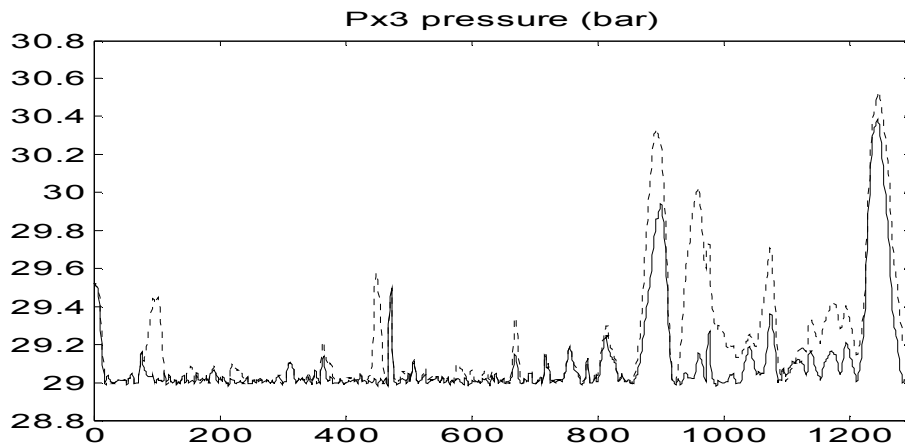
Figure 5.19 Px3 pressure from 1.3.2003 00:00 to 9.3.2003 24:00. Solid line: j_b=16, dashed line: case1, j_b=8.

If we consider the optimiser's ability to keep Px3 as close as possible to its minimum limit to be a performance measure, j_b=16 gives a somewhat better result than j_b=8. However, the change is not large, because there still seems to be room for improvement. This issue will be further discussed below in section 5.11.4.

5.11.2 Cost function approximation no.2

Next, we revert to the second cost function approximation with linear flow and linear pressure dependence (5.43).

Case 3

The values of the tuning parameters are: j_b=8, N_b=4 and P=100. No input variable damping is used, i.e. **R**=0. The values of the cost function approximation parameters are as shown in Appendix D. The time period is 1.1.2003 00:00 to 17.3.2003 22:00, or 2436 control intervals. The results are presented in figures 5.20 to 5.24 below.
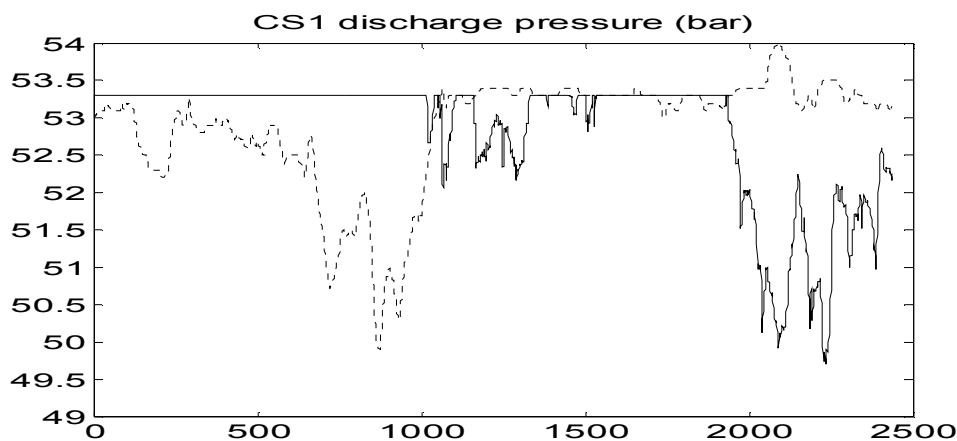
Figure 5.20 CS1 discharge pressure from 1.3.2003 00:00 to 17.3.2003 22:00. Solid line: optimiser, dashed line: as operated.
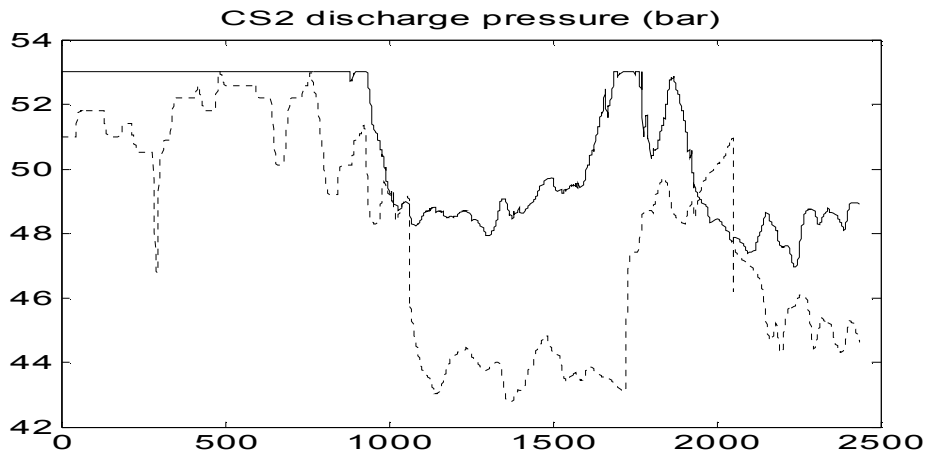
Figure 5.21 CS2 discharge pressure from 1.3.2003 00:00 to 17.3.2003 22:00. Solid line: optimiser, dashed line: as operated. Note, that CS2, as operated manually, is shut down for the second time at 15.3.2003 06:00 (time point 2050).
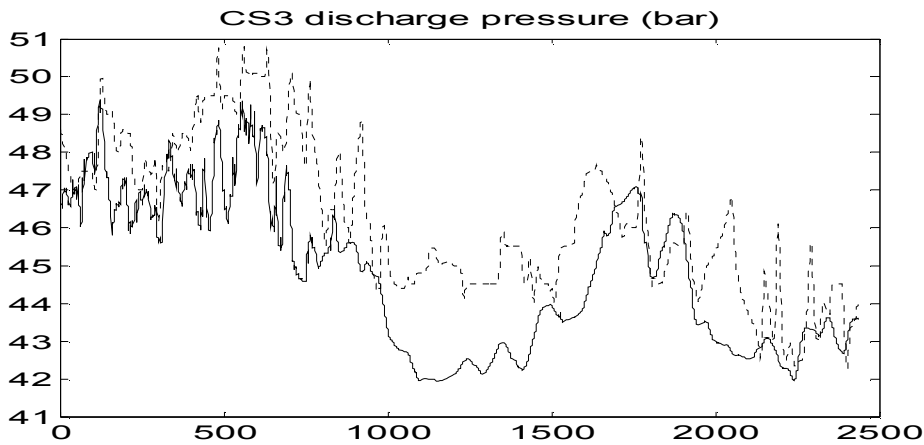
Figure 5.22 CS3 discharge pressure from 1.3.2003 00:00 to 17.3.2003 22:00. Solid line: optimiser, dashed line: as operated.
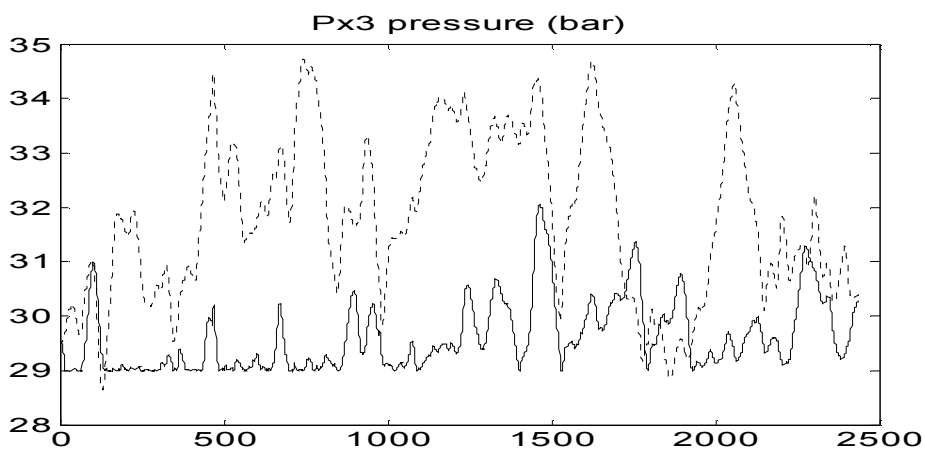
Figure 5.23 Px3 pressure from 1.3.2003 00:00 to 17.3.2003 22:00. Solid line: optimiser, dashed line: as operated.
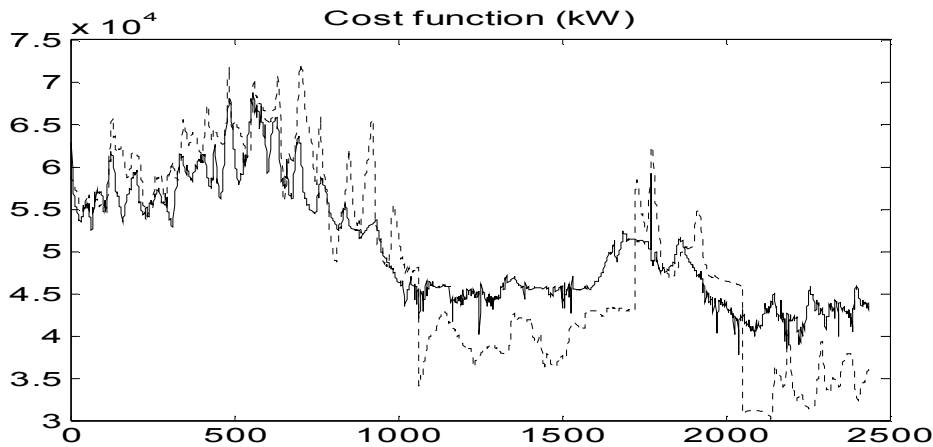
Figure 5.24 Cost function (kW) as optimised (solid line) and operated (dashed line) over the time period 1.3.2003 00:00 to 17.3.2003 22:00.

As can be seen in figure 5.24, the cost function is lower for the operating data in the ranges 1060...1720 and 2050...2436, due to the shutdown of CS2. The effect of the idle power of CS2 (parameter b_2 in the cost function) is the main reason for the cost difference.

For each type of constraint (12 CS envelope constraints and the Px3 minimum limit) and for each optimal solution, the optimiser monitors the number of active (scalar) constraints in the prediction horizon. The maximum number of active constraints for each type is equal to the length of the prediction horizon, P. In figure 5.25, the number of active constraints for this case is shown. In the beginning of the time period (until 1060) the active constraint monitoring was switched off. An observation to be further discussed in section 5.11.4 is that CS2 and CS3 minimum speed limits seem to be highly active over the whole period.
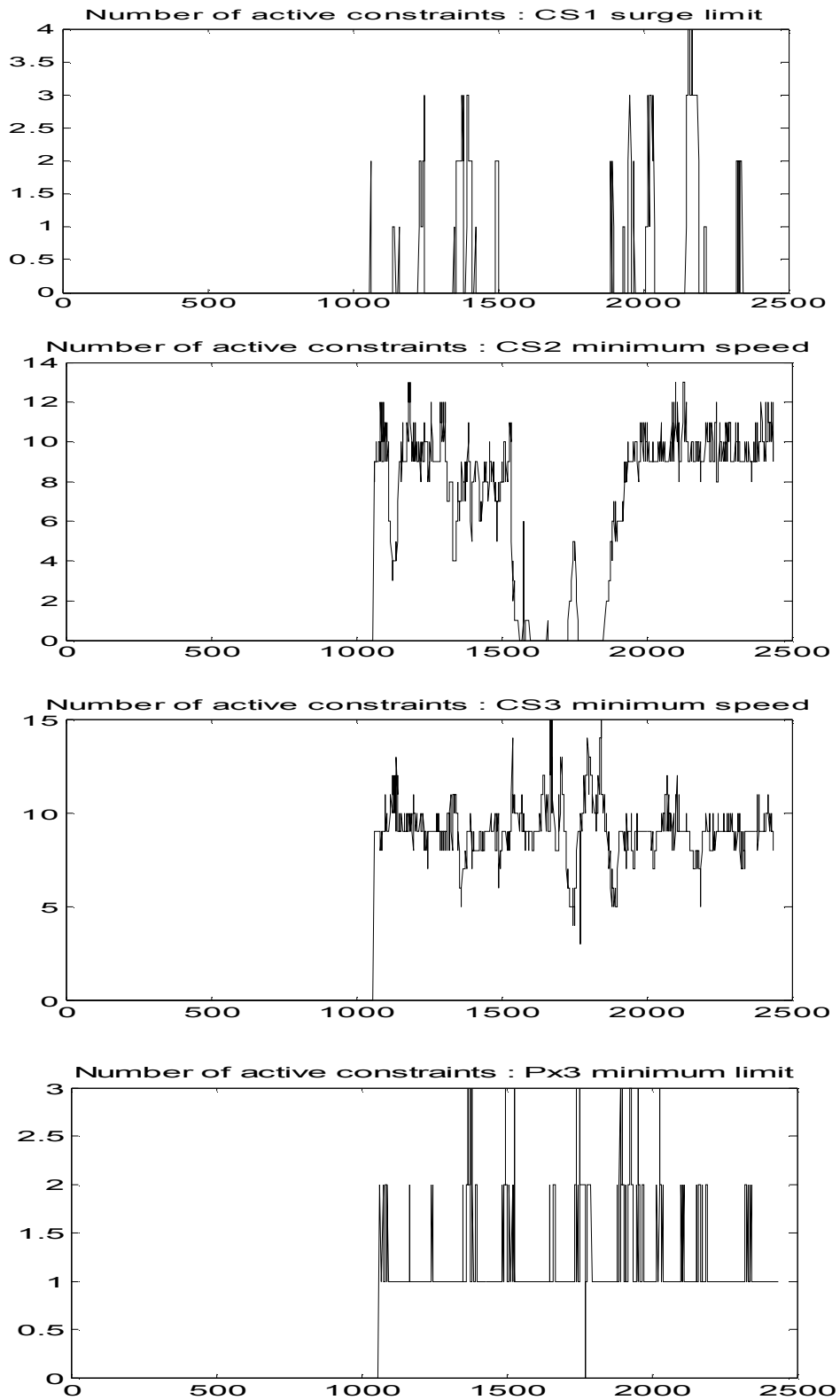
Figure 5.25 Number of active constraints from 1.3.2003 00:00 to 17.3.2003 22:00 (Top) CS1 surge limit, (Next to top) CS2 minimum sped limit, (Next to bottom) CS3 minimum speed limit and (Bottom) Px3 minimum limit

Case 4

The optimisation run of case 3 is repeated, but with j_b=16, which gives a control horizon M=61. The time period is 1.3.2003 00:00 to 12.3.2003 16:00. CS1 and CS2 discharge pressures behave very much as they do in case 3, so only CS3 discharge pressure and Px3 pressure are shown in figures 5.26 and 5.27 below.
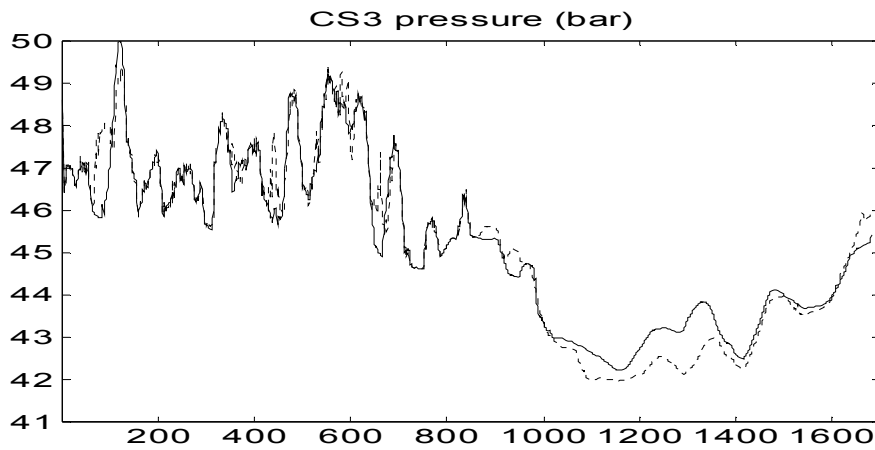
Figure 5.26 CS3 discharge pressure with j_b=16 (solid line) and from case 3 (dashed line) over the time period 1.3.2003 00:00 to 12.3.2003 16:00.
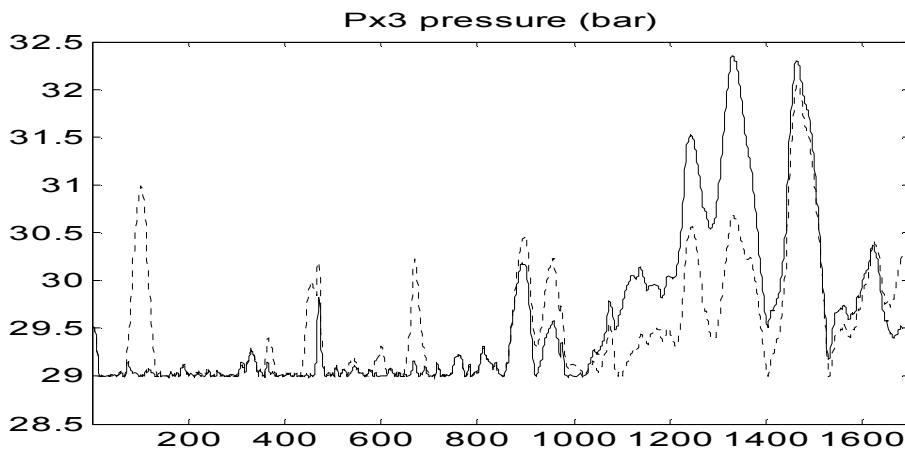
Figure 5.27 Px3 pressure with j_b=16 (solid line) and from case 3 (dashed line) over the time period 1.3.2003 00:00 to 12.3.2003 16:00.

Case 5

The optimisation run of case 3 is repeated, but with j_b=10 and P=64. The time period is 1.3.2003 00:00 to 12.3.2003 16:00. Only Px3 pressure is shown in figure 5.28 below together with Px3 pressure from case 4.
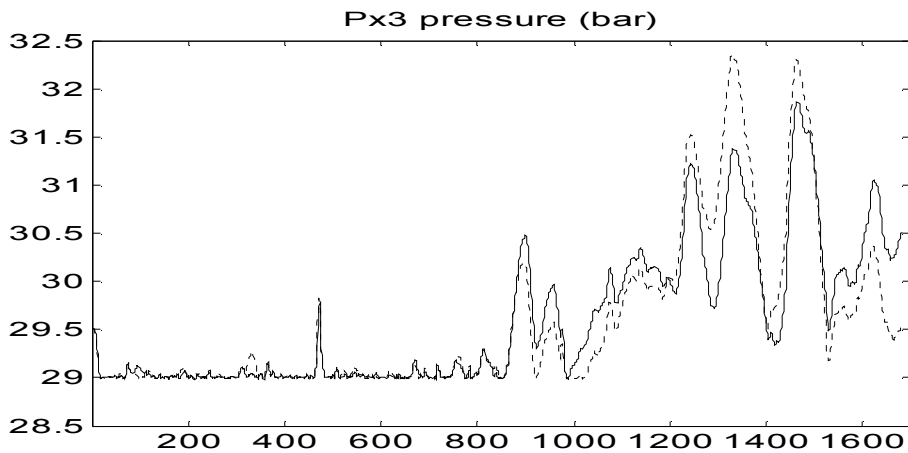
Figure 5.28 Px3 pressure with new parameters (solid line) and from case 4 (dashed line) over the time period 1.3.2003 00:00 to 12.3.2003 16:00.

5.11.3 Maximisation of energy consumption

Case 6

This optimisation run is a *maximisation* of the cost function. The only motive for this is to test the optimisation method because it will encounter other constraints than in the previous cases. The cost function approximation no. 2 with linear flow and linear pressure dependence (5.43) is used, the time period is 1.1.2003 00:00 to 11.3.2003 24:00 and the values of the tuning parameters are: j_b=16, N_b=4 and P=100, **R**=0. The results are shown in figures 5.29 to 5.32 below.
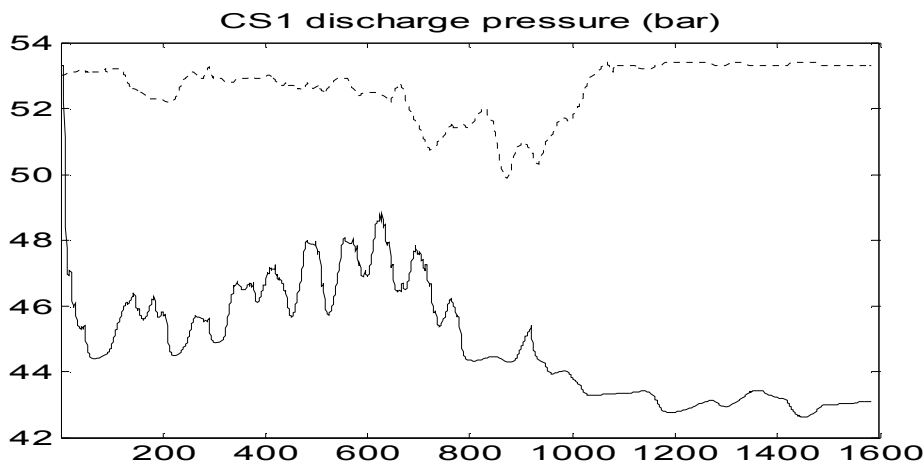
Figure 5.29 CS1 discharge pressure (solid line) and as operated (dashed line) over the time period 1.3.2003 00:00 to 11.3.2003 24:00.

88
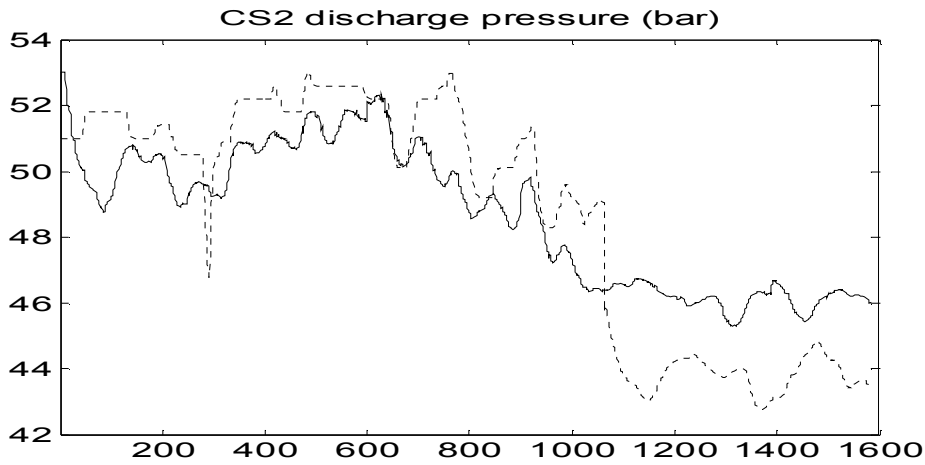
Figure 5.30 CS2 discharge pressure (solid line) and as operated (dashed line) over the time period 1.3.2003 00:00 to 11.3.2003 24:00.
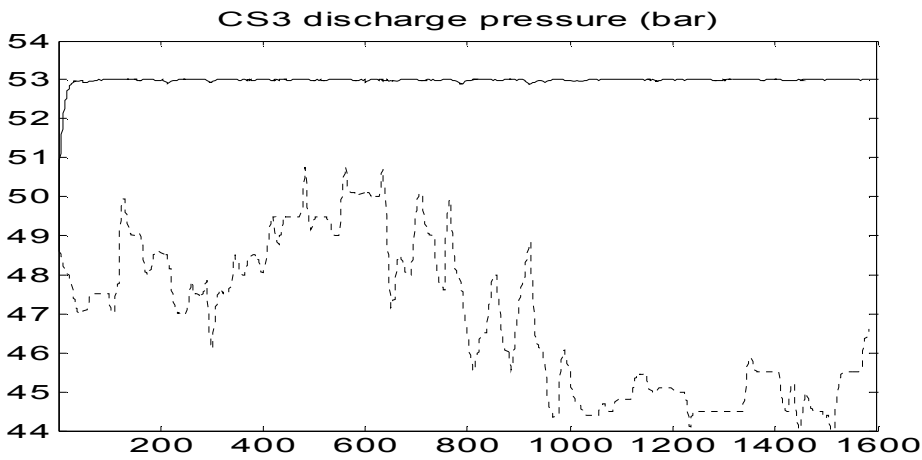
Figure 5.31 CS3 discharge pressure (solid line) and as operated (dashed line) over the time period 1.3.2003 00:00 to 11.3.2003 24:00.
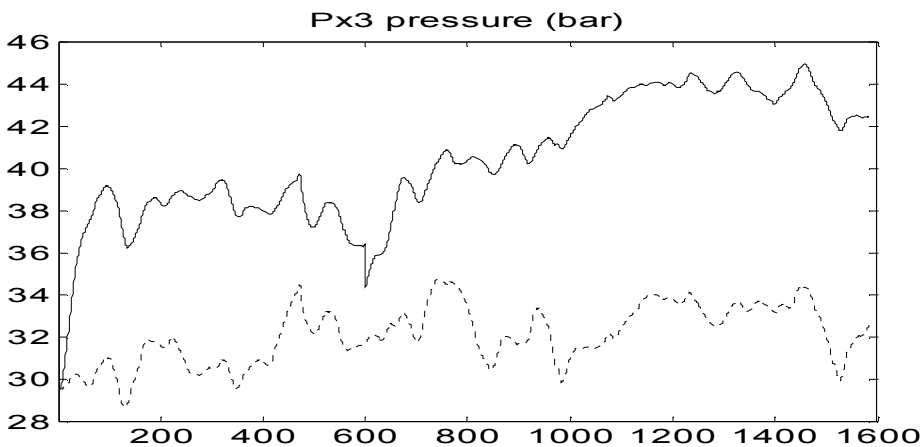
Figure 5.32 Px3 pressure (solid line) and as operated (dashed line) over the time period 1.3.2003 00:00 to 11.3.2003 24:00.

As expected (see the steady-state optimisation in section 5.9), CS1 and CS2 discharge pressure take small values and CS3 discharge pressure is high, this means that Px3 temporarily reaches pressures of up to 45 bar.

In figure 5.33, the number of active constraints in the prediction horizon at each optimisation interval is shown. CS2 and CS3 maximum speed constraints are active which certainly maximises energy consumption. Both CS1 surge and choke limits being active reveals that the operating point of CS1 makes large excursions within the envelope constraints over the control horizon M. CS1 minimum speed and CS2 surge constraints were also active at sporadic moments with the number of active constraints less than 3, but these are not shown in the figure.
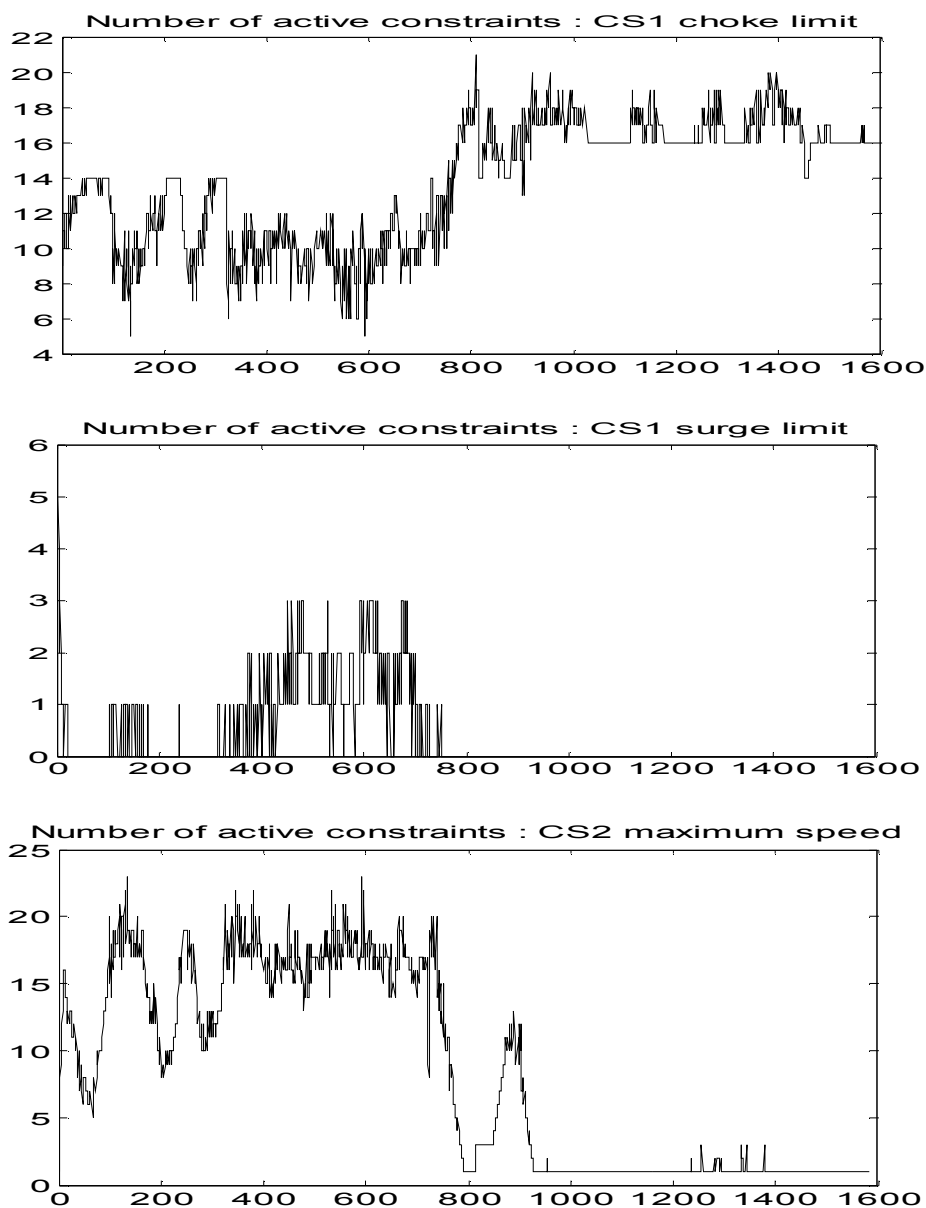
Figure 5.33 a)…c) Number of active constraints from 1.3.2003 00:00 to 11.3.2003 24:00. **a)** (Top) CS1 choke limit, **b)** (middle) CS1 surge limit, **c)** (bottom) CS2 maximum speed limit
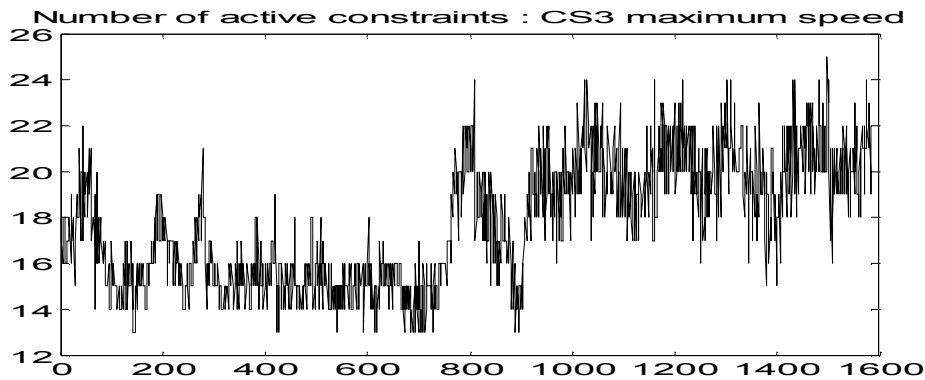
Figure 5.33 d) Number of active constraints from 1.3.2003 00:00 to 11.3.2003 24:00. CS3 maximum speed limit

5.11.4 Sub-optimal behaviour of the checkpoint pressure

In the ideal situation at hand, where the consumption forecasts are perfectly known over the prediction horizon, the optimiser should be able to keep Px3 very close to the minimum limit (29 bar). It actually achieves this aim, but it seems difficult to achieve significant improvement by selecting cost function approximation or varying the values of the tuning parameters. There is some modelling error, i.e. the linear model from CS3 discharge pressure to Px3 does not exactly match the dynamics of "Simone", but error in this SISO sub-system should not be harmful. Moreover, the fresh free response prediction obtained from "Simone" at each optimisation interval should help up the situation. There is one unique feature of this pipeline system, which can be generalised to any gunbarrel system.

Suppose that the current operating point of CS3 is close to the minimum speed limit (see figure 5.34). As a matter of fact, the optimal strategy is often to run CS3 this way (see figure 5.25). If gas consumption is predicted to decrease downstream CS3, then predicted Px3 values will increase, and the optimal decision would be to decrease CS3 discharge pressure. However, the CS3 minimum speed limit will not allow this, or it will allow only an extremely minimal decrease. Obviously, decreasing CS2 discharge pressure would decrease CS3 suction pressure *after a certain time* (see figure 5.34 b), leading to increased CS3 head and a movement away from the CS3 minimum speed limit. The central issue is that the magnitude of the CS2 discharge pressure decrease must be large enough to compensate for the fast dynamics of the CS3 discharge to suction pressure. From a strict optimisation point of view, it is *not* optimal to significantly decrease CS2 discharge pressure just to be able to make a small reduction in CS3 discharge pressure. Hence, Px3 is just allowed to float well above its minimum limit in a "suboptimal" manner.

91
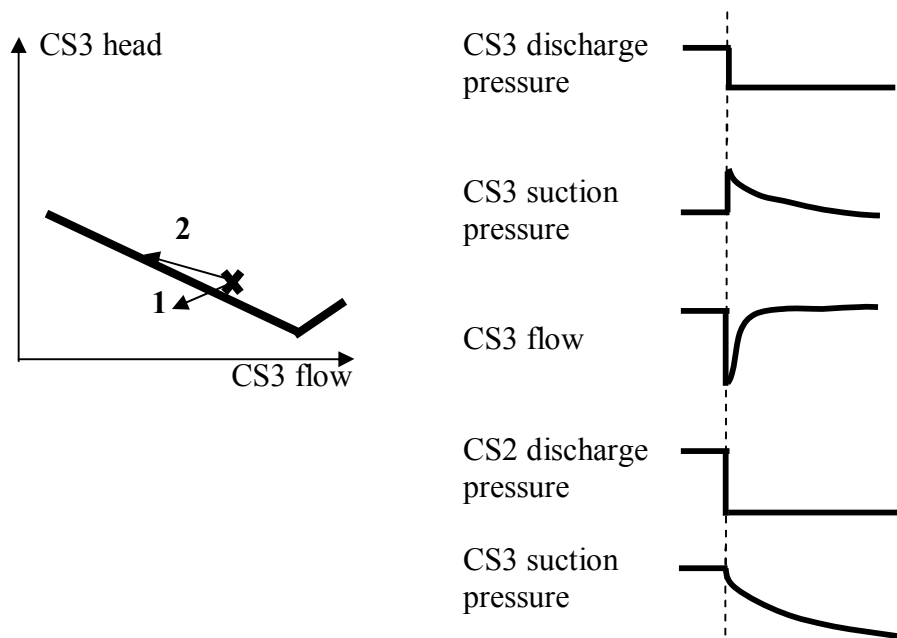
Figure 5.34 a) (left) A movement within the CS3 envelope in direction "1" from the current operating point **x** is not possible, direction "2" requires a CS2 discharge pressure decrease. **b)** (right) response sketches to illustrate, that for CS2 to enable a movement from x to the left, a large CS2 discharge pressure decrease is needed.

5.11.5 Energy consumption calculation and comparison

The optimal discharge pressure, suction pressure and CS gas flow evolution in the different cases are substituted into the *original* cost function (5.35) using the value P=0 to obtain the cost function as a function of time and the "current" simulated pressure and flow values at each optimisation interval. The average cost function values of the respective time periods are calculated and shown in table 5.2. The longer the optimisation time period, the smaller the cost because gas consumption and therefore CS gas flows decrease. The relative difference between operated data and optimiser results are compared up to 8.3.03 09:00 only, as this is the moment of time the operators shut down CS2 for the first time. The relative difference, 4.81%, is the energy saving the optimiser can achieve in case 3 compared to how the pipeline was actually operated in the beginning of March 2003.

The influence of the type of cost function approximation and tuning parameters is very small, which indicates that the cost function is "flat". Comparing the case 3 optimal cost function with case 6, where maximisation was performed, the difference is 17.48%.

Case	1.3.03 00:00-8.3.03 09:00	1.3.03 00:00-9.3.03 24:00	1.3.03 00:00-17.3.03 22:00	1.3.03 00:00-12.3.03 16:00	1.3.03 00:00-11.3.03 24:00
Operated	**59397**	-	-	-	-
Case 1	56524	54386			
Case 2	56478	54332			
Case 3	**56542**	54439	50235		**52831**
Case 4	56506	54509	-	52574	
Case 5	56550	54490	-	52617	
Case6					**64023**
Relative difference	4.81 %				17.48 %

Table 5.2 Average cost function values (kW) over different time periods and the different optimisation cases discussed.

Chapter 6

Optimisation with discrete decision variables

In this chapter, discrete decision variables, namely the start-up and shutdown commands of compressor stations (CSs) will be added to the receding horizon optimisation problem. This leads to a Mixed Integer Quadratic Programming (MIQP) problem. A systematic approach to defining an MIQP for a dynamic optimisation problem is to formulate it as a Mixed Logical Dynamical (MLD) system.

6.1 Shutting down and starting up compressor stations

As shown in Chapter 4, the dynamics of a pipeline system changes when the running status of CSs changes. We evaluated a number of linear dynamic models with respect to discharge pressure and off-take consumption flow changes at *steady-state* conditions. Steady-state in this respect means, that the models were evaluated after all transients related to shut down or start up had levelled out.

A CS shutting down at some time point $k + k_s$ in the prediction horizon may be illustrated as in figure 6.1. The optimal choice of the shutdown time k_s can be given to the receding horizon optimiser.
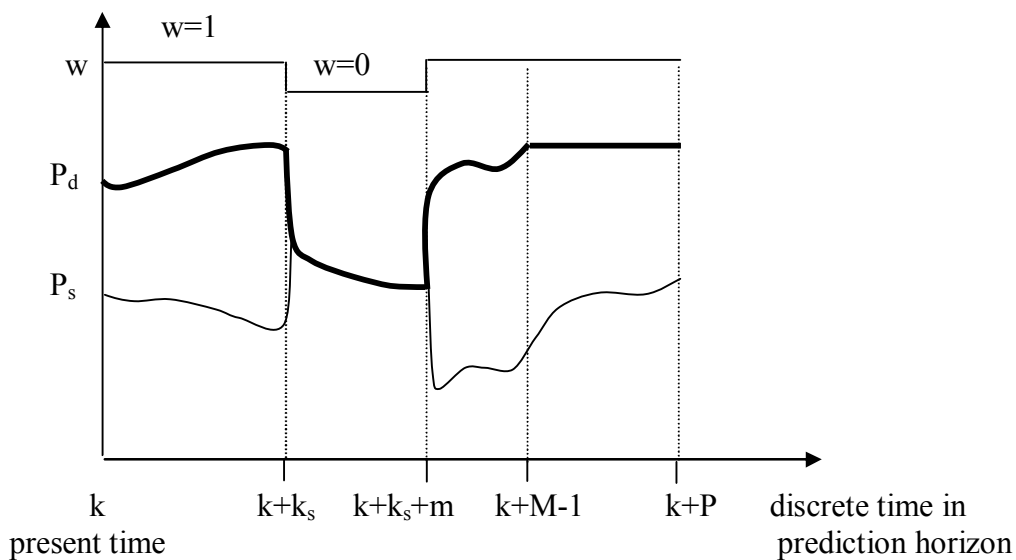
Figure 6.1 Shutting down a CS at time $k+k_s$ and restarting at $k+k_s+m$. "w" is the switch variable, P_d is the discharge pressure and P_s is the suction pressure. The control horizon is M<P implying that no CS status changes may occur past M.

95

If possible, for each CS, the optimiser should calculate an optimal sequence of running status values and, based on the receding horizon principle, implement the first values of the sequence and delete the rest of them, while the optimisation is repeated in the next cycle. "w" is defined as an integer valued decision or "switch" variable for the CS, where w(k)=1 means that the station is running and w(k)=0 is shut down. Before shutting down the CS, the discharge pressure of the CS follows the optimal values calculated by the optimiser. At shutdown time, the shutdown transient (see Chapter 4, section 4.6) is initiated.

From k_s and onwards in the prediction horizon, we lose the discharge pressure as a decision variable and from that moment we must use the linear models valid for the CS shut down in the optimiser.

6.2 A linearised pipeline system model

The pipeline system may be approximated by a series of pressure vessels as in figure 6.2, with the pressure of each vessel depicted by the shaded area. At some locations, CSs are used to raise the pressure. From a pure dynamic modelling perspective, the CSs are simply linear controllers capable of manipulating the gas flow from one vessel to a subsequent one. Thus, the pressure of the vessel immediately downstream the CS, i.e. the discharge pressure is ideally controlled by the gas flow, and no other variables of the system have any influence on that pressure. Accordingly, the pressure of the vessel immediately upstream the CS is the suction pressure of the station. The accuracy of this *space-discretised* model may be increased at wish by decreasing the volumes of the pressure vessels. The requirement that the discharge and suction pressures are equal when a CS is shut down may as well be met by using small enough vessel volumes.
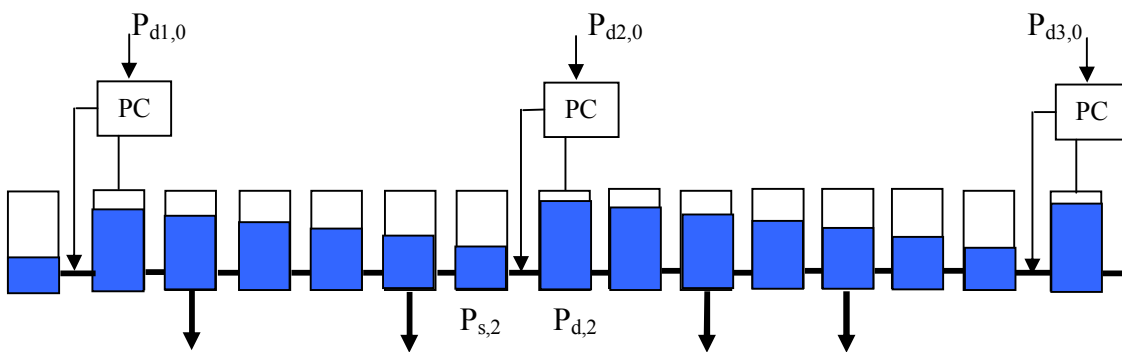
Figure 6.2 Space-discretised pressure vessel model of a pipeline system with three CSs and four off-takes. $P_{d1,0}$, $P_{d2,0}$ and $P_{d3,0}$ are the set points of the CS discharge pressure controllers (PC).

If we linearise and discretise this model, we obtain:

$$\mathbf{x}(k+1) = \mathbf{A}_1\mathbf{x}(k) + \mathbf{B}_1\mathbf{u}(k) + \mathbf{E}_1\mathbf{d}(k) \quad , \quad \mathbf{x}(0) = \mathbf{x}_0$$
$$\mathbf{y}(k) = \mathbf{C}_1\mathbf{x}(k)$$

(6.1)

Note, that linearisation is done with respect to some operating point (usually a steady-state point) $\mathbf{x}=\mathbf{x_s}$, $\mathbf{u}=\mathbf{u_s}$ and $\mathbf{d}=\mathbf{d_s}$. For simplicity, we will leave these out from the expressions below. Note also, that for the time being, we assume that the linear models also contain the contribution of off-take flows $\mathbf{d}$.

The output vector $\mathbf{y}$ of the system contains all relevant output variables needed: CS suction pressures, flow rates and checkpoint pressures. The subscript "1" for the model matrices means, that this is a nominal or "base case" model, where all CSs are running.

Note also, that for the disturbance contribution, the following expression holds approximately over the prediction horizon, within the linearisation error, if the linear model matrices in (6.1) are compatible with the simulator model (i.e. the matrices are obtained by linearising the same simulator model which provides the free response prediction $\mathbf{Z_{0,p}}(k)$ (see section 5.6, expression (5.33) and it's definitions):

$$\mathbf{C_{1,p}}\left[\mathbf{A_1^j x_0} + \sum_{i=0}^{j-1}\mathbf{A_1^{j-1-i}E_1 d}(k+i)\right] \approx z_{0,p}(k+j) \qquad (6.2)$$

where $\mathbf{C_{1,p}}$ is a row of the matrix $\mathbf{C_1}$ corresponding to the output variable "p" , $p=1,2,...,2N_c+N_x$ and $\mathbf{x_0} \triangleq \hat{\mathbf{x}}(k|k-1)$, see section 5.4, expressions 5.24 and 5.25.

We will use the *mixed logical dynamical system* (MLD system) approach (Bemporad and Morari, 1999) for the modelling needed for shut down and start up optimisation. Let us assume that we have linear models $\mathbf{A_1,B_1,E_1,C}$; $\mathbf{A_2,B_2,E_2,C}$; ..., $\mathbf{A_n,B_n,E_n,C}$, for n different modes of operation and binary variables $\delta_i(k)$, $i=1,2,...,n$. Then, a *piecewise linear system* may be defined using auxiliary variables $\mathbf{z}$ and δ:

$$\mathbf{z}(k) = \sum_{i=1}^{n}(\mathbf{A_i x}(k) + \mathbf{B_i u}(k) + \mathbf{E_i d}(k))\delta_i(k),$$
$$\mathbf{x}(k+1) = \mathbf{z}(k) \qquad (6.3)$$
$$\sum_{i=1}^{n}\delta_i(k) = 1$$

δ is binary valued and controls the model change, for example, $\delta_1(k)=1$ may stand for all CSs running, $\delta_2(k)=1$ means CS1 is shut down, $\delta_3(k)=1$ means CS2 shut down, and so on. All possible combinations yield $n=2^{N_c}$, where N_c is the number of CSs.

Assume now, that a CS shuts down at the moment $k+k_s$, whereby the linear model $\mathbf{A_1,B_1,E_1,C}$ will be replaced by the model $\mathbf{A_2,B_2,E_2,C}$, i.e. $\delta_1(k+j)=1$, $\delta_2(k+j)=0$, $j=1,2,...$ k_s and $\delta_1(k+j)=0$, $\delta_2(k+j)=1$, when $j= k_s+1, k_s+2,...$ For any output variable y_p we may write:

$$y_p(k+k_s)=\mathbf{C_p}\left[\mathbf{A_1^{ks} x_0} + \sum_{i=0}^{ks-1}\mathbf{A_1^{ks-1-i}B_1 u}(k+i) + \sum_{i=0}^{ks-1}\mathbf{A_1^{ks-1-i}E_1 d}(k+i)\right] \qquad (6.4)$$

$$y_p(k+k_s+1) = C_p[A_2A_1^{ks}x_0 + \sum_{i=0}^{ks-1} A_2A_1^{ks-1-i}B_1u(k+i) + B_2u(k+k_s) +$$

$$\sum_{i=0}^{ks-1} A_2A_1^{ks-1-i}E_1d(k+i) + E_2d(k+k_s)]$$

(6.5)

and for any $k_s' \geq m \geq 1$, where $k+k_s+k_s'$ is the moment of the next model change:

$$y_p(k+k_s+m) = C_p[A_2^m A_1^{ks}x_0 + \sum_{i=0}^{ks-1} A_2^m A_1^{ks-1-i}B_1u(k+i) + \sum_{i=0}^{m-1} A_2^{m-1-i}B_2u(k+k_s+i) +$$

$$\sum_{i=0}^{ks-1} A_2^m A_1^{ks-1-i}E_1d(k+i) + \sum_{i=0}^{m-1} A_2^{m-1-i}E_2d(k+k_s+i)]$$

(6.6)

Now, let y_p stand for the suction pressure of the CS "p" shutting down at time $k+k_s$. Up to this time in the prediction horizon, optimal values of discharge pressures, $u_p(k)$, may be determined by the optimiser, but after that moment of time, the shut down takes over and determines the behaviour of the discharge pressure. Separating u_p from the input vector **u** after the moment of shut-down and rearranging (6.6) yields:

$$y_p(k+k_s+m) = C_p[A_2^m A_1^{ks}x_0 + \sum_{i=0}^{ks-1} A_2^m A_1^{ks-1-i}B_1u(k+i) + \sum_{i=0}^{ks-1} A_2^m A_1^{ks-1-i}E_1d(k+i)$$

$$\sum_{i=0}^{m-1} A_2^{m-1-i}B_2M_{NP}u(k+k_s+i) + \sum_{i=0}^{m-1} A_2^{m-1-i}B_2M_Pu(k+k_s+i) + \sum_{i=0}^{m-1} A_2^{m-1-i}E_2d(k+k_s+i)]$$

(6.7)

where M_{NP} is an N_c times N_c identity matrix with a zero entry on the diagonal at (p,p) and M_P is an N_c times N_c zero matrix with a "one" on the diagonal at (p,p). The term containing the latter in (6.7) is the suction pressure response of CS "p" to the discharge pressure of the same CS.

The discharge pressures of the other CSs, u_i ,i=1,2,...,N_c, i≠p and the off-take flows, d_i ,i=1,2,...,N_d ,will now affect the discharge pressure $P_{d,p}$ through very nearly the same dynamics as the suction pressure y_p. Recalling, that the difference in the dynamics can be made arbitrarily small by choosing small enough pressure vessel volumes in the linear model (see figure 6.2), the resulting discharge pressure at time $k+k_s+m$ is:

$$P_{d,p}(k+k_s+m)=$$

$$u_p(k+k_s+m-1) + C_p\sum_{i=0}^{m-1} A_2^{m-1-i}B_2M_{NP}u(k+k_s+i) + C_p\sum_{i=0}^{m-1} A_2^{m-1-i}E_2d(k+k_s+i)$$

(6.8)

where $u_p(k+k_s+m-1)$ represents the discharge pressure value as determined by the shutdown transient.

Equating (6.7) and (6.8), while the discharge and suction pressures must be equal when the CS "p" is shut down, the fourth and sixth terms in (6.7) are cancelled out by the second and third terms in (6.8), respectively, leaving us with m equations from which the m unknown values $u_p(k+k_s),..., u_p(k+k_s+m-1)$ can be solved:

$$C_p[A_2^j A_1^{ks} x_0 + \sum_{i=0}^{ks-1} A_2^j A_1^{ks-1-i} B_1 u(k+i) + \sum_{i=0}^{ks-1} A_2^j A_1^{ks-1-i} E_1 d(k+i) + \sum_{i=0}^{j-1} A_2^{j-1-i} B_2 M_P u(k+k_s+i)] =$$

$$u_p(k+k_s+j-1) \tag{6.9}$$

where j=1,2,...,m. Because of the definition of M_P, no discharge pressures $u_i(k+k_s+j)$,i≠p are present in this equation when j≥0.

(6.9) is called the "equation constraint" because it will be used as such when setting up the receding horizon optimisation problem, as will be seen below.

Note 1. The second and third terms on the left side of (6.9) are "rest responses" to inputs and disturbances (discharge pressures and off-take flows), respectively, prior to the shut-down.

Note 2. Any output variable y_p of the pipeline system is calculated using expressions of type (6.6), where the discharge pressures of any CS being shut down are calculated by expressions of type (6.9) over the shut down period.

Let us now assume that the CS "p" restarts at time $k+k_s+k_s$'< k+M. From a modelling and optimisation perspective, it is much easier to start (or restart) a CS, as we only have to stop applying the equation (6.9) and allow the optimiser to again calculate values for $u_p(k+k_s+k_s'+1)$, $u_p(k+k_s+k_s'+2)$,...

If CS "p" is not running when the optimisation at cycle "k" commences, the equation constraint (6.9) is applied for time points k+1,..., k+k_s, until a CS start-up. Over this period, $\delta_1(i)=0$ and $\delta_2(i)=1$ and the model A_2, B_2, E_2, C is valid.
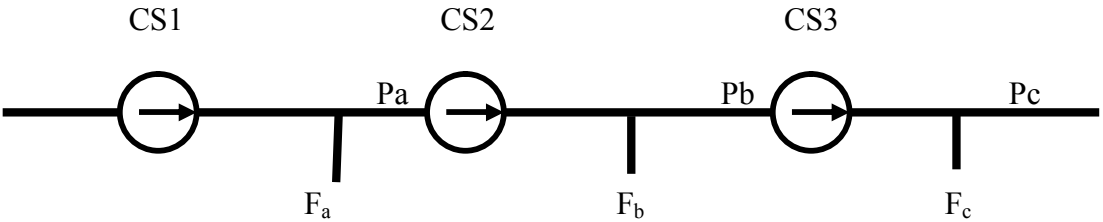
6.3 The free response prediction with compressor station shutdown and start -up

The simulator calculates the free response prediction vector $Z_0(k)$ once per optimisation cycle "k" prior to the optimisation calculations. The simulator uses the latest information available including CS running status and discharge pressures, which are considered to be constant over the whole prediction horizon.

The equation constraint (6.9) would require a rest response to the off-take flows before the shutdown moment k+k_s, which the simulator does *not* provide. Using expression (6.6) to calculate any output variables y_p would require the simulator to provide predictions corresponding to the model A_2, B_2, E_2, C which is valid after CS shutdown. This is not provided by the simulator either. In other words, the data in $Z_0(k)$ is in principle not *consistent* with the shutdown or start-up speculations made by the optimiser. The missing off-take flow models could be obtained by identifying linear models as was done for the inputs, but this is a large extra burden, especially when the pipeline system contains a large number of off-takes.

The question remains: do we have to revise the optimisation method to *iterate* between simulator runs and optimisations to reduce the error in cases where the optimiser wants to change CS status?

The largest error caused by the inconsistency comes from the fact that the "isolating" effect in the downstream direction of a running CS disappears when it shuts down. In reverse, the isolating effect appears when a CS is started up. Consider the example of a simulation study with "Simone" on the Finnish pipeline system in operating point no.1 (See Appendix A) in figure 6.3. All off-take flows are at constant steady-state values, but one off-take flow F_a is varying 40000 Nm3/h, as shown in figure 6.4. This flow variation is 7.1 % of the steady-state flow through CS2 in operating point no.1. When CS2 is running, F_a does not have any effect on pressure P_b (CS3 suction pressure), but after CS2 shut down, P_b will have a response to changes in F_a. The distance from CS1 to F_a is 85 km.

Figure 6.3 Pipeline simulation case to show effect of off-take flow F_a on P_b when CS2 is shutting down.

The free response prediction of P_b with CS2 running would remain a constant 38.7 bar, see the horizontal dashed line in figure 6.4 b). A CS2 shutdown is simulated with a *constant* off-take flow F_a, which is equivalent to assuming that there is no effect from F_a to P_b, which is what the simulator assumes when it calculates the free response prediction without knowing the plans to shut down CS2. Another shutdown is simulated with the F_a variations shown in figure 6.4. The values of P_b from both simulations are graphed in figure 6.4 b). The difference between these results, which is equal to the error in P_b made by using the constant free response prediction, is graphed in figure 6.4 c).
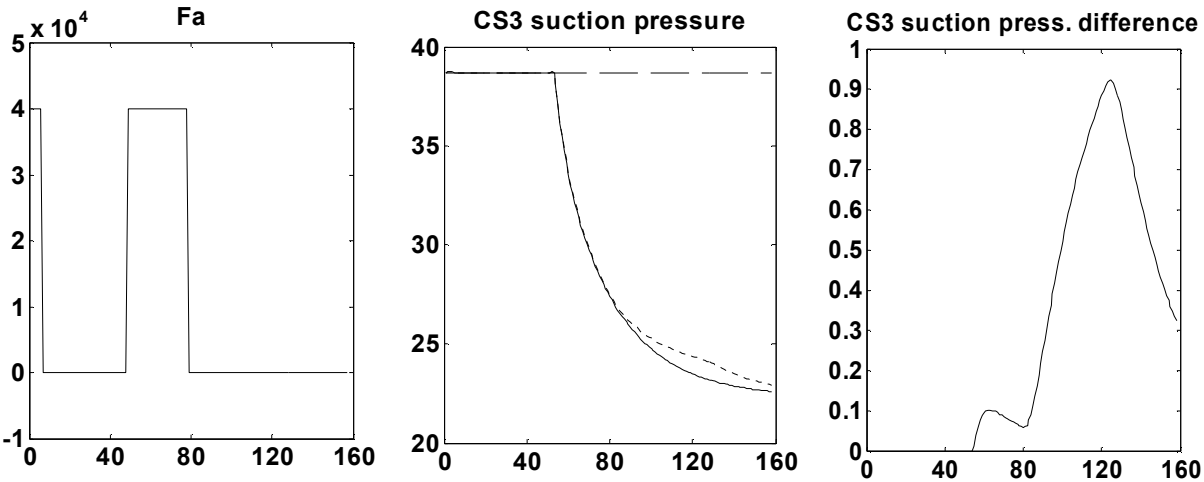

Figure 6.4 a) (left) F_a flow changes from 40000 Nm^3/h to 0 and back again. **b)** (middle) P_b responses to CS2 shut down at time point 51 **c)** (right) The difference between the two P_b curves in b). The time axis in all graphs are expressed in 10-minute time steps.

CS status changes do not influence responses in the upstream direction nearly as dramatically, as can be seen from the step response graphs in Appendix A. For example, P_a will always respond to off-take flows F_a, F_b and F_c irrespective of the status of CS1, CS2 and CS3. Figure 6.5 shows some cases collected from Appendix A.

The shut-down transient of a CS clearly dominates over effects caused by off-take flow changes when CSs shut down from high discharge pressures. The same is true for start-up transients, while the CS cannot usually stay at low discharge pressure after starting up. There are, however, cases where moderate discharge pressures are used (see CS3 shut-down simulation runs in section 6.8.2. below). In such cases, the inconsistency may generate some error.

If the off-take flow changes over the prediction horizon are small, then the error caused by the inconsistency is small as well.
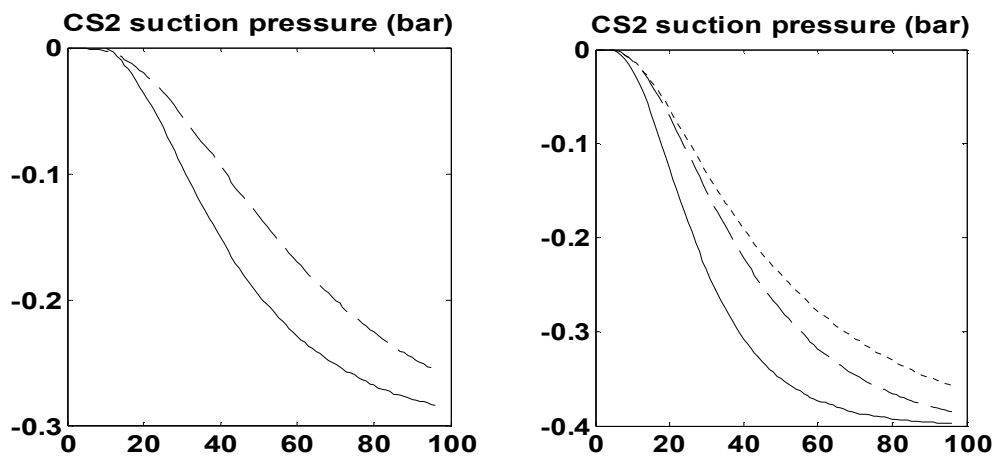
Figure 6.5 a) (left) CS2 suction pressure P_a response to Px3 flow rate change of 10000 Nm3/h in operating point no. 1 when all CSs are running (solid line) and CS2 shut down (dashed line) from figures A.10 b and A.18 b in Appendix A. **b)** (right) P_a response to Px3 flow rate change in operating point no. 2 when all CSs are running (solid line), CS2 is shut down (dashed line) and CS3 is shut down (dashed-dotted line) from figures A.10 b, A.18 b and A.26 b in Appendix A

Despite the inconsistency, no iterations between the receding horizon optimiser and the simulator will be introduced and optimiser development will continue to be based on the single free response prediction $\mathbf{Z_0}(k)$.

6.4 A mixed logical dynamical system

In this section we will formulate the receding horizon optimisation problem including CS shutdown and start-up optimisation using a *mixed logical dynamical system* (MLD system) (Bemporad and Morari, 1999). Note, that we have already defined the piecewise linear model in (6.3), which is an essential part of that system concept. The general form is:

101

$$x(k+1) = \mathbf{A}x(k) + \mathbf{B_1}\mathbf{u}(k) + \mathbf{B_2}\boldsymbol{\delta}(k) + \mathbf{B_3}\mathbf{z}(k)$$
$$y(k) = \mathbf{C}x(k) + \mathbf{D_1}\mathbf{u}(k) + \mathbf{D_2}\boldsymbol{\delta}(k) + \mathbf{D_3}\mathbf{z}(k) \qquad (6.10)$$
$$\mathbf{F_2}\boldsymbol{\delta}(k) + \mathbf{F_3}\mathbf{z}(k) \leq \mathbf{F_1}\mathbf{u}(k) + \mathbf{F_4}x(k) + \mathbf{F_5}$$

The state **x**, input **u** and output **y** are each partitioned into continuous parts (subscript "c") and logical, i.e. integer- or binary-valued parts (subscript "l"):
$\mathbf{x} \triangleq \begin{bmatrix} \mathbf{x_c^T} & \mathbf{x_l^T} \end{bmatrix}^T$, $\mathbf{u} \triangleq \begin{bmatrix} \mathbf{u_c^T} & \mathbf{u_l^T} \end{bmatrix}^T$, $\mathbf{y} \triangleq \begin{bmatrix} \mathbf{y_c^T} & \mathbf{y_l^T} \end{bmatrix}^T$. In the case of pipeline optimisation, only the logical inputs $\mathbf{u_l}$ will be needed.

The non-linearity involved with multiplying integer variables (δ) with continuous ones (**u**, see expression (6.3)) is taken care of by introducing the so-called "big M" concept. Defining auxiliary variables $\mathbf{z_i}(k) = \mathbf{A_i}x(k) + \mathbf{B_i}\mathbf{u}(k) + \mathbf{E_i}\mathbf{d}(k)$, i=1,2,...n, (6.3) is equivalent to the following set of inequalities, written as vector inequalities which have to be satisfied component-wise:

$$\mathbf{z_i}(k) \leq \mathbf{M}\delta_i(k)$$
$$\mathbf{z_i}(k) \geq \mathbf{m}\delta_i(k)$$
$$\mathbf{z_i}(k) \leq \mathbf{A_i}x(k) + \mathbf{B_i}\mathbf{u}(k) + \mathbf{E_i}\mathbf{d}(k) - \mathbf{m}(1-\delta_i(k)) \qquad (6.11)$$
$$\mathbf{z_i}(k) \geq \mathbf{A_i}x(k) + \mathbf{B_i}\mathbf{u}(k) + \mathbf{E_i}\mathbf{d}(k) - \mathbf{M}(1-\delta_i(k))$$

where **m** (**M**) is a vector of minimum (maximum) values of the state vector **x**. Only one $\mathbf{z_i}$-vector is non-zero at one time, the other n-1 vectors being forced to zero by (6.11). While the free response prediction $\mathbf{Z_0}(k)$ is used, all matrices $\mathbf{E_i} \equiv \mathbf{0}$, i=1,2,...,n in (6.11) and instead the outputs of the MLD system over the prediction horizon, j=0,1,…,P-1, are calculated as:

$$y_i(k+j) = \mathbf{C_i}\sum_{p=1}^{n} \mathbf{z_p}(k+j) + z_{0,i}(k+j) \qquad (6.12)$$

The initial state of the system $x_0=0$, because the contribution of the initial state is actually accounted for in $\mathbf{Z_0}(k)$, see expression (6.2).
We will relax the normal requirement within MLD systems that the coefficient matrices in (6.10) are time invariant so that we allow $\mathbf{F_5}$ (or a part of it) to be the carrier of the free response prediction values. Define an extra auxiliary variable vector $\mathbf{z_{n+1}}$ of the same dimension $2N_c+N_x$ as the output vector **y**. The equality $\mathbf{z_{n+1}}(k) = \mathbf{C_0}(k)\mathbf{Z_0}(k)$, where $\mathbf{C_0}$ is a matrix ($\mathbf{C_0}$ (i,j)=1, when i=1,.., $2N_c+N_x$, j=P(i-1)+k, otherwise 0) used to pick values from $\mathbf{Z_0}$, is implemented as $4N_c+2N_x$ extra inequalities in (6.10). Then, defining $\mathbf{C_1} = \mathbf{D_1} = \mathbf{D_2} = \mathbf{0}$ and $\mathbf{D_3} = \begin{bmatrix} \mathbf{C} & \mathbf{C} & ... & \mathbf{C} & \mathbf{I} \end{bmatrix}$ in (6.10) we obtain:

$$y(k) = \begin{bmatrix} \mathbf{C} & \mathbf{C} & ... & \mathbf{C} & \mathbf{I} \end{bmatrix} \begin{bmatrix} \mathbf{z_1}(k) \\ \mathbf{z_2}(k) \\ ... \\ \mathbf{z_n}(k) \\ \mathbf{z_{n+1}}(k) \end{bmatrix} \qquad (6.13)$$

Let us define a new set of binary variables, "w", constituting the logical part of the input vector $\mathbf{u}$, $\mathbf{u}_l = \mathbf{w}$, and defined as the running statuses of the CSs. The number of w-variables is N_c and $n=2^{N_c}$. The variables w_i and δ_j are related as shown in figure 6.6.

Case	w_1	w_2	w_3		δ_1	δ_2	δ_3	δ_4	δ_5	δ_6	δ_7	δ_8
All CSs running	1	1	1		1							
CS 1 off	0	1	1			1						
CS 2 off	1	0	1				1					
CS 3 off	1	1	0					1				
CS1 and CS2 off	0	0	1						1			
CS1 and CS3 off	0	1	0							1		
CS2 and CS3 off	1	0	0								1	
All CS off	0	0	0									1

Figure 6.6 Table relating model change variables δ_i with CS running status variables w_i for $N_c=3$ and $n=8$. $w_i=1$ means CS number "i" is running, otherwise CS "i" is shut down. The empty table entries for δ_i contain zeros.

It is easy to verify that the following set of inequalities and one equality determines the values for $\delta_i(k+j)$, $j=0,1,...P-1$, satisfying the relations in figure 6.6:

$$-\delta_1(k+j)+w_1(k+j)+w_2(k+j)+w_3(k+j) \le 2$$
$$-\delta_2(k+j)+1-w_1(k+j)+w_2(k+j)+w_3(k+j) \le 2$$
$$-\delta_3(k+j)+w_1(k+j)+1-w_2(k+j)+w_3(k+j) \le 2$$
$$-\delta_4(k+j)+w_1(k+j)+w_2(k+j)+1-w_3(k+j) \le 2$$
$$-\delta_5(k+j)+1-w_1(k+j)+1-w_2(k+j)+w_3(k+j) \le 2 \qquad (6.14)$$
$$-\delta_6(k+j)+1-w_1(k+j)+w_2(k+j)+1-w_3(k+j) \le 2$$
$$-\delta_7(k+j)+w_1(k+j)+1-w_2(k+j)+1-w_3(k+j) \le 2$$
$$-\delta_8(k+j)+1-w_1(k+j)+1-w_2(k+j)+1-w_3(k+j) \le 2$$
$$\delta_1(k+j)+\delta_2(k+j)+\delta_3(k+j)+\delta_4(k+j)+\delta_5(k+j)+\delta_6(k+j)+\delta_7(k+j)+\delta_8(k+j)=1$$

Writing the equality as two inequalities, we obtain n+2 inequalities which are added to the matrix inequality in (6.10).

The final MIQP problem we are going to obtain, or the time required to solve it, will benefit if we can limit the number of searches in the tree of binary decision alternatives. In addition, it is not at all recommended to shut down and start up CSs frequently. If $w_i(k)$, $w_i(k+k_1)$, $w_i(k+k_1+k_2)...$, $w_i(k+k_1+k_2+...+k_{Jw-1})$, where $k_i>1$, can be freely manipulated by the optimiser, but intermediate values must be frozen, we can define equalities $w_i(k+1) - w_i(k)=0$, $w_i(k+2) - w_i(k+1)=0,...$; $w_i(k+k_1+1) - w_i(k+k_1)=0,....$ The total number of equalities for one CS is $\sum_{i=1}^{J_w} k_i - J_w$, where k_i are the lengths of the freezing intervals and J_w is the total number of those intervals. For the whole MIQP problem, with N_c CSs, we obtain $2N_c(\sum_{i=1}^{J_w} k_i - J_w)$ *in*equalities.

The limiting equality technique is the same as that used in multi-rate control (Ling and Lim, 1996) and is illustrated in figure 6.7.
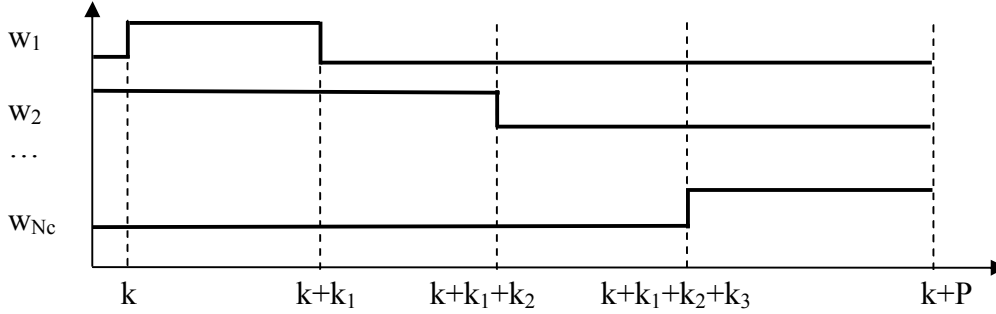
Figure 6.7 Example on limiting the w_i-variables over the prediction horizon P. Each value of w_i is frozen over k_r sample intervals so, that $k_1+k_2+ ... +k_{Jw} = P$. In the figure, $J_w =4$.

If considered necessary, it is possible to block the continuous decision variables $\mathbf{u_i}$ using the same technique as in Chapter 5, section 5.10. However, Bemporad and Morari (1999) do not recommend using even a shorter control horizon, M < P, as savings in the computational load will not be significant. They do not mention blocking, but presumably blocking is not recommended either on the same grounds.

The $4N_cP$ CS envelope constraints (see Chapter 5, the matrix inequalities (5.51)) can now be written as scalar inequalities:

$$
a_{ij}\left[\sum_{p=0}^{r}\Delta u_i(k+p)+u_i(k\text{-}1)\right]+b_{ij}\left[\mathbf{C}_i\sum_{p=1}^{n}\mathbf{z_p}(k+r)+z_{0,i}(k+r)\right]+
$$
$$
c_{ij}\left[\mathbf{C}_{Nc+i}\sum_{p=1}^{n}\mathbf{z_p}(k+r)+z_{0,Nc+i}(k+r)\right]\leq M'\sum_{q\in Qi0}\delta_q(r) \tag{6.15}
$$

where i=1,2,..., N_c , j=1,..,4 and r=0,1,...,P-1. M' is a sufficiently large number to *relax the compressor constraints* when CS "i" is shut down, which is true for the values of q belonging to the set Q_{i0}. (For the example in figure 6.6, if i=2, then Q_{20}={3,5,7,8}, i.e. when $\delta_3(k)$, $\delta_5(k)$, $\delta_7(k)$ or $\delta_8(k)$=1, then CS2 is shut down and the constraints must be relaxed).

The constraints on checkpoint pressures are:

$$
\mathbf{C}_{2Nc+i}\sum_{p=1}^{n}\mathbf{z_p}(k+r)+z_{0,2Nc+i}(k+r) \geq P_{x,i,min} \tag{6.16}
$$

where i=1,2,..., N_x and r=0,1,...,P-1.

The minimum and maximum CS discharge pressure limits and the discharge pressure change limits are, both relaxed when a CS is shut down:

$$u_i(k+r) \leq P_{d,i,max} + M' \sum_{q \in Qi0} \delta_q(r)$$

$$\text{(6.17)}$$

$$u_i(k+r) \geq P_{d,i,min} - M' \sum_{q \in Qi0} \delta_q(r)$$

and:

$$u_i(k+r) - u_i(k+r-1) \leq \Delta u_{i,Max}(r) + M' \sum_{q \in Qi0} \delta_q(r)$$

$$\text{(6.18)}$$

$$u_i(k+r) - u_i(k+r-1) \geq \Delta u_{i,Min}(r) - M' \sum_{q \in Qi0} \delta_q(r)$$

where $i=1,2,..., N_c$ and $r=0,1,...,P-1$.

We can calculate the values of all output variables (see (6.13)) needed for calculating the value of the quadratic cost function. However, we have to add the contribution of the CS status changes to the cost function so that the "zero degree term" of the CS power consumption, b_i, $i=1,2,...,N_c$ (see section 5.7, expression (5.35)) is added to the cost when the CS is running, but otherwise not. In this way, we obtain zero cost for a CS in shut down status, while discharge pressure equal to suction pressure yields zero for the adiabatic head of the CS. The cost contribution of start-up and shutdown optimisation is:

$$\sum_{i=1}^{Nc} b_i \sum_{j=0}^{P-1} w_i(k+j) \qquad \text{(6.19)}$$

which replaces the term $\sum_{i=1}^{P} \sum_{j=1}^{Nc} b_j$ in (5.35).

If there is a need to consider an extra cost associated with the status changes of the CSs, a *start-up* cost may be defined. First, we must detect whether some $w_i(k+j) > w_i(k+j-1)$ and, if this is the case, "raise a flag" or more precisely, collect all start-ups for each CS into a variable. Let the total start-up cost for the CSs be a linear expression: $\sum_{i=1}^{Nc} C_{S,i} \sum_{j=0}^{P-1} v_i(k+j)$, where $C_{s,i}$ is the cost in power units and $v_i(k+j)=1$ if $w_i(k+j) > w_i(k+j-1)$. If the $v_i(k+j)$:s are binary variables, then the inequalities (6.20) apply over $j=0,...,P-1$. $w_i(k-1)$ is the current running status of CS "i" when entering the optimisation cycle.

$$-w_i(k+j) + v_i(k+j) \leq 0$$
$$w_i(k+j-1) + v_i(k+j) \leq 1 \qquad \text{(6.20)}$$
$$w_i(k+j) - w_i(k+j-1) - v_i(k+j) \leq 0$$

These $3N_cP$ additional inequalities must be added to the set of inequalities in (6.10).

The final effort needed to obtain a complete MLD system with all relevant variables and inequalities is to set up the equation constraint within the MLD framework. Before that, we will inspect the dimensions of the resulting MIQP problem using the auxiliary variables and inequalities obtained so far.

6.5 The MIQP problem

The optimal control, or dynamic optimisation, problem based on an MLD system will result in an MIQP problem (Bemporad and Morari, 1999) with the variables defined as follows:

$$\mathbf{X_1} = \begin{bmatrix} \mathbf{u}(k) \\ \dots \\ \mathbf{u}(k+P-1) \\ w_1(k) \\ w_2(k) \\ \dots \\ w_{N_c}(k+P-1) \end{bmatrix}, \ \mathbf{X_2} = \begin{bmatrix} \delta_1(k) \\ \delta_2(k) \\ \dots \\ \delta_n(k+P-1) \\ v_1(k) \\ v_2(k) \\ \dots \\ v_{N_c}(k+P-1) \end{bmatrix}, \ \mathbf{X_3} = \begin{bmatrix} \mathbf{z_1}(k) \\ \mathbf{z_2}(k) \\ \dots \\ \mathbf{z_{n+1}}(k+P-1) \end{bmatrix} \quad (6.21)$$

For $\mathbf{X} = [\mathbf{X_1^T} \ \mathbf{X_2^T} \ \mathbf{X_3^T}]^T$, the MIQP problem is:

$$\text{Min.} \frac{1}{2} \mathbf{X^T Q X} + \mathbf{b^T X}$$

$$\text{Subject to } \mathbf{AX} \leq \mathbf{B} \quad (6.22)$$

The matrices $\mathbf{Q}$, $\mathbf{b}$, $\mathbf{A}$ and $\mathbf{B}$ can be calculated from the expressions given in section 6.4 and from the cost function expressions in section 5.7.

Table 6.1 summarises the number and dimensions of the variables in the MIQP problem. The term "expanded" means the total number of scalar variables over the whole prediction horizon.

Variable	Name	Dimension	Number	Expanded
Auxiliary variable	$\mathbf{z_i}$	r	n	rnP
Auxiliary variable	$\mathbf{z_{n+1}}$	$2N_c + N_x$	1	$(2N_c + N_x)P$
Input variable	$\mathbf{u}$	N_c	1	$N_c P$
Auxiliary binary variable	δ_i	1	n	nP
Auxiliary binary variable	v_i	1	N_c	$N_c P$
Input binary variable	w_i	1	N_c	$N_c P$

Table 6.1 Variables of the MIQP problem

The total number of MIQP variables is $[rn+3N_c+N_x]P$ continuous and $(n+2N_c)P$ binary variables. Table 6.2. summarises the linear inequalities of the MIQP problem.

The total number of MIQP inequalities is $[17N_c+3N_x+4rn+n+2]P -2N_c J_w$

If each of the outputs y_i is represented by three states, the dimension of the state vector $\mathbf{x}$, $r=3(2N_c+N_x)$, which is equal to the dimension of all auxiliary variables $\mathbf{z_i}$. Using this assumption, for $N_c=3$, $N_x=1$, $n=2^{N_c}=8$, $J_w=6$ and $P=100$ we obtain 17800 as the total number

(expanded) of continuous variables; 1400 as the total number of discrete variables and 73564 as the total number of inequalities.

Inequality	Dimension	Number	Expanded
big-m inequalities for z_i (6.11)	$4r$	n	$4rnP$
$z_{n+1} = C_0 Z_0$ equations	$2N_c + N_x$	2	$2(2N_c + N_x)P$
δ_i to w_i relations (6.14)	$n+2$	1	$(n+2)P$
CS envelope constraint (6.15)	$4N_c$	1	$4N_c P$
Checkpoint pressure limits (6.16)	N_x	1	$N_x P$
Discharge pressure limits (6.17)	$2N_c$	1	$2N_c P$
Input increment limits (6.18)	$2N_c$	1	$2N_c P$
Limiting w_i (figure 6.7)	$2N_c$	$(P-J_w)$	$2N_c(P-J_w)$
Startup cost management (6.20)	$3N_c$	1	$3N_c P$

Table 6.2 Linear inequalities of the MIQP problem

If we limit the number of CS status combinations in figure 6.6. in order not to accept "All CS off" (δ_8), "CS2 and CS3 off" (δ_7) and "CS1 and CS3 off" (δ_6), we have n=5, giving 11500 continuous variables, 1100 discrete variables and 48064 inequalities.

If we further reduce P from 100 to 50, we obtain 5750 continuous variables, 550 discrete variables and 24014 inequalities.

It is not at all surprising to obtain such a large dimension of the MIQP problem.

We did not yet implement the equation constraint into the MLD system and further into the MIQP problem. We have good ground to assume that it can be done, since the equation constraint is linear. On the other hand, we can also assume that some additional auxiliary variables and inequalities are required. As at this point we already saw a dimensional explosion, we will *not* develop the MLD system-based MIQP problem any further.

6.6 Step response models revisited

In Chapter 5 we used step response models in the optimiser. So far, in this chapter we have used state-space models. The reason for using state-space models is that MLD systems are defined based on state-space models and the background for the shutdown transient, which is determined through the equation constraint, is easier to explain this way.

If we want to use step response (matrix) models in our MLD system, we would need some kind of state-space model of type (6.3) including model change variables δ_i. Consider a non-minimal state-space model $X(k+1) = M_{ss}X(k) + S_1\Delta u(k)$; $y(k) = HX(k)$ which is slightly modified from (5.19) so, that we use a shift matrix M_{ss} consisting of P x P M_s-matrices, where the last row and last column of M_s (5.20) are deleted, and S_1 (5.21) is modified to use step response vectors of length P instead of length P+1. Moreover, we will use an output matrix H (a modified matrix T, see (5.22)) : $H(i,j)=1$, if $j=P(i-1)+1$, otherwise $H(i,j)=0$. It is easy to verify that propagating this

model over $\Delta\mathbf{u}$(k), $\Delta\mathbf{u}$(k+1),…, $\Delta\mathbf{u}$(k+P-1) with the initial condition $\mathbf{X}$(k)=0, the sequence of outputs $\hat{\mathbf{y}}(k+1), \hat{\mathbf{y}}(k+2),..., \hat{\mathbf{y}}(k+P)$ is the predicted control response of the system, i.e. the predicted outputs excluding the contribution of the free response prediction $\mathbf{Z_0}$(k). If we now issue a model change at time k+k$_s$, we will start to use another step response matrix, say $\mathbf{S_2}$, instead of $\mathbf{S_1}$ in our model, while the matrix $\mathbf{M_{ss}}$ remains unchanged.

This is an acceptable state-space model and can be used as a basis for an MLD system and a changing model with a common state vector is obtained here also. Johansen and Murray-Smith (1997) in Chapter 1, page 19, recommend a common state vector for the separate local models involved in a modelling problem where different local models apply in different operating regimes. This is satisfied by both the model (6.3) and by the non-minimal model presented here.

Recalling section 6.2, expressions (6.5) and (6.6) we see that a model change at time k+k$_s$, causes a "mixed dynamic model" while model $\mathbf{C},\mathbf{A_1},\mathbf{B_1}$ mixes with $\mathbf{C},\mathbf{A_2},\mathbf{B_2}$ in the lower left sub-matrix of the impulse response matrix:

$$\mathbf{H} = \begin{pmatrix} \mathbf{CB_1} & 0 & 0 & \cdots & 0 & 0 & 0 \\ \mathbf{CA_1B_1} & \mathbf{CB_1} & 0 & \cdots & 0 & 0 & 0 \\ \vdots & \vdots & \vdots & & & & \\ \mathbf{CA_1^{ks-1}B_1} & \mathbf{CA_1^{ks-2}B_1} & \mathbf{CA_1^{ks-3}B_1} & \cdots & \mathbf{CB_1} & 0 & \cdots & 0 \\ \hline \mathbf{CA_2A_1^{ks-1}B_1} & \mathbf{CA_2A_1^{ks-2}B_1} & \mathbf{CA_2A_1^{ks-3}B_1} & \cdots & \mathbf{CA_2B_1} & \mathbf{CB_2} & & 0 \\ \vdots & \vdots & \vdots & & & & \\ \mathbf{CA_2^{P-ks}A_1^{ks-1}B_1} & \mathbf{CA_2^{P-ks-1}A_1^{ks-2}B_1} & \mathbf{CA_2^{P-ks-2}A_1^{ks-3}B_1} & \cdots & & \cdots & \mathbf{CA_2B_2} & \mathbf{CB_2} \end{pmatrix}$$

(6.23)

the step response matrix $\mathbf{S}$ corresponding to $\mathbf{H}$ contains matrices $\sum_{k=0}^{i-j}\mathbf{CA_1^kB_1}$, $i \le k_s$, $j \le i$ in the left upper sub-matrix, $\sum_{k=0}^{ks-j}\mathbf{CA_2^{i-ks}A_1^kB_1} + \sum_{k=0}^{i-ks-1}\mathbf{CA_2^kB_2}$, $i \ge k_s+1$, $j \le k_s$ in the left lower sub-matrix and $\sum_{k=0}^{i-j}\mathbf{CA_2^kB_2}$, $i \ge k_s+1$, $k_s+1 \le j \le i$ in the right lower sub-matrix.

Propagating the non-minimal state space model and implementing a model change at k+k$_s$ yields predictions over the whole horizon for the system output, excluding the contribution of the free response prediction $\mathbf{Z_0}$(k) : $\mathbf{S}\Delta\tilde{\mathbf{u}}(k)$, where $\mathbf{S}$ has the structure (5.17) and each sub-matrix of $\mathbf{S}$ is:

$$\mathbf{S_{ij}} = \left(\begin{array}{cc|cc} s_{ij}^1(1) & 0 & & \\ \vdots & & & \\ s_{ij}^1(k_s) & s_{ij}^1(k_s\text{-}1) & \cdots & 0 \\ \hline s_{ij}^1(k_s\text{+}1) & s_{ij}^1(k_s) & s_{ij}^2(1) & 0 \\ s_{ij}^1(k_s\text{+}2) & s_{ij}^1(k_s\text{+}1) & s_{ij}^2(2) & s_{ij}^2(1) \quad \cdots \\ \vdots & & \vdots & \\ s_{ij}^1(P) & s_{ij}^1(P\text{-}1) & s_{ij}^2(P\text{-}k_s\text{-}1) & s_{ij}^2(P\text{-}k_s\text{-}2) \end{array} \right) \qquad (6.24)$$

where the superscript 1 refers to step response coefficients in the step response matrix $\mathbf{S_1}$ and superscript 2 for $\mathbf{S_2}$. No mixed dynamics is seen in any part of the matrix $\mathbf{S_{ij}}$.

The non-minimal state-space model leaves effects of $\mathbf{\Delta u}(k)$, $\mathbf{\Delta u}(k+1),\ldots$, $\mathbf{\Delta u}(k+k_s\text{-}1)$ on the output predictions un-updated after a model change, i.e. it behaves in a "conservative" way. The model change applied by Bemporad and Morari (1999) can be considered "abrupt". The model change of a physical system may in reality be something in between: Johansen and Murray-Smith (1997) address a piecewise linear model of exactly the same structure as (6.3), but the δ_i 's are *not* restricted to binary values, while they can accept any values $0 \le \delta_i \le 1$, because there is a need for *smooth* model changes. Smooth weighing functions for selecting dynamic models from a model bank in multiple model adaptive control applications are also discussed by Schott and Bequette (1997).

Note: Smooth model changes can also be implemented with the piecewise models (6.3) by defining a proper number N of intermediate models $(\mathbf{A_{11},B_{11}})$, $(\mathbf{A_{12},B_{12}})$, $\ldots,(\mathbf{A_{1N},B_{1N}})$, "between" models $(\mathbf{A_1,B_1})$ and $(\mathbf{A_2,B_2})$, and associated switch variables δ_{11}, $\delta_{12},\ldots \delta_{1N}$.

If the "conservative" model change offered by the use of step response model matrices is not satisfactory, then state-space models can be used instead, whereby "abrupt" model changes follow. Smooth model change potentially means introducing some additional model change (or transition) dynamics. In such a case, an *ad-hoc* model change method for step response matrices may be constructed: define a first-order model change dynamics, operating on the step response matrix elements in the lower left sub-matrix (see (6.24)):

$$\mathbf{S^{12}}(i,j) = \alpha(i\text{-}k_s)\mathbf{S^1}(i,j) + (1-\alpha(i\text{-}k_s))\mathbf{S^2}(i,j) \qquad (6.25)$$

where $i= k_s\text{+}1$, $k_s\text{+}2,..,P$ and $j=1,2,.. k_s$ and $\alpha(i)=\left[e^{-\Delta T/T_M} \right]^i$, when $i>0$ and $\alpha(i)=0$ otherwise, and where ΔT is the optimisation interval and T_M is a suitable time constant value. For the sub-matrices $\mathbf{S_{kj}}$ $(k=1,..,n$; $j=1,\ldots,m)$ of a multivariable step response matrix $\mathbf{S}$ we can use different values $\alpha_{kj}(i)=\left[e^{-\Delta T/T_{M,k,j}} \right]^i$.

The extension to multiple step response model changes is straightforward. For example, changing to a third model $\mathbf{S^3}$ at time $k+k_s+k_s'$ yields:

$$\mathbf{S} = \left(\begin{array}{ccc} \mathbf{S^1} & \mathbf{0} & \mathbf{0} \\ \mathbf{S^{12}} & \mathbf{S^2} & \mathbf{0} \\ \mathbf{S^{123}} & \mathbf{S^{23}} & \mathbf{S^3} \end{array} \right) \qquad (6.26)$$

where

$$\mathbf{S^{12}}(i,j) = \alpha_1(i\text{-}k_s)\mathbf{S^1}(i,j) + (1 - \alpha_1(i\text{-}k_s))\mathbf{S^2}(i,j) \tag{6.27}$$

where i= k_s+1, k_s+2,.., k_s+k_s' and j=1,2,.. k_s

$$\mathbf{S^{23}}(i,j) = \alpha_2(i\text{-}k_s\text{-}k_s^{'})\mathbf{S^2}(i,j) + (1 - \alpha_2(i\text{-}k_s\text{-}k_s^{'}))\mathbf{S^3}(i,j) \tag{6.28}$$

where i= k_s+k_s'+1, k_s+k_s'+2,..,P and j= k_s+1, k_s+2,.. k_s+k_s'

$$\mathbf{S^{123}}(i\text{-}k_s\text{-}k_s^{'},j) = \alpha_2(i\text{-}k_s\text{-}k_s^{'})[\alpha_1(i\text{-}k_s)\mathbf{S^1}(i,j) + (1 - \alpha_1(i\text{-}k_s))\mathbf{S^2}(i,j)] +$$
$$(1 - \alpha_2(i\text{-}k_s\text{-}k_s^{'}))\mathbf{S^{23}}(i,j) \tag{6.29}$$

where i= k_s+ k_s'+1, k_s+k_s'+2,..,P and j= 1,2,.. k_s

The ad-hoc model change introduces error in the left lower sub-matrices of the modified step response matrices. The larger the difference of the models, the larger the error. To get an idea of the error introduced, let us compare the step responses of the Finnish natural gas pipeline system which are presented in Appendix A. In particular, we collect responses from figures A1 b, A7 b, A7c and A12 b, A15 b, A15 c , the solid lines corresponding to operating point no.1. In figure 6.8 the CS2 and CS3 suction pressure step responses for CS2 is running and CS2 shut-down are presented. The responses are in fact different, but some similarity in shape and direction (sign of gain) is seen.
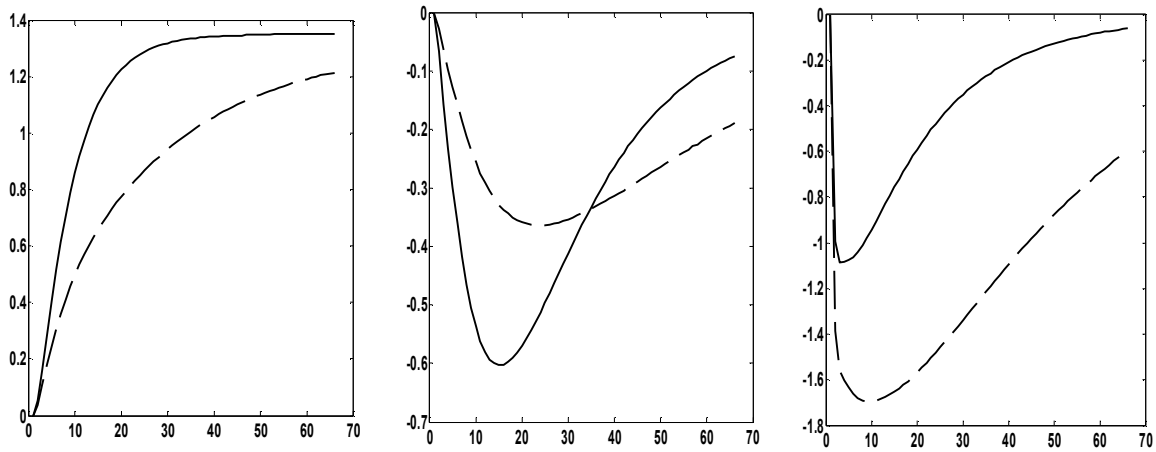
Figure 6.8 a) (left) CS2 suction pressure response to CS1 when CS2 running (solid line) and shut down (dashed line) **b)** (middle) CS2 suction pressure response to CS3 when CS2 running (solid line) and shut down (dashed line) and **c)** (right) CS3 suction pressure response to CS3 when CS2 running (solid line) and shut down (dashed line)

Assume, that we have available a *candidate* CS shut down – start up sequence in $\mathbf{w} = [\mathbf{w_1^T}\ \mathbf{w_2^T}\ ...\mathbf{w_{Nc}^T}]^T$. Using the P($2^{Nc}$+2) inequalities (6.14), we may solve $\delta_i(k+1),...,$ $\delta_i(k+P-1)$, i=1,…, 2^{Nc} to obtain the model change moments k_s, k_s', ... and then modify step response matrices $\mathbf{S^P}$, $\mathbf{S^X}$ and $\mathbf{S^F}$ using suitable model change time constants.

The terms $C_p[\sum_{i=0}^{ks-1} A_2^j A_1^{ks-1-i} B_1 u(k+i) + \sum_{i=0}^{j-1} A_2^{j-1-i} B_2 M_P u(k+k_s+i)]$ of (6.9) can in step

response matrix form be written as, when index "p" is changed to "i" :

$$S_i^{P,R} \Delta \tilde{u}(k) \triangleq [S_{i,1}^{P,R} \ S_{i,2}^{P,R} \ ... S_{i,i-1}^{P,R} \ S_{i,i}^{P,R} \ S_{i,i+1}^{P,R} \ ...S_{i,Nc}^{P,R}] \Delta \tilde{u}(k) \tag{6.30}$$

where

$$S_{ij}^{P,R} = \left(\begin{array}{cc|c} s_{ij}(1) & 0 & \begin{array}{c} 0 \end{array} \begin{array}{c} \mathbf{0} \end{array} \\ s_{ij}(2) & s_{ij}(1) & \begin{array}{c} 0 \end{array} \\ & \vdots & \begin{array}{c} \vdots \end{array} \\ \hline s_{ij}(k_s) & s_{ij}(k_s - 1) & \cdots \\ \alpha(1)s_{ij}(k_s+1) + (1-\alpha(1))s_{ij}^2(k_s+1) & \alpha(1)s_{ij}(k_s) + (1-\alpha(1))s_{ij}^2(k_s) & \\ \alpha(2)s_{ij}(k_s+2) + (1-\alpha(2))s_{ij}^2(k_s+2) & \alpha(2)s_{ij}(k_s+1) + (1-\alpha(2))s_{ij}^2(k_s+1) & \begin{array}{c} \mathbf{S_L} \end{array} \\ & \vdots & \\ \alpha(P-k_s)s_{ij}(P) + (1-\alpha(P-k_s))s_{ij}^2(P) & \alpha(P-k_s)s_{ij}(P-1) + (1-\alpha(P-k_s))s_{ij}^2(P-1) & \end{array}\right)$$

$$(6.31)$$

where $\mathbf{S_L} = \mathbf{0}$ when i≠j and

$$\mathbf{S_L} = \begin{pmatrix} s_{ij}^2(1) & 0 & & 0 \\ s_{ij}^2(2) & s_{ij}^2(1) & \cdots & 0 \\ & & \vdots & \\ s_{ij}^2(P-k_s-1) & s_{ij}^2(P-k_s-2) & & s_{ij}^2(P-M+1) \end{pmatrix} \tag{6.32}$$

when i=j.

The superscript "2" for step response coefficients in (6.31) and (6.32) stands for the model to change to at k_s. α is the model change coefficient. The equation constraint for CS "i" can now be written, recalling, that M´ is a large-valued constant for relaxing constraints:

$$-M' I_w w_i \leq S_i^{P,R} \Delta \tilde{u}(k) + Z_{0,i}(k) - S_0 \Delta u_i(k) - u_i(k-1) I_P \leq M' I_w w_i \tag{6.33}$$

while the relation $u_i(k+j) = \sum_{r=0}^{j} \Delta u_i(k+r) + u_i(k-1)$, j=0,1,..M-1 is true, where S_0 is defined in

(5.37) and I_w is a P x J_w matrix which resolves the blocking of w_i :

$$I_W = \begin{pmatrix} I_{w,1} & \mathbf{0} & & \\ \mathbf{0} & I_{w,2} & \mathbf{0} & \\ & & & \ddots \\ \mathbf{0} & \cdots & & I_{w,Jw} \end{pmatrix} \tag{6.34}$$

where each $I_{w,j}$ is a k_j-vector of ones.

As was seen in Chapter 5, blocking of $\Delta\mathbf{u}$ is conveniently implemented with step response models. We can easily see that the model change procedure introduced above can as such be applied on blocked step response matrices. However, care must be taken, when the equation constraint is considered. The origin of this is the idea to equate discharge and suction pressure at every point in the prediction horizon where a CS is shut down. If $\Delta\mathbf{u}$ is blocked, $N_b > 1$ (see (5.57) in section 5.10), for a shutdown period of, say, P_1 time points, we can find only P_1/N_b distinct values of the blocked vector $\Delta\mathbf{u_i}$, the number of equations being P_1. This over-determined set of equations cannot be supplied as equation constraints to a QP solver, since some of those cannot be satisfied, and the QP solver will announce an infeasible solution. Let us define an averaging matrix $\mathbf{A_m}$:

$$\mathbf{A_m} = \begin{pmatrix} \mathbf{I_{jb}} & 0 & & & \\ 0 & \mathbf{I_{jb}} & & \mathbf{0} & \\ & & \ddots & & \\ & \mathbf{0} & & \mathbf{I_{jb}} & 0 \\ & & & 0 & \mathbf{I_{pmb}} \end{pmatrix} \tag{6.35}$$

where the vectors $\mathbf{I_{jb}} = \dfrac{1}{N_b}[11...1]^T$ are of length N_b and the vector $\mathbf{I_{pmb}} = \dfrac{1}{P-M}[111..1]^T$ is of length P-M. The equation constraint (6.33) is modified as follows:

$$-M'\mathbf{A_m^T}\mathbf{I_w}\mathbf{w_i} \le \mathbf{A_m^T}[\mathbf{S_i^{P,R}}\Delta\tilde{\mathbf{u}}(k) + \mathbf{Z_{0,i}}(k)] - \mathbf{I_u}\Delta\mathbf{u_i}(k) - u_i(k-1)\mathbf{I_M} \le M'\mathbf{A_m^T}\mathbf{I_w}\mathbf{w_i} \tag{6.36}$$

where we have replaced $\mathbf{I_p}$ as multiplier of $u_i(k-1)$ with $\mathbf{I_M}$, which is a j_b-vector filled with ones.

The compressor envelope constraints (5.51), checkpoint pressure limits (5.52) and the discharge pressure limits are now, respectively, written as:

$$a_{ij}(\mathbf{S_0}\Delta\mathbf{u_i}(k) + \mathbf{I_p}u_i(k-1)) + b_{ij}(\mathbf{S_i^P}\Delta\tilde{\mathbf{u}}(k) + \mathbf{Z_{0,i}}(k)) +$$
$$c_{ij}(\mathbf{S_i^F}\Delta\tilde{\mathbf{u}}(k) + \mathbf{Z_{0,Nc+i}}(k)) \le M'(\mathbf{I_P} - \mathbf{I_w}\mathbf{w_i}) \tag{6.37}$$

$$\mathbf{S_i^X}\Delta\tilde{\mathbf{u}}(k) + \mathbf{Z_{0,2Nc+i}}(k) \ge \mathbf{P_{x,i,min}} \tag{6.38}$$

$$\mathbf{I_u}\Delta\mathbf{u_i}(k) + \mathbf{I_M}u_i(k-1) \le \mathbf{P_{d,i,max}} + M'(\mathbf{I_M} - \mathbf{J_w}\mathbf{w_i})$$
$$\mathbf{I_u}\Delta\mathbf{u_i}(k) + \mathbf{I_M}u_i(k-1) \ge \mathbf{P_{d,i,min}} - M'(\mathbf{I_M} - \mathbf{J_w}\mathbf{w_i}) \tag{6.39}$$

$$\Delta\mathbf{u_i}(k) \le \mathbf{Du_{i,max}} + M'(\mathbf{I_M} - \mathbf{J_w}\mathbf{w_i})$$
$$\Delta\mathbf{u_i}(k) \ge \mathbf{Du_{i,min}} - M'(\mathbf{I_M} - \mathbf{J_w}\mathbf{w_i}) \tag{6.40}$$

where $\mathbf{J_w}$ is a M x J_w matrix which resolves the blocking of $\mathbf{w_i}$ with respect to the control horizon:

$$J_W = \begin{pmatrix} J_{w,1} & 0 & & \\ 0 & J_{w,2} & 0 & \\ & & & \ddots \\ 0 & \cdots & & J_{w,Jw} \end{pmatrix} \qquad (6.41)$$

where each $J_{w,i}$ is a vector of ones with length k_i/N_b except for $J_{w,Jw}$, whose length is

$$\min\left(\frac{k_{Jw}}{N_b}, j_b - \frac{1}{N_b}\sum_{i=1}^{Jw-1} k_i\right)$$

The value of the control horizon, M, the $\Delta\mathbf{u}$-blocking and $\mathbf{w}$-blocking must be synchronised so that at least some input increments are available after the last CS shutdown or start-up event in order to be able to set up the equation constraint or to conduct a decent CS start-up. In other words, we have to require $k_1 + k_2 + \ldots + k_{Jw-1} < M$. (See figure 6.7). Also, the $\mathbf{w}$ and $\Delta\mathbf{u}$ blocking intervals must be multiples, i.e. k_i/N_b = integer.

As a cost function update we will substitute zeros for the cost parameters when CS "i" is shut down : i.e. $a_i=0$ over the period(s) CS "i" is, by $\mathbf{w_i}$, projected to be shut down in the prediction horizon. Possible CS start-up costs can be treated as explained in section 6.4.

6.7 Simplified, step-response matrix based enumeration method

In section 6.6 we actually described a *procedure* for modifying the step response matrices involved and for setting up the constraints for the final QP problem, once a *candidate* CS shut down and start up sequence is given. No auxiliary variables are needed and only the equation constraint for each CS is added to the set of constraints. The total number of (scalar) decision variables is $N_c j_b$. The constraints are $N_c(4P+4j_b)$ CS envelope and variable limit constraints and $N_x P$ constraints for pressure check points and finally the equation constraint, equivalent to $2N_c j_b$ inequality constraints.

One *practical* detail to consider is the set of admissible switching options. Some values of $\mathbf{w}$ may not be allowed either temporarily (for example, CS is being serviced and may not be started up) or permanently (for example, too frequent shutdowns / start-ups can not be allowed for given CSs). We will use a look-up table of admissible switching options, where the user has entered pre-selected values. Too frequent start-up/shutdown activities can be taken care of in this way. In addition, we will use a limitation external to the optimisation procedure: once a CS has been started up by the optimiser, it is not allowed to shut the same CS down until after a pre-defined number of optimisation cycles, a different valued parameter for each CS, N_{Ri}, i=1,2,...,N_c. The same cannot be applied in the other direction: if a CS is shut down by the optimiser, it must always have the opportunity to re-start the CS in case of an unpredicted gas consumption increase.

The algorithm sequence is as follows:

1. Select a vector $\mathbf{w} \triangleq \begin{bmatrix} \mathbf{w_1^T} & \mathbf{w_2^T} & \ldots \mathbf{w_{Nc}^T} \end{bmatrix}^T$ from a given set (table) of switching options
2. Modify the step response matrices $\mathbf{S^P}$, $\mathbf{S^F}$ and $\mathbf{S^X}$ as explained in section 6.6.
3. Modify the cost parameter vector $\mathbf{a_j}$ to be zero-valued for all the time steps that any CS j is projected to be in a shut down state (as determined by $\mathbf{w}$)

4. Calculate matrices $\mathbf{Q_j}$, $\mathbf{b_j}$ (j=1 or 2 depending on the chosen cost function alternative), $\mathbf{A}$ and $\mathbf{B}$.

5. Solve the QPproblem : $\text{Min. J} = \dfrac{1}{2}\Delta\tilde{\mathbf{u}}^T\mathbf{Q_j}\Delta\tilde{\mathbf{u}} + \mathbf{b_j^T}\Delta\tilde{\mathbf{u}}$, $\mathbf{A}\Delta\tilde{\mathbf{u}} \leq \mathbf{B}$. Add the contribution of

   the idle power $\displaystyle\sum_{i=1}^{N_c} b_i \mathbf{I_W}\mathbf{w_i}$ to the cost function value J.

   Tabulate the result :
       optimal $\Delta\tilde{\mathbf{u}}$
       switching option $\mathbf{w}$
       optimal cost function value J
       feasible/infeasible flag (i.e. is the solution feasible or can no feasible solution
           be found)

6. If all switching options have been checked, go to 7, if not go to 1.

7. From the QP result table, select from among the feasible solutions the one with the smallest value of the cost function end exit.

The CS cost parameter a_j, $j=1,\ldots,N_c$ multiplies vectors in $\mathbf{D_F}$ of (5.40) and $\mathbf{I_p}$ in (5.46) and (5.47). It is easy to redefine $\mathbf{a_j}$ as vectors and use component-wise multiplication (or notation diag($\mathbf{a_j}$) $\mathbf{D_F}$ and diag($\mathbf{a_j}$) $\mathbf{I_p}$). The value of the vector $\mathbf{a_j}$ is calculated as $\mathbf{a}_j = a_j \mathbf{I_W}\mathbf{w}_j$. Zeroing the cost function parameter in this way ensures that the CS j disappears completely from the cost function when CS "j" is shut down.

The simplified procedure is much smaller in size than the MLD-based MIQP problem with its many auxiliary variables. Recall that the latter was not finalised, as the equation constraint was not yet included. The property of the rapidly growing complexity and size of the optimisation problems containing discrete decision variables is well known (Stursberg and Engell, 2002; Perea-Lopez et al., 2003) among others. Growing complexity can also be seen in the gas supply system example of Bemporad and Morari (1999). Bemporad and Morari (2001) mention a risk that hybrid problems of practical interest cannot be solved with present mixed-integer methods because of the so-called NP-hardness: the solution time grows exponentially with the problem size. If so, only small problems are practically solvable. One possible way of tackling this problem is to take advantage of special structures of each particular problem in order to develop good rather than strictly optimal solutions.

6.8 Simulation results

Receding horizon optimisation including CS start-up and shutdown optimisation of the Finnish natural gas pipeline system is simulated in the same fashion as described in section 5.11.

6.8.1 Start-up and shutdown optimisation of CS2

Case 1

As a first simulation run, start-up/shutdown optimisation of CS2 is tested. In addition, the discharge pressures of all three CSs are optimised. The simulation period is from 1.3.2003 00:00 to 13.3.2003 21:00. It is not possible (feasible) to shut down CS2 in the very first days of March because of the large gas consumption and consequently larger pressure drops in the pipeline segments. The values of the tuning parameters are j_b=8, N_b=4, P=100, $\mathbf{R}$=0. For $\mathbf{w_2}$, we define

$J_w=7$, $k_1= k_2 = \ldots = k_6 = 4$ and $k_7=76$. The admissible values for $\mathbf{w_2}$ are shown in table 6.3. The only admissible values for $\mathbf{w_1}$ and $\mathbf{w_3}$ are [1 1 1 1 1 1 1]. Note that we define different admissible sets for situations where CS2 is shut down and when it is running. Undoubtedly, the sets can be the same, but when CS2 is running, a very fast re-start is not considered (0 1 1 1 1 1 1 would allow only 40 minutes, since $N_b=4$, shutdown time before re-start). A larger number of distinct values is used when CS2 is shut down in order to let a possible projected start-up moment approach in a natural way

The start-up cost parameters $C_{s,i}$ (see section 6.4) are zero in this simulation.

Another restriction imposed on the optimiser is that if CS2 is re-started, it has to remain running for $N_{Ri}=12$ optimisation cycles (2 hours) before it may try to shut down again.

Admissible $\mathbf{w_2}$ values, CS2 running	No.
0 0 0 0 0 0 0	1
0 0 0 0 0 0 1	2
0 0 0 0 0 1 1	3
0 0 0 0 1 1 1	4
1 1 1 1 1 1 1	5
Admissible $\mathbf{w_2}$ values, CS2 shut down	No.
0 0 0 0 0 0 0	1
0 0 0 0 0 0 1	2
0 0 0 0 0 1 1	3
0 0 0 0 1 1 1	4
0 0 0 1 1 1 1	5
0 0 1 1 1 1 1	6
0 1 1 1 1 1 1	7
1 1 1 1 1 1 1	8

Table 6.3 Admissible $\mathbf{w_2}$ values for CS2.

The step response matrices are modified using the ad-hoc method described in section 6.6. The time constants for suction pressure model changes in the matrix $\mathbf{S^P}$ between the two modes: CS2 running and CS2 shut down, can be presented as the matrix:

$$\mathbf{T_M} = \begin{pmatrix} - & - & - \\ 200 & 0 & 200 \\ 350 & 0 & 500 \end{pmatrix}$$, where the elements $T_M(i,j)$ are the time constants in minutes used for

model changes within $\mathbf{S^P}$. The top row indicates that there are no models for CS1 suction pressure and the zero entries mean that no smooth model change is needed while the response of the CS2 suction pressure must as such be available all the time over the prediction horizon. For the step response matrix of the gas flows, $\mathbf{S^F}$, no model changes are applied, while the gas flow responses are very similar even for different CS running statuses.

The results of the optimisation run are presented in figures 6.9 to 6.15 below.
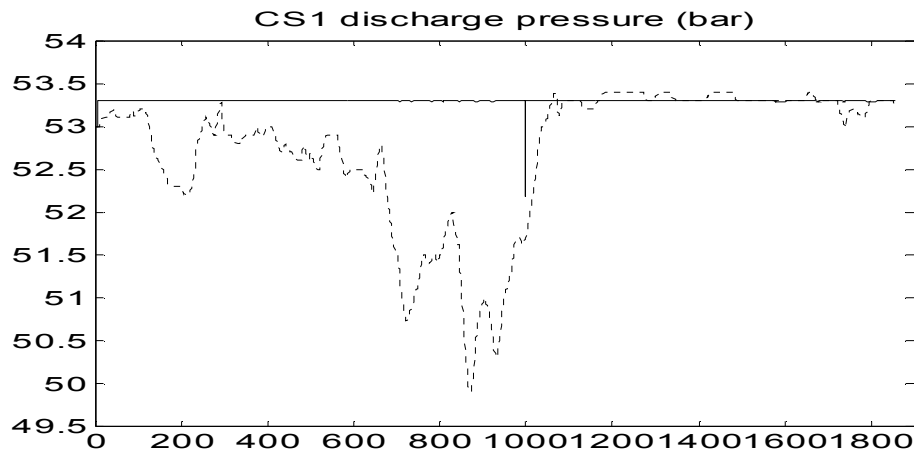
Figure 6.9 CS1 discharge pressure from 1.3.2003 00:00 to 13.3.2003 21:00. Optimiser (solid line), as operated (dashed line).
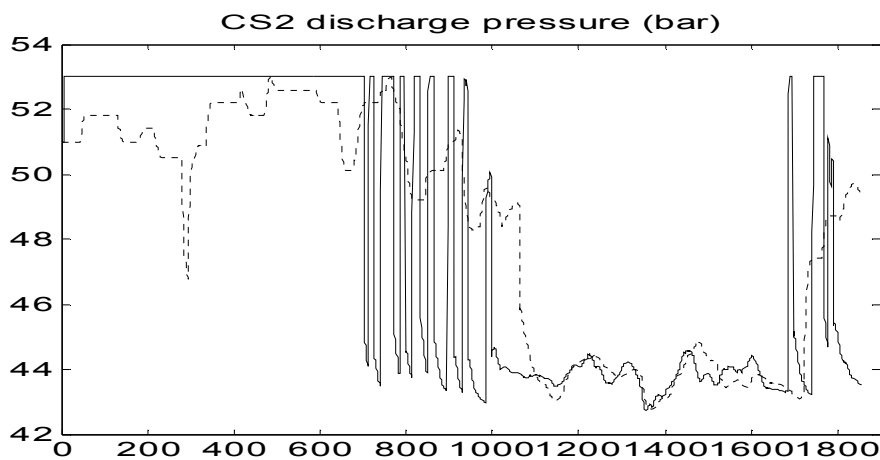
Figure 6.10 CS2 discharge pressure from 1.3.2003 00:00 to 13.3.2003 21:00. Optimiser (solid line), as operated (dashed line).
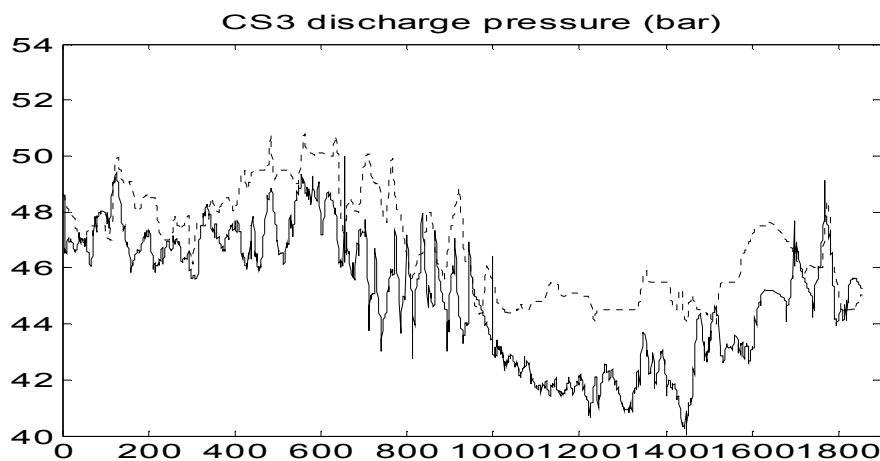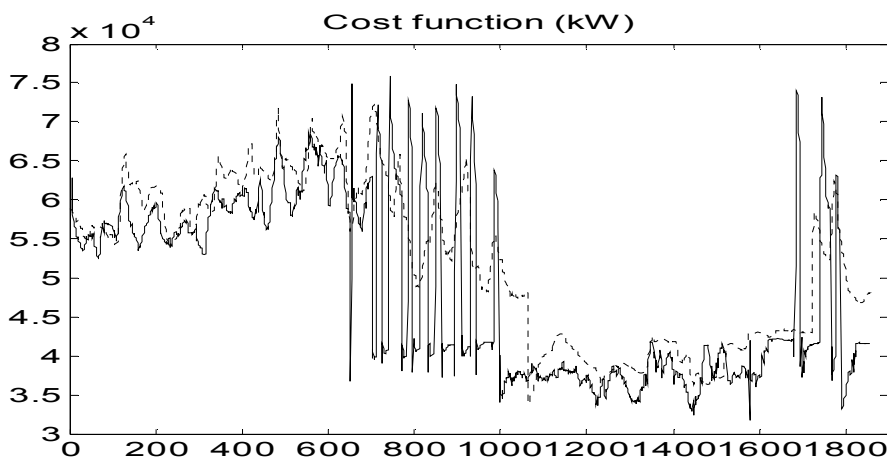

Figure 6.11 CS3 discharge pressure from 1.3.2003 00:00 to 13.3.2003 21:00. Optimiser (solid line), as operated (dashed line).
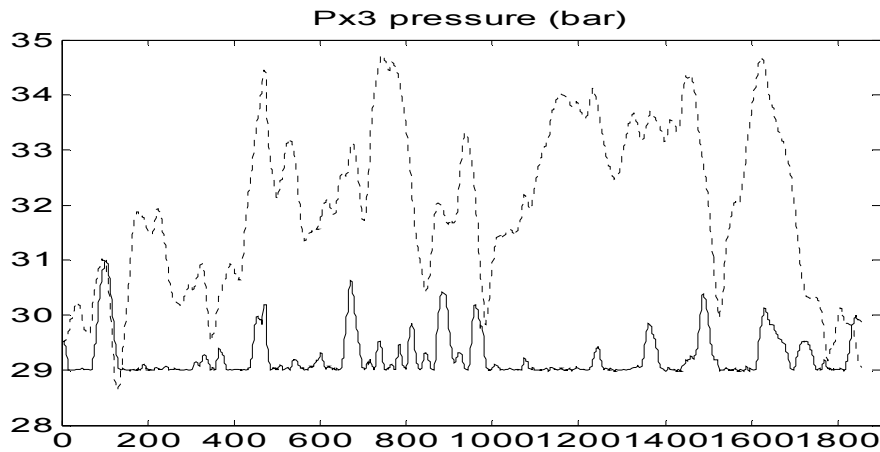
Figure 6.12 Px3 checkpoint pressure from 1.3.2003 00:00 to 13.3.2003 21:00. Optimiser (solid line), as operated (dashed line).

The optimiser shuts down CS2 quite early on 5.3.2003 21:00 (time point 700), but re-starts CS2 eight times before it remains shut down for a longer period, while the human operator shuts down CS2 at time point 1062 (8.3.2003 09:00) "once and for all", i.e. he does not need to restart at all (figure 6.10). The optimiser starts CS2 after a long period of down time, at 12.3.2003 16:00 (time point 1680), which is 7 hours before the human operator starts it, 12.3.2003 23:00 (time point 1720).

The energy consumption from this optimisation run is graphed together with the corresponding values as operated in figure 6.13.

Figure 6.13 Cost function from 1.3.2003 00:00 to 13.3.2003 21:00. Optimiser (solid line), as operated (dashed line).

The average cost for the optimised case over the whole time period is 48929 kW and as operated 52078 kW; the difference is 5.99%. From the moment the optimiser begins to shut down CS2 (time point 700) and to the end of the period, the corresponding numbers are: 43337 kW , 47049 kW and 7.89%.

117

The optimiser increases CS3 discharge pressure every time CS2 shuts down (figure 6.14), while the optimiser predicts that CS3 suction pressure will, in the near future, decrease considerably because of the shutdown. In this situation, CS3 would have to decrease its discharge pressure not to violate the maximum speed limit, but the Px3 minimum limit requires some CS3 discharge pressure level. The optimiser solves this trade-off situation by *a short-term gas deposit* into the pipeline segment downstream CS3: Immediately at CS2 shutdown, it is possible to increase the CS3 discharge pressure for a short time, followed by a decrease, but this is enough to keep Px3 above the minimum limit for a longer time. As seen in figure 6.15, the CS3 maximum speed limit activity correlates with CS2 being shut off. These actions are seen as non-optimal behaviour of Px3, since it escapes from the minimum line (figure 6.12). Every time CS2 restarts, a temporary decrease in CS3 discharge pressure is observed, as the optimiser recognises return of the capabilities to control Px3 optimally.
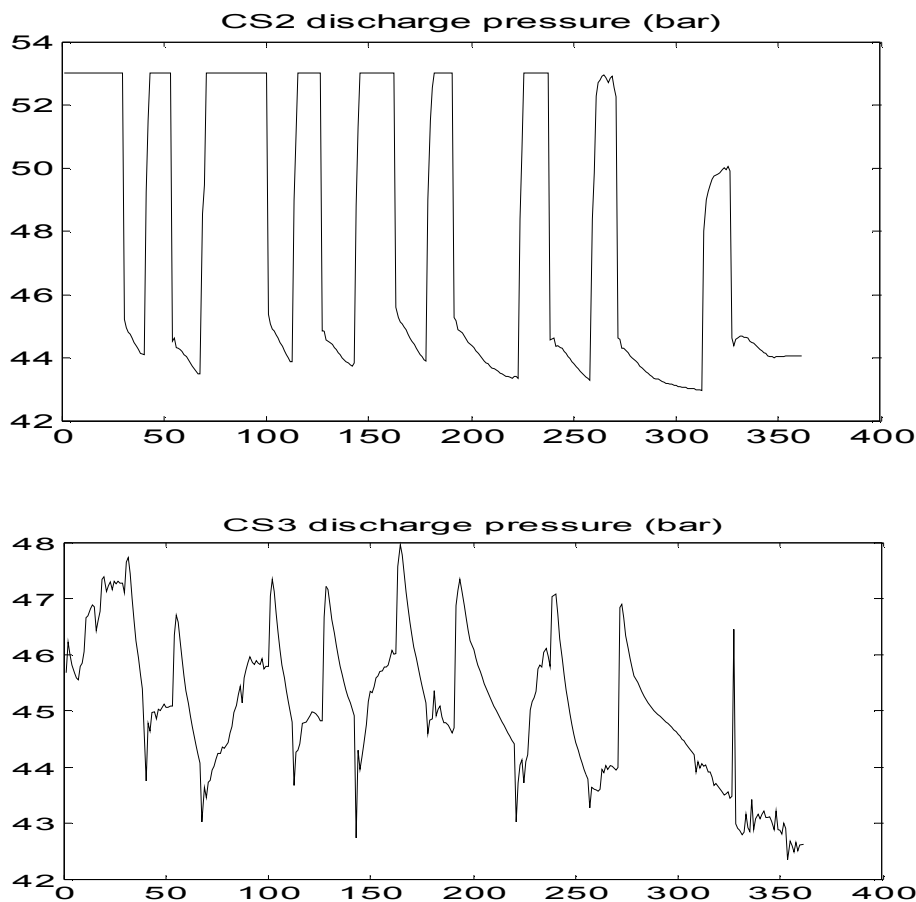
Figure 6.14 CS2 (upper graph) and CS3 (lower graph) discharge pressure from 5.3.2003 16:30 (time point 672 in figures 6.10 and 6.11) to 8.3.2003 04:00 (time point 1032).

The active constraints in the prediction horizon are shown in figure 6.15. Only a few constraints other than those shown are active: the CS2 minimum speed limit is somewhat active at the end of the period with CS2 running, because gas consumption is decreasing. The CS2 choke line is activated every time CS2 starts up. CS1 has no active constraints except for a short surge line activation at time point 1000, when there is a temporary CS1 discharge pressure decrease (figure 6.9).
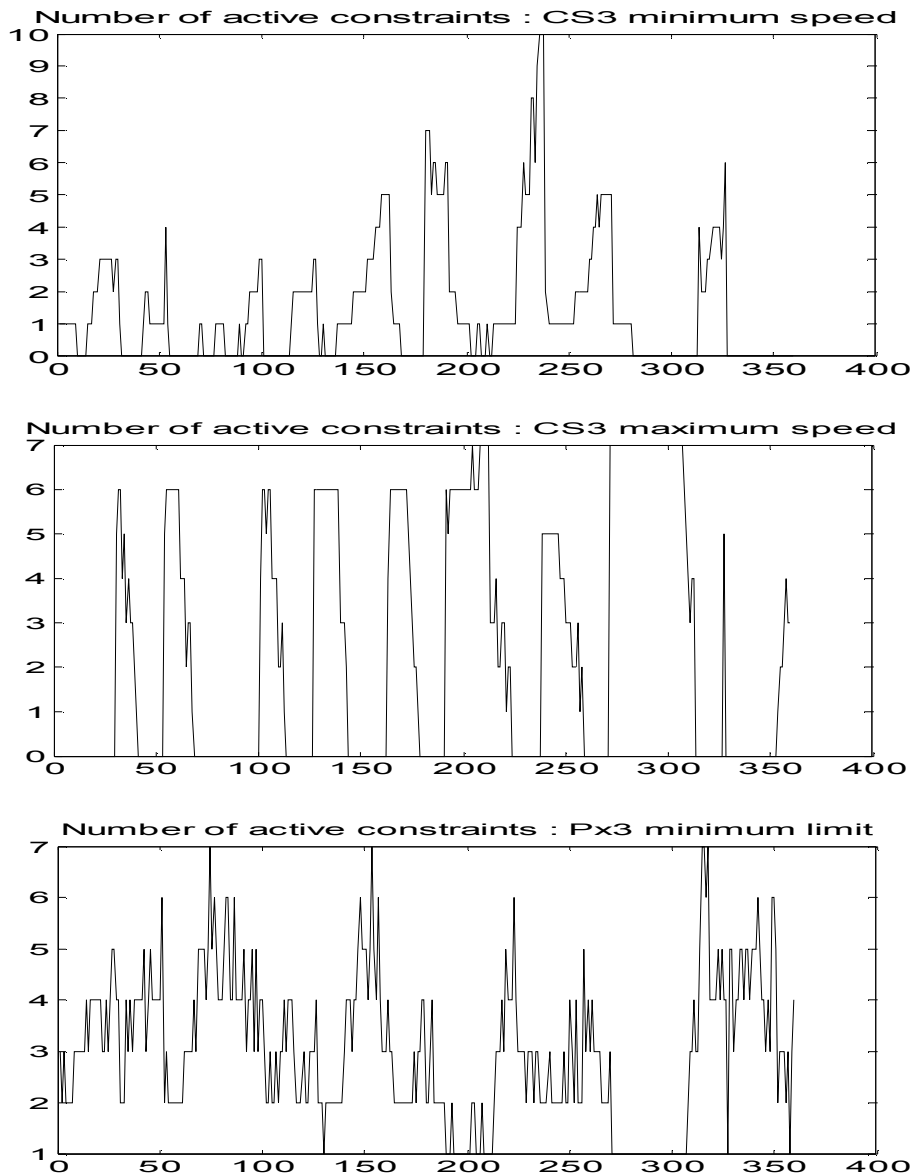
Figure 6.15 CS3 minimum speed constraint activity (upper graph), CS3 maximum speed constraint activity (middle graph) and Px3 minimum limit activity (lower graph) from 5.3.2003 16:30 (time point 672) to 8.3.2003 04:00 (time point 1032).

If eight restarts cannot be accepted, then a suitable start-up cost can be defined, or the patterns for w_2 can be more strict. If we allow only [1 1 1 1 1 1 1] and [0 0 0 0 0 0 0], we would actually mimic the human operator in that the optimiser allows no re-starts within the control horizon M (M=29 control intervals = 290 minutes) when shutting down CS2.

In order to get an idea of the optimiser's ability to predict the actual down time of CS2, data for the eight short shut down periods in figure 6.14 are listed in table 6.4. "First pattern" means the optimal and feasible value of w_2 found by the optimiser at the beginning of each shutdown period. The "Predicted shut down time" is obtained by multiplying the number of zeros in "First pattern" with N_b, which is 4 in this case. The "actual shutdown time" is obtained by counting the number of optimisation intervals when CS2 is shut down. Table 6.4 reveals that the actual deviates from the predicted times, the reasons being mainly modelling error and the use of a

119

single free response prediction (see section 6.3). Note, that the largest difference is for "0 0 0 0 0 0 1", which comes as no surprise, as this is the pattern with the longest down time stating that *sometime* in the future CS2 must restart. "0 0 0 0 0 0 0" allows no re-start at all.

No. of shut down period	First pattern (w)	Predicted shut down time	Actual shut down time (fig. 6.14)
1	0 0 0 0 1 1 1	16	10
2	0 0 0 0 1 1 1	16	15
3	0 0 0 0 1 1 1	16	13
4	0 0 0 0 0 1 1	20	17
5	0 0 0 0 0 1 1	20	16
6	0 0 0 0 0 0 1	24	32
7	0 0 0 0 0 1 1	20	20
8	0 0 0 0 0 0 1	24	42

Table 6.4 Predicted and actual shut down times of CS2 corresponding to the short shut down periods in figure 6.14.

Figure 6.16 below shows the predicted behaviour of CS3 suction pressure when CS2 is shutting down for the first time (time moment 30 in figure 6.14, the upper graph) as calculated by the optimiser as explained in section 6.6 (In summary: the optimal $\Delta \mathbf{u_2}$ –vector is obtained through the equation constraint, and CS3 suction pressure prediction is then equal to: $\mathbf{S_{31}^P}[\Delta \mathbf{u_1}(k) \ 0 \ ... \ 0]^T + \mathbf{S_{32}^P} \Delta \mathbf{u_2} + \mathbf{S_{33}^P}[\Delta \mathbf{u_3}(k) \ 0 \ ... \ 0]^T + \mathbf{Z_{0,3}}(\mathbf{k})$, see Chapter 5, section 5.6). The CS3 discharge pressure over the prediction horizon as returned by "Simone" as the free response prediction for the next cycle is $\mathbf{Z_{0,3}}(k+1)$. The predictions are quite close to each other. The effect of the averaging matrix (see section 6.6, expression (6.35)) is seen as a "knee" in the response at time point 29, where the control horizon ends.
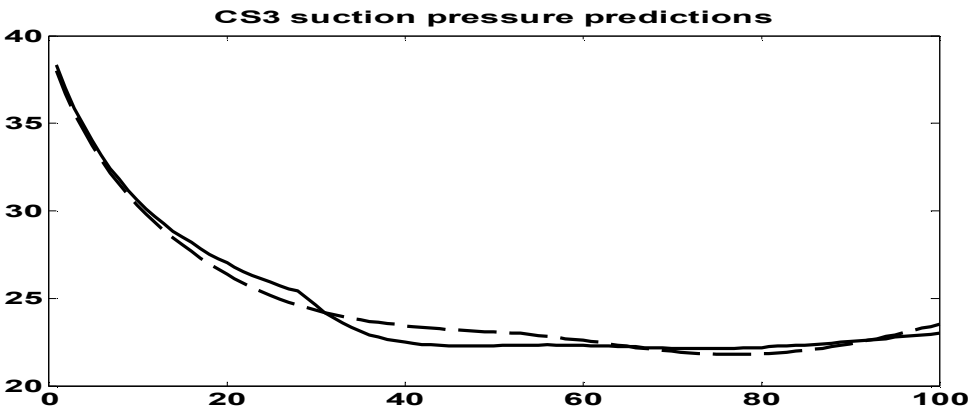
Figure 6.16 Predicted behaviour along the prediction horizon of CS3 suction pressure when CS2 shuts down: by optimiser using linear model (solid line) and by "Simone" (dashed line)

Figure 6.17 shows the free response prediction of the Px3 pressure prior to shutting down CS2. As can be seen, the first 5 to 6 points are very close to the minimum limit, but later on in the prediction horizon the pressure is well above the limit.
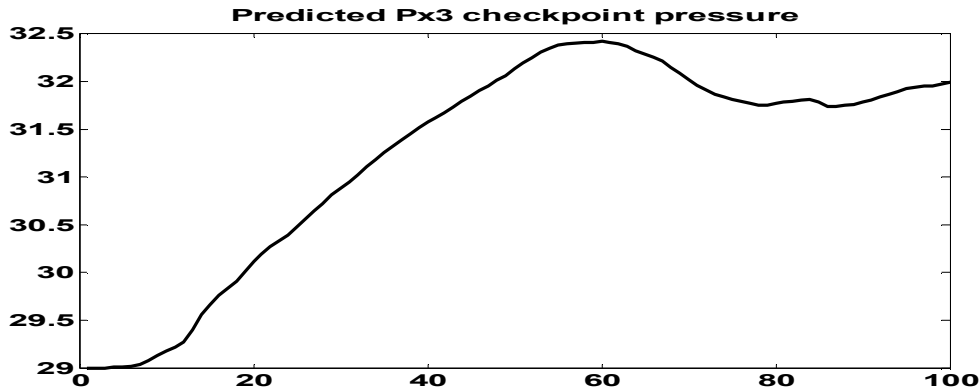
Figure 6.17 Predicted behaviour along the prediction horizon of Px3 pressure prior to shutting down CS2: the free response prediction from "Simone"

### 6.8.2 Start-up and shutdown optimisation of CS3

Case 2

The optimisation period is from 1.3.2003 00:00 to 13.3.2003 21:00 but the optimiser does not find it feasible to shut down CS3 before 6.3.2003, and therefore the results below are graphed from 6.3.2003 12:00 to 13.3.2003 21:00 .

The parameters are the same as in CS2 shutdown/start-up optimisation (j_b=8, N_b=4, P=100, **R**=0. J_w=7, k_1= k_2 = … = k_6 = 4 and k_7=76) and for $\mathbf{w_3}$, the admissible values are the same as shown in table 6.3 for the CS2 case.

As the model change time constants for the suction pressure step response matrix $\mathbf{S^P}$ we use:

$\mathbf{T_M} = \begin{pmatrix} - & - & - \\ 200 & 200 & 0 \\ 500 & 500 & 0 \end{pmatrix}$. In CS3 shutdown /start-up cases we need to define the model change

constant between the response model from CS3 to Px3 and CS2 to Px3, for which a value of 125 minutes was chosen. The start-up cost parameters $C_{s,i}$ (see section 6.4) are zero in this simulation. If CS3 is re-started, it has to remain running for N_{Ri}=6 optimisation cycles (1 hour) before it may try to shut down again. The results are shown in figures 6.18 to 6.24 below.

121
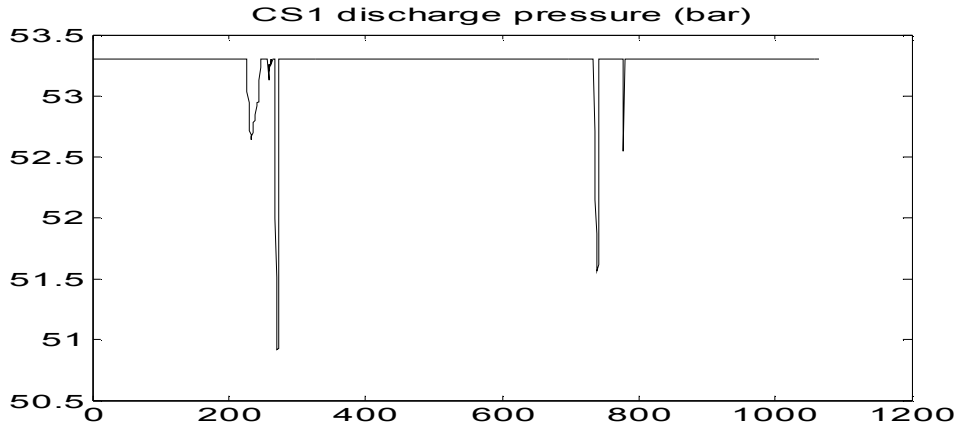
Figure 6.18 CS1 discharge pressure from 6.3.2003 12:00 to 13.3.2003 21:00
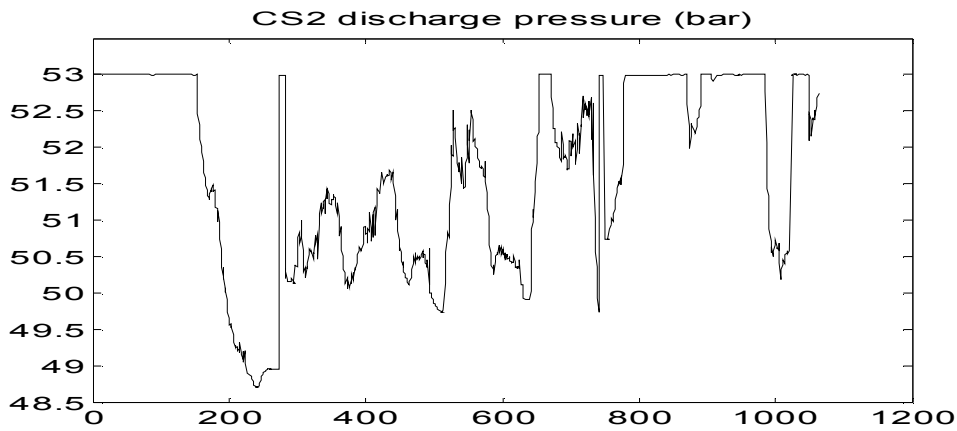
Figure 6.19 CS2 discharge pressure from 6.3.2003 12:00 to 13.3.2003 21:00
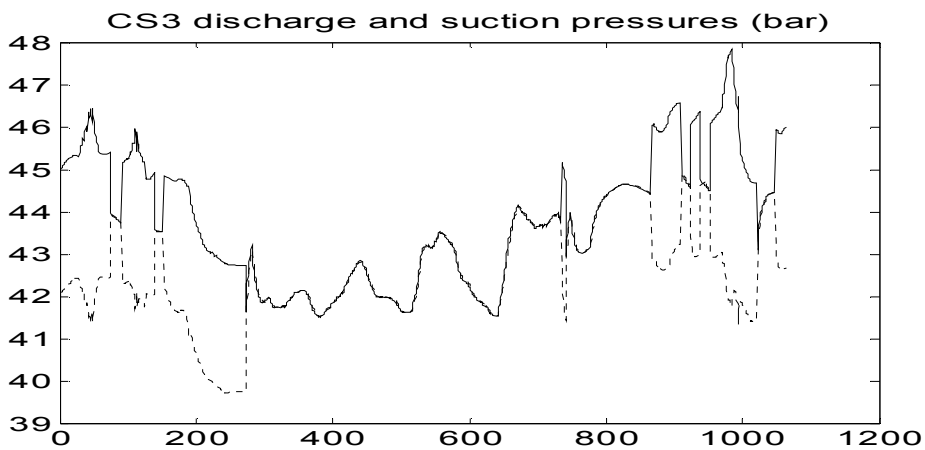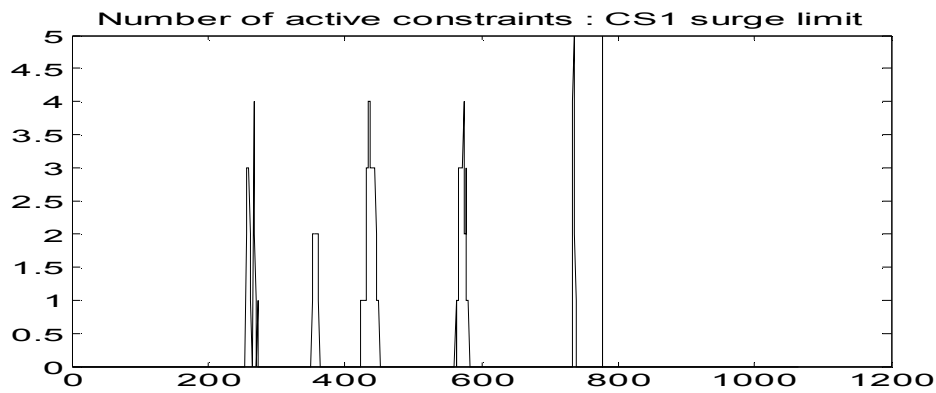

Figure 6.20 CS3 discharge (solid line) and suction (dashed line) pressure from 6.3.2003 12:00 to 13.3.2003 21:00. Suction pressure is graphed only to make it easier to follow when CS3 is shut down and when it is running.
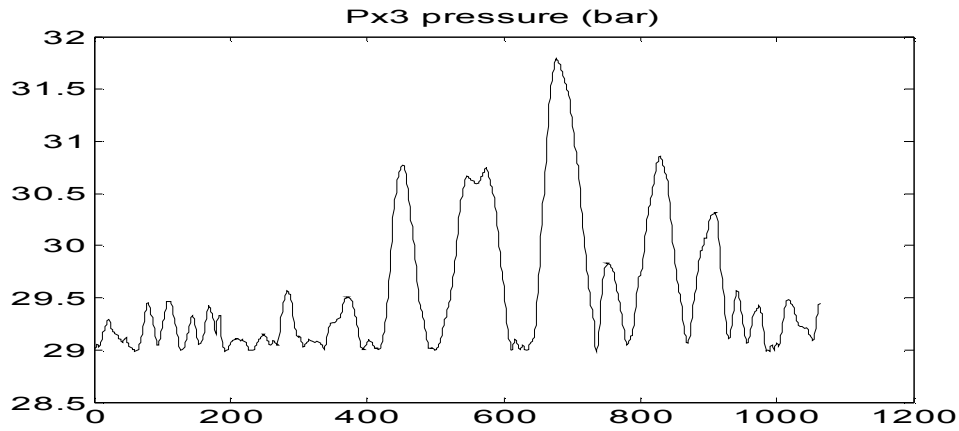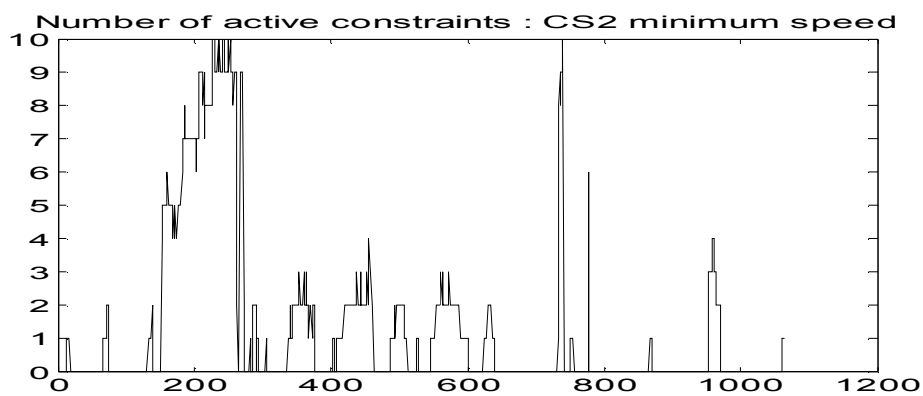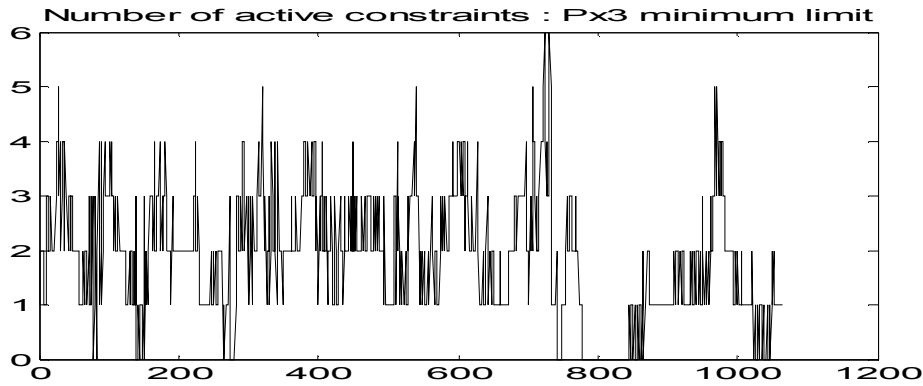
Figure 6.21 Px3 checkpoint pressure from 6.3.2003 12:00 to 13.3.2003 21:00.

Figure 6.22 Number of active CS1 surge limit constraints from 6.3.2003 12:00 to 13.3.2003 21:00.

Figure 6.23 Number of active CS2 minimum speed limit constraints from 6.3.2003 12:00 to 13.3.2003 21:00.

Figure 6.24 Number of active Px3 minimum pressure constraints from 6.3.2003 12:00 to 13.3.2003 21:00.

Comparing the average energy consumption over the interval 5.3.2003 18:00 to 13.3.2003 21:00 (the start of this interval is slightly before the first shutdown of CS2) we obtain 42943 kW for case 1 and 43985 kW for this case. The result is obvious as it can be seen that CS3 is not capable of being shut down as much as CS2.

The first CS3 shutdown appears a lot later than the first CS2 shutdown (see section 6.8.1). The reason is that the behaviour of the optimiser is somewhat contradictory, while it simultaneously minimises Px3 pressure against the minimum limit and looks for opportunities to shut down CS3. The optimiser cannot shut down CS3 if it can not compensate a predicted Px3 decrease below the minimum limit with CS2 discharge pressure, and with Px3 predictions largely varying, there are few such opportunities. The total number of CS3 re-starts is 7 (figure 6.20). The third re-start period at about time point 730 is very short, as are some shutdown periods. The shutdown/ start-up behaviour is somewhat "nervous".

Note, that CS3 shuts down from a much lower discharge pressure level than CS2, and the disturbing effect of the error introduced by using a single free response prediction may now be visible, while the shutdown transient is less dominating.

CS2 takes over the task of minimising Px3 against the minimum limit when CS3 is shut down. As seen in figure 6.21, Px3 keeps quite close to the limit at the beginning of the period, but later on the familiar sub-optimality appears. The active constraint graphs in figures 6.22 to 6.24 show that the CS2 minimum speed limit is constraining and that it is a familiar reason (see section 5.11.4) for the sub-optimality. The CS1 surge limit is also somewhat active, which in combination with the aforementioned really constitutes a "lock-up" situation giving very few opportunities to decrease CS2 discharge pressure. The sub-optimal increase of Px3 around time point 700 is not due to the CS2 minimum speed limit, but the increased activity of the Px3 minimum limit suggests that a considerable Px3 decrease is predicted in the future, which requires CS2 to prepare for this in good time because of the slow dynamics.

Case 3

Inspired by the observation in case 2 above, that CS3 has more difficulties shutting down than CS2 has, we will test the admissible patterns in table 6.5, which project a *future* CS3 shut down and a possible subsequent start up in the three added table entries in boldface. The parameters

are otherwise the same as in case 2 above. The optimisation period is 6.3.2003 00:00 to 8.3.2003 21:00.The results are shown in figures 6.25 to 6.27 below, together with results from the previous case over the same period.

Admissible w_3 values, CS3 running	No.
0 0 0 0 0 0 0	1
0 0 0 0 0 0 1	2
0 0 0 0 0 1 1	3
0 0 0 0 1 1 1	4
1 1 1 0 0 0 0	**5**
1 0 0 0 0 0 1	**6**
1 0 0 0 0 1 1	**7**
1 1 1 1 1 1 1	8
Admissible w_3 values, CS3 shut down	No.
0 0 0 0 0 0 0	1
0 0 0 0 0 0 1	2
0 0 0 0 0 1 1	3
0 0 0 0 1 1 1	4
0 0 0 1 1 1 1	5
0 0 1 1 1 1 1	6
0 1 1 1 1 1 1	7
1 1 1 1 1 1 1	8

Table 6.5 Admissible w_3 values for CS3. New table entries for CS3 running are no's 5 (shutdown after 12 intervals and leaving it shut down) and no's 6 and 7 (shutdown after 4 intervals and later re-start).
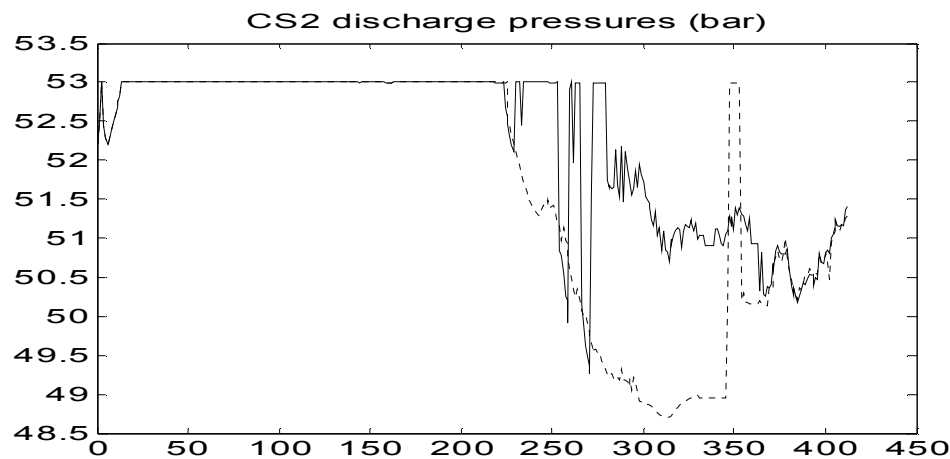
Figure 6.25 CS2 discharge pressure from 6.3.2003 00:00 to 8.3.2003 21:00. Solid line: present case, dashed line: case 2
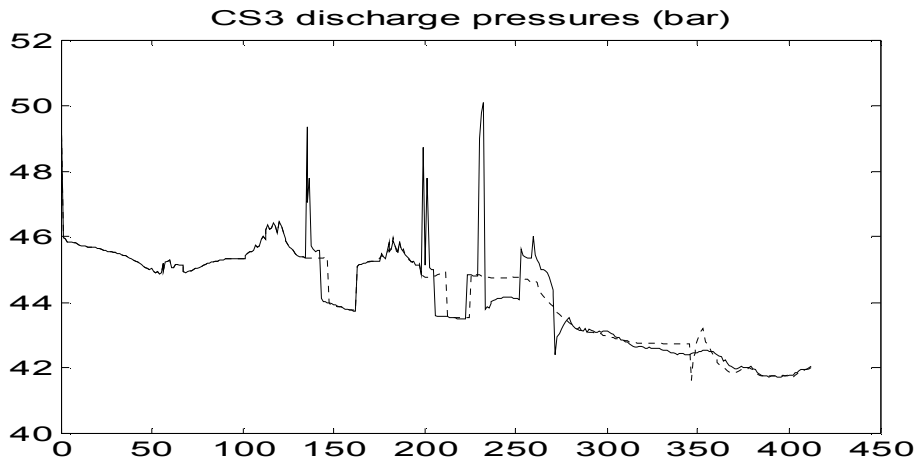
Figure 6.26 CS3 discharge pressure from 6.3.2003 00:00 to 8.3.2003 21:00
Solid line: present case, dashed line: case 2
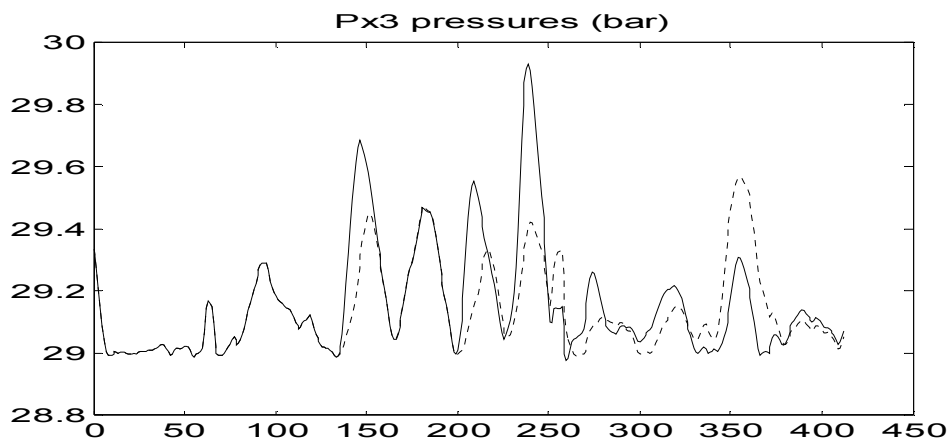
Figure 6.27 Px3 pressure from 6.3.2003 00:00 to 8.3.2003 21:00. Solid line: present case, dashed line: case 2

The optimiser makes large changes in CS3 discharge pressure (the three "spikes" in figure 6.26) and is actually capable of shutting down CS3 earlier than in the previous case. In case 2, the optimiser could not make the third shut down at all (time points 230 to 250, figure 6.26). The largest difference is that the fourth shut down takes place at time point 260, whereas the (third) shutdown in case 2 is delayed until time point 350. As expected, because of the CS3 "spikes", Px3 makes somewhat larger excursions.

The average cost over the time period considered is 44836 kW and for the comparison case, 47104 kW, the relative difference being 4.8%. Consequently, it is beneficial to let the optimiser "prepare" for CS3 shutdowns by making short-term gas deposits. The average cost over the period used in this case for the cost function obtained in case 1 with CS2 shutdown optimisation yields 44858 kW, which is 18 kW more. In practice, CS2 and CS3 shutdown optimisation produces the same energy consumption. However, the time period for comparison is too short for a final conclusion.

6.8.3 Optimisation with erroneous consumption forecasts

Case 4

Until now, all simulation studies have been conducted using perfectly known gas consumption forecasts, i.e. all off-take flows are known in advance. In this case we choose four off-takes, to which randomly generated disturbances are added. The disturbances are white noise with the maximum amplitudes shown in table 6.6. To make the disturbance more realistic, the duration of each sample from the random population with a normal distribution is given a length, which is also a random number from a normal distribution between 5 and 20 control intervals (50 to 200 minutes). See figure 6.28 for an example of a disturbance sequence.

Location of disturbed off-take	Max. disturbance amplitude, Nm^3/h
154 km downstream CS1 (in Kotka branch)	6000
52 km downstream CS2	6000
45 km downstream CS 3 (in Helsinki branch)	12000
178 km downstream CS3 (in Tampere branch)	2500

Table 6.6 Disturbances added to selected consumption forecasts. See figure 4.1 for a pipeline system schematic.

The sum of the maximum disturbance amplitudes is 26500 Nm^3/h, which is equal to 3.47% of the total gas flow through CS1 in operating point 1 (763400 Nm^3/h, see table A.1, Appendix A). A 3.47 % forecast error is not particularly high according the experience of Gasum Oy's operating personnel. However, adding an unknown disturbance 2500 Nm^3/h to the fourth selected off-take, which is the off-take located near check point Px3 is a demanding case, as Px3 pressure upsets will be large.

At each optimisation cycle, the values picked from the four random sequences are added to the original off-take flows stored in a file for "Simone" (see Appendix C) over the whole prediction horizon. This is a quite radical thing to do compared to the ideal forecast philosophy, where changes in off-take flows appear at the far future end of the prediction horizon and definitely not in the very beginning of it.
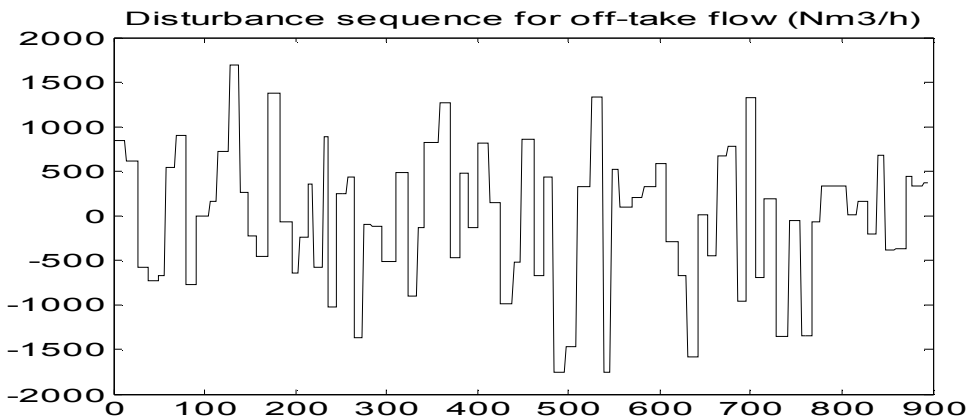

Figure 6.28 The random disturbance sequence of the fourth disturbed off-take (178 km downstream CS3, table 6.6)

The simulated case is comparable to case 1 in section 6.8.1 above, but here CS2 is enabled for shutdown/start-up optimisation later than in case 1, which is at 7.3.2003 00:00. Otherwise, the parameters are the same as described in case 1. The results are shown in figures 6.29 to 6.32 below. For comparison, a corresponding disturbance-free simulation, with CS2 shutdown enabled at 7.3.2003 00:00 is run and CS2 discharge pressure from this run is presented in figure 6.33 The simulation period is from 7.3.2003 00:00 to 13.3.2003 05:00.
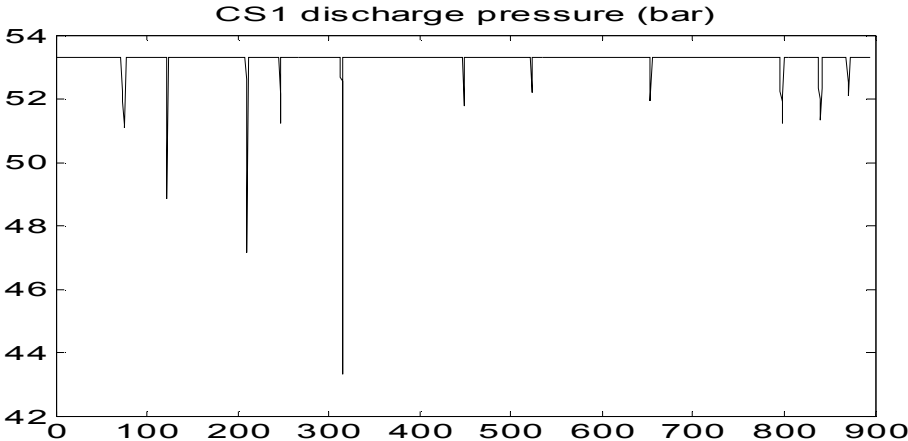
Figure 6.29 CS1 discharge pressure from 7.3.2003 00:00 to 13.3.2003 05:00 when off-take flows are disturbed.
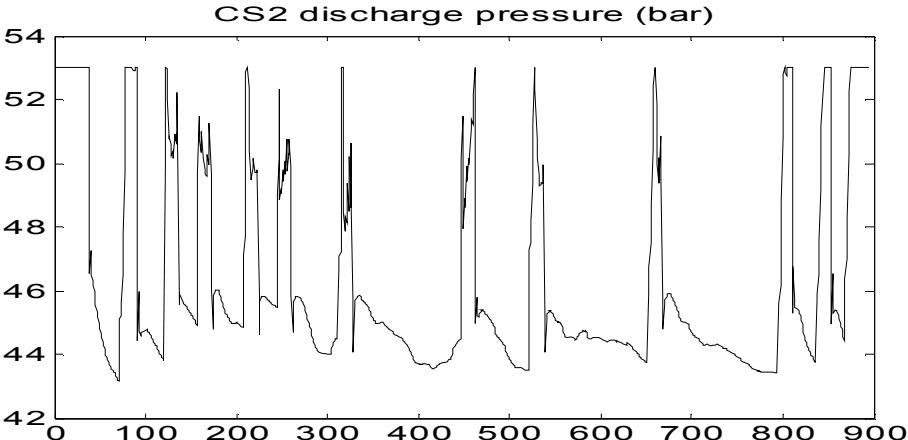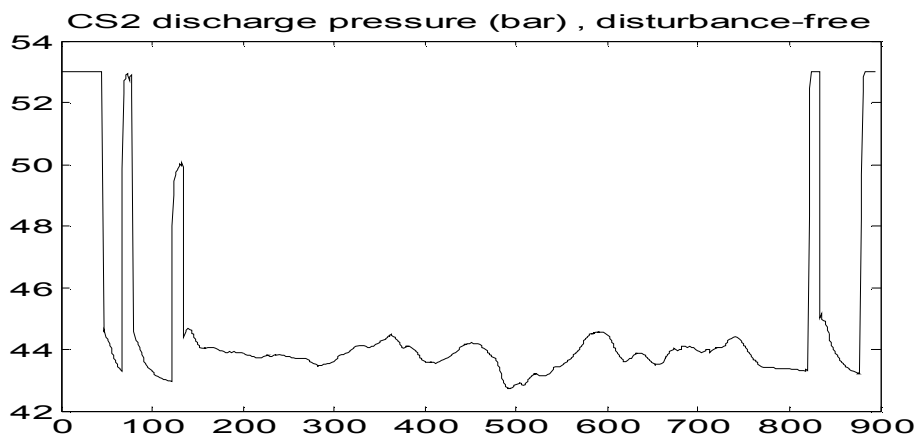

Figure 6.30 CS2 discharge pressure from 7.3.2003 00:00 to 13.3.2003 05:00 when off-take flows are disturbed.
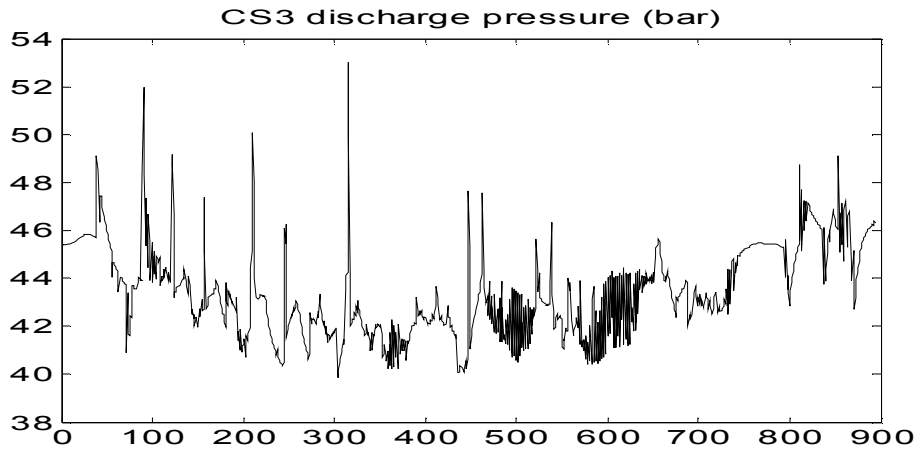
Figure 6.31 CS3 discharge pressure from 7.3.2003 00:00 to 13.3.2003 05:00 when off-take flows are disturbed.
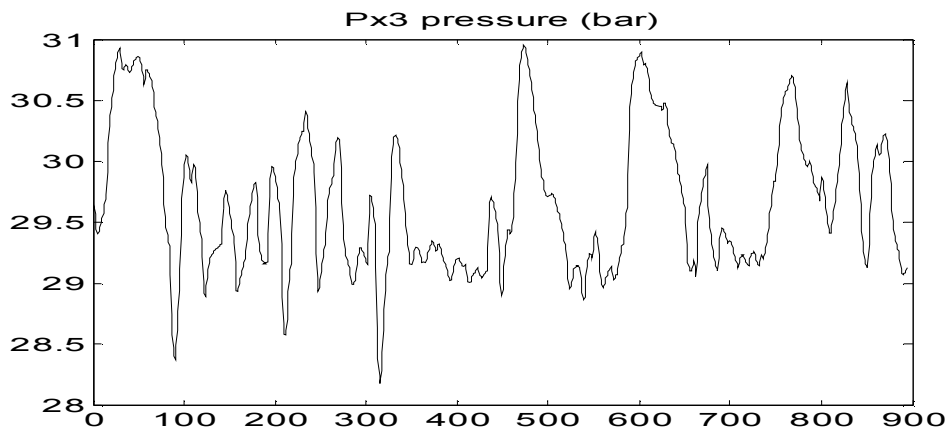
Figure 6.32 Px3 pressure from 7.3.2003 00:00 to 13.3.2003 05:00 when off-take flows are disturbed.

Figure 6.33 CS2 discharge pressure from 7.3.2003 00:00 to 13.3.2003 05:00 in the disturbance-free case.

129

CS1 discharge pressure makes rather deep but temporary excursions from the familiar maximum pressure policy. CS2 makes 8 extra restarts compared to the disturbance-free case. CS3 discharge pressure makes high-frequency and high-amplitude movements, but is still not capable of keeping Px3 above the minimum limit at all times during the simulation. Obviously, a sudden positive off-take flow disturbance (at the Px3 off-take) in the very beginning of the prediction horizon (or in the current value as well) causes a rapid Px3 pressure decrease, which cannot be compensated for by any admissible increase in CS3 discharge pressure (maximum limit is 53bar). The constraint relaxation mechanism for the minimum limit of Px3 (see section 5.10) has particular value, as can be seen from figure 6.32.

The extra re-starts of CS2 suggest that CS2 should be kept running for most of the time without trying to shut it down. The re-starts are related to the fact that CS3 is forced to make a discharge pressure increase in order to keep Px3 above the minimum limit, which cannot be implemented with CS2 being shut down, as CS3 suction pressure is too low. Examining closely figures 6.30 and 6.31, it can be seen in all eight extra re-start cases that CS3 discharge pressure increases simultaneously with CS2 re-starts. In order to obtain better results in a disturbed case, constraint relaxation mechanisms must be further developed: the Px3 limit relaxation must be further tuned and relaxation for CS envelope constraints must be implemented.

6.8.4 Execution times

The simulation test bench is implemented in two interconnected computer workstations as described in Appendix C. Table 6.7 below shows the execution time for one receding horizon optimisation cycle *without* shut-down/startup optimisation. The "Simulation task" consists of simulating one interval for obtaining the "current values" and P+1 intervals for obtaining the predictions (see Appendix C, section C.3). The time for data transfer between the two computers is included in the execution time of the simulation task. The optimisation task is defined as setting up the step response matrices, as well as the linear constraint and cost function matrices for the QP problem for one **w**-pattern per CS only and solving the QP problem. The parameter values are $j_b=8$, $N_b=4$ and $P=100$. For larger values of j_b and P the execution time increases.

Task	Execution time, seconds
Simulation task	80
Optimisation task	10
Total execution time	90

Table 6.7 Execution times for one optimisation cycle

The execution time for shutdown/start-up optimisation can be calculated when the number of **w**-patterns the optimiser must solve for is known. For example, in table 6.5, the optimiser evaluates 8 patterns for CS3, which then would give a total execution time of 160 seconds for one cycle. However, the "fmincon" solver spends considerable less time when it does not find a feasible solution, and on average, the optimisation task executes faster than calculated by this simple formula. If the total execution time exceeds 10 minutes, real-time operation would not be possible with a 10-minute optimisation interval. However, the execution time of the receding horizon optimiser can be decreased considerably keeping in mind that Matlab script files are not the correct tool with which to implement fast executing program code.

Chapter 7

Conclusions

In this work, it was shown that adequate results were obtained from real-time receding horizon optimisation, based on free response predictions obtained from a pipeline system simulator, using linear control variable models and approximate quadratic cost functions. Representative tests in a simulation test bench were performed and the results were compared with actual operational data. Receding horizon optimisation including discrete decision variables was implemented using a simple, sequential, enumerative procedure instead of using a Mixed Logical Dynamical model which would result in a large and possibly non-solvable MIQP problem. The simple procedure requires users to *pre-define* the shutdown and start-up patterns they wish to use. This is a drawback of the method and the price to be paid for simplicity. In principle, the MIQP solver itself is capable of finding optimal solutions, without the need to pre-define shutdown and start-up patterns or to otherwise significantly limit the search space.

The results of the receding horizon optimiser were compared with actual operational data from the Finnish natural gas pipeline system. The savings in compressor station energy consumption was shown to be in the order of 5 to 8% depending on the case. One might ask why the energy savings often reported in literature, 10 ... 25 % could not be achieved. One answer is that the operating personnel at Gasum Oy actually operates the pipeline system not far away from the typical, recommended "high -pressure strategy". Another reason is that the short-term (daily and weekly) gas consumption variation is rather moderate in the Finnish pipeline system. Thirdly, we might question whether the 25-% savings potential promises are realistic. Nevertheless, one outcome of this study is the simple idea of evaluating the savings potential of a pipeline system: let the optimiser both minimise and maximise the energy consumption and then calculate the difference between the minimum energy and the maximum energy. An energy maximisation run with the receding horizon optimiser showed a 17.5% relative difference with respect to the minimum energy case, which was the maximum savings potential in the Finnish pipeline system in March 2003. It may also be concluded, that the optimisation method searches the constrained solution space effectively.

The basic nature of the optimal strategy found in this study coincides with the results on gunbarrel pipelines presented in the literature: keep pressures high in those pipeline segments with downstream compressor stations, otherwise keep pressures low. Using the simple gain formula derived in Chapter 4 combined with the fact that segment gain is always greater than one, we arrive at a brand new interpretation of this strategy: a control engineer's point of view. "Because any discharge pressure increase produces a larger suction pressure increase at a downstream compressor station, then the cost increase of the upstream station is smaller than the cost decrease of the downstream station. Hence, the pressure should be as high as possible".

Two quadratic cost function variants for approximating the energy consumption of the compressor stations (see Chapter 5) were developed. The first variant showed unattractive numerical properties. Although the second variant showed more approximation error than the first one, it had better numerical properties and was selected as the preferred cost function approximation for the study.

The optimum solution is usually constrained, i.e. multiple constraints are active at the optimum. This was seen to be true for both steady-state and dynamic optimisation. This suggests that the shape of the cost function is not overly important, and the approximate quadratic cost functions can be used despite the approximation error. Taking it a step further, we might ask whether the optimisation of a gunbarrel system is so constrained that the cost function can be simplified to something like "maximise the pressure in segments, except the last one, where pressure should be minimised". Before such a simplification can be made, the effect of different values for the compressor station cost parameters on the optimum solutions must be investigated.

It was shown that step response matrices, which are popular within Model Predictive Control practice, can successfully be used when constructing the QP sub-problems used in start-up/shutdown optimisation. In particular, it was easy to set up the "equation constraint", which is needed to model the shutdown period of a compressor station in the prediction horizon. However, it was shown, that step response matrices do not offer the same model change characteristics in the prediction horizon as state-space models do. For model change with step response matrices, an ad-hoc model change dynamics is required.

In the literature, a fear for gas inventory depletion was seen which generates complicated optimisation schemes to ensure that the pipeline system enters an adequate final state. The receding horizon optimiser developed in this work does not contain any kind of inventory depletion protection or final state considerations. Still, it successfully performs receding horizon optimisation without explicitly recognising, for example, calendar day changes.

Further development of the optimisation method

The simple gain formula in Chapter 4 is useful as such. However, it is necessary to have the steady-state pressure distribution of the pipeline system under consideration available. Alternatively, suitable average values of pipeline pressures over long enough time periods can be used as approximate steady-state pressure values.

There seem to be no simple formulas available for pipeline system time constants. As a further development scenario, it would be useful to develop formulas for both gains and time constants for pipeline segments of any shape and branching structure, as functions of pipeline geometry and possibly gas content and gas flow.

State estimation, which was not evaluated in detail in this study, is an important issue. As the free response predictions are obtained from an external simulator, there is in most cases no access to the complete internal state of the simulator. The simple and intuitive "state reconstruction" method described in Chapter 5, where gas consumption or supply forecasts assumed to be the source of error as they are updated proportionally to the error in measured variables, may not work correctly in all cases. As was seen in Chapter 5, rigorous state estimation tends to require the possibility to adjust estimated state values over the prediction horizon in some controlled way. It may be desirable to develop some ad-hoc method, where constant-valued forecast updates would be replaced by functions of time along the prediction horizon.

The results of this work indicate that constraint relaxation techniques need to be further developed. In some cases, the optimiser was overly cautious or "nervous", as it has interrupted an otherwise good-looking optimal policy for a short time (for example, a compressor station was started up just to compensate for a limit violation of 0.1 bar 6 hours in the future). The nervous behaviour was observed especially in the simulation run with erroneous forecasts in Chapter 6.

In principle, receding horizon optimisation could be implemented on any gas pipeline system of a suitable size and structure. A practical detail must, however, be considered. The compressor stations are geographically spread out over a large area. Are operating personnel prepared to give an optimiser running in some control centre, the authority to a) manipulate discharge pressures b) shut down and start up compressor units at remote locations? This cultural issue should be discussed *before* making the final decision to implement an optimiser.

Extensions of the optimisation method

For looped pipeline systems, the second quadratic cost function approximation (see Chapter 5) must be used, as gas flow through compressor stations is better accounted for in this one. A straightforward looped pipeline system implementation can be based on the fact that the looped system is divided into branched gunbarrel systems with interconnecting gas flow streams, the latter being new decision variables of the optimisation problem.

In this study, compressor stations contain only one running compressor unit. The extension to multiple unit stations includes the following steps:
- Evaluate the parameters of the linearised envelopes of the new compressor units
- Implement new decision variables: a) gas flow through individual units in a parallel unit configuration; b) discharge pressures of individual units in a serial unit configuration
- Implement the dynamic responses of the new intra-station decision variables noting, that they will not extend from inside the station out to the pipeline system. The dynamic responses of variables inside the stations are very fast, almost instantaneous.

Scope limits are an important issue and may be even more important in looped and/or complicated pipeline systems. The "Scope limit" defines the limits for the pipeline system to be optimised. In this study, we found the Finnish-Russian border to be a scope limit, but generally speaking, there are others, for example responsibility and ownership limits, which more or less artificially divide a pipeline system into parts, across which very little information on gas consumption forecasts or pipeline system status is shared.

The changing natural gas delivery principles, where short-term ("spot") deliveries and pipeline capacity utilisation become more important, do not constitute major challenges to the receding horizon optimisation method developed in this study. In case future short-term deliveries can be quantified, they can be added to the consumption forecast data storage, from which the optimiser picks the data and solves the optimisation problem as usual. The real-time 10-minute stepping can be modified so that the optimiser performs "look ahead optimisation", i.e. it steps forward a given number of steps with maximum speed. Also, the prediction and control horizon and the shutdown/start-up patterns can be adapted for off-line use. Typically, off-line applications would need larger control and prediction horizons. All in all, the real-time receding horizon optimiser can be extended towards a planning tool.

References

Abou-Jeyab R. A., Y. P. Gupta, J. R. Gervais, P.A. Branchi and S.S. Woo (2001), Constrained multivariable control of a distillation column using a simplified model predictive control algorithm. Journal of Process Control, Vol. 11, pp. 509-517

Batey E. H., H. R. Courts and K. W. Hannah (1961), Dynamic approach to gas-pipeline analysis, Oil and Gas Journal, Vol. 59, pp. 65-78, December 1961

Bemporad A. and M. Morari (1999), Control of systems integrating logic, dynamics, and constraints, Automatica, Vol. 35, pp. 407-427

Bemporad A. and M. Morari (2001), Optimisation-Based Hybrid Control Tools, Proceedings of the American Control Conference, Arlington, VA, June 25-27,2001, pp. 1689-1703

Botros K.K., B. J. Jones and D. J. Richards (1996), Recycle Dynamics during Centrifugal Compresor ESD, Start-up and Surge Control, ASME International Pipeline Conference, Volume 2, pp. 957-966

BP Statistical Review of Word Energy (2004), www.bp.com

Broadbent G. E. and T. Williams (1990), Flexibility, savings chief returns of new pipeline system, Oil and Gas Journal, April 30, 1990, pp. 55-61.

Brown R. and P. Chui (1996), Custom Optimisation Program used by Dispatchers, Pipeline Simulation Interest Group, Annual Conference October 23-25,1996, San Francisco, USA, www.psig.org/papers

Bryant M. and R. L. Varo'n (2002), Advanced application enhances operation for US Gulf Coast gas pipeline, Oil and Gas Journal February 25, 2002, pp. 64-71

Carter R. G. (1996) , Compressor Station Optimisation: Computational Accuracy and Speed, Pipeline Simulation Interest Group, Annual Conference October 23-25,1996, San Francisco, USA, www.psig.org/papers

Carter R. G. (1998), Pipeline Optimisation: Dynamic Programming after 30 years, Pipeline Simulation Interest Group, Annual Conference October 28-30,1998, Denver, Colorado, USA, www.psig.org/papers

Clarke D.W., C. Mohtadi and P.S. Tuffs (1987 **A**) Generalized Predictive Control – Part I. The Basic Algorithm. Automatica, Vol. 23, no.2 , pp. 137-148.

Clarke D.W., C. Mohtadi and P.S. Tuffs (1987 **B**), Generalized Predictive Control – Part II. Extensions and Interpretations. Automatica, Vol. 23, no.2 , pp. 149-160.

Coker A. K. (1994), Selecting and sizing process compressors, Hydrocarbon Processing, July 1994.

Cutler, C. R. and Ramaker, B. L. (1980), Dynamic Matrix Control- A Computer Control Algorithm. Joint American Control Conference, San Francisco, USA, paper WP5-B.

Ferrari-Trecate G., E. Gallestey, A. Stothert, G. Hovland, P. Letizia, M. Spedicato, M. Morari and M. Antoine (2002), Modelling and control of co-generation power plants under consideration of lifetime consumption: a hybrid system approach. Proceedings of the IFAC 15th Triennal World Congress, Barcelona, Spain

Finnish Natural Gas Association (2004) , www.maakaasu.fi, English pages

Furey B. P. (1993), A Sequential Quadratic Programming-based Algorithm for Optimization of Gas Networks, Automatica, Vol. 29, No. 6, pp. 1439-1450, 1993

Gallestey E., A. Stothert, D. Castagnoli, G. Ferrari-Trecate and M. Morari (2003), Using Model Predictive Control and Hybrid Systems for Optimal Scheduling of Industrial Processes. Automatisierungstechnik, Vol. 51, no. 6, pp. 285-293.

Gattu G. and E. Zafiriou (1992), Nonlinear Quadratic Dynamic Matrix Control with State estimation, Ind. Eng. Chem. Res., Vol. 31, pp. 1096-1104.

Gattu G. and E. Zafiriou (1995), Observer Based Nonlinear Quadratic Dynamic Matrix Control for State Space and Input/Output Models. The Canadian Journal of Chemical Engineering, Vol. 73, pp. 883-895.

Goslinga J., M. Kaulback, K. Witczak and B. McNeill (1994), A method for pipeline network optimization, 13. International Conference on Offshore Mechanics and Arctic Engineering (OMAE-13), Houston, Texas (USA), 27 Feb-3 Mar 1994, pp. 31-43.

Graham J. T., V. J. Wukovits and J. D. Yurchevich (1996), On-line Modeling, a Diamond in the Rough, Pipeline Simulation Interest Group, Annual Conference October 23-25,1996, San Francisco, USA, www.psig.org/papers

Grelli G. J. and J. Gilmour (1986), Western U. S. gas pipeline optimisation program, Oil & Gas Journal, July 14, 1986

Henson M. A. (1998), Nonlinear model predictive control: current status and future directions, Computers & Chemical Engineering, Vol. 23, pp. 187-202.

Henttonen J. (1996), Receding Horizon Control Approach to Multivariable Systems, Doctoral thesis, Tampere University of Technology Publications no. 192, 1996

Hoeven van der T. and T. Fournier (1995), Steady State Modelling based on Piecewise Linear Programming, Pipeline Simulation Interest Group, Annual Conference October 18-20,1995, Albuquerque, New Mexico, USA, www.psig.org/papers

Imam A., R.A. Startzman and M. A. Barrufet (2004), Multicyclic Hubbert model shows global conventional gas output peaking in 2019, Oil & Gas Journal, August 16, 2004, pp. 20-28

Jeni'cek T., J. Kra´lik, P. Stiegler, Ž. Vostry´, J. Sterba, J. Zaworka and H. Scheerer, (1991), Simone, User's Manual, Czechoslovak Academy of Sciences and Liwacom Informationstechnik GmbH.

Johnson A. T., B. D. Marquart , M. L. Istre and R. K. Walloopillai (2000), Integrating an Expert System and Pipeline Simulator to Enhance Gas Pipeline Operation, Profitability and Safety, Pipeline Simulation Interest Group, Annual Conference October 18-20, 2000, Savannah, Georgia, USA, www.psig.org/papers

Kelling C., K. Reith and E. Sekirnjak (2000), A Practical Approach to Transient Optimisation for Gas Networks, Pipeline Simulation Interest Group, Annual Conference October 18-20, 2000, Savannah, Georgia, USA, www.psig.org/papers

de Keyser R. M. C. and A.R. van Cauwenberghe (1981), A Self-Tuning Multistep Predictor Application, Automatica, Vol. 17, no.1 , pp. 167-174.

de Keyser R. M. C., Ph. G. A. van de Velde and F. A. G. Dumortier (1988), A Comparative Study of Self-adaptive Long-range Predictive Control Methods, Automatica, Vol. 24, no.2 , pp. 149-163.

Kinnaert M. (1989), Adaptive generalized predictive controller for MIMO systems, International Journal of Control, Vol. 50, no.1 , pp. 161-172.

Kra´lik J. (1993), Compressor stations in SIMONE, Proceedings of the SIMONE Congress, Prague, Sept. 27-30, 1993, pp. 93-117.

Kra'lik J., P. Stiegler, Z. Vostry' and J. Za'vorka (1984 A), Modeling the Dynamics of Flow in Gas Pipelines, IEEE Trans. on Systems, Man and Cybernetics, Vol SMC-14, No. 4, July/August 1984, pp. 586-596

Kra'lik J., P. Stiegler, Z. Vostry' and J. Za'vorka (1984 B), A Universal Dynamic Simulation Model of Gas Pipeline Networks, IEEE Trans. on Systems, Man and Cybernetics, Vol SMC-14, No. 4, July/August 1984, pp. 597-606

Lee J. H., M. Morari and C. E. Garcia (1994), State-space Interpretation of Model Predictive Control. Automatica, Vol. 30, no.4, pp. 707-717.

Lee J. H. and N. L. Ricker (1994), Extended Kalman Filter Based Nonlinear Model Predictive Control, Ind. Eng. Chem. Res., Vol. 33, pp. 1530-1541.

Li S., K. Y. Lim and D.G. Fisher (1989), A State Space Formulation for Model Predictive Control. AIChe Journal, Vol. 35, no. 2, pp. 241-249.

Ling K.V. and K. W. Lim (1996), A State Space GPC with Extensions to Multirate Control, Automatica, Vol. 32, No. 7, pp. 1067-1071.

Lundström P., J. H. Lee, M. Morari and S. Skogestad (1995), Limitations of dynamic matrix control, Computers & Chemical Engineering, Vol. 19, no. 4, pp. 409-421.

Luongo C. A., B. J. Gilmour, M. J. Goodreau and D. W. Schroeder (1991), Optimal Operation of Gas Transmission Networks, 18th World Gas Conference, Berlin, July 1991

Marque´s D.and M. Morari (1988), On-line Optimisation of Gas Pipeline Networks, Automatica, Vol. 24, No. 4, pp. 455-469

Martin, G.D. (1981), Long-Range Predictive Control, AIChE Journal, Vol. 27, no. 5, pp. 748-753.

Matlab Optimisation Toolbox User's Guide (2000), The MathWorks, Inc., 306 pages

Morari M. and J. H. Lee (1999), Model predictive control: past, present and future. Computers & Chemical Engineering, Vol. 23 , pp. 667-682

Murray-Smith R. and T. A. Johansen (1997), The Operating Regime Approach to Nonlinear Modelling and Control, in : Murray-Smith and Johansen, Multiple Model Approaches to Modelling and Control, Chapter 1, pp. 3 − 72, Taylor and Francis, 1997

Muske K. R. and J. B. Rawlings (1993), Model Predictive Control with Linear Models, AIChe Journal, Vol. 39, No. 2, pp. 262-287

Osiadacz A. J. (1996), Different Transient Models- Limitations, Advantages and Disadvantages, Pipeline Simulation Interest Group, Annual Conference October 23-25,1996, San Francisco, USA, www.psig.org/papers

Osiadacz A. J. (1998), Hierarchical Control of Transient Flow in Natural Gas Pipeline Systems, International Transactions on Operational Research, Vol. 5, No.4, pp 285-302

Osiadacz A. J. and M. Chaczykowski (2001), Comparison of isothermal and non-isothermal pipeline gas flow models, Chemical Engineering Journal, Vol. 81, pp. 41-51

Ostromuhov L. A. (1998), Economic and operational pressure and flow gas network optimization, Erdöl-Erdgas-Kohle, Vol. 114, no. 7/8, 1998, pp. 373 − 377

Perea-Lo'pez E., B. E. Ydstie and I. E. Grossman (2003), A model predictive control strategy for supply chain optimisation, Computers & Chemical Engineering, Vol. 27 , pp. 1201-1218.

Pietsch U., R. G. Carter and H. H. Rachford (2001), Investigating Real-World Applications of Transient Optimization, Pipeline Simulation Interest Group, Annual Conference October 17-19, 2001, Salt Lake City, Utah, USA, www.psig.org/papers

Piggott J. (2003), Accurate Load Forecasting - "You cannot be serious", Pipeline Simulation Interest Group, Annual Conference October 15 − 17, 2003, Bern, Switzerland, www.psig.org/papers

Piggott J., T. Perchard and C. Whitehand (2000), Short Term Gas Demand Forecasting, Pipeline Simulation Interest Group, Annual Conference October 18 − 20, 2000, Savannah, Georgia, USA, www.psig.org/papers

Poe W., U. Basu, G. Venkataramanan and P. Ferber (1999), Gas pipeline optimisation and control, Hydrocarbon Engineering, Vol 4, no. 10, pp. 81-85

Rachford H. H. and R. G. Carter (2000), Optimising Pipeline Control in Transient Gas Flow, Pipeline Simulation Interest Group, Annual Conference October 18 – 20, 2000, Savannah, Georgia, USA, www.psig.org/papers

Revell N.J. and M. G. Thorne (1998), An Overview of the Gas Transmission System in Great Britain- Operating Challenges and Modelling Solutions, Pipeline Simulation Interest Group, Annual Conference October 28 – 30,1998, Denver, Colorado, USA, www.psig.org/papers

Ricker N. L. (1985), Use of Quadratic Programming for Constrained Internal Model Control, Ind. Eng. Chem. Process Des. Dev., Vol. 24, pp. 925-936.

Ricker N. L. (1990), Model Predictive Control with State Estimation, Ind. Eng. Chem. Res., Vol. 29, pp. 374-382.

Riikonen A. (1993) , Maakaasun ja nestekaasun koostumus ja ominaisuudet ("Composition and properties of natural gas and liquefied petroleum gas"), Publication M1, Gasum Oy, July 1993, ISSN 0785-8183. In Finnish.

Sandercock W. G. (1994), Union Gas applies expert system to optimize pipeline, Pipeline Industry, September 1994

Sandler H. J. and E. T. Luckiewicz, (1987), Practical Process Engineering, McGraw-Hill, 1987, 638 pages.

Schoder W. and R. D. Brandt (1999), Gas Management Systems for Changing Gas Markets, OIL GAS European Magazine, No. 3, 1999, pp. 17-23

Schott K. D. and B. W. Bequette (1997), Multiple Model Adaptive Control, Chapter 11, pp. 269- 291, in : Murray-Smith and Johansen, Multiple Model Approaches to Modeling and Control, Taylor and Francis, 1997

Schroeder D. W. (2001), A Tutorial on Pipe Flow Equations, Pipeline Simulation Interest Group, Annual Conference October 17-19, 2001, Salt Lake City, USA, www.psig.org/papers

Seferlis P. and N. F. Giannelos (2003), A Two-Layered Optimisation-Based Control Strategy for Multi-Echelon Supply Chain Networks, European Symposium on Computer Aided Process Engineering-13 (edited by A. Kraslawski and I. Turunen), Lappeenranta, Finland.

Sekirnjak E. (1996), Practical Experiences with Various Optimisation Techniques for Gas Transmission and Distribution Systems, Pipeline Simulation Interest Group, Annual Conference October 23-25, 1996, San Francisco, USA, www.psig.org/papers

Shaw H. C., M. L. Wheeler and R. S. Whaley (1997), On-line Simulations for the Gas Controller, Pipeline Simulation Interest Group, Annual Conference October 15-17, 1997, Tuscon, Arizona, USA, www.psig.org/papers

Smeulers J. P. M., W. J. Bouman and H. A. van Essen (1999), Model predictive control of compressor installations, International Conference on Compressors and their Systems, London (UK), 13-15 Sep 1999, pp 555-565

Stursberg O. and S.Engell (2002), Optimal Control of Switched Continuous Systems using Mixed-Integer Programming, Proceedings of the IFAC 15th Triennal World Congress, Barcelona, Spain

Uraikul V., C. W. Chan and P. Tontiwachwuthikul (2000), Development of an expert system for optimizing natural gas pipeline operations, Expert Systems with Applications, Vol. 18, 2000, pp. 271-282

Wheeler M. L. and R. S. Whaley (2001), Automating Predictive Model Runs for Gas Control, Pipeline Simulation Interest Group, Annual Conference October 17-19, 2001, Salt Lake City, Utah, USA, www.psig.org/papers

Vostry′ Z., J. Zaworka and T. Jeni′cek (1994), Optimum Control of Gas Transport, Pipeline Simulation Interest Group, Annual Conference October 13-14, 1994, San Diego, California, USA, www.psig.org/papers

Wright S., M. Somani and C. Ditzel (1998), Compressor Station Optimisation, Pipeline Simulation Interest Group, Annual Conference October 28-30, 1998, Denver, Colorado, USA, www.psig.org/papers

Wu S., R. Z. Rios-Mercado, E. A. Boyd and L. R. Scott (2000), Model relaxations for the fuel cost minimization of steady-state gas pipeline networks, Mathematical and Computer Modelling, Vol. 31, no 2-3, pp. 197-220

Zhu G., M. A. Henson and L. Megan (2001), Dynamic modeling and linear model predictive control of gas pipeline networks, Journal of Process Control, Vol. 11, 2001, pp. 129-148

Åström K. J. (1970), Introduction to Stochastic Control Theory. Academic Press, New York, USA.

Appendix A. Dynamic responses of the Finnish natural gas pipeline system

A.1 Introduction

The step responses of selected pressure and flow variables of the Finnish natural gas pipeline system are obtained by using the "Simone" pipeline simulator in three different operating points, which are characterised by different gas flow throughput: Operating point no. 1 has a gas flow distribution corresponding to beginning of March 2003, operating point no. 2 has a gas flow corresponding to April 2003 and operating point no. 3 is extrapolated from operating points 1 and 2 so, that operating point 2 represents an intermediate value. See table A.1 for details. In all operating points, discharge pressures for CS1, CS2 and CS3, respectively, are 53, 51 and 48.6 bar.

Operating point	1	2	3
Gas flow CS1, Nm3/h	763400	655900	555800
Gas flow CS2, Nm3/h	560900	469600	378600
Gas flow CS3, Nm3/h	506300	422200	347500
CS1 suction pressure	40	40	40
CS2 suction pressure	40.17	43.48	46.18
CS3 suction pressure	38.65	42.45	45.40
PX1 pressure	41.15	44.27	46.55
PX2 pressure	43.11	45.66	47.50
PX3 pressure	29.52	40.26	42.55

Table A.1 Steady state values at operating points no. 1,2 and 3 when all CSs are running

If CS2 is shut down (by-passed), a long pipeline segment connects CS1 and CS3. Table A.2 shows details when CS2 is shut down in the three operating points defined above. The gas flows and CS discharge pressures are the same as the values in table A.1. As can be seen in table A.2, CS3 suction pressure in operating point no.1 decreases down to 22.34 bar. With this suction pressure, a CS3 discharge pressure of 48.6 bar can not be maintained unless the CS envelopes within "Simone" are disabled (the so called "free mode", see Appendix C).

Operating point	1	2	3
CS1 suction pressure	40	40	40
CS2 suction pressure	40.29	43.48	46.18
CS3 suction pressure	22.34	32.90	39.88
PX1 pressure	41.26	44.10	46.55
PX2 pressure	29.58	37.05	42.25
PX3 pressure	29.53	40.26	42.55

Table A.2 Steady state values at operating points when CS2 is shut down.

If CS3 is shut down (by-passed), a long pipeline segment now connects CS2 and the checkpoint PX3. Table A.3 shows details when CS3 is shut down in the three operating points defined above. The gas flows and CS discharge pressures are the same as the values in table A.1.

PX3 pressure decreases far below the 29 bar minimum limit, which is not acceptable. Moving over to operating point no. 2 increases the PX3 pressure with nearly 14 bar, a typical feature of a long pipeline segment with a small average diameter.

Operating point	1	2	3
CS1 suction pressure	40	40	40
CS2 suction pressure	41.27	43.48	46.18
CS3 suction pressure	39.65	42.46	45.43
PX1 pressure	42.13	44.10	46.55
PX2 pressure	44.52	45.67	47.50
PX3 pressure	20.49	34.07	38.87

Table A.3 Steady state values of operating points when CS3 is shut down.

In tables A.4 to A.6 below, gains of the responses are calculated using the gain formula (4.4), when applicable (a response exists and it is not zero-gain). These gains may be verified by comparing with the graphs in this appendix, unless the responses are so slow, that they do not reach steady state within the time frame of the graph.

Operating point	1			2			3		
	CS1	CS2	CS3	CS1	CS2	CS3	CS1	CS2	CS3
CS1 suction pressure									
CS2 suction pressure	1.32			1.22			1.15		
CS3 suction pressure		1.32			1.20			1.12	
PX1 pressure	1.29			1.20			1.14		
PX2 pressure		1.18			1.17			1.07	
PX3 pressure			1.65			1.21			1.14

Table A.4 Gains calculated with gain formula (4.4) using data from table A.1 Column headers CS1, CS2 and CS3 mean, that the discharge pressure of those respective CSs are the input to the models, which produce responses for the variables on the table rows with the gains as specified.

Operating point	1			2			3		
	CS1	CS2	CS3	CS1	CS2	CS3	CS1	CS2	CS3
CS1 suction pressure									
CS2 suction pressure	1.32			1.22			1.15		
CS3 suction pressure	2.37	-		1.61	-		1.33	-	
PX1 pressure	1.28			1.20			1.14		
PX2 pressure	1.79	-		1.43	-		1.25	-	
PX3 pressure			1.65			1.21			1.14

Table A.5 Gains calculated with gain formula (4.4) using data from table A.2.

Operating point	1			2			3		
	CS1	CS2	CS3	CS1	CS2	CS3	CS1	CS2	CS3
CS1 suction pressure									
CS2 suction pressure	1.28			1.22			1.15		
CS3 suction pressure		1.29			1.20			1.12	
PX1 pressure	1.26			1.20			1.14		
PX2 pressure		1.15			1.12			1.07	
PX3 pressure		2.49	-		1.50	-		1.31	-

Table A.6 Gains calculated with gain formula (4.4) using data from table A.3

As CS2 is shut down (table A.5), CS2 discharge pressure is not an input to any model. CS2 is not isolating, and CS1 discharge pressure acts on CS3 suction pressure and checkpoint PX2. Accordingly, when CS3 is shut down (table A.6), CS3 "disappears" as an input and CS2 discharge pressure acts on checkpoint PX3.

Step tests for control response are performed by making a +1 bar discharge pressure change at each CS in turn. The disturbance responses are obtained by making a +10000 Nm3/h step change in gas off-take flow near checkpoint PX3. All step tests are initiated at steady state operating point conditions.

To visualise the influence of operating point on pipeline dynamics, each graph below presents responses at all three operating points so, that a solid line represents operating point no.1, a dashed line operating point no.2 and a dotted (or short-dashed) line operating point no. 3.

The graphs are presented as CS1 (or PX1) pressure or flow to the left, CS2 (or PX2) in the middle and CS3 (PX3) to the right. This same order is preserved even, if there is no response due to the CS's isolating effect, but an empty space is left for the zero response. The leftmost figure is referred to as figure "a", the middlemost figure as "b" and the rightmost as "c", for example, figure A.4 b.

CS1 suction pressure is not shown because there is a virtual pressure controller at CS1 suction point keeping the suction pressure constantly at 40 bar, as explained in section 4.2.

The time axes have been selected based on the settling times of the responses. The shortest settling times are for CS flows (especially the flow of the station, where a discharge pressure step change has been made), for which a time axis length of 6 hours is usually used. Typically, an 11 hour time axis is used, but for very slow responses, 16 hours is used. All time axes in the graphs below are presented using a sample time interval (or "scale tick") of 10 minutes.

A.2 Pipeline system responses when all compressor stations are in operation

CS2 suction pressure, bar

CS1 suction pressure is fixed at 40 bar
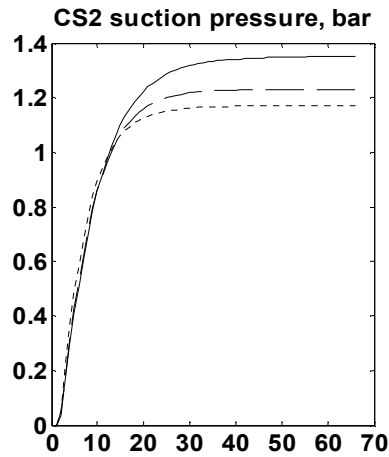
Figure A.1 Responses of suction pressures to CS1 discharge pressure. CS1 suction pressure is fixed, CS2 responses are shown, and CS3 responses are all zero.
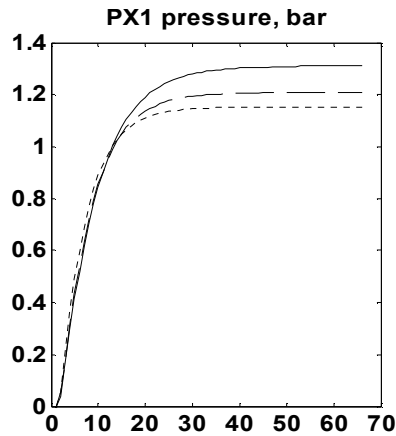
Figure A.2 Responses of pipeline checkpoint pressures to CS1 discharge pressure. PX2 and PX3 are all zero.
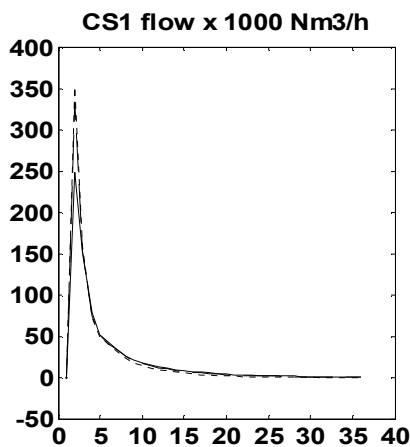
Figure A.3 Responses of station flows to CS1 discharge pressure. CS2 and CS3 flow rates are all zero. The flow rate peak is lower in operating point 1 but higher and almost equal in operating points 2 and 3.

A - 4

CS1 suction pressure is
fixed at 40 bar

CS2 suction pressure, bar

CS3 suction pressure, bar
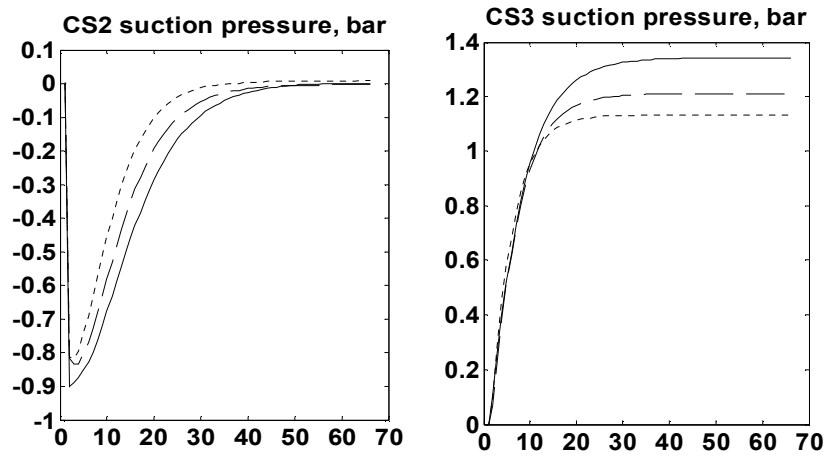
Figure A.4 Responses of CS2 and CS3 suction pressures to CS2 discharge pressure.

PX1 pressure, bar

PX2 pressure, bar
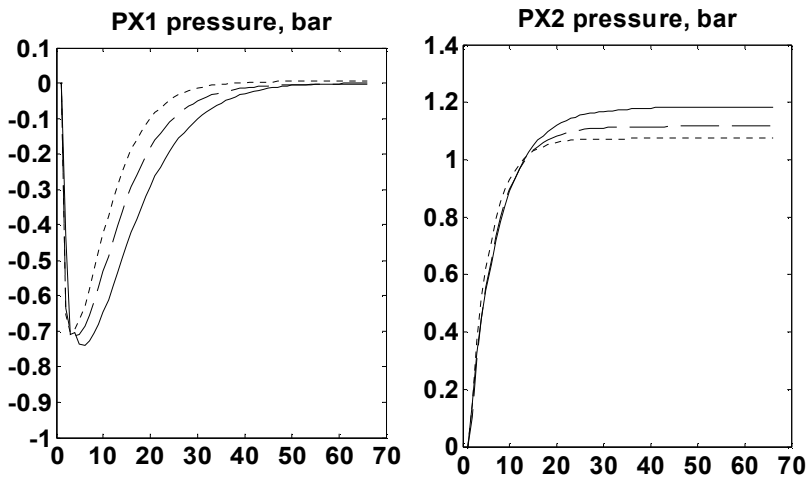
Figure A.5 Responses of PX1 and PX2 checkpoint pressures to CS2 discharge pressure

CS1 flow x 1000 Nm3/h

CS2 flow x 1000 Nm3/h
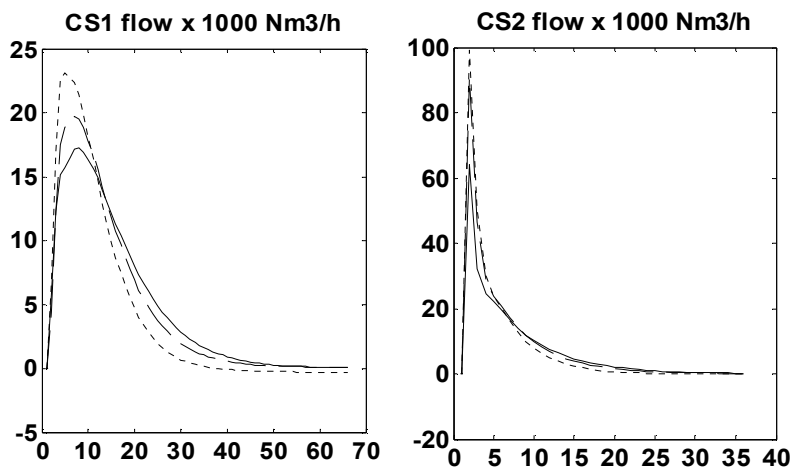
Figure A.6 Responses of CS1 and CS2 flow rates to CS2 discharge pressure.

CS1 suction pressure is fixed at 40 bar

CS2 suction pressure, bar

CS3 suction pressure, bar
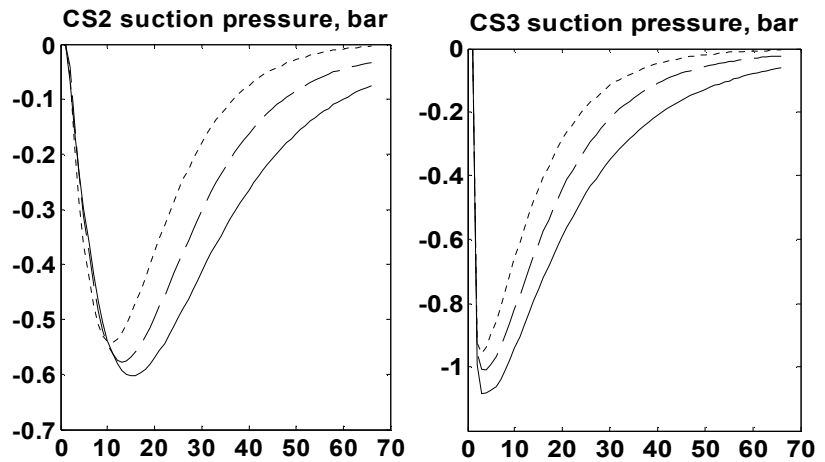
Figure A.7 Responses of CS2 and CS3 suction pressures to CS3 discharge pressure.

PX1 pressure, bar

PX2 pressure, bar

PX3 pressure, bar
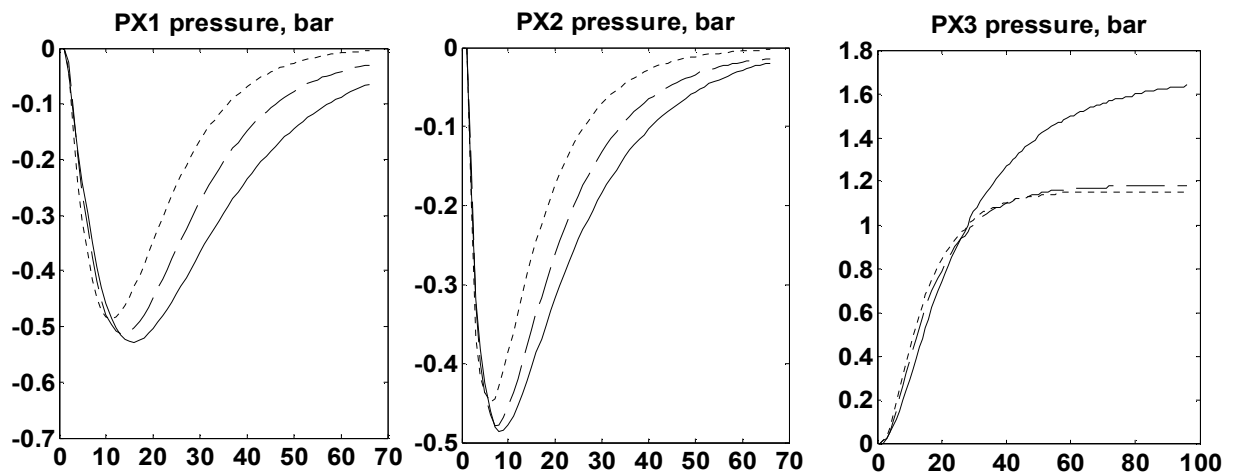
Figure A.8 Responses of PX1, PX2 and PX3 checkpoint pressures to CS3 discharge pressure.

CS1 flow x 1000 Nm3/h

CS2 flow x 1000 Nm3/h

CS3 flow x 1000 Nm3/h
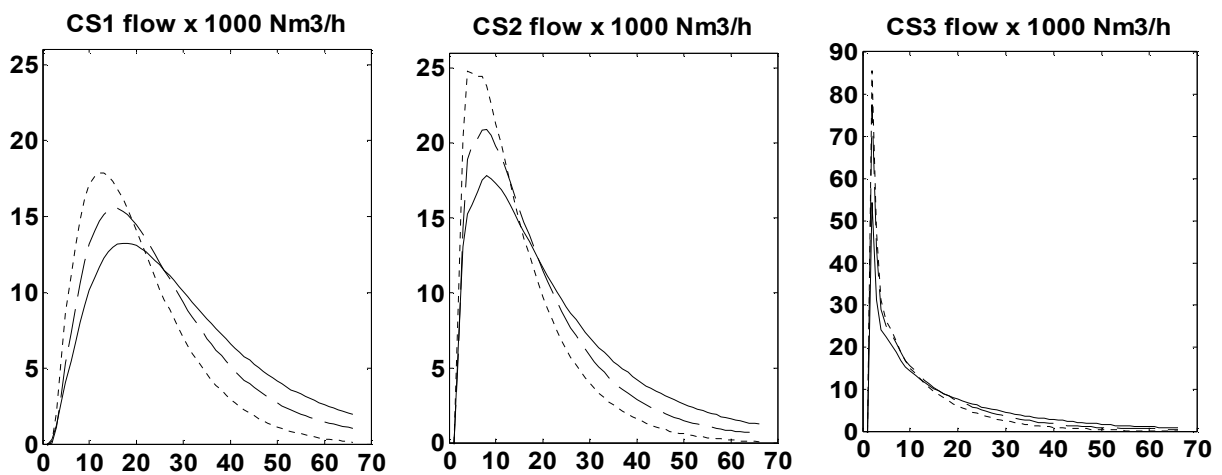
Figure A.9 Responses of CS1, CS2 and CS3 flow rates to CS3 discharge pressure.

A - 6

For CS3 the flow rate peak is lower in the operating point no. 1 but higher and almost equal in operating points no. 2 and 3. CS3 is flow graphed on an 11 hour time axis because flow differences are seen also after an initial period.

CS1 suction pressure is fixed at 40 bar

CS2 suction pressure, bar

CS3 suction pressure, bar
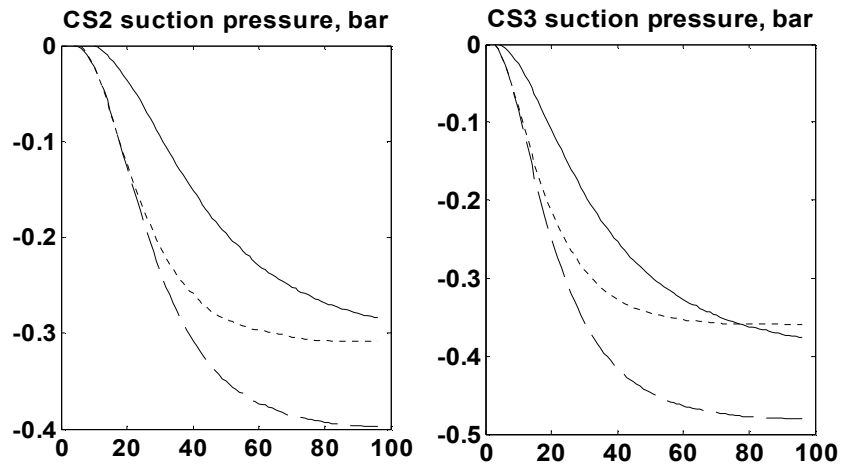
Figure A.10 Responses of CS2 and CS3 suction pressures to a 10000 Nm3/h step change in gas flow rate at off-take PX3.

PX1 pressure, bar

PX2 pressure, bar

PX3 pressure, bar
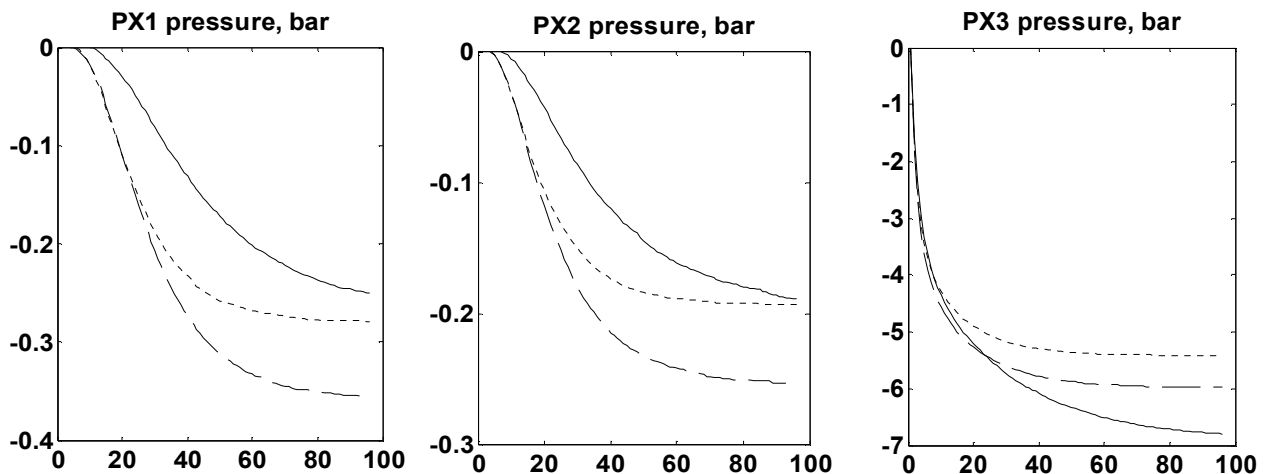
Figure A.11 Responses of checkpoint pressure PX1, PX2 and PX3 to a 10000 Nm^3/h step change in gas flow rate at off-take PX3.

A.3 Pipeline system responses when compressor station CS2 is shut down

CS1 suction pressure is fixed at 40 bar
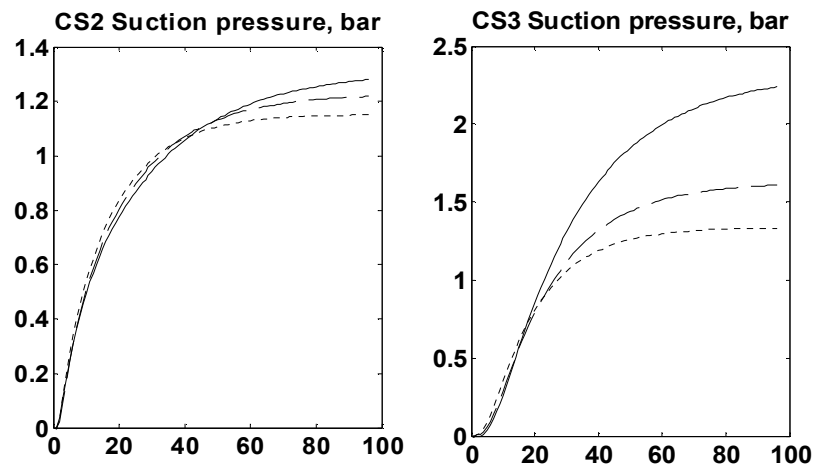
Figure A.12 Responses of CS2 and CS3 suction pressures to CS1 discharge pressure
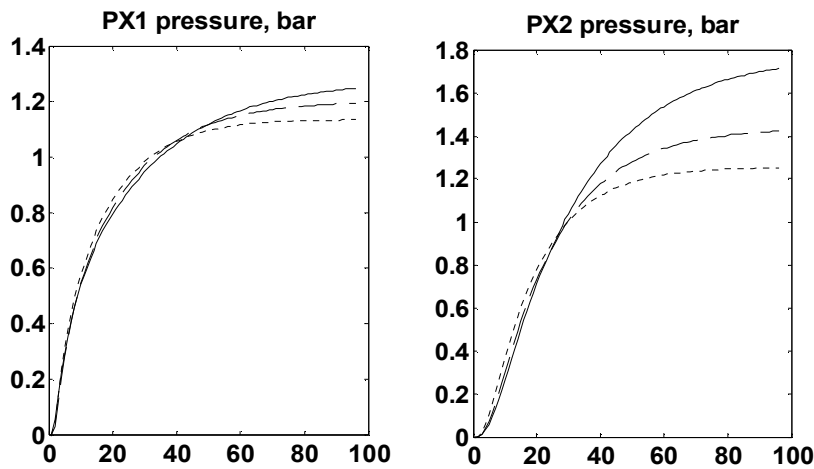
Figure A.13 Responses of PX1 and PX2 checkpoint pressures to CS1 discharge pressure
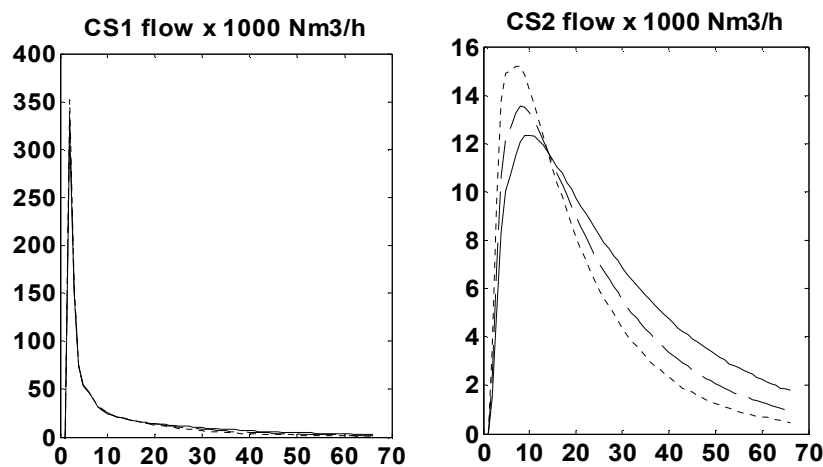
Figure A.14 Responses of CS1 and CS2 flow rates to CS1 discharge pressure. Note, that CS1 flow rate curves coincide, practically speaking.

CS2 suction pressure, bar

**CS3 Suction pressure, bar**

CS1 suction pressure is
fixed at 40 bar
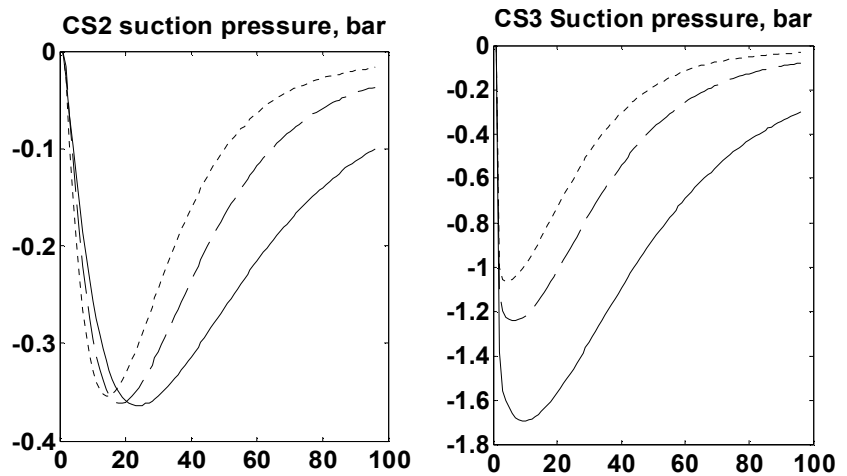
Figure A.15 Responses of CS2 and CS3 suction pressures to CS3 discharge pressure.

PX1 pressure, bar

PX2 pressure, bar

PX3 pressure, bar
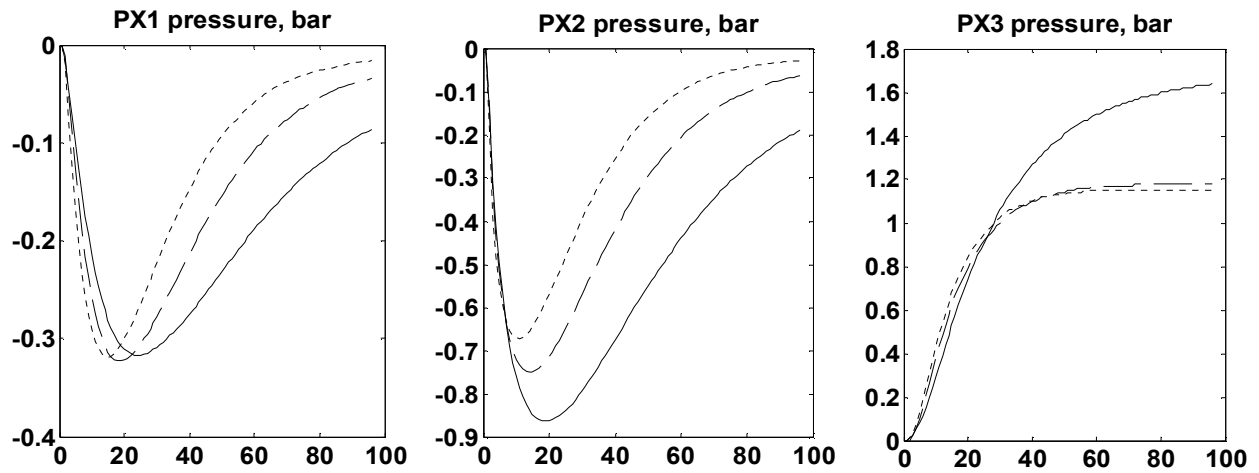
Figure A.16 Responses of PX1, PX2 and PX3 checkpoint pressures to CS3 discharge pressure. PX3 response to CS3 is the same as in the case with all CSs in operation (figure A.8 c), since CS3 isolates pipeline segments.

CS1 flow x 1000 Nm3/h

CS2 flow x 1000 Nm3/h

CS3 flow x 1000 Nm3/h
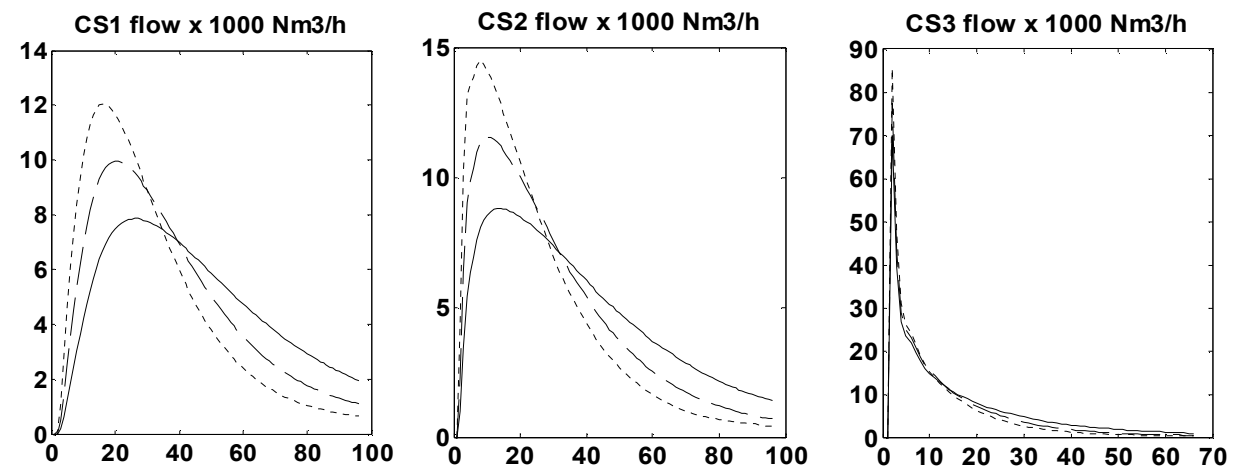
Figure A.17 Responses of CS1, CS2 and CS3 flow rates to CS3 discharge pressure

CS1 suction pressure is
fixed at 40 bar
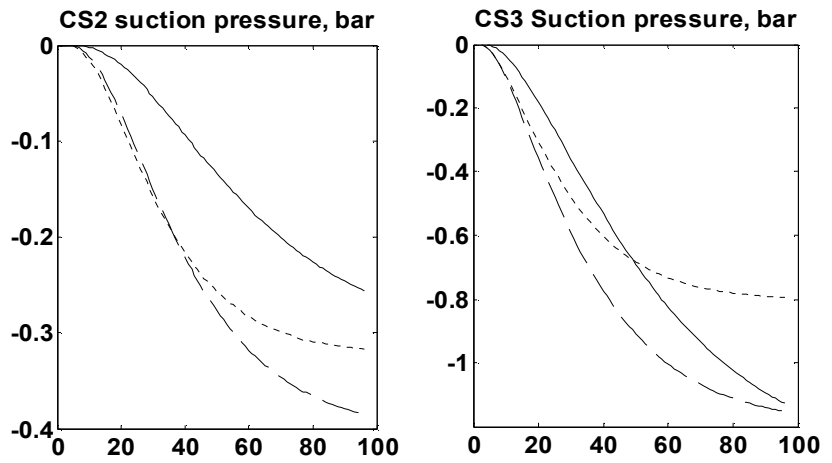
Figure A.18 Responses of CS2 and CS3 suction pressures to PX3 off-take flow rate
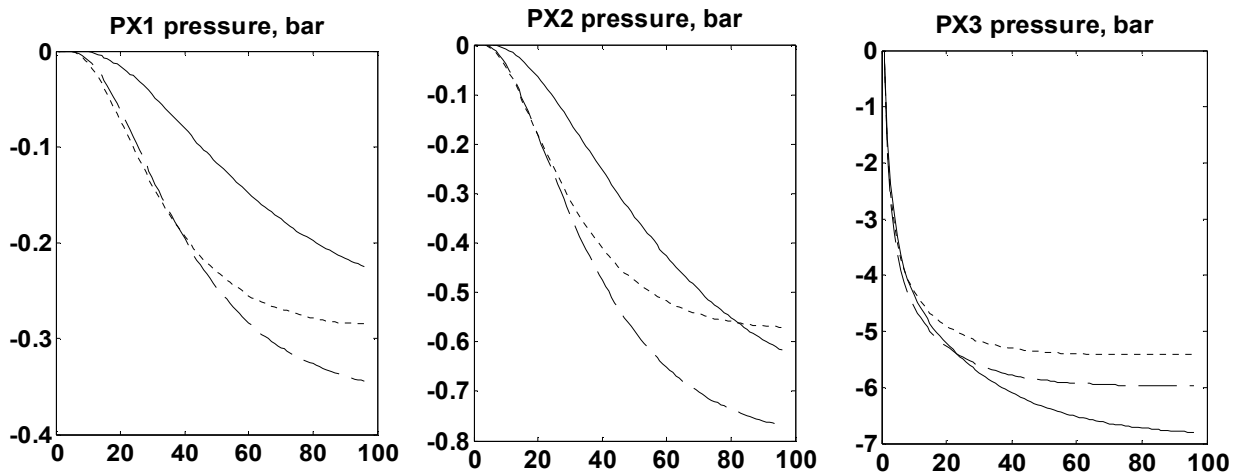
Figure A.19 Responses of PX1, PX2 and PX3 checkpoint pressures to PX3 off-take flow rate

A -10

A.4 Pipeline system responses when compressor station CS3 is shut down

The situation where CS3 is shut down in operating point no.1, which shows the largest gas consumptions, is near gas exhaust. As can be seen in table A.3 above, the pressure at PX3 decreases to about 20 bar, which is far below the minimum limit (29 bar) and thus this is not an acceptable operating point. Here we use it only to demonstrate the dynamical behaviour. In operating point 1 with CS3 shut down, it is not possible to make a 10 000 Nm3/h increase in gas off-take flow at PX3, and therefore, in figures A.26 and A.27 below, only responses for operating points no. 2 and 3 are shown.

CS1 suction pressure is fixed at 40 bar
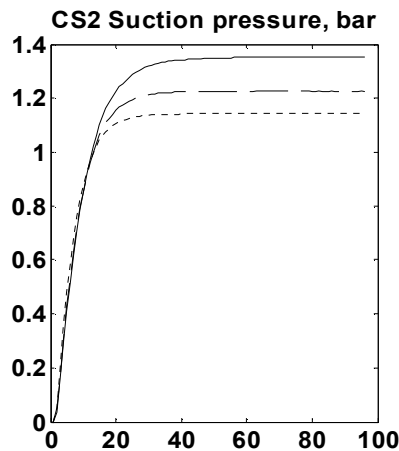
**Figure A.20** Responses of CS2 suction pressure to CS1 discharge pressure
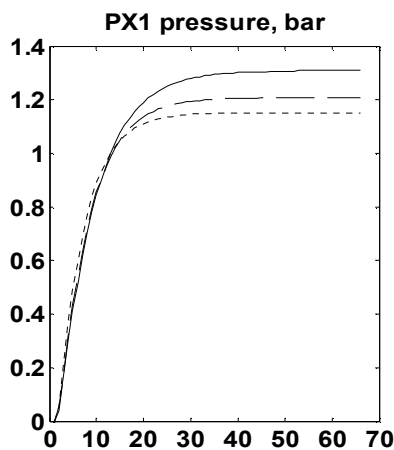
Figure A.21 Responses of PX1 checkpoint pressure to CS1 discharge pressure. Note, that PX1 responses equals those when all CSs are running (figure A.2 a)

A -11

CS1 flow x 1000 Nm3/h
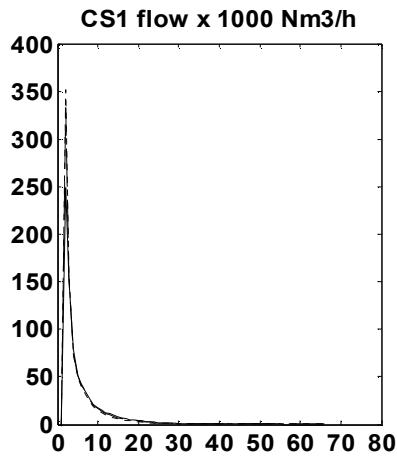
Figure A.22 Responses of CS1 gas flow rate to CS1 discharge pressure

CS2 Suction pressure, bar

CS3 Suction pressure, bar

CS1 suction pressure is
fixed at 40 bar
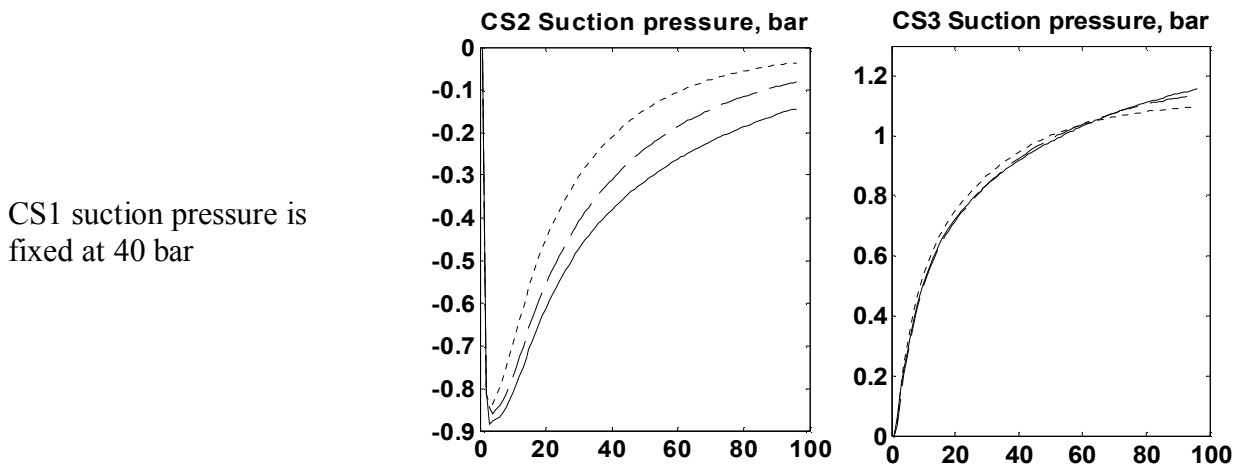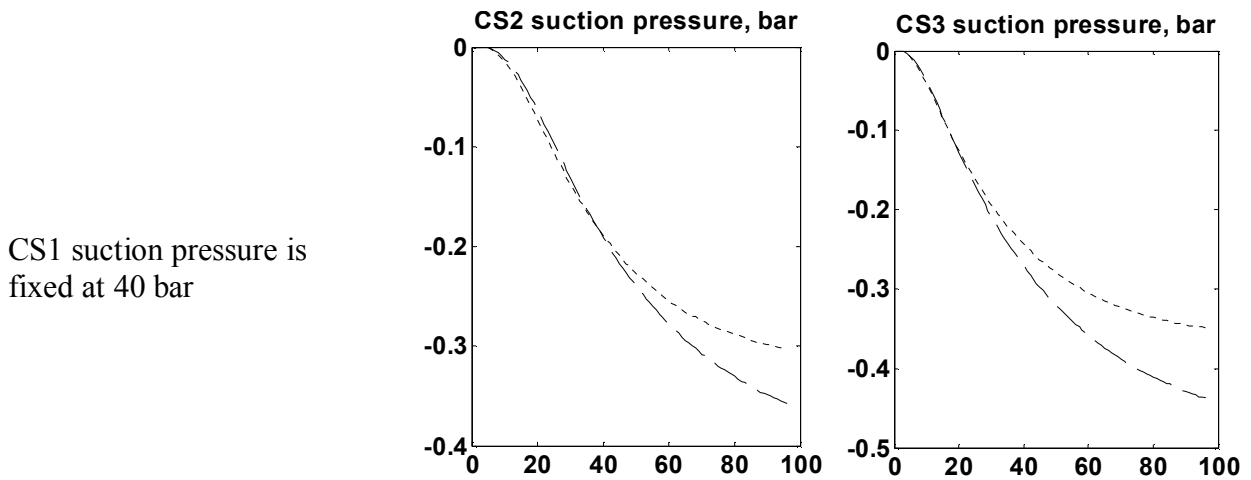
Figure A.23 Responses of CS2 and CS3 suction pressures to CS2 discharge pressure.
Note the slow dynamics of CS3 suction pressure.

**PX1 pressure, bar**

PX2 pressure, bar

PX3 pressure, bar
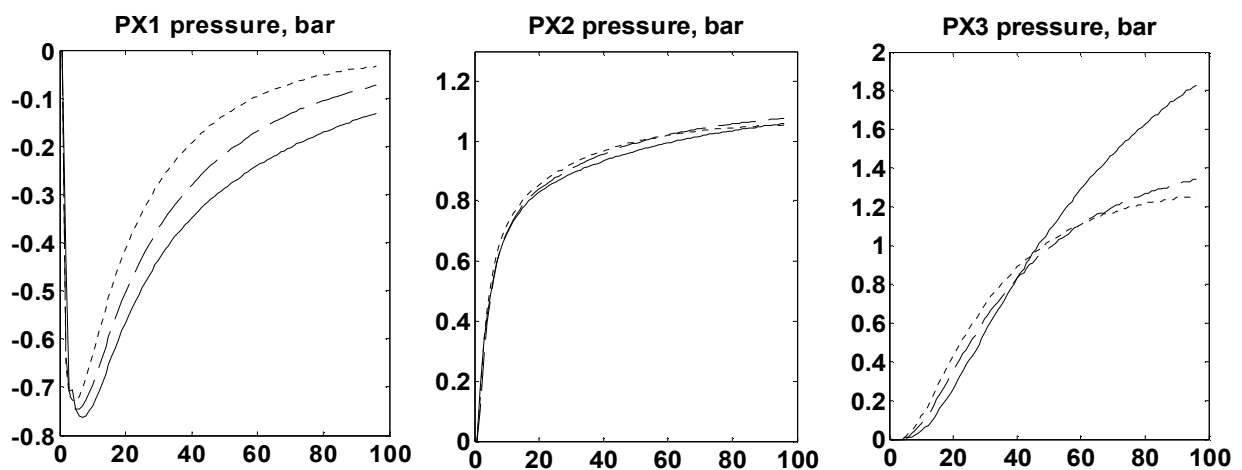
Figure A.24 Responses of PX1, PX2 and PX3 checkpoint pressures to CS2 discharge pressure.
Note the very slow dynamics of PX3 especially in operating point no. 1.

A -12
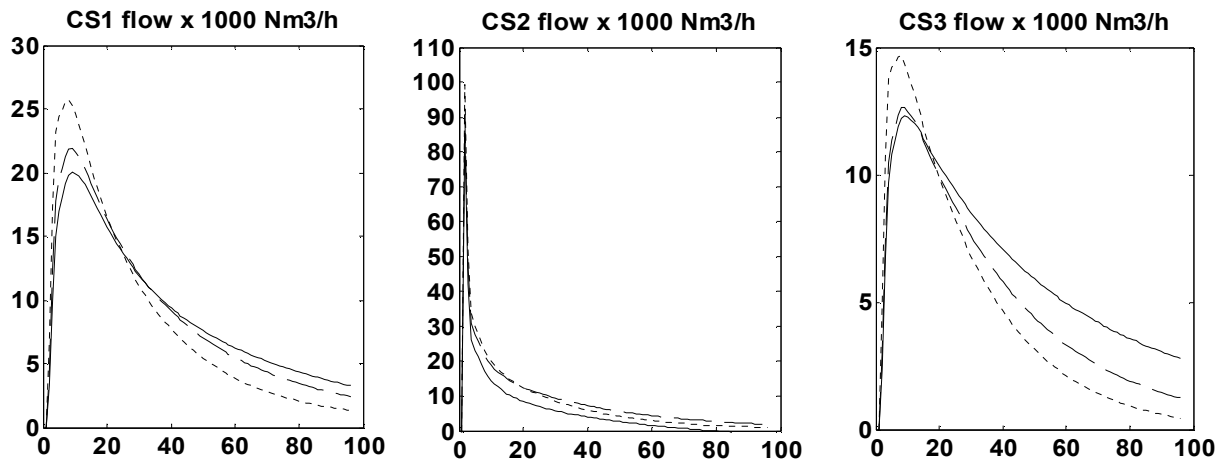
Figure A.25 Responses of CS1, CS2 and CS3 flow rates to CS2 discharge pressure.

CS1 suction pressure is fixed at 40 bar

Figure A.26 Responses of CS2 and CS3 suction pressures to off-take flow rate change at PX3. Responses in operating point 1 not shown.
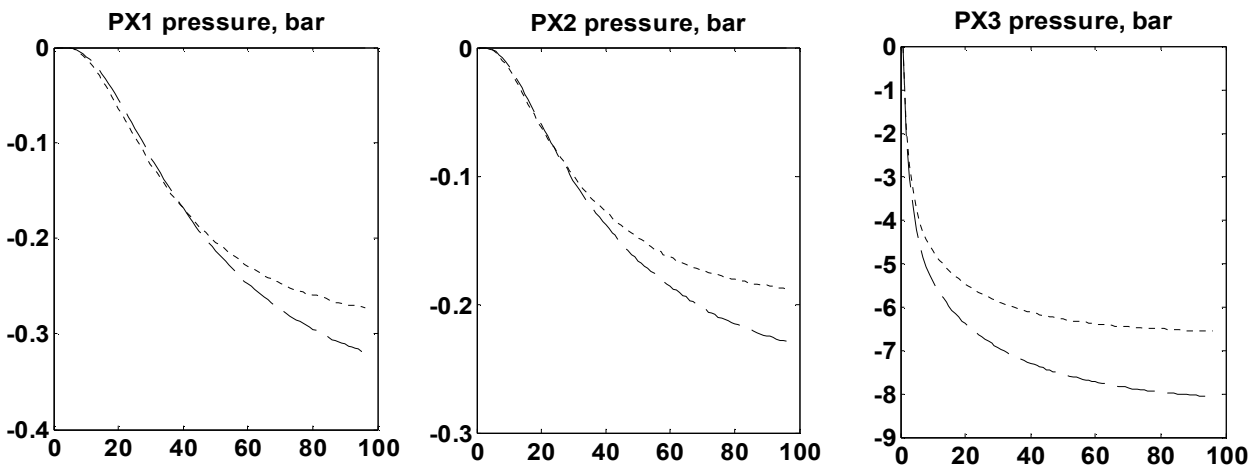

Figure A.27 Responses of PX1, PX2 and PX3 pressures to off-take flow rate change at PX3. Responses in operating point 1 not shown.

A.5 Effect of discharge pressure level on pipeline dynamics.

With the gas flow rates used in operating point no. 2, the CS discharge pressures are significantly decreased in order to obtain a fourth operating point, in which we once again will run a series of step tests. The steady state values of this operating point are shown in the table below together with steady state values of operating point no. 2 for comparison. All CSs are running.

|	New operating point	Oper. point 2 (Table A.1)
CS1 discharge pressure	50	53
CS2 discharge pressure	47	51
CS3 discharge pressure	43	48.6
CS1 suction pressure	40	40
CS2 suction pressure	39.70	43.48
CS3 suction pressure	37.48	42.45
PX1 pressure	40.40	44.27
PX2 pressure	41.14	45.66
PX3 pressure	34.74	40.26

Pressure level does not have a very large impact on pipeline dynamics. Below, only some selected step responses to CS discharge pressures are shown. In all graphs, a solid line represents the original operating point no. 2 and the dashed line the operating point with reduced pressure level. A slight gain increase can be seen in figures A.28 and A.29 c, but the otherwise the dynamics has not changed significantly.

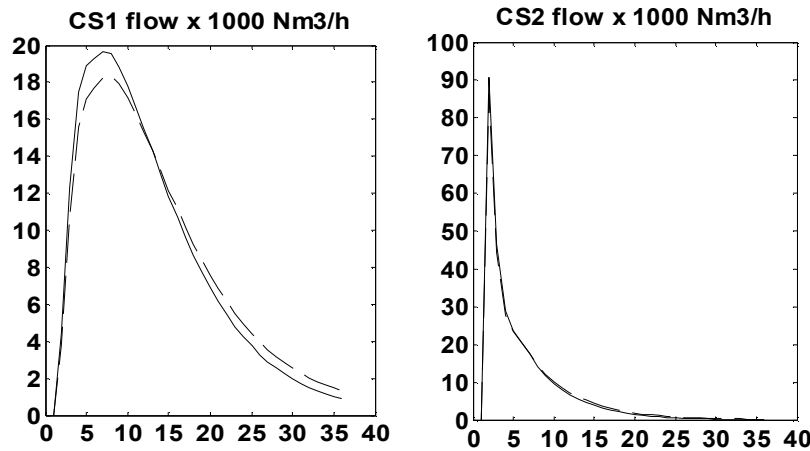CS1 suction pressure is fixed at 40 bar
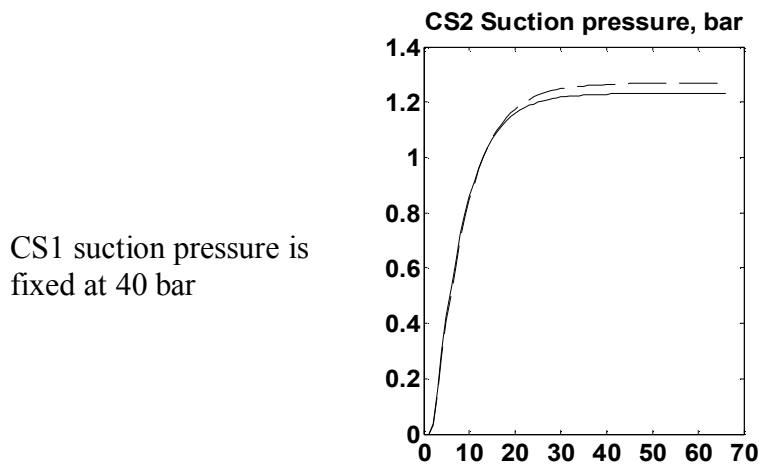
**Figure A.28** Response of CS2 suction pressure to CS1 discharge pressure

CS1 suction pressure is
fixed at 40 bar
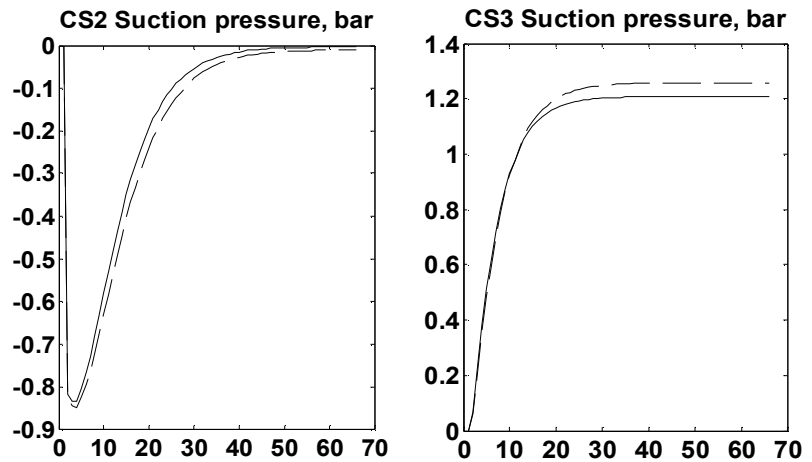
Figure A.29 Response of CS2 and CS3 suction pressures to CS2 discharge pressure

Figure A.30 Responses of CS1 and CS2 flow rates to CS2 discharge pressure. CS2 flow rates are practically speaking identical. Some differences are seen in CS1 flows, obviously because of the change in pipeline segment dynamics due to the pressure level change.
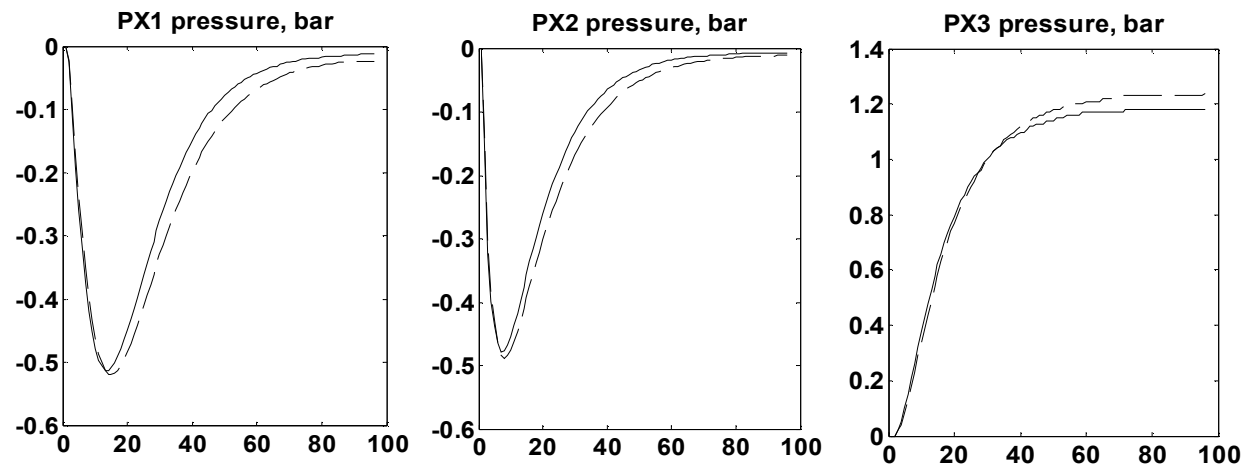
Figure A.31 Responses of PX1, PX2 and PX3 checkpoint pressures to CS3 discharge pressure

Appendix B. Linear transfer functions for the Finnish natural gas pipeline system

Transfer function models obtained from identification on simulated data together with graphs visualising the modelling error are presented below for selected cases.

Relative error is in all cases calculated as the difference between linear, identified model and simulated outputs divided by maximum absolute value of identified output. If the relative error is large, usually greater than 5%, then the step response of the identified linear model is graphed together with the step response from "Simone", otherwise the relative error is graphed, because for small errors, the two step response curves are almost overlapping.

The graphs and transfer functions in all figures below are shown in the same order: for operating point 1 at the left (figure "a") , for operating point no. 2 in the middle (figure "b") and for operating point no. 3 to the right (figure "c"). For each figure below, a corresponding figure in Appendix A can be found showing the "Simone" step response.

The identification strategy is to find decent but not too high order linear models, in other words, good model fit is not bought with the price of using more model parameters. It seems that for operating point no.1, low order models give a larger relative error suggesting higher order models to be used. For operating points no. 2 and 3, low order models give smaller errors, indicating that lower gas throughput in the pipeline system decreases the complexity of the dynamics. For compressor station gas flows, a higher order model would obviously provide better results, but at this stage, we will use low order models. See figure B.2 below.

For all transfer functions shown below, gains are in appropriate units (dimensionless, i.e. bar/bar) for pressures and $Nm^3/(h, bar)$ for gas flow rates. Time constants are expressed in minutes.

## B.1 Linear models for operating points no.1, 2 and 3 when all compressor stations are in operation

$\dfrac{1.36}{83s+1}$	$\dfrac{1.24}{69s+1}$	$\dfrac{1.17}{57s+1}$
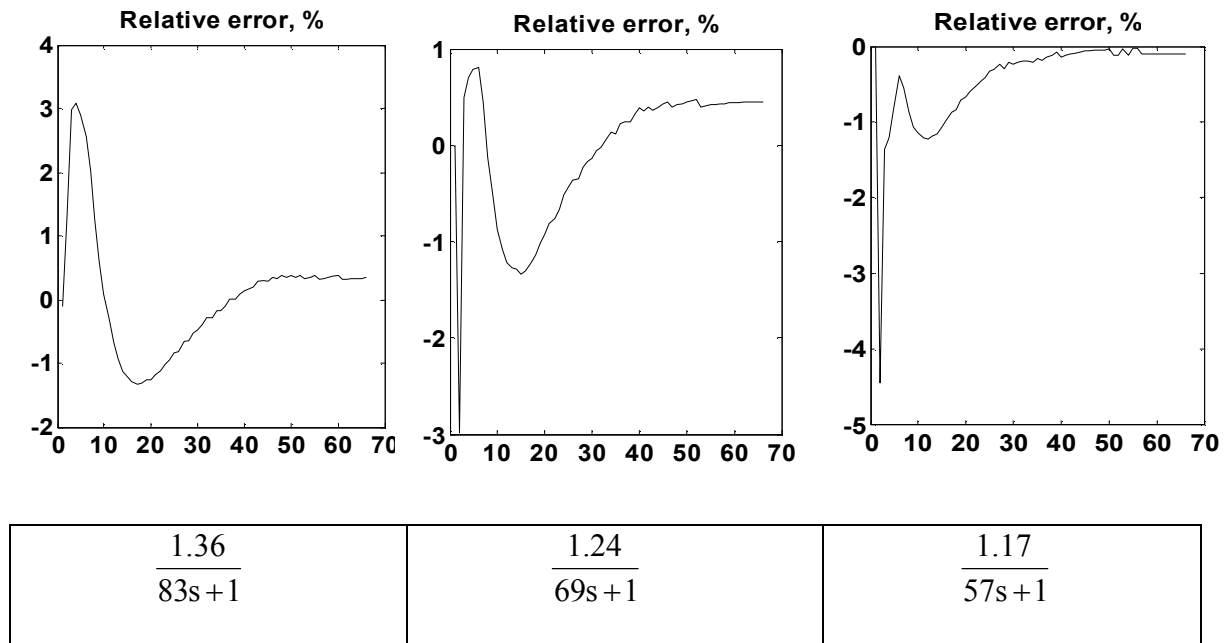
Figure B.1 CS2 suction pressure response to CS1 discharge pressure. Compare figure A.1 b , Appendix A.

| $270000\left[1-\dfrac{1}{30s+1}\right]$	$330000\left[1-\dfrac{1}{18s+1}\right]$	$350000\left[1-\dfrac{1}{17s+1}\right]$
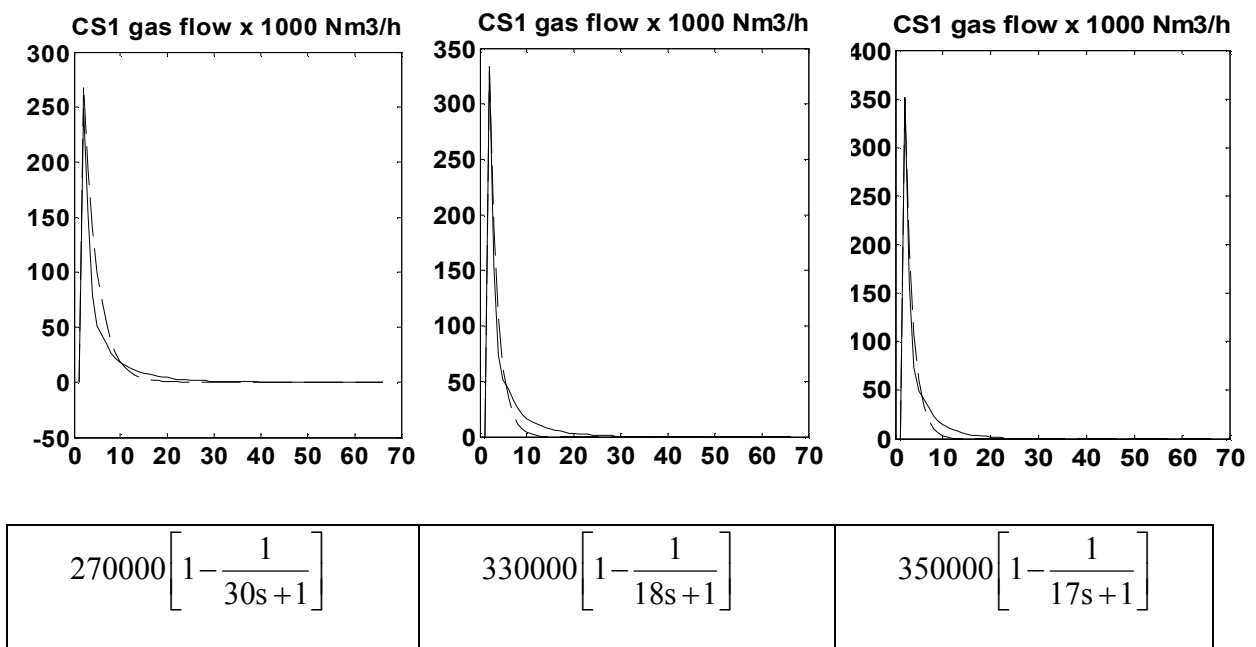
Figure B.2 CS1 gas flow response to CS1 discharge pressure. Maximum relative errors are for figures a, b and c, respectively, 24 % , 10.7 % and 10.1 %. Compare figure A.3 a , Appendix A.
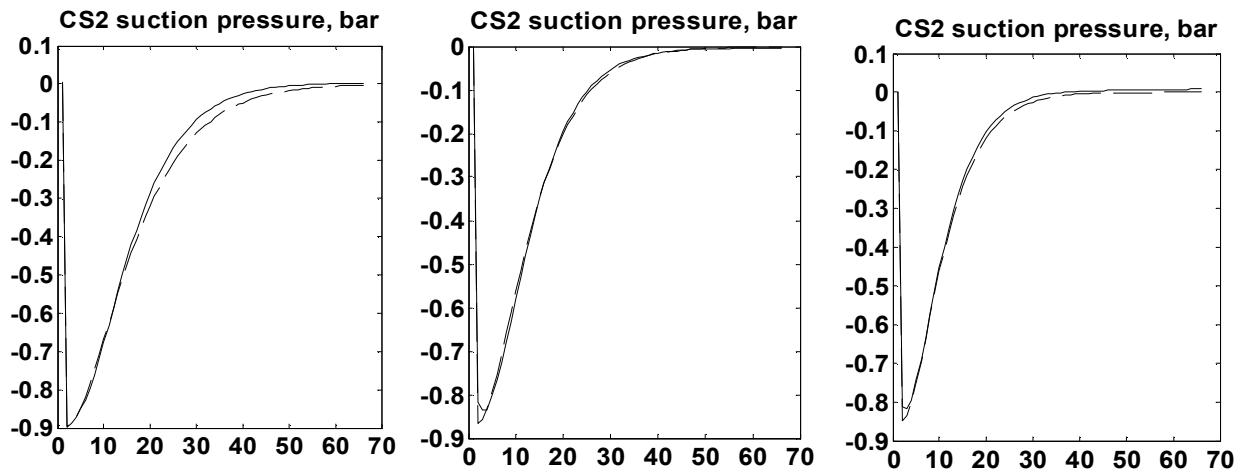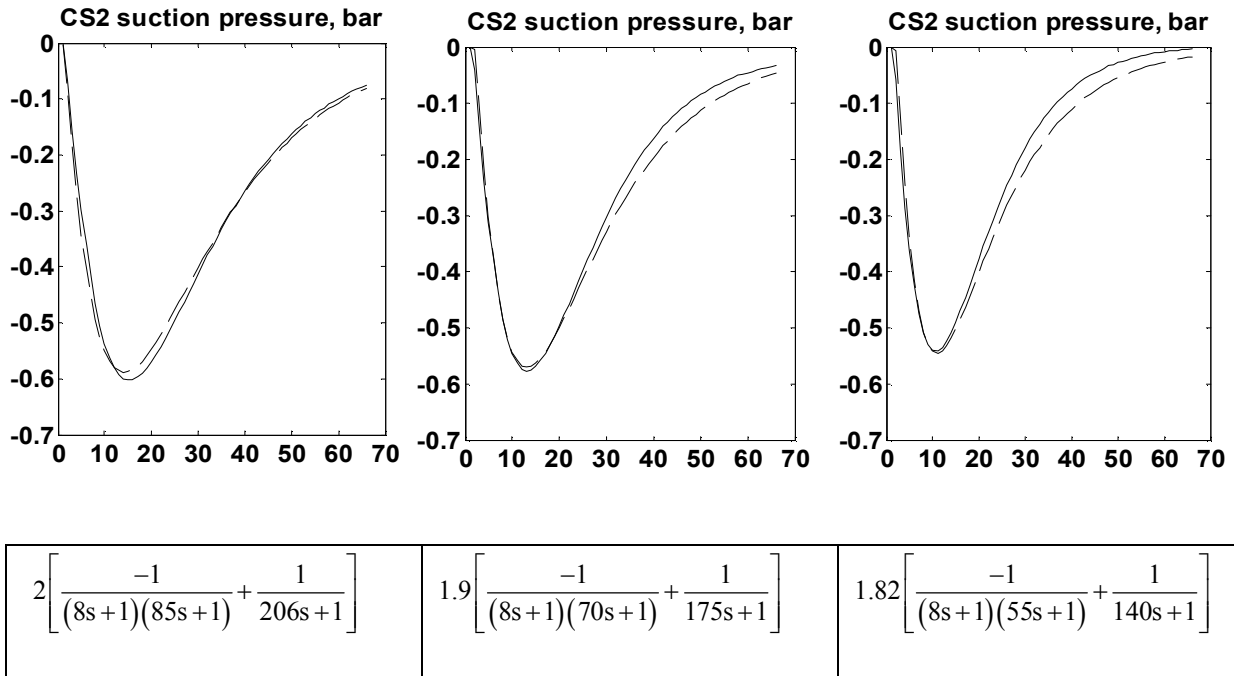
$0.9\left[-1+\dfrac{1}{(81s+1)(83s+1)}\right]$	$0.87\left[-1+\dfrac{1}{(63s+1)(66s+1)}\right]$	$0.85\left[-1+\dfrac{1}{(55s+1)^2}\right]$

Figure B.3 CS2 suction pressure response to CS2 discharge pressure. Maximum relative errors are for figures a, b and c, respectively, 4.2% , 5.8 % and 4.4 %. Compare figure A.4 b , Appendix A.
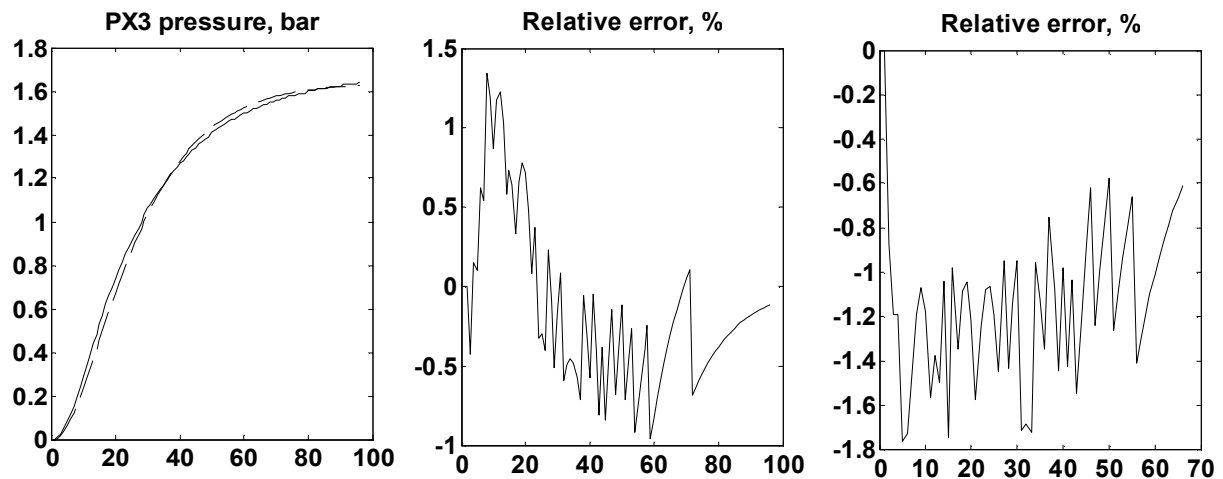

$\dfrac{1.64}{(117s+1)(155s+1)}$	$\dfrac{1.18}{(25s+1)(135s+1)}$	$\dfrac{1.15}{(25s+1)(120s+1)}$

Figure B.4 Px3 pressure response to CS3 discharge pressure. Maximum relative error for figure a is 4.5 %.. The high frequency fluctuations of the relative error in figures b and c are due to the 2 decimal places presentation accuracy of Px3 in the "Simone" output data files. Compare figure A.8 c , Appendix A.

|		
$2\left[\dfrac{-1}{(8s+1)(85s+1)}+\dfrac{1}{206s+1}\right]$	$1.9\left[\dfrac{-1}{(8s+1)(70s+1)}+\dfrac{1}{175s+1}\right]$	$1.82\left[\dfrac{-1}{(8s+1)(55s+1)}+\dfrac{1}{140s+1}\right]$

Figure B.5 CS2 suction pressure response to CS3 discharge pressure. Maximum relative errors are for figures a, b and c, respectively, 6.5% , 5.89% and 11.9 %. Compare figure A.7 b, Appendix A.

B.2 Linear models for operating points no.1, 2 and 3 when CS2 is shut down

$\dfrac{1.31}{216s+1}$	$\dfrac{1.23(85s+1)}{(200s+1)(60s+1)}$	$\dfrac{1.16(96s+1)}{(180s+1)(60s+1)}$
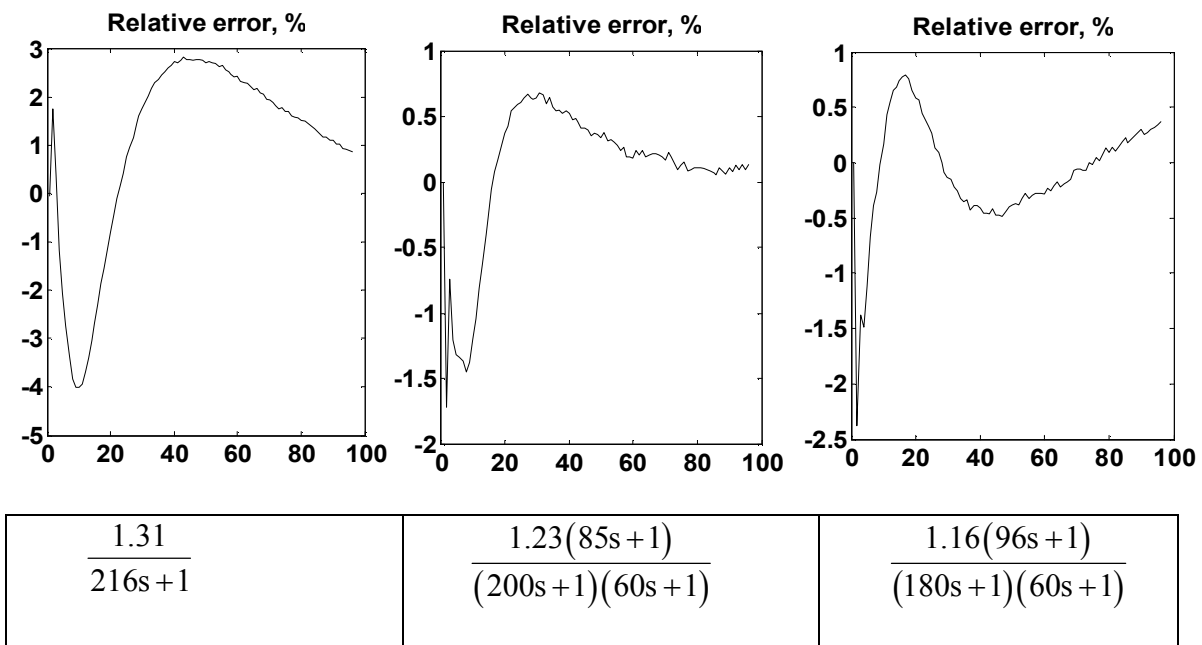
Figure B.6 CS2 suction pressure response to CS1 discharge pressure. Most obviously, the relative error in figure "a" could be made smaller using a higher order model. Compare figure A.14 b , Appendix A.

$\dfrac{2.31}{(216s+1)(102s+1)}$	$\dfrac{1.63}{(184s+1)(56s+1)}$	$\dfrac{1.34}{(155s+1)(35s+1)}$
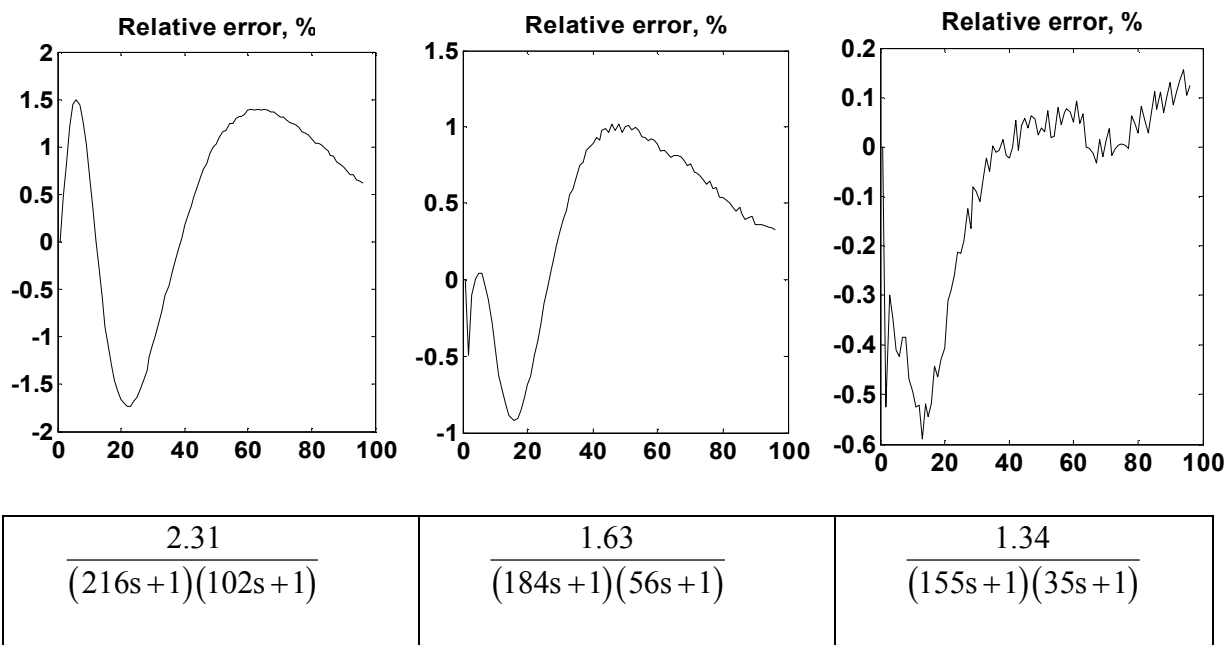
Figure B.7 CS3 suction pressure response to CS1 discharge pressure. Note that CS2 being bypassed, we have a very long pipeline segment consequently with slow dynamics. Compare figure A.14 c , Appendix A.

$318000\left[1-\dfrac{1}{25s+1}\right]$	$327000\left[1-\dfrac{1}{26s+1}\right]$	$350000\left[1-\dfrac{1}{24s+1}\right]$

Figure B.8 CS1 gas flow response to CS1 discharge pressure. Maximum relative errors are for figures a, b and c, respectively, 21.3 % , 22.9 % and 21.8 %. Compare figure A.14 a , Appendix A.
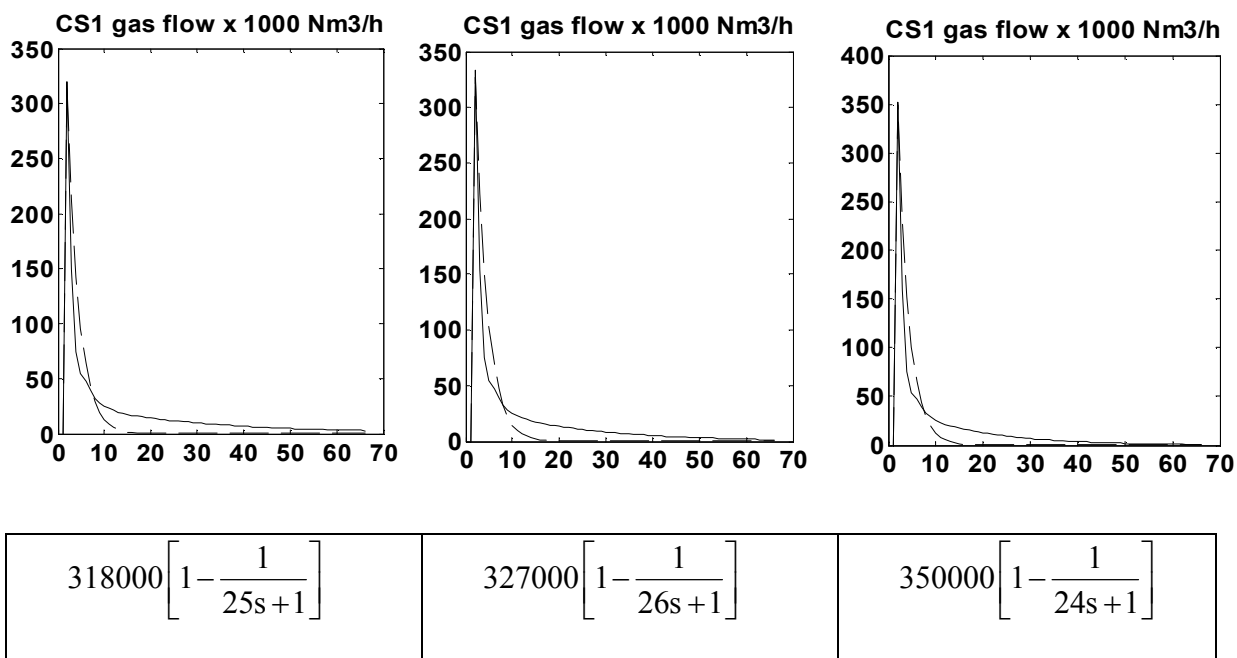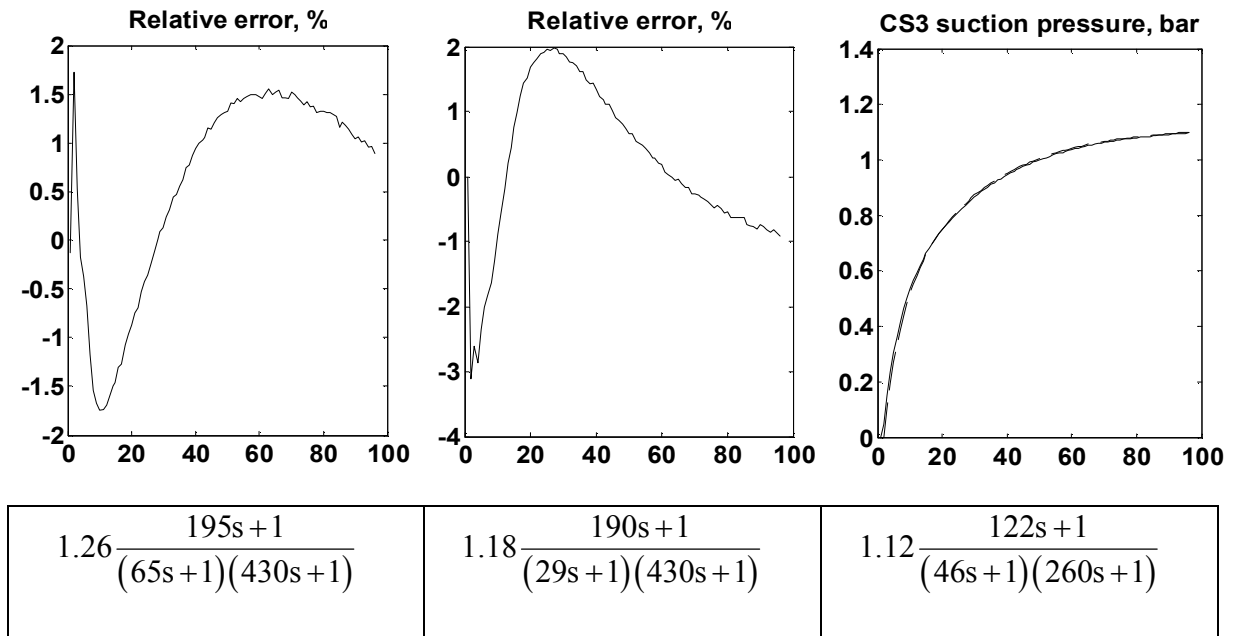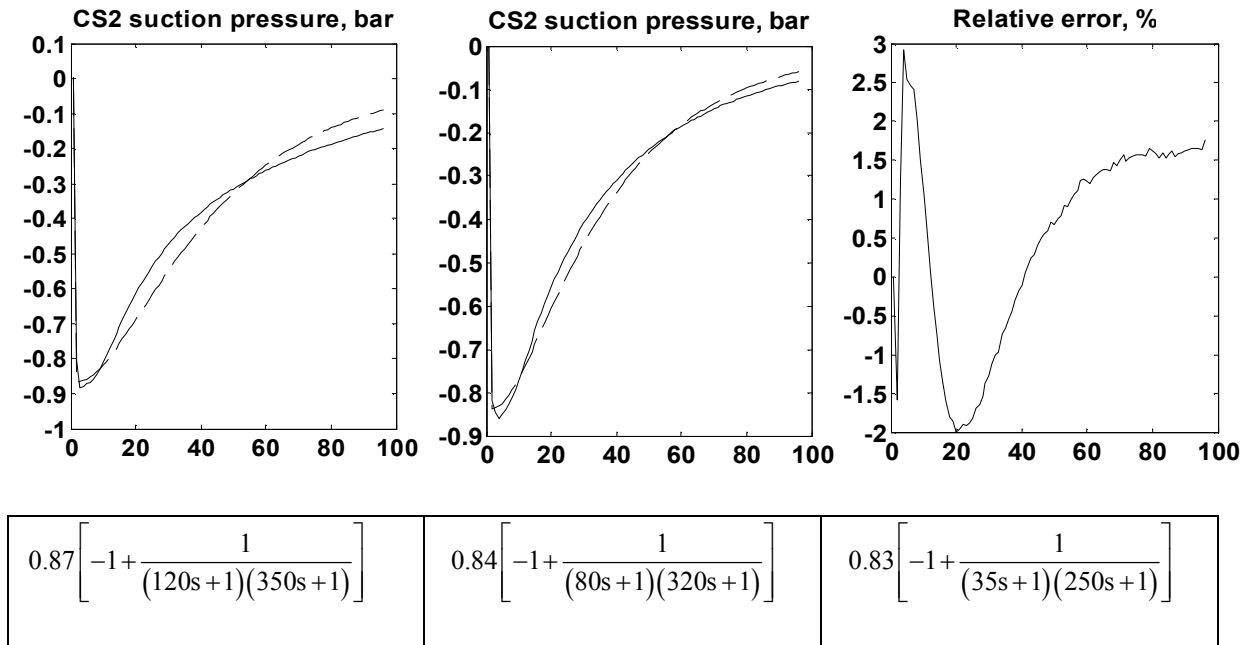
B.3 Linear models for operating points no.1, 2 and 3 when CS3 is shut down

|		
$1.26\dfrac{195s+1}{(65s+1)(430s+1)}$	$1.18\dfrac{190s+1}{(29s+1)(430s+1)}$	$1.12\dfrac{122s+1}{(46s+1)(260s+1)}$

Figure B.9 CS3 suction pressure response to CS2 discharge pressure. Maximum relative error in figure c is 4.5 % Compare figure A.23 c , Appendix A.

|		
$0.87\left[-1+\dfrac{1}{(120s+1)(350s+1)}\right]$	$0.84\left[-1+\dfrac{1}{(80s+1)(320s+1)}\right]$	$0.83\left[-1+\dfrac{1}{(35s+1)(250s+1)}\right]$

Figure B.10 CS2 suction pressure response to CS2 discharge pressure. Maximum relative errors are in figure a: 9.2 % and figure b: 6.2 % Compare figure A.23 b , Appendix A.

$\dfrac{2.35}{(280s+1)(350s+1)}$	$\dfrac{1.44}{(140s+1)(260s+1)}$	$\dfrac{1.30}{(105s+1)(220s+1)}$
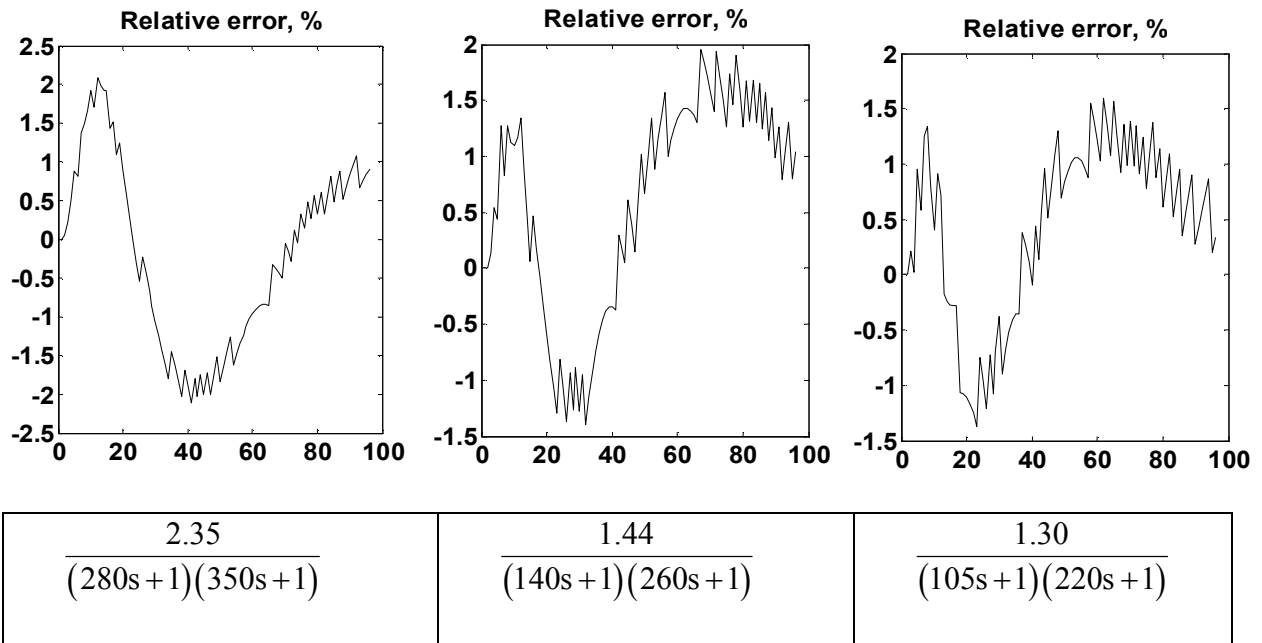
Figure B.11 Px3 response to CS2 discharge pressure. Compare figure A.24 c , Appendix A.

$1.14\dfrac{250s+1}{(29s+1)(430s+1)}$	$1.10\dfrac{148s+1}{(26s+1)(270s+1)}$	$1.06\dfrac{138s+1}{(25s+1)(240s+1)}$
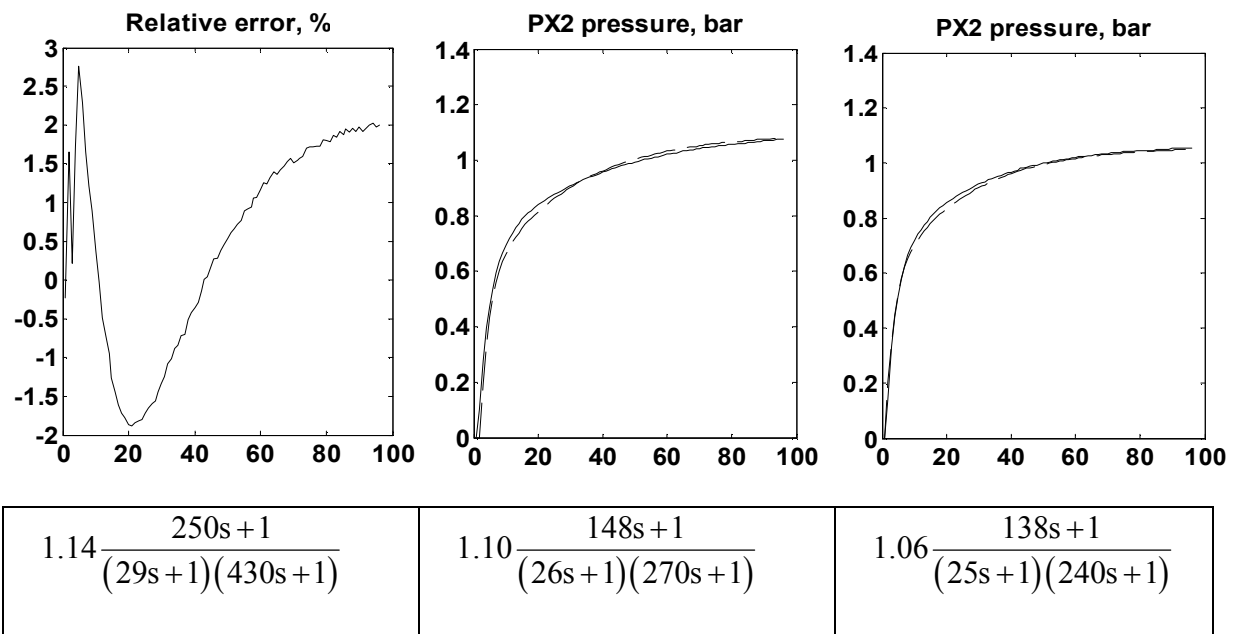
Figure B.12 PX2 response to CS2 discharge pressure. Maximum relative errors in figure b 4.6 % and in figure c 4.8 %. Compare figure A.24 b , Appendix A.

Appendix C. Software description

C.1 The program structure of "Simone"

The "Simone" ("simulation of memory optimised networks)"natural gas pipeline system simulator, version 3.2, 1991 is used (Jeni'cek et. al., 1991). This is a software program, which runs under an MS-DOS window under the Windows 95 operating system. This version was chosen because of practical reasons and the age of the program is not an issue, since the dynamical model of the Finnish natural gas pipeline system has been continuously been kept up to date on this version, although newer "Simone" versions are in use in parallel. "Simone", version 3.2, is not, as such, capable of fulfilling the needs of a real time receding horizon optimiser, but it has an excellent program structure, which enables the necessary modifications.

The kernel of "Simone" consists of a few executable files, which are controlled by a number of MS-DOS Batch command files. "Simone" uses a number of central data input files as well. The most important ones are (see figure C.1):
- A "Boundary condition file, BCA" containing gas flow rate profiles (flow rate data vectors) for all off-takes.
- A "Run command file, CRD" used to control the simulation. Specific commands are:
  - Set a value for a compressor station's discharge pressure
  - Switch a compressor station's status to "run" or "bypass" (means shut down)
  - Set a compressor station to "free mode" (do not obey envelope limits) or to "normal mode" (obey envelope limits)
  - Modify the gas flow rate of a given off-take from the values in the boundary condition file.
- Definition file for compressor station envelope curves and power consumption characteristics, CSED
- "Tabular output definition file, TDF" for controlling the ASCII output format of simulation data results
- "Initial conditions, ICU" file. Contains initial conditions of all state variables of the simulation model

The most important output files from "Simone" are:
- The ASCII output data file , "OUT", defined by the TDF-file
- The "Final conditions, FCU" file. Contains values of all state variables at the end of the simulation period.

For the identification experiments described in chapter 4, a BCA file with constant steady state values of the off-take flow rates was used. Step changes of compressor station discharge pressures and the off-take flow near the check point Px3 were implemented in the CRD file.

C.2 Extensions to "Simone"

"Simone" has a very limited capability on simulation time. With the 10 minute sampling interval chosen, only about 22 hours can be simulated. Also, the CRD file may host only a limited number of commands. Therefore, the "Simone" was extended with a number of auxiliary programs as follows, see figure C.1
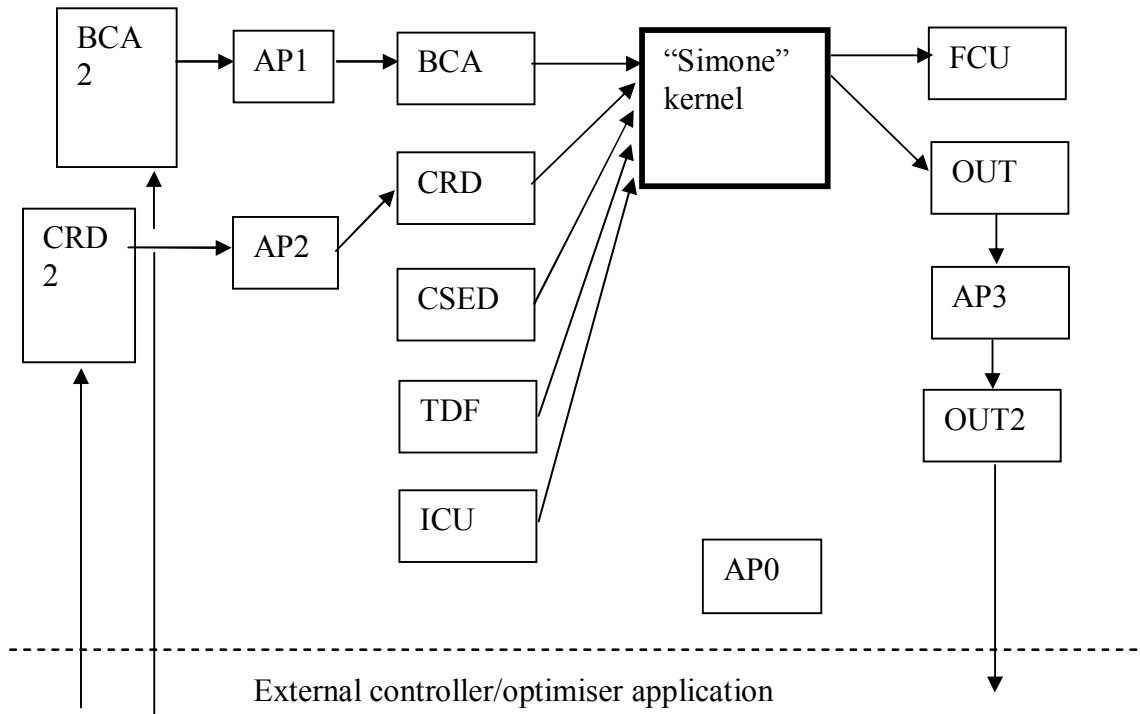
Figure C.1 The "Simone" simulator with it's associate files and auxiliary programs

The auxiliary program AP1 re-samples (from 60 to 10 minutes) the off-take flow rate data from the large BCA2 file containing gas flow values for all 194 off-takes for the whole month of March 2003 and writes the data to a smaller BCA file which "Simone" is capable of handling. Analogously, AP2 takes re-sampled and filtered discharge pressure values and compressor station start up / shut down commands for the three compressor stations as operated during the spring of 2003 from CRD2 and writes the data to the CRD file. A third program, which takes care of overall sequencing and administration, AP0, keeps track of the actual simulation time (which within "Simone" is the "physical time", starting 1.3.2003 00:00 and steps forward with 10 minute increments). The sequencing program starts simulation with the FCU-file from the previous simulation cycle copied to the ICU file of the present cycle and updates the time tick to a data file (not shown in the figure) which AP1 and AP2 can read in order to pick the correctly timed values from the BCA2 and CRD2 files. The ASCII data output file OUT is updated with simulated results after each 10-minute simulation and the program AP3 is collecting this data into OUT2 which spans the whole simulated period.

The auxiliary programs AP0 to AP3 are all implemented by the author in the Pascal programming language. Modifications of the DOS BATCH files used by "Simone" are done by the author as well.

C.3 Real time operation and predictions with "Simone"

The auxiliary programs presented above are extended to perform prediction calculations, which simply means, that the simulation period is extended from 10 minutes (or any basic interval) to any longer interval. In this case, "Simone" picks gas off-take flow values, as usual, from the

BCA file, which is updated from BCA2, but values for each off-take over the prediction horizon (P) are needed (see figure C.2 for an illustration). The compressor station discharge pressures and shut down/start up commands (decision variables) are received from an external control or optimisation application. In the case described in this study, these values are assumed to be constant over the whole prediction horizon. The main co-ordination program AP0 conducts two simulation steps at each time it is acknowledged by the external application, that decision variables have been updated:

1. Simulate one interval (10 minutes) into the future to obtain the new "measured" (or "current") values of pressure and gas flow variables
2. Simulate P+1 intervals into the future to obtain the *free response predictions* of pressure and gas flow variables.

The simulation results are collected into the file OUT2 and the external application is acknowledged, that the simulation is completed.
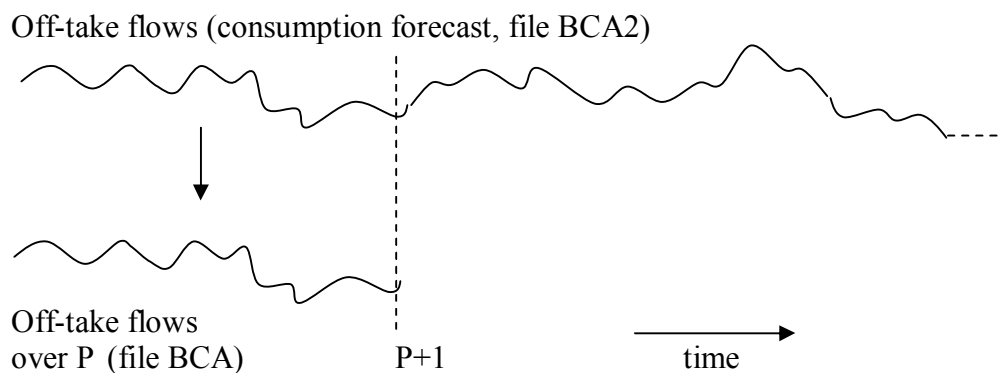
Figure C.2 Off-take flows over the prediction horizon are obtained by picking values from a "long term storage" of off-take flows

The auxiliary programs also allow off-take flow values in the BCA2 file to be updated from an external application (arrow towards BCA2 in figure C.1). This feature is used when testing the effect of erroneous forecasts on the optimisation (See Chapter 6, section 6.8.3)

With the auxiliary programs described above, "Simone" is capable of operating in a real-time mode, if the simulation cycles above are timed to start when fresh, measured data is available *and* the controller or optimiser has fresh decision variables available. If state estimation schemes (see Chapter 5) are needed, then at least the method of updating off-take flows (over the prediction horizon) based on differences between measured and simulated pressures can be implemented in a straightforward way.

Typically, in real-time operation, BCA2 holds *gas consumption forecasts* for each off-take and is possibly updated from a separate forecasting application.

C.4 The real-time receding horizon optimiser

The optimiser is built upon Matlab 6.5 and Matlab's Optimisation Toolbox. While "Simone" runs under MS-DOS, and it's memory usage did not allow network software to operate on the computer, a separate computer running the Windows NT operating system for the optimiser was used and a serial communication link was set up between the two computers. Matlab 6.5. contains good support and existing functions for serial communication. The optimiser consists of a number of "M-files" (script files written in Matlab's script language). As explained in Chapter 5, the kernel of the optimiser is the solver "fmincon" of the Optimisation Toolbox. For the optimiser, a graphical user interface was built, also for which good support and a multitude of functions exist within Matlab 6.5.

Appendix D. Details of the dynamic simulation model of the Finnish natural gas pipeline system

The composition of the natural gas entering the Finnish pipeline system is as shown in table 2.1, Chaper 2. The average molecular weight of the gas is 16.4 kmol/kg.

In all simulations performed in this work, isothermal conditions are assumed, the constant temperature being 5 °C, which is one degree less than the yearly average temperature of the pipeline system. As the compressibility expression, the following simplified expression is used (Riikonen, 1993)

$$z = 1.0016 - \frac{P}{476},$$

where P is the absolute pressure in bar. The expression is valid in the range 0...100 bar.

The cost parameters for compressor stations CS1, CS2 and CS3 are, respectively:

a_1=0.2969, b_1=10270 kW
a_2=0.30484, b_2 =9540 kW
a_3=0.32618, b_3=7230 kW

These parameters have been obtained by fitting the cost function expression (5.35) in Chapter 5 to the compressor station gas consumption of each station calculated by "Simone". The data used for the parameter fit is the true operating data from 1.3.2003 to 31.3.2003. "Simone" uses compressor models of type (3.16) in Chapter 3. The values of the various parameters of those models are automatically calculated by "Simone" when the user enters value pairs of adiabatic head and volume flow rate. The compressor models are kept up to date while the operating personnel of Gasum Oy enters new data into "Simone" whenever changes in compressor characteristics (ageing effects, compressor and/or gas turbine maintenance and so on) are changed.

The value of γ is 0.22.

The parameters of the quadratic cost function approximation, the first variant with quadratic head approximation and independent gas flow, are:

a= -0.00005926
b=   0.0001064
c= -0.00002731
d=   0.011525
e= -0.013052
f=   0.028312

The parameters of the quadratic cost function approximation, the second variant with linear head approximation and linear gas flow, are:

a_L=0.0049
b_L=-0.0072
c_L=0.0862

This approximation is accurate for pressure ratios (P_d/P_s) in the higher end, 1.4 … 1.7.

In figures D.1 to D.3 below, the compressor envelopes for the three units used in the simulations are shown. The non-linear, original limit curves as they are configured into "Simone" as points in the (volume flow, Head) co-ordinate system, are shown as dashed lines. They are actually piecewise linear, because the number of points used is small.

CS1 Head (kJ/kg) as a function of volume flow (m3/s) at suction conditions
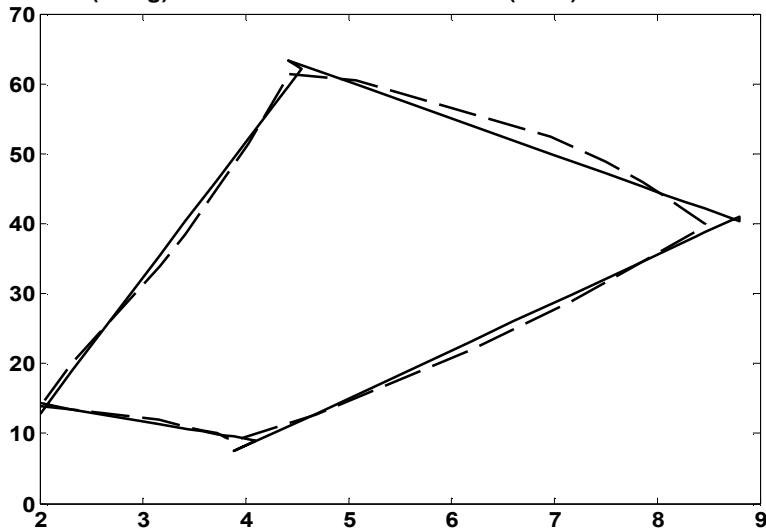
Figure D.1 CS1 envelope approximation. True envelope curves from "Simone" (dashed lines) and linear approximations.
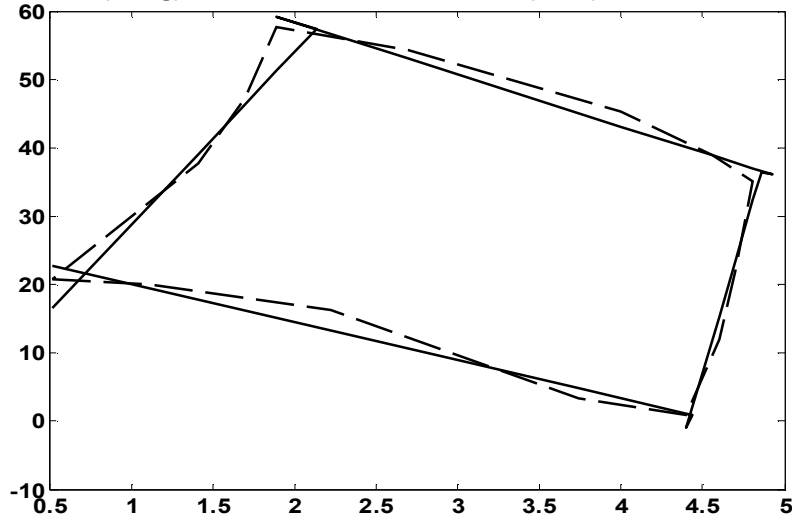

CS2 Head (kJ/kg) as a function of volume flow (m3/s) at suction conditions
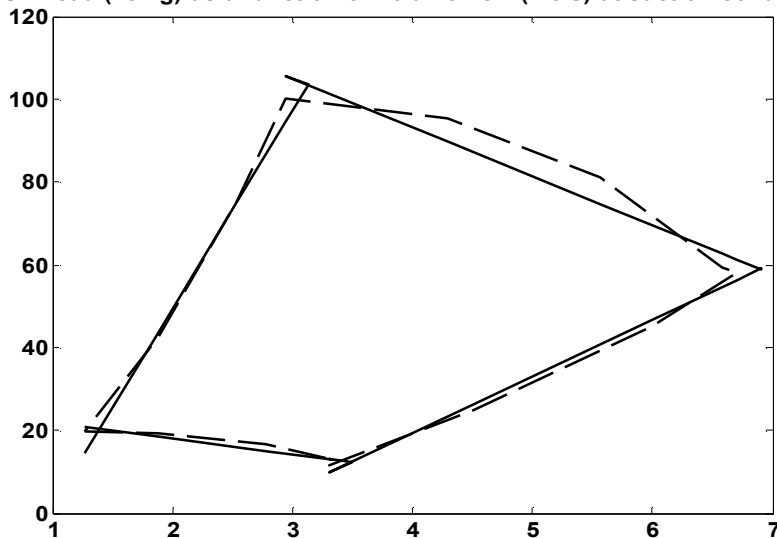
Figure D.2 CS2 envelope approximation. True envelope curves from "Simone" (dashed lines) and linear approximations.

Figure D.3 CS3 envelope approximation. True envelope curves from "Simone" (dashed lines) and linear approximations.

The linear compressor station envelope constraints, $a_{ij}H + b_{ij}q_{VOL} + c_{ij} \leq 0$, i=1,2,...,$N_c$, j=1,...4, see section 5.7, Chapter 5, have the following parameter values:

Constraint	a_{ij}	b_{ij}	c_{ij}
CS1 minimum speed	1	2.5137	-19.3257
CS1 choke line	1	-6.8298	19.0749
CS1 surge line	1	-19.3353	25.7433
CS1 maximum speed	1	5.2260	-86.4505
CS2 minimum speed	1	3.8001	-25.6039
CS2 choke line	1	-13.6946	35.4812
CS2 surge line	1	-47.9946	44.0984
CS2 maximum speed	1	11.8167	-140.4125
CS3 minimum speed	1	5.5417	-25.549
CS3 choke line	1	-81.5262	359.763
CS3 surge line	1	-25.2874	5.9534
CS3 maximum speed	1	7.6084	-73.5893

For the steady state optimisation in section 5.9, Chapter 5, the *quadratic* constraint approximations $H - a^q q_{VOL}^2 - b^q q_{VOL} - c^q \leq 0$ are used:

Constraint	a^q	b^q	c^q
CS1 minimum speed	1.161	-4.321	-9.8834
CS1 choke line	-0.4807	-0.8302	-1.5968
CS1 surge line	-2.2355	-4.8863	4.0823
CS1 maximum speed	1.205	-10.2868	-39.4746
CS2 minimum speed	2.4383	-7.6044	-13.915
CS2 choke line	-1.2907	-0.6014	4.3555
CS2 surge line	-10.6086	-3.4298	1.6358
CS2 maximum speed	3.4072	-21.4871	-66.356
CS3 minimum speed	0.9316	0.9324	-21.9072
CS3 choke line	-128.2	1097.9	-2348.9
CS3 surge line	-16.9539	14.2716	-23.5829
CS3 maximum speed	1.9963	-5.8246	53.6028